Immune Evasion in Glioma

Helen Judith Close

Submitted in accordance with the requirements for the degree of Doctor of Philosophy

The University of Leeds
Faculty of Medicine and Health
School of Medicine

September 2016

The candidate confirms that the work submitted is her own and that appropriate credit has been given where reference has been made to the work of others.

Acknowledgements

I wish to thank my supervisor Graham Cook for his continued support and guidance throughout my project. Although chaotic in the lab, his positive attitude and kind nature have enabled me to explore scientific ideas in a receptive environment. I also wish to thank my co-supervisor Erica Wilson for technical guidance, ideas and constructive feedback. I am indebted to previous lab members Laura Wetherill and Emma Black for both emotional support as well as technical guidance. I'm also entirely grateful to colleagues Sarah Phillips, Gary Grant, Aarren Mannion, Adam Odell and Misian for constructive unwavering ridicule and endless lab bants. This project would also not have been possible without the love and support of my friends and family, especially my parents Robyn and Chris, Anthony Aimon, Ruth Norman, Alethea Peters and Helene Taylor. I would also like to thank Cancer Research UK for funding the project.

Abstract

Glioblastoma multiforme (GBM) is the most common form of primary brain cancer and the current prognosis for patients is poor. New therapies are required that target the invasive cells that are characteristic of GBM. GBM is infiltrated by immune cells but, as with other cancers, immune evasion pathways minimise productive anti-tumour immunity. Natural killer (NK) cells are able to recognise and kill tumour cells and are being developed for the immunotherapy of other cancers. The aim of this work was to analyse the interaction between human NK cells and GBM cells *in vivo* and *in vitro*, as a prerequisite to future NK cell based immunotherapy of GBM. Analysis of the cell surface phenotype for GBM infiltrating NK and T cells revealed that the tumour microenvironment exerts localised immune evasion mechanisms which downregulate activation receptors and upregulate inhibitory receptors. The interaction of NK cells with patient-derived GBM stem cells, which are thought to be responsible for recurrent disease, was investigated *in vitro*. A high-throughput, multiplex flow cytometry-based screen of tumour cells revealed the expression of a number of cell surface molecules that regulate NK cell activation. Furthermore, GBM cells were more susceptible to NK cell lysis *in vitro* compared to a non-cancerous neural progenitor cell line, revealing specificity in the NK cell response. Furthermore, this screen identified potential mechanisms by which GBM might evade immune surveillance *in vivo*. Targeting these pathways and restoring functional immune surveillance provides a potential route for future immunotherapy of this disease. However, GBM patients often experience cerebral oedema and are treated with immunosuppressive corticosteroids, such as dexamethasone; this induces a similar immunosuppressed phenotype to that observed with the GBM infiltrating NK cells, and inhibits their lytic function. Gene expression profiling identified the transcription factor c-Myc as a key regulator of NK cell activation and as a hub for the immunosuppressive action of steroids and the immunosuppressive cytokine TGF-β. The demonstration that therapeutic steroids target the same pathway as TGF-β and induce immunosuppression has important implications for the use of steroids in patients undergoing immunotherapy.

Table of Contents

Figures

Tables

Abbreviations

ADCC	Antibody-dependent cell-mediated cytotoxicity
AF	Alexa Fluor
APC	Antigen presenting cell
APC	Allophycocyanin
APS	Ammonium persulfate
BBB	Blood brain barrier
BDP	Beclomethasone dipropionate
BSA	Bovine serum albumin
BTIC	Brain tumour-initiating cell
CD	Cluster of differentiation
CD122	IL-2 receptor β chain
CD132	Common cytokine-receptor γ-chain
cDNA	Complementary DNA
CFSE	Carboxyfluorescein succinimidyl ester
CML	Chronic myeloid leukaemia
CNS	Central nervous system
CSC	Cancer stem cell
CSF	Cerebrospinal fluid
cSMAC	Central supramolecular activation cluster
CTLA-4	Cytotoxic T-lymphocyte-associated antigen 4 ; CD152
CUSA	Cavitron ultrasonic surgical aspirator
D	Dexamethasone
DAP10	DNAX activation protein of 10kDa
DAP12	DNAX activation protein of 12kDa
DBD	DNA-binding domain
DC	Dendritic cell
DCLN	Deep cervical lymph nodes
DMEM	Dulbecco's Modified Eagle Medium
DMEM-F12	Dulbecco's Modified Eagle Medium: Nutrient Mixture F-12
DNA	Deoxyribonucleic acid
DNAM-1	DNAX accessory molecule-1, CD226
dNK	Decidual NK
EDTA	Ethylenediaminetetraacetic acid
EGF	Epidermal growth factor
EGFR	Epidermal growth factor receptor
eIF4E	Eukaryotic translation initiation factor 4E
FACS	Fluorescence-activated cell sorting
FADD	Fas-associated death domain
FAK	Focal adhesion kinase
FasL	Fas ligand
FBS	Foetal bovine serum
Fc	Constant region
FCS	Foetal calf serum

FGF	Fibroblast growth factor
FITC	Fluorescein
FSC	Forward scatter
g	Gravitational constant
GBM	Glioblastoma multiforme
GC	Glucocorticoid
G-CSF	Granulocyte colony-stimulating factor
GM-CSF	Granulocyte macrophage colony stimulating factor
GR	Glucocorticoid receptor
GRE	GR response element
GSC	Glioma stem cells
HLA	Human leukocyte antigen
HPC	Hematopoietic progenitor cell
HSP	Heat shock protein
ICAM3	Intercellular adhesion molecule 3
IDO	Indoleamine 2,3-dioxygenase
IFNγ	Interferon gamma
Ig	Immunoglobulin
IL	Interleukin
ILCs	Innate lymphoid cells
IS	Immunological synapse
ITAM	Immunoreceptor tyrosine-based activation motif
ITIM	Immunoreceptor tyrosine-based inhibitory motif
ITSM	Immunoreceptor tyrosine-based switch motif
IU	International unit
IκBα	Inhibitor of kappa B
JAK	Janus-associated kinases
kDa	Kilodalton
KIR	killer cell immunoglobulin receptor
KLR	killer lectin like receptor
LAG-3	Lymphocyte-activation gene 3
LAK	Lymphokine-activated killer
LAMP-1	Lysosomal-associated membrane protein 1; CD107a
LBD	C-terminal ligand-binding domain
LRC	Leukocyte receptor complex
Ly75	Lymphocyte antigen 75; CD205
M	Molar
MAPK	Mitogen-activated protein kinase
MDSC	Myeloid-derived suppressor cell
mg	Milligram
MGMT	O^6-methylguanine-DNA methyltransferase
MHC	Major histocompatibility complex
MIC A	MHC class I polypeptide-related sequence A
MIC B	MHC class I polypeptide-related sequence B
mL	Millileter

MM	Multiple myeloma
mM	Millimolar
MP	Methylprednisolone
mRNA	Messenger RNA
MTOC	Microtubule organising centre
mTOR	Mammalian target of rapamycin
n.s	Not significant
NCR	Natural cytotoxicity receptor
ng	Nanogram
NICE	National Institute for Health and Care Excellence
NIR	Near infrared
NK	Natural killer
NKp30	Natural cytotoxicity triggering receptor 3; NCR3, CD337
NKp44	Natural cytotoxicity triggering receptor 1; NCR2, CD336
NKp46	Natural cytotoxicity triggering receptor 1; NCR1, CD335
NSCLC	Non-small cell lung cancer
NTD	N-terminal transactivation domain
oHSV	Oncolytic Herpes simplex virus
OS	Overall survival
PBMCs	Peripheral blood mononuclear cells
PBMCs	Peripheral blood mononuclear cell
PBS	Phosphate buffered saline
PCA	Principal component analysis
PD-1	Programmed cell death protein 1; CD279
PD-L1	Programmed death ligand 1; CD274
PD-L2	Programmed death ligand 2; CD273
PDNA	Prednisolone acetate
PE	Phycoerythrin
PGE2	Prostaglandin E2
PIGF	Placental growth factor
PIP_2	Phosphatidylinositol-3,4-bisphosphate
PIP_3	Phosphatidylinositol-3,4,5-trisphosphate
PNS	Peripheral nervous system
pSMAC	Peripheral supramolecular activation cluster
PVDF	Polyvinylidene difluoride
REMBRANDT	Repository of Molecular Brain Neoplasia Data
RNA	Ribonucleic acid
RPMI	Roswell Park Memorial Institute medium
RT	Room temperature
s.d	Standard deviation
SAP	SLAM associated protein
SAS	Sub arachnoid space
SH2	Src homology 2
SIRPβ1	Signal-regulatory protein beta-1; CD172b
SLT	Secondary lymphoid tissue

SSC	Side scatter
STAT	Signal transducer and activator of transcription
TAA	Tumour associated antigen
TCGA	The Cancer Genome Atlas
TCR	T-cell receptor
TGF-β	Transforming growth factor beta
TIL	Tumour infiltrating lymphocyte
TNF	Tumour necrosis factor
TRAIL	TNF-related apoptosis-inducing ligand
Tregs	Regulatory T cells
ULBP1	UL16 binding protein 1
v/v	Volume per volume
VEGF	Vascular endothelial growth factor
w/v	Weight per volume
WHO	World Health Organisation
°C	Degrees celsius
µl	Microliter
µm	Micrometer
µM	Micromolar
4E-BP1	4E-binding protein 1

Chapter 1 Introduction

1.1 The immune system and cancer

Cancer is an umbrella term for a group of diseases that can arise in almost any tissue. In 2000, Hanahan and Weinberg summarised that most, if not all cancers, are characterised by the following 'hallmarks'; a limitless replicative potential, sustained angiogenesis, evading apoptosis, self-sufficiency in growth signals, insensitivity to anti-growth signals and the ability to invade tissue and metastasise (Hanahan & Weinberg 2000). Cancer is one of the leading causes of death in the UK, accounting for more than 25% of deaths (Cancer Research UK 2016a) and it is estimated that 50% of people in the UK born after 1960 will develop cancer within their lifetime (Ahmad et al. 2015).

Accordingly, a vast amount of research has been conducted to try to depict the aetiology of each cancer and how it progresses. As our understanding grows, so too does the advancement of treatments. Although overall cancer survival rates have doubled since the 1970s to around 50% (Quaresma et al. 2015), the prognosis for some patients, such as those with a brain tumour known as glioblastoma multiforme (GBM) has remained poor, with just 12% survival at 3 years post diagnosis (Jovčevska et al. 2013). There is a real need to find new therapies to improve the outlook for these patients.

In the last 15 years there has been a shift in the way we think about and study cancer; from a cancer cell based focus to one which recognises that cancers are complex tissues that act as parasitic organs, recruiting and manipulating healthy cells to propagate their growth. In light of this insight, the list of cancer hallmarks has been expanded. It is now established that in order for tumours to prevail they must not only sustain division but also evade the body's defence mechanism against external and internal threats; namely the immune system (Hanahan & Weinberg 2011).

1.1.1 Immunosurveillance

The notion that the immune system could suppress tumour formation is as old as immunology itself, being first proposed by Paul Ehrlich in 1909 (Ichim 2005). However, it was not until 1957, when tumour specific antigens were discovered, that Burnet and Thomas proposed the theory of 'cancer immunosurveillance'. They suggested that it

was evolutionarily necessary to be able to eliminate transformed cells and that the mechanism responsible was immunological (Burnet 1970). The discovery of natural killer (NK) cells and their ability to spontaneously kill tumour cells supported this theory (Herberman & Holden 1978), yet a lack of characterisation and knowledge of NK cell regulation, coupled with the use of unsuitable animal models rendered the theory controversial until the mid 1990s (Dunn et al. 2002). The tumour suppressive nature of the cytokine interferon gamma (IFNγ) (Dighe et al. 1994) and the observation that perforin, a key constituent of NK cell cytolytic granules, prevents chemically induced tumours in a mouse model (Russell & Ley 2002) helped to silence the critics. Furthermore, an increase in the incidence of certain tumours in immunocompromised patients strongly supports the cancer immunosurveillance theory (Vajdic & van Leeuwen 2009).

1.1.2 Immune evasion and immunoediting

If the immune system is capable of eliminating transformed cells then its stands to reason that patients' tumours acquire mechanisms to escape detection or destruction. In fact this requirement for a tumour to 'evade immune destruction' is listed as one of the hallmarks of cancer (Hanahan & Weinberg 2011). As is often seen in nature, when a selective pressure is applied to a population, those that have variations allowing them to survive will propagate to form similarly adapted offspring. This Darwinian mechanism thus not only applies at the level of the organism, but also at the cellular level. Transformed cells that are highly immunogenic are destroyed by the immune system, allowing only weakly immunogenic cells to remain, expand and colonise until the cancer is a clinically detectable entity. This sculpting effect of the immune system is known as 'immunoediting' and has been demonstrated in experiments involving transplanted tumours from both immuno- compromised and competent mice (Kim et al. 2007; Teng et al. 2008).

1.1.3 Pro-tumour immune cells

Not only is cancer able to evade the immune system but an increasing volume of research supports the counterintuitive finding that some immune cells actually promote tumour progression. This is achieved in a multitude of ways. For example, by

the release of tumour growth factors such as EGF (Qian & Pollard 2010), the secretion of the proangiogenic growth factor VEGF, the synthesis of prometastatic matrix-degrading proteins (Murdoch et al. 2008) and the suppression of cytotoxic immune cells (Nguyen & Ohashi 2015).

1.1.4 Immunotherapy for cancer treatment

Therapies involving the manipulation of the immune system are known as immunotherapies. These are already being used in the clinic to treat cancer and many more are currently being developed. For example, antibodies such as trastuzumab and rituximab target ERBB2-positive breast cancer and CD20-positive B cell malignancies respectively. Tumour regression in patients treated with these antibodies is, in part, due to antibody-dependent cell-mediated cytotoxicity (ADCC) (Scott et al. 2012). In 2011, ipilimumab, an antibody that blocks cytotoxic T-lymphocyte-associated antigen 4 (CTLA-4) expressed on T cells, was approved by the FDA to treat patients with metastatic melanoma (Fellner 2012). CTLA-4 acts as an 'immune checkpoint' by preventing the activation of T cells. In doing so it plays an important role in thwarting autoimmunity. By inhibiting this immune checkpoint, ipilimumab is believed to enhance the antitumor T-cell response (Fellner 2012). Cellular based immunotherapies and viral therapies are also being developed with the goal of turning the immune evasion pathways operating in patients into productive anti-tumour immunity.

Immunotherapy offers a new avenue of treatment, especially for cancers such as GBM that have a poor prognosis with the current treatment options. To make effective immunotherapy a reality for the treatment of GBM it is essential to establish the mechanisms of immune evasion in the diseased state.

1.2 Glioblastoma Multiforme

1.2.1 Current treatment and outlook

GBM is the most common type of primary brain tumour and has a 5 year survival rate of just 6% (Cancer Research UK 2016b). The current standard treatment involves surgical resection followed by radiation in conjunction with temozolomide chemotherapy and a further 6 rounds of temozolomide treatment (Stupp et al. 2005). However, tumours inevitably become resistant to treatment and the patients no longer respond. Accordingly, the median survival is only 12-15 months (Ahmed et al. 2014).

1.2.2 Glial cells

On a simplified level, the central nervous system (CNS) can be categorized into two cell types; neurons and glial cells. The neurons principally act to relay electrical signals, whilst the glial (Greek for glue) cells support the neurons. The glial cells can be further subdivided into four groups; astrocytes, oligodendrocytes, ependymal cells and microglia (Figure 1.1). Astrocytes have a star-like morphology with long protrusions. They help to support neurons, maintain chemical concentrations in the extracellular space, remove waste, repair tissue damage and form an integral part of the blood brain barrier (BBB). Oligodendrocytes have a similar role to Schwann cells found in the peripheral nervous system (PNS), insulating axons by synthesizing a myelin sheath (Hall 2006). Ependymal cells are specialized ciliated cells that line the ventricles of the brain. Their cilia help to circulate the cerebrospinal fluid (CSF) which is made within the choroid plexus. The CSF acts as a protective cushion for the brain, as well as contributing to CNS metabolism and homeostasis. Microglia are brain-resident macrophages and provide innate immune defence in the brain (Perry & Teeling 2013). They are discussed in more depth in section 1.2.4.

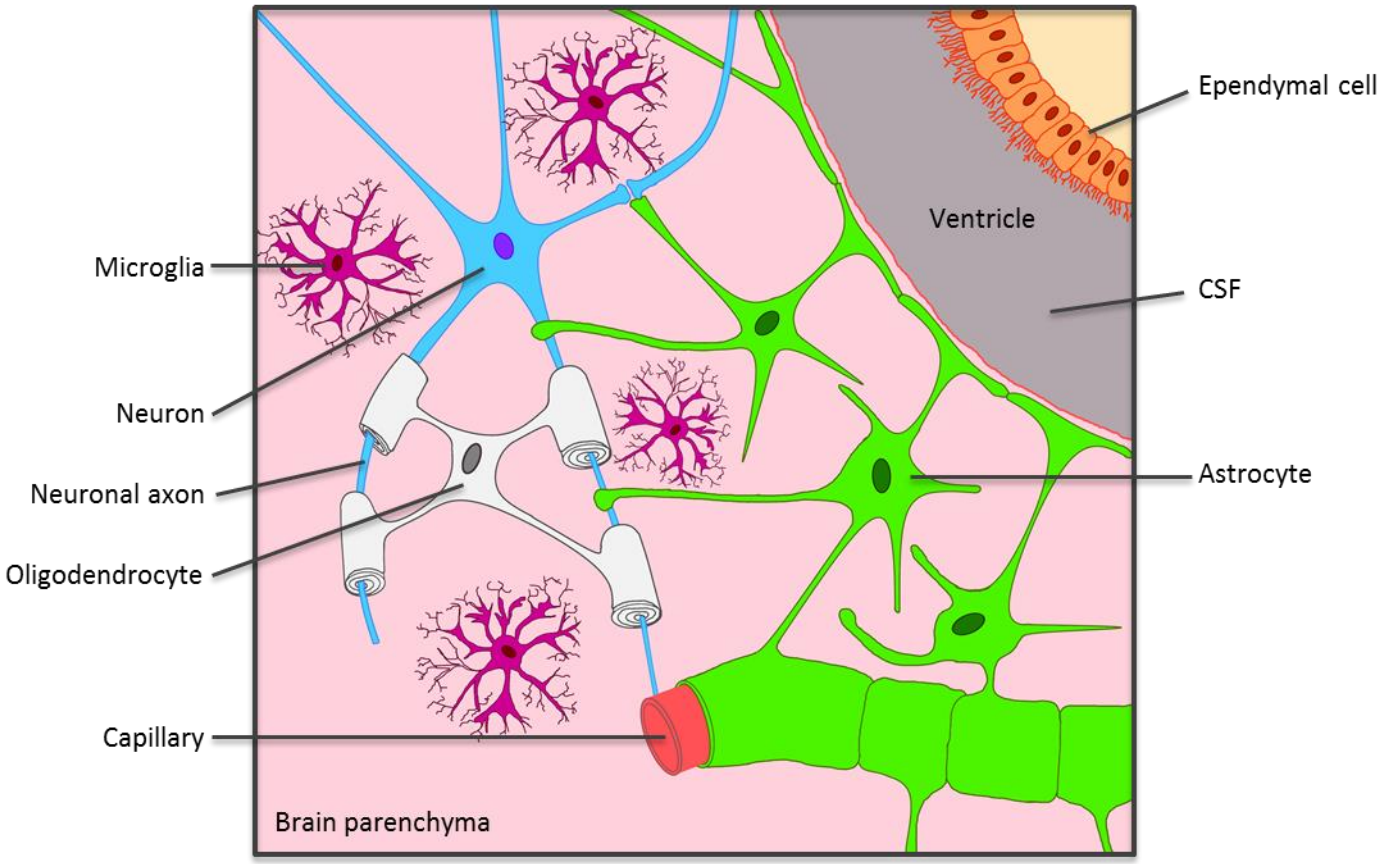

Figure 1.1. Central nervous system glial cells. Oligodendrocytes (white), astrocytes (green) and microglia (violet) are located in the brain parenchyma. Microglia are brain-resident macrophages. Oligodendrocytes insulate the axons of neurons (blue). Astrocytes support neurons, facilitate tissue homeostasis and their foot processes form an integral part of the blood brain barrier (BBB). Ependymal cells (orange) line the ventricles and help to circulate CSF.

1.2.3 Tumour grading

Gliomas are currently graded according to their malignancy as described by the WHO classification system (Louis et al. 2007). This system is based on seminal research done by Bailey and Cushing in 1926 (Bailey & Cushing 1926). Tumours were grouped according to patient prognosis and subsequently the histological morphology was used to annotate the groups. Tumours dubbed astrocytomas and oligodendrogliomas resembled astrocytes and oligodendrocytes respectively. The cells within tumours from patients with the worst prognosis mirrored less differentiated precursor cells. Therefore, malignant astrocytomas were coined astroblastomas. (Louis et al. 2001). Although tumour cells morphologically mimic other cell types, and are named accordingly, the tumour initiating cells are still unknown. It is speculated that malignant gliomas could arise from a number of cells including neural stem cells, neural/glial progenitors, oligodendrocytes or astrocytes (Hadjipanayis & Van Meir 2009). Currently four groups of astrocytomas are defined; pilocytic, grade I: diffuse, grade II: anaplastic, grade III and glioblastoma multiforme (GBM), grade IV. GBM is highly invasive into surrounding healthy tissue (Denysenko et al. 2010) and it is therefore difficult to excise all of the malignant cells during surgery. In general cancer nomenclature, a primary cancer is one that originates within a certain region and a secondary cancer is one that metastasizes to the location. However, a primary GBM is one that arises de novo and a secondary GBM is one that has progressed from a lower grade. Secondary GBMs account for 10% of cases (Van Meir et al. 2010)). An overview of the grading system is shown in figure 1.2.

Over the past 30 years an increasing number of genetic alterations have been identified within GBM that correlate, to some extent, with the response to different treatments and patient prognosis (Van Meir et al. 2010). Research by The Cancer Genome Atlas (TCGA) consortium has confirmed and expanded our knowledge about genes and key pathways that are implicated in GBM (Cancer Genome Atlas Research Network 2008). Further investigation by the same group using DNA, mRNA and microRNA analysis have led to subtypes being described (Verhaak et al. 2010). Characteristic alterations are listed in figure 1.2. It is hoped that over time these subtypes will help to establish a tailored treatment plan for each group of patients and improve survival outcomes. The importance of the molecular changes that define the

subtypes is recognised by their inclusion in the recently amended WHO classification system (Louis et al. 2016). As molecular profiling becomes a more routine component of diagnosis it will enable the use of the updated system.

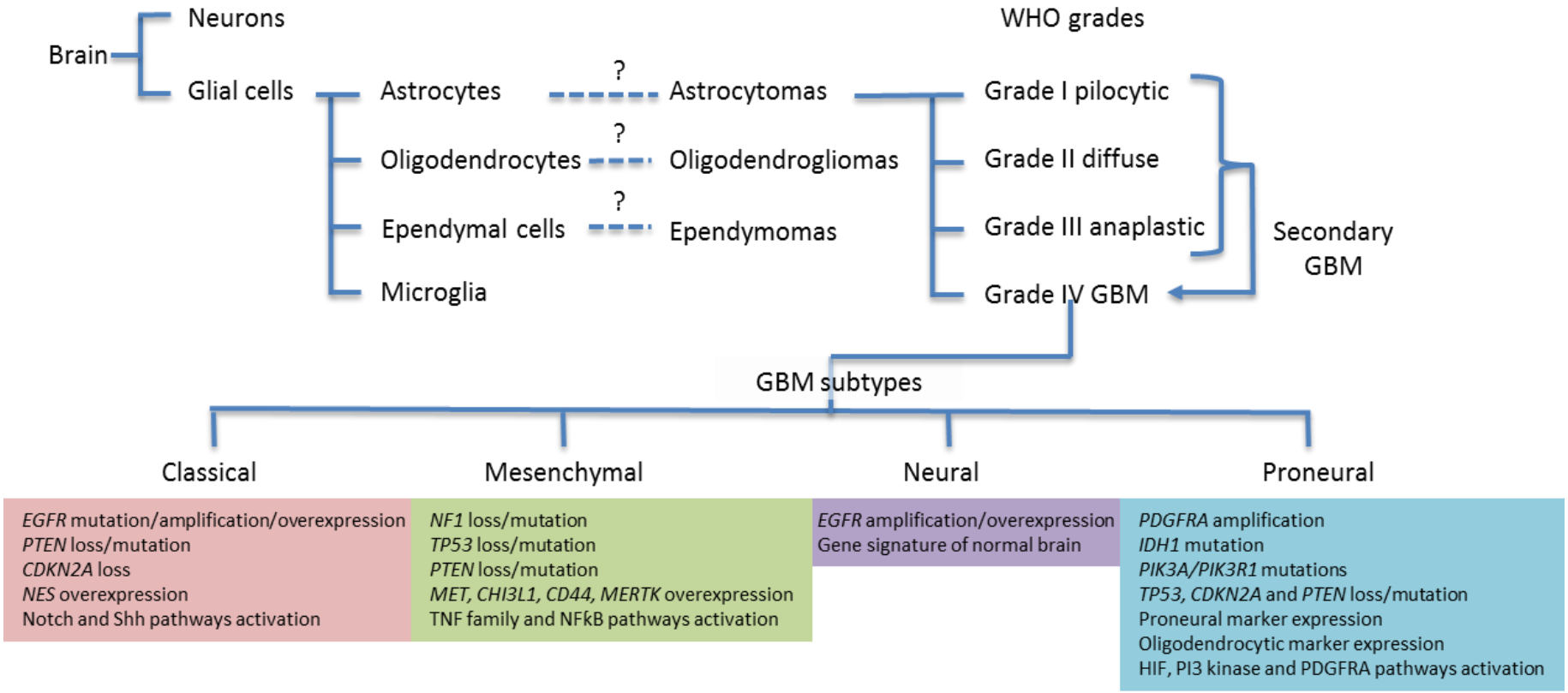

Figure 1.2. An overview of astrocytoma grading and GBM subtypes. The brain consists of neurons and glial cells (astrocytes, oligodendrocytes, ependymal cells and microglia). The cell of origin of glial neoplasms (astrocytomas, oligodendrogliomas and ependymomas) is unknown but they are named according to resemblance. There are four grades of astrocytoma based on the WHO grading system; grade IV is known as GBM. Lower grade tumours that progress to GBM are referred to as secondary GBM. Subgroups of GBM have been established based on DNA, RNA and microarray analysis; classical, mesenchymal, neural and proneural. Typical characteristics are listed in the coloured boxes (Van Meir et al. 2010).

1.2.4 Brain anatomy and immune surveillance

In order to understand the challenges faced when treating GBMs it is important to understand the anatomy and immune surveillance of the brain.

1.2.4a Meninges and the blood brain barrier

The brain is a critical organ and thus has evolved unique defence mechanisms that are employed to protect it. Neurons reside in the brain parenchyma, a tissue that is subject to maximum security achieved by three encasing membranes known as meninges. Namely, the pia, arachnoid and dura maters lie sequentially from parenchyma to skull. The region between the pia and arachnoid membranes is known as the sub arachnoid space (SAS). CSF is found within the SAS, along with arachnoid trabeculae that entwine the two membranes (Figure 1.3b). This space is also occupied by arterial vessels that sink into the parenchyma to deliver nutrients to the brain (Figure 1.3c). As these vessels penetrate, so too do the arachnoid and pia maters, creating perivascular spaces that are continuous with the SAS (Ransohoff & Engelhardt 2012). In order to prevent harmful agents from the blood entering the parenchyma, regulation is tightly controlled by the BBB. The BBB is a physical barrier that prohibits substances with a molecular weight of greater than 500 Da from entering the brain parenchyma (a five amino-acid peptide has a molecular weight of ~550 Da) (Daga et al. 2011). It comprises three cellular components (Figure 1.4); endothelial cells held together by tight junctions form an impenetrable barrier, contractile pericytes help control the blood flow within the brain and astrocytes protrude foot-like processes that tightly enclose the vessel wall and are critical in the formation and maintenance of tight junctions (Ballabh et al. 2004).

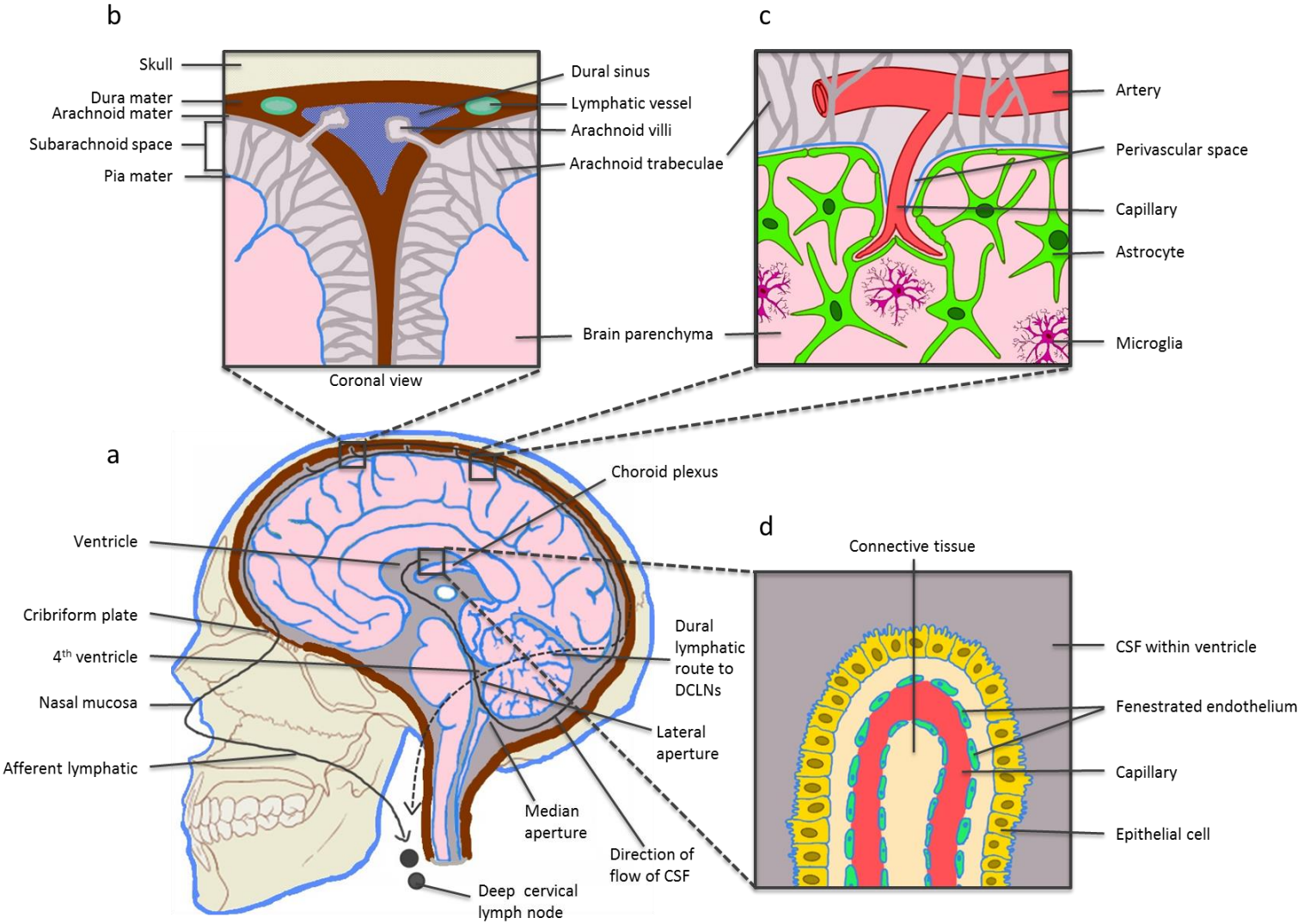

Figure 1.3. Brain anatomy. a) A sagittal view of the brain and skull showing the routes taken by the CSF to enter the DCLNs. The majority of the CSF is produced in the ventricles. It circulates around the brain and is reabsorbed into the blood through the arachnoid villi. CSF is also trafficked to the DCLN either by dural lymphatic vessels or along olfactory rootlets through the cribriform plate to the nasal mucosa and eventually to the deep cervical lymph nodes (DCLN) via afferent lymphatic vessels. b) A coronal view of the meninges, dural sinus and the adjacent dural lymphatic vessels. The meninges (dura mater, arachnoid mater and pia mater) are concealed beneath the skull. Arachnoid villi protrude into dural sinuses. c) Astrocytic foot process provide a barrier that protects the brain parenchyma. See figure 1.4. d) A choroid plexus villi. CSF is made by the epithelial cells which filter fluid from the blood that has passed through the fenestrated endothelium. The epithelial layer is the blood-CSF barrier. Adapted from (Ransohoff & Engelhardt 2012) and (Louveau et al. 2015).

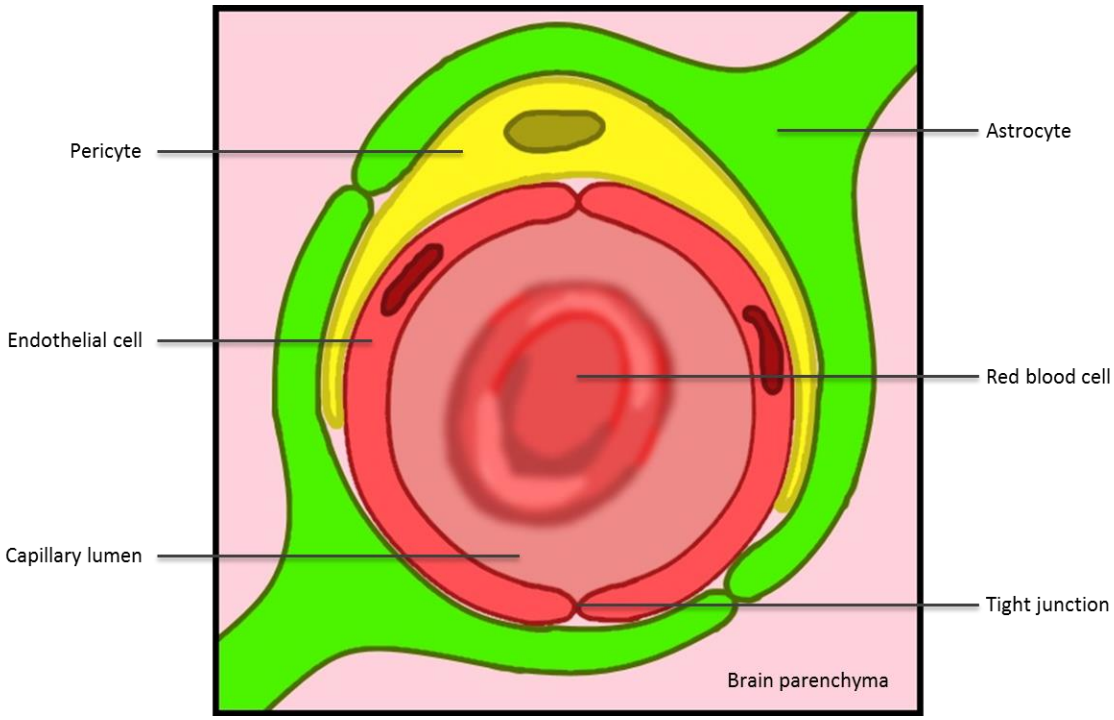

Figure 1.4. The blood brain barrier (BBB). Endothelial cells (red) joined by tight junctions, pericytes (yellow) and astrocytic foot processes (green) make up the BBB.

1.2.4b Blood-CSF barrier

The blood-CSF barrier displays a different architecture to the BBB but is also a tightly controlled checkpoint of entry into the brain. The blood-CSF barriers are located in the four ventricles of the brain in regions known as the choroid plexus. The choroid plexus is organized into villi that consist of an outer epithelial layer embodying a fenestrated capillary, stromal cells and connective tissue (Figure 1.3d). The epithelial cells are closely conjugated by tight junctions and it is this layer that is termed the blood-CSF barrier (Lun et al. 2015). These epithelial cells are also responsible for the production of CSF.

1.2.4c Immune surveillance- CSF

In addition to physical barriers, the immune system plays an important role in protecting the brain. For obvious reasons it is difficult to fully elucidate how the immune system functions in a healthy human brain and a lot of the current understanding has been based on animal models. Researchers using rodent models in the early 1920s reported the observation that antigens or tumours placed in the brain parenchyma failed to mount an immune response but this was not the case elsewhere in the body. These findings pioneered the conception of the idea in 1953 by Billingham and Boswell that the brain is 'immunologically privileged' (Galea et al. 2007). Anatomical observations supported this idea. For example the presence of the restrictive BBB (Galea et al. 2007) and, until 2015, the belief that the brain lacked conventional lymphatic vessels (Walker et al. 2002). However, this concept has been revised based on the existence of autoimmune diseases of the CNS, such as multiple sclerosis (Ransohoff & Engelhardt 2012), and that immune cells have been shown to infiltrate brain tumours and play a role in anti-tumour immunity (Brodbelt & Stoodley 2007). Furthermore, with the newly discovered meningeal lymphatic vessels (Louveau et al. 2015), it is now more apparent than ever that immune regulation within the CNS is not absent, but is highly specialised.

The CSF plays an important role in CNS immunity. In addition to the CSF made by choroid plexus epithelial cells mentioned above, a small proportion of the CSF originates from the interstitial fluid from the brain parenchyma via the perivascular spaces (Ransohoff & Engelhardt 2012). The CSF flows from the lateral ventricles,

through the third and into the fourth ventricle. From here some of the fluid continues to flow downwards and lubricate the spinal cord but the majority will exit the brain to the surrounding SAS via two lateral and one median apertures (Brodbelt & Stoodley 2007). Once in the SAS, the CSF flows from posterior to anterior and is reabsorbed into the venous blood stream through the arachnoid villi (Hall 2006). The seminal discovery that lymphatic vessels are located within the brain has undoubtedly improved our knowledge of immune surveillance within the CNS. Lymphatic vessels were observed in a mouse model lining the dural sinuses and were shown to be the major route for CSF and cellular components into the deep cervical lymph nodes (DCLN). Similar structures were also identified in the human brain (Louveau et al. 2015). A proportion of CSF is also trafficked along olfactory rootlets through the cribriform plate to the nasal submucosa where it enters lymphatic vessels. Animal studies show that some of this subsequently drains to the DCLNs via afferent lymphatic vessels (Koh et al. 2005) (Figure 1.3a). These separate routes enable antigens from the parenchyma to reach secondary lymphoid tissue (SLT). In effect, the CSF acts as a component of the CNS's lymphatic system.

1.2.4d Cellular surveillance

The cellular components of the immune system operating in the brain are different in different anatomical regions. It is, perhaps, helpful to think of the brain as two sections; the parenchyma and everything exterior; the meninges, perivascular spaces and the ventricles. Microglia are the only immune cells routinely reported to be present in the healthy parenchyma. They help maintain homeostasis in the parenchyma, for example, by removing neurotransmitters (Shaked et al. 2005) and modifying and eliminating certain synapses (Tremblay et al. 2010). Immunologically, they are capable of antigen presentation and T cell activation in response to pathological insults (Ford et al. 1996). Myeloid cells outside the parenchyma include meningeal macrophages, perivascular macrophages and choroid plexus macrophages. The residence of these cells is indicated by their names. Their location is ideal to sample CSF from both parenchyma drainage and that originating within the ventricles. Mast cells are also present in the meninges and perivascular spaces. Perivascular macrophages are optimally positioned to activate extravasated lymphocytes by antigen presentation and also stringently control lymphocyte entry into the

parenchyma (Ransohoff & Engelhardt 2012). It is commonly reported that the most abundant cell type in CSF is T cells. However, there are conflicting accounts of the type and proportion of T cell present. This could be due to the method used to assess the composition, for example a lumbar puncture extracts CSF from the bottom region of the spine compared to autopsy tissue where CSF can be viewed in the SAS. It is also possible that the immune composition within the brain could change following death despite a lack of neurological disease. Some groups report a high proportion of CD4+ memory T cells (Kivisäkk et al. 2003). It is thought that these T cells predominantly gain access to the brain via the choroid plexus (Ransohoff et al. 2003). Here they can interact with the antigen presenting cell and traffic to the DCLN via the cribriform plate (Goldmann et al. 2006).

The historic theory the brain is 'immune privileged' has now been revised and accounts for the differential surveillance in separate compartments. The new definition acknowledges that privilege is restricted to the parenchyma but is not absolute, it is not present in the meninges, choroid plexus or ventricles and it is not maintained during inflammation (Galea et al. 2007). The immune cell composition within the brain changes during disease, including cancer.

1.2.5 Immune cell composite within glioblastoma multiforme

Many studies have been undertaken to characterise immune cell infiltration within GBM and different results have been reported. This can partly be due to different markers used to define the cells and the techniques employed for identification, such as flow cytometry and immunohistochemistry, but it could also reflect the different response seen between patients. For example, within a study of just 9 patients the composition of macrophages in the tumour varied widely from 31-90% of total cells (Morantz et al. 1979). It is also feasible that the stage of disease progression correlates with the immune composition, as regulatory T cells (Tregs) have been shown to accumulate in a time dependent fashion in an animal model (Grauer et al. 2007). Another critical consideration to note is that the categorisation of certain infiltrates, such as tumour infiltrating lymphocytes (TILs) incorporates subsets of cells that have opposing roles in tumour biology; CD3+CD8+ T cells correlate with prolonged survival in GBM patients (Kmiecik et al. 2013), but CD4+CD25+ Tregs inhibit anti-tumour immune activation. Similarly, subpopulations of macrophages exist and whilst M1 macrophages are linked with a pro-inflammatory response, M2 macrophages exhibit anti-inflammatory, pro-tumour behaviour (Mantovani & Sica 2010). In glioma patients, high levels of M2 macrophages correlated with higher WHO pathological grades and poor prognosis, whereas the opposite was true of M1 macrophages (Ding et al. 2014).

It is widely reported that the most abundant immune cell within GBMs are myeloid derived macrophages (resident microglia and infiltrating macrophages) and they can constitute a high proportion of cells within the tumour mass (Dunn et al. 2007). In conjunction with M2 macrophages, microglia have also been implicated in tumour progression. Microglia have been reported to secrete anti-inflammatory molecules such as interleukin (IL)-10 (Seo et al. 2004) and prostaglandin E2 (Watters et al. 2005) which acts to reduce the expression of class II major histocompatibility complex (MHC) on antigen presenting cells (APCs) (Hishii et al. 1995), limiting antigen presentation to T cells. In addition to engaging an MHC complex, T cells must bind to costimulatory molecules such as CD86, CD80 and CD40. Microglia within GBM reportedly lacked the expression of such molecules (Hussain et al. 2006). Without sufficient costimulation, T cells can become anergic (Schwartz 2003) and fail to respond appropriately to tumour antigens.

Other immune cells of both myeloid and lymphoid origin have been reported in GBMs and either play a direct role in immune evasion or have been evaded by the tumour. Myeloid-derived suppressor cells (MDSCs) are thought to accumulate in tumours due to the presence of cytokines and growth factors, such as granulocyte macrophage colony stimulating factor (GM-CSF), granulocyte colony-stimulating factor (G-CSF), IL-2, and VEGF (Ostrand-Rosenberg 2010). They exhibit several methods to inhibit T cell activity, such as the production of arginase that reduces the availability of L-arginine, which is critical for T cell function (Rodríguez & Ochoa 2008), and the secretion of nitric oxide and reactive oxygen species that also act to repress T cell activation (Nagaraj & Gabrilovich 2007). Different numbers of TILs have been observed in GBMs (Dunn et al. 2007) and numerous immune evasion strategies prevent tumour elimination by TILs. For example, expression of the Fas ligand (FasL) on tumour cells can induce T cell death by engaging with Fas receptor, a tumour necrosis factor (TNF) receptor superfamily member (Saas et al. 1997). Some tumour cells also lack the co stimulatory molecules required to effectively activate naïve T cells, such as CD80 and CD86 (Wintterle et al. 2003).

It is clear that both innate and adaptive immune cells play a role in tumour surveillance and many tactics are employed by the tumour to evade the onslaught of multiple cellular defence mechanisms. To develop successful cell based immunotherapies it is vital to improve our understanding of immune interactions within GBMs.

1.2.6 Immunotherapies for GBM

The last major advancement for the treatment of GBM patients occurred in 2005. Stupp and colleagues reported an increase in overall survival (OS) for patients who had undergone debulking surgery and were subsequently treated with radiotherapy and chemotherapy (specifically temozolomide) compared to radiotherapy alone (Stupp et al. 2005). Although this treatment trumps its predecessors and is now the current standard of care for patients in the UK, the reality is that a patient's life has been extended by just 2.5 months; a survival prognosis of only 14.6 months. With a better understanding of the immunosuppressive microenvironment of GBM and the frequent mutations that occur, scientists have begun to develop immunotherapies that could improve their prognosis. The immune system can be manipulated in many different ways and as such there are different categories of immunotherapy; active

immunotherapy, passive immunotherapy, immunomodulator therapy and virotherapy. Numerous trials have been conducted within each category. Some of the more prominent are discussed below.

1.2.6a Active immunotherapies

Active immunotherapies include cancer vaccines that aim to eliminate the tumour, primarily by activating cytotoxic T lymphocytes (CTLs). To prime the CTLs specifically against the tumour, tumour associated antigens (TAA) must be presented to them by APCs such as dendritic cells (DCs) (Bielamowicz et al. 2013). This can be achieved by loading the DCs outside of the body or by injecting the TAA into the body. Additional costs are associated with the former method. One TAA that has been the focus of many vaccine trials (reviewed in (Xu et al. 2014) is a mutant epidermal growth factor receptor (EGFR), EGFRvIII that has been shown to be overexpressed in 31% of GBM samples (Heimberger et al. 2005). The mutation involves a deletion in part of the extracellular domain of the growth factor receptor which causes it to become constitutively active (Prigent et al. 1996). Early clinical trials involved pulsing DCs with modified EGFRvIII peptides and delivering them to patients intradermally (Sampson et al. 2009). The vaccine was deemed safe and further trials revealed that the treatment successfully eliminated EGFRvIII positive cells (Sampson et al. 2008). A collective analysis of 3 phase II trials that used a synthetic EGFRvIII peptide, rindopepimut, resulted in a promising overall survival of 24 months from diagnosis (Zussman & Engh 2015). However in March 2016, the subsequent double-blind phase III trial (ACT IV) was discontinued as the results showed no benefits over the placebo (NCT01480479).

1.2.6b Passive immunotherapes

Passive therapies include adoptive cell therapies and monoclonal antibodies. During adoptive immunotherapy effector cells are introduced into the patient to induce anti-tumour activity. In a recent phase II trial, lymphokine-activated killer (LAK) cells were placed directly into the tumour cavity by the surgeon after debulking surgery. These cells were generated by isolating peripheral blood mononuclear cells (PBMCs) from the patient and activating them with interleukin-2 (IL-2) for 3 to 5 days. The median survival from original diagnosis was 20.5 months and the 1-year survival rate was 75% (Dillman et al. 1997). Other cell therapies currently being investigated involve the use of genetically modified T cells (Bielamowicz et al. 2013).

As mentioned previously, antibodies are already used in the clinic to treat cancer. The first, rituximab which targets CD20 on B cells, was licensed by the FDA in 1997 to treat B cell non-Hodgkin lymphoma (Teo et al. 2016). GBM tumours are highly vascularised and the sprouting of new vessels (angiogenesis) is a key process in tumour progression (Jain et al. 2007). Angiogenesis is promoted by VEGF which is released by the glioma cells (Ahmed et al. 2014). Following promising early clinical trials, a monoclonal antibody targeting VEGF-A (bevacizumab) was given FDA approval for the treatment recurrent glioma in 2009. A number of further studies investigating the use of bevacizumab for newly diagnosed patients revealed worrying side effects, such as hypertension, thromboembolic events, intestinal perforation, and neutropenia, with no survival advantage (Gilbert et al. 2014). More concerning are reports that bevacizumab promotes invasion and metastasis in both animal models (Pàez-Ribes et al. 2009) and patients (Tuettenberg et al. 2009). Bevacizumab is not approved for treating GBM in the UK.

Other antibody therapies currently in trials (for example NCT02017717 and NCT02617589) for GBM patients include the checkpoint inhibitors nivolumab and ipilimumab that target programmed cell death protein 1 (PD-1) and CTLA-4 respectively. T cell activation is determined by the integration of both stimulatory and inhibitory signals. PD-1 is a membrane protein that is able to provide an inhibitory signal when it interacts with its ligands PD-L1 and PD-L2 (Nguyen & Ohashi 2015)(Figure 1.5). CTLA-4 competes with the costimulatory receptor CD28 to bind the dual ligands CD80 and CD86; in doing so it helps to prevent T cell activation (McCoy & Le Gros 1999). Simultaneously blocking both of these inhibitory signals using antibodies has proved effective in the treatment of advanced melanoma in clinical trials (NCT01927419) and in June 2016 the treatment was approved by the National Institute for Health and Care Excellence (NICE).

Lymphocyte activation gene 3 (LAG-3) is also an immune checkpoint receptor that is upregulated on Tregs and anergic T cells. It binds a region of MHC class II with greater affinity than CD4 and downregulated T cell proliferation. LAG-3 antibodies are being developed for cancer immunotherapy (He et al. 2016).

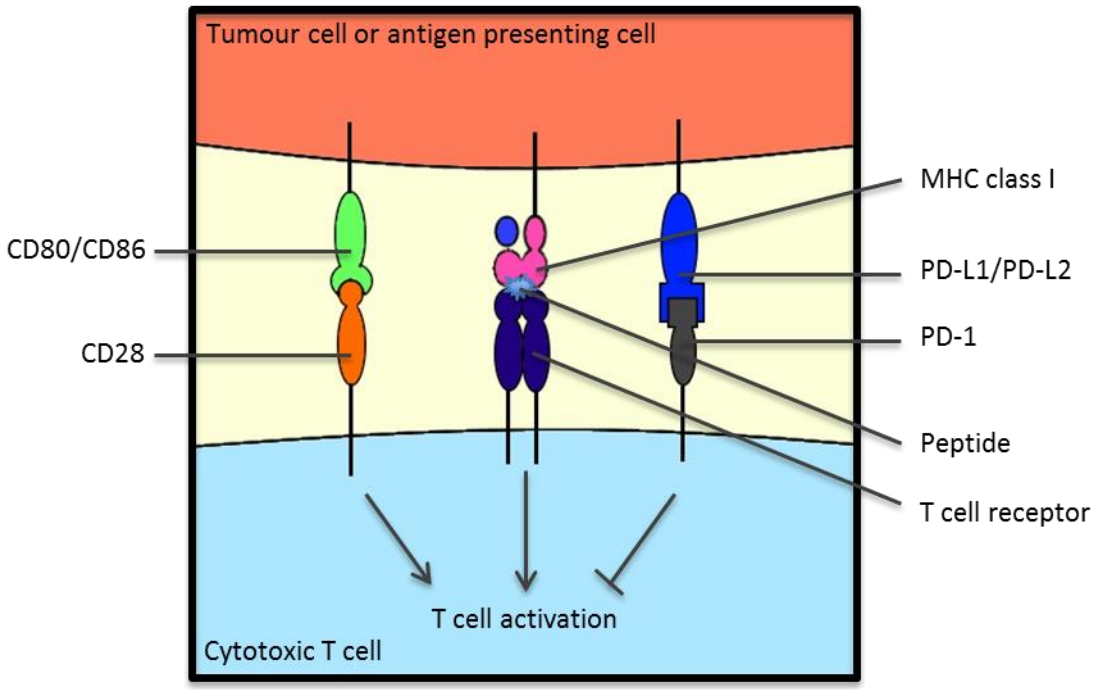

Figure 1.5. T cell regulation by PD-1. T cells are activated when their T cell receptors recognise a peptide presented on an MHC class I complex, in addition to CD28 binding a costimulatory protein such as CD80 or CD86. To prevent collateral damage to healthy tissue during chronic inflammation, suppression of T cells is required. PD-L1 and PD-L2 interact with PD-1 to down regulate T cells. Tumour cells have exploited this mechanism by displaying these inhibitory ligands. Diagram based on (McDermott & Atkins 2013).

1.2.6c Virotherapies

The use of viruses to treat patients, virotherapy, is also being explored. Although the concept of virotherapy is more than 100 years old (Kelly & Russell 2007), no virotherapy has yet been approved for the treatment of GBM patients. A number of viruses are currently in clinical trials such as poliovirus, adenovirus, herpes simplex virus and reovirus (Koks et al. 2015). Originally it was thought that viruses exerted their effect by selectively replicating in tumour cells and thereby causing specific tumour cell lysis. However, given that non-virulent virus strains are also able to elicit an anti-tumour response, it is now understood that the presence of the virus also acts as an adjuvant and helps to recruit and activate immune cells (Melcher et al. 2011). An ongoing phase I trial (NCT01491893) to treat recurrent GBM patients with a modified poliovirus has sparked excitement in America. The non-virulent virus is thought to gain entry into tumour cells via the CD155 surface protein. The group report a 23% 2 year survival rate compared to 13.7% in historical controls (Desjardins et al. 2016). A double blind study needs to be performed to establish if this treatment has a statistically significant survival advantage over the existing one. Paradoxically, the efficiency of the innate immune system has been implicated in hampering the efficacy of virotherapy in a murine model of GBM. NK cells, which have evolved to target viral infection, were shown to impede treatment with oncolytic Herpes simplex virus (oHSV) (Alvarez-Breckenridge et al. 2012) but this has since been prevented by the administration of transforming growth factor beta (TGF-β) prior to oHSV administration (Han et al. 2015).

Evidently, a vast amount of research is being done to develop immunotherapies in order to improve the outlook for patients. However, very little progress has actually been made to advance the survival statistics and, as of yet, the great potential of immunotherapies is still to be harnessed for the treatment of patients with GBM.

1.2.7 Cancer stem cells

Cancer stem cells (CSCs) are defined as having the ability to self-renew, differentiate into different lineages within the tumour and recapitulate the original disease phenotype in animal models (Singh et al. 2003). The CSC hypothesis states that CSCs exist at the top of the cellular hierarchy within a tumour and can differentiate to form

the diverse progeny of the tumour bulk. Once differentiated, the cells lose the capacity to self-renew (Pointer et al. 2014). Glioma stem cells (GSCs) are CD133+ (Singh et al. 2004) and are known to be resistant to current radio- and chemotherapies (Bao et al. 2006; Liu et al. 2006). Their resistance to treatment implicates these cells in relapse and future therapies should target these cells with the aim of reducing recurrence.

1.3 NK cells

1.3.1 Overview

Natural killer (NK) cells are large granular lymphocytes that exhibit both cytotoxicity and cytokine-producing effector functions (Vivier et al. 2008). They were discovered in 1975 by Rolf Kiessling whilst investigating cell mediated cytotoxicity against cancer cells. He identified a lymphocyte population isolated from mouse spleens that was able to 'naturally kill' mouse leukaemia cells *in vitro* without prior immunisation (Kiessling et al. 1975). It is now established that, in addition to transformed cells, NK cells are capable of recognising and killing virus infected cells and play a key role in regulating the adaptive immune system (Kruse et al. 2014). Accordingly, recurring virus infections and an increase in the incidence of some cancers are observed in patients with NK cell deficiencies (Orange 2013).

Leukocytes are often defined according to the presence or absence of surface molecules that have been designated a 'cluster of differentiation' (CD) number which provides information about the cell's function (Chan et al. 1988). NK cells originate from CD34+ hematopoietic progenitor cells (HPCs) (Freud & Caligiuri 2006) and constitute 2-18% of lymphocytes within human peripheral blood (Grégoire et al. 2007). NK cells are typically identified as lacking the T cell receptor complex (including CD3gamma and delta chains), but display neural cell adhesion molecule (CD56) or natural cytotoxicity triggering receptor 1 (NCR1, also known as NKp46 or CD335); CD3-CD56+ or CD3-NKp46+ (Morvan & Lanier 2016). Broadly speaking, NK cells can be categorised as $CD56^{bright}$ and $CD56^{dim}$ cells. The $CD56^{bright}$ subset primarily function to release cytokines, but exhibit little or no cytotoxic activity (Cooper et al. 2001), whereas the opposite is true for $CD56^{dim}$ cells (Walzer et al. 2007). $CD56^{dim}$ cells also express CD16, a low affinity Fc receptor, allowing them to participate in ADCC when they encounter cells coated in IgG antibody. Therefore NK cells are important effectors in antibody therapies (Seidel et al. 2013). A more recent nomenclature system has been proposed to categorise innate lymphoid cells (ILCs) based on their cytokine secretion profile and transcription factors. NK cells are a prototypical group 1 ILC as defined by their ability to produce IFNɣ (Spits et al. 2013) that plays an important role in shaping the immune response. IFNγ can induce upregulation of MHC class I

expression on APCs (Wallach et al. 1982), induce macrophage killing of intracellular pathogens (Filipe-Santos et al. 2006) and prevent the division of aberrant cells (Maher et al. 2007).

1.3.2 Mechanisms for killing

Natural killer cells can kill target cells either by releasing the cytotoxic contents within their granules or by engaging death receptors such as Fas or the TNF-related apoptosis-inducing ligand (TRAIL) receptor on the surface of target cells (Caligiuri 2008).

1.3.2a Granule exocytosis

Activation or inhibition signals are generated at the site of contact between the NK cell and target cell known as the immunological synapse (IS). These synapses can be activating, inhibitory or regulatory depending on the receptor-ligand complexes present (Krzewski & Strominger 2008). Activating ISs are highly organised and contain an outer region known as the peripheral supramolecular activation cluster (pSMAC) and a central region; central supramolecular activation cluster (cSMAC) (Figure 1.6). Adhesion molecules such as LFA-1 (CD11a/CD18) and Mac-1 (CD11b/CD18) are located in the pSMAC whilst the NK cell activating receptors (see section 1.3.3b) occupy the cSMAC. Engagement of the activating receptors causes an intracellular signalling cascade that results in polarisation of the microtubule organising centre (MTOC) and the recruitment of lytic granules to the IS where the granules are exocytosed (Krzewski & Coligan 2012). The granules contain the pore-forming protein, perforin, that allows the entry of the proteolytic granzymes into the cytoplasm of the target cell (Catalfamo & Henkart 2003). Granzymes are serine proteases and, to date, five have been identified in humans; A, B, H, K and M. Once within the target cell cytosol, granzymes proteolytically cleave their target proteins, leading to apoptosis through activation of caspases, induction of mitochondrial damage, and DNA fragmentation (Figure 1.6) (Krzewski & Coligan 2012).

1.3.2b Death receptor

Apoptosis of the target cell can also be induced by signalling through membrane-bound death receptors. The interaction of NK cell Fas ligand or TRAIL with their corresponding receptors on target cells, Fas (CD95) or TRAIL receptors, causes the

activation of the caspase cascade. Ligand binding results in receptor oligomerization, recruitment of adaptor proteins such as Fas-associated death domain (FADD) and cleavage of procaspase 8 to the active form. The resulting cell death is similar to granzyme induced apoptosis (Figure 1.6) (Warren & Smyth 1999).

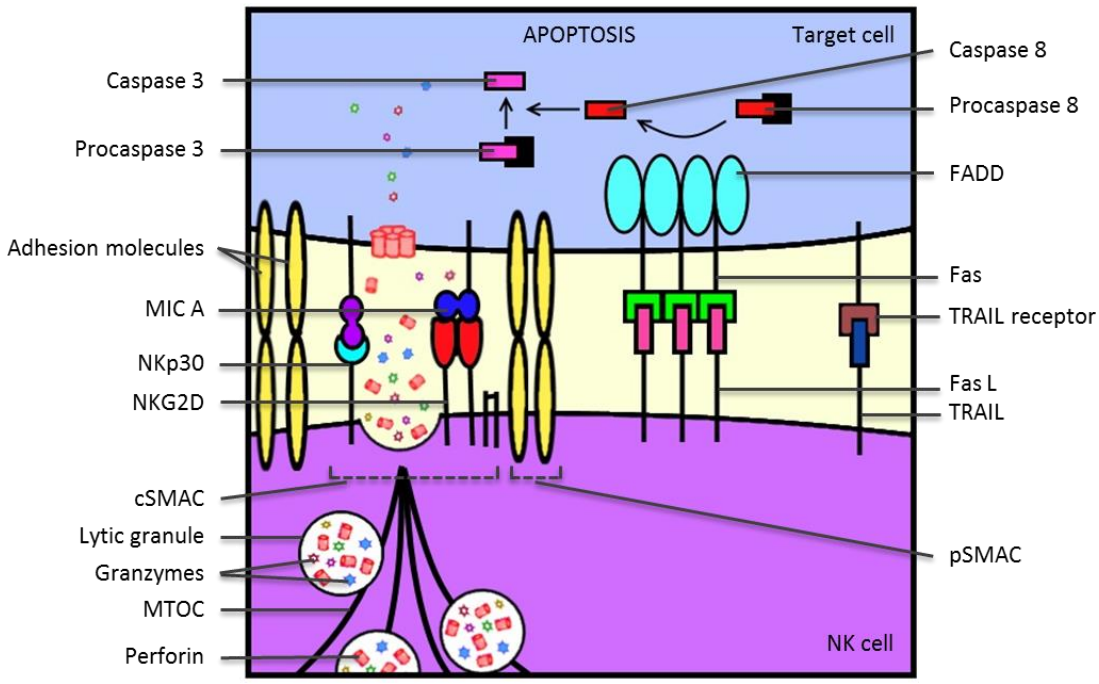

Figure 1.6. Mechanisms of NK cell target killing. The left hand side depicts the exocytosis of NK cell cytotoxic granules leading to the apoptosis of the target cell. An activating immunological synapse (IS) causes the polarisation of the microtubule organising centre (MTOC) and the recruitment and release of lytic granules. Perforin allows the entry of granzymes into the cytosol of the target cell where they exert their proteolytic action. The right hand side details induction of the target cell apoptosis by the engagement of death receptors. Adapted from (Krzewski & Coligan 2012; Warren & Smyth 1999).

1.3.3 Regulation of NK cells

With the ability to kill cells and induce an immune response, the activity of NK cells must be tightly regulated and this is achieved by the integration of signals from both activating and inhibitory receptors, including those for cytokines and chemokines.

1.3.3a Cytokines/chemokines

There are many different cytokines that act to regulate NK cells. For example, interleukin 2 (IL-2), interleukin 15 (IL-15), type I IFN, interleukin 12 (IL-12) and interleukin (IL-18) are potent activators of NK cell effector function (Walzer et al. 2005; Trinchieri 1989) whereas molecules such as prostaglandin E2 (PGE2), indoleamine 2,3-dioxygenase (IDO), adenosine and TGF-β are known to inhibit NK cells (Morvan & Lanier 2016).

Two of the best characterised activating cytokines are IL-2 and IL-15 and they bind to membrane bound receptors, the IL-2 receptor (IL-2R) and IL-15 receptor (IL-15R) respectively. The receptors are heterotrimeric, of which 2 subunits are common to both receptors; the common cytokine-receptor γ-chain (γ_c or CD132) and the IL-2 receptor β chain (CD122) (Waldmann 2006). The third subunits are the IL-2Rα and IL-15Rα chains. These can either be membrane bound or presented together with the cytokine (Mishra et al. 2014). When IL-15Rα and IL-15 are displayed together by one cell to interact with the IL-15Rβ and γ subunits on another, it is called trans-presentation. Trans-presenting cells include neutrophils, monocytes and dendritic cells (Stonier & Schluns 2010). Intracellular signalling of IL-15 leads to NK cell activation and uses Janus-associated kinases (JAK) and signal transducer and activator of transcription (STAT)(Johnston et al. 1995). The binding of IL-15 causes activation on JAK1 and subsequent phosphorylation of STAT3 that is mediated by the β chain (CD122). Likewise, the γ chain coordinates JAK3/STAT5 activation (Lin et al. 1995; Miyazaki et al. 1994). Once phosphorylated, STAT5 and STAT3 form a complex that translocates to the nucleus and activates transcription of the anti-apoptotic protein bcl-2 and proto-oncogenes c-myc, c-fos and c-jun (Mishra et al. 2014). IL-15 activation has also been reported to signal through the PI3K/AKT and Ras/MAPK pathways (Mishra et al. 2014).

The established immunosuppressive cytokine TGF-β is produced by tumour cells and is thought to promote cancer metastasis through its actions in the tumour microenvironment, including enhancement of tumour cell invasion and by inhibiting the function of immune cells (Flavell et al. 2010; Massagué 2008). TGF-β prevents NK cell effector functions by preventing IFNγ production and cytotoxic activity (Laouar et al. 2005; Rook et al. 1986). TGF-β signals through its tetrameric membrane receptor complex made up of two TGF-βRI chains and two TGF-βRII chains. When bound by TGF-β, the type I chains trans-phosphorylates the type II chains which enables the phosphorylation of transcription factors Smad2 and Smad3 (Smad2/3). The SMAD2/3 complex is then able to translocate to the nucleus where it interacts with Smad4 and other proteins to regulate transcription (Derynck & Zhang 2003).

1.3.3b Activating and inhibiting receptors

Following the discovery of NK cells in 1975, the next logical step was to discover how cytotoxicity was regulated. In 1981 Klas Kärre, PhD student of Rolf Kiessling, published his thesis which contained the first version of the, then somewhat controversial, 'missing-self' recognition concept, whereby the absence or incomplete expression of host MHC class I molecules in a normal cell would be sufficient to render it susceptible to NK cells. The theory was postulated following the observed 'hybrid resistance' in animal transplant models; an (A x B) F1 recipient rejects A or B grafts of parental origin (A and B referring to MHC genotypes). The absence of some MHC class I genes in a parental to F1 graft led to rejection by NK cells (Kärre 2002). Further evidence supported the 'missing-self' theory; cells lacking MHC class I were susceptible to NK cell death (Stern et al. 1980) and interferon upregulated MHC class I expression reduced susceptibility to NK cell lysis (Trinchieri & Santoli 1978). NK cells complement T cell immune surveillance as the downregulation of MHC class I proteins, a strategy commonly employed by tumour and virally infected cells as a way of avoiding T cell recognition (Alcami & Koszinowski 2000; Algarra et al. 2004), will render cells susceptible to NK cell lysis.

Although the 'missing self' theory was first coined in the early 1980s, it would be another 10 years before the inhibitory receptors that interact with MHC molecules were discovered. It is now known that there are both activating and inhibitory

receptors and NK cell activity depends on the integration of signals from both types of receptor (Long et al. 2013). There are many different NK cell receptors but two of the main groups, based on their structure, are the killer cell immunoglobulin receptors (KIRs) and the killer lectin like receptors (KLRs) (Lanier 2008). Perhaps confusingly, the groups contain activating and inhibitory receptors; the key difference occurs in the intracellular and membrane regions of the receptors that allow the recruitment of specific proteins and subsequent differential downstream effects. This section aims to give an overview of activating and inhibitory receptors, highlighting the importance of integrating signals with a key focus on receptors investigated as part of this PhD.

The killer cell immunoglobulin-like receptor (KIR) genes are encoded on chromosome 19 in a region known as the leukocyte receptor complex (LRC) (Barrow & Trowsdale 2008). KIRs are monomeric type I glycoproteins (Lanier 2008) and consist of an extracellular region containing either two or three immunoglobulin domains (KIR2D or KIR3D), with either a long or short cytoplasmic tail. Long-tailed KIRs contain either one or two immunoreceptor tyrosine-based inhibitory motifs (ITIMs) and are inhibitory (Figure 1.7). Conversely, short-tailed receptors have a positively charged lysine residue within the membrane region of the protein that mediates coupling to DAP12, a protein containing an immunoreceptor tyrosine-based activation motif (ITAM). Inhibitory KIRs are better characterised than activation KIRs and, whilst many inhibitory KIRs have well-defined MHC class I ligands, activating KIRs show only weak binding (Rajagopalan & Long 2005). When inhibitory KIRs bind their ligands, the tyrosine residue within the ITIM is phosphorylated which leads to the recruitment of phosphatases that compete with kinases linked to activating receptors to prevent the phosphorylation of proteins within the activation cascade. For example, SHIP-1 dephosphorylates phosphatidylinositol-3,4,5-trisphosphate (PIP_3) to phosphatidylinositol-3,4-bisphosphate (PIP_2), whereas SHP-1 and SHP-2 dephosphorylate the guanine nucleotide exchange factor Vav1 (Figure 1.8). The inhibitory KLRs, such as CD94-NKG2A, also signal using ITIMs (Figure 1.7) (Lanier 2008).

In a similar fashion, the ITAM is used by many of the activation receptors including activating KIRs, the natural cytotoxicity receptors (NCRs; NKp30, NKp44 and NKp46)), CD16 and activating KLRs (Figure 1.7). In general, the receptor has a positively charged residue within the membrane domain through which it interacts with a negatively

charged residue within the membrane domain of a membrane anchored accessory protein that contains one or more ITAMs in the cytoplasmic domain. The exception is CD16 that has a negatively charged residue, aspartic acid (D) in the membrane region. The ITAM containing proteins include DAP12, FcεRI-γ and CD3-ζ (Lanier 2008; Long et al. 2013). An overview of the receptors, including their ITAM associated proteins and ligands are summarised in figure 1.7. Many of the receptors, including KIRs, NCRs and CD16, contain immunoglobulin domains in the extracellular region of the protein so belong to the immunoglobulin superfamily (Kruse et al. 2014; Mandelboim et al. 1999). CD16 is a strong activating receptor and recognises the constant region (Fc) of IgG antibodies (Long et al. 2013). CD16 mediates ADCC by NK cells in antibody therapies (Seidel et al. 2013). The NCRs were discovered in the late 1990s (Sivori et al. 1997) and, despite having different amino acid sequences and structures (Joyce & Sun 2011), they have been grouped together based on their functions. NKp46 (CD335) is present on NK cells, regardless of activation status (Sivori et al. 1997) and has been used in this study to facilitate NK cell identification. Many ligands have been suggested for the NCRs (Kruse et al. 2014; Morvan & Lanier 2016) but the only one that has been confirmed with a receptor-ligand co-crystal structure is NKp30 with B7-H6. B7-H6 is a surface transmembrane protein and is not detected in healthy tissue but is detected on many tumour cell lines (Brandt et al. 2009). When the receptors bind their ligands, the tyrosine residues within the ITAMs of associated proteins are phosphorylated, probably by Src family kinases (Lanier 2008). This allows the recruitment of kinases Syk and ZAP-70 via their Src homology 2 (SH2) domains and activation of downstream pathways including PI3K and phospholipase Cγ (Figure 1.8)(Long et al. 2013).

NKG2D (CD314) is an activation receptor of the KLR family and the human form exists as a hexamer composed of an NKG2D homodimer and two DAP10 homodimers. NKG2D recognises stress induced proteins MHC class I polypeptide-related sequence A/B (MIC A/B) and the UL16 binding proteins (ULBPs) that are present on cancer cells (Raulet 2003). As with DAP12, DAP10 contains a signalling motif that results in the activation of signalling cascades. However, it is not an ITAM but a tyrosine-isoleucine-asparagine-methionine (YINM) motif which when phosphorylated is able to recruit PI3K through the P85 subunit or Grb2 (Lanier 2008).

DNAM-1 (DNAX accessory molecule-1, CD226) is an immunoglobulin activation receptor found on both NK and CD8 T cells (Shibuya et al. 1996). It recognises related proteins Nectin-2 (CD112) and the poliovirus receptor (CD155) (Bottino et al. 2003), both of which are upregulated on tumour cells. The cytoplasmic domain of DNAM-1 contains signalling motifs that enable the recruitment of tyrosine kinases Fyn and serine-threonine kinase PKC (Shibuya et al. 1998). DNAM-1 works in conjunction with LFA-1, which is important for the tyrosine phosphorylation by Fyn and subsequent downstream activation (Shibuya et al. 1999).

2B4 is an immunoglobulin-like co-receptor of the signalling lymphocytic activating molecule (SLAM) receptor family that recognises CD48 (Veillette 2010). Although its positive cytolytic functions were originally identified (Garni-Wagner et al. 1993), subsequent studies have reported inhibitory functions (Schatzle et al. 1999; Dong et al. 2009). Although some discrepancy exists as to the circumstances of activation or inhibition, Veillette proposes that associated proteins that interact with the immunoreceptor tyrosine-based switch motif (ITSM) within the cytoplasmic domain of 2B4 are a key determinant of effector functions; SLAM associated protein (SAP) and Fyn confer activation, whereas EAT2 inhibits activation (Veillette 2010; Veillette et al. 2007).

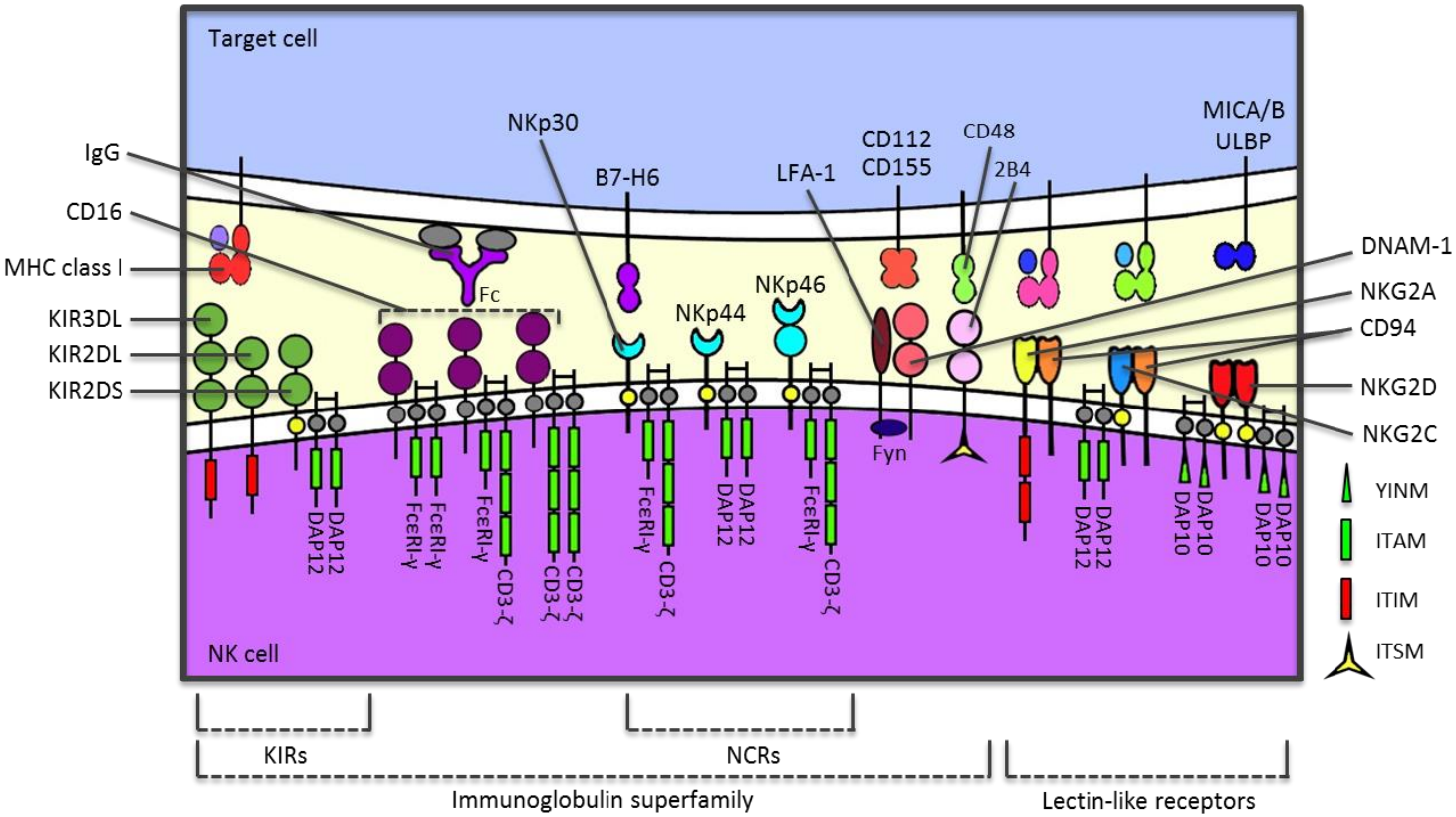

Figure 1.7. NK cell receptors and ligands. The activity of NK cells is regulated by the integration of signals from a repertoire of activation and inhibitory receptors. NK cell receptors that are part of the immunoglobulin (Ig) superfamily include killer cell immunoglobulin receptors (KIRs), CD16, natural cytotoxicity receptors (NCRs; NKp30, NKp44 and NKp46), DNAM-1 and 2B4. Both the Ig superfamily and killer lectin-like receptors contain activation and inhibitory receptors. Inhibitory receptors signal through immunoreceptor tyrosine-based inhibitory motifs (ITIMs) (red), whereas activation receptors interact with accessory proteins such as DAP12, FcεRI-γ and CD3-ζ which contain immunoreceptor tyrosine-based activation

motifs (ITAMs) (green rectangle) or DAP10 which contains a YINM (green triangle). Based on information in (Lanier 2008; Kruse et al. 2014; Long et al. 2013).

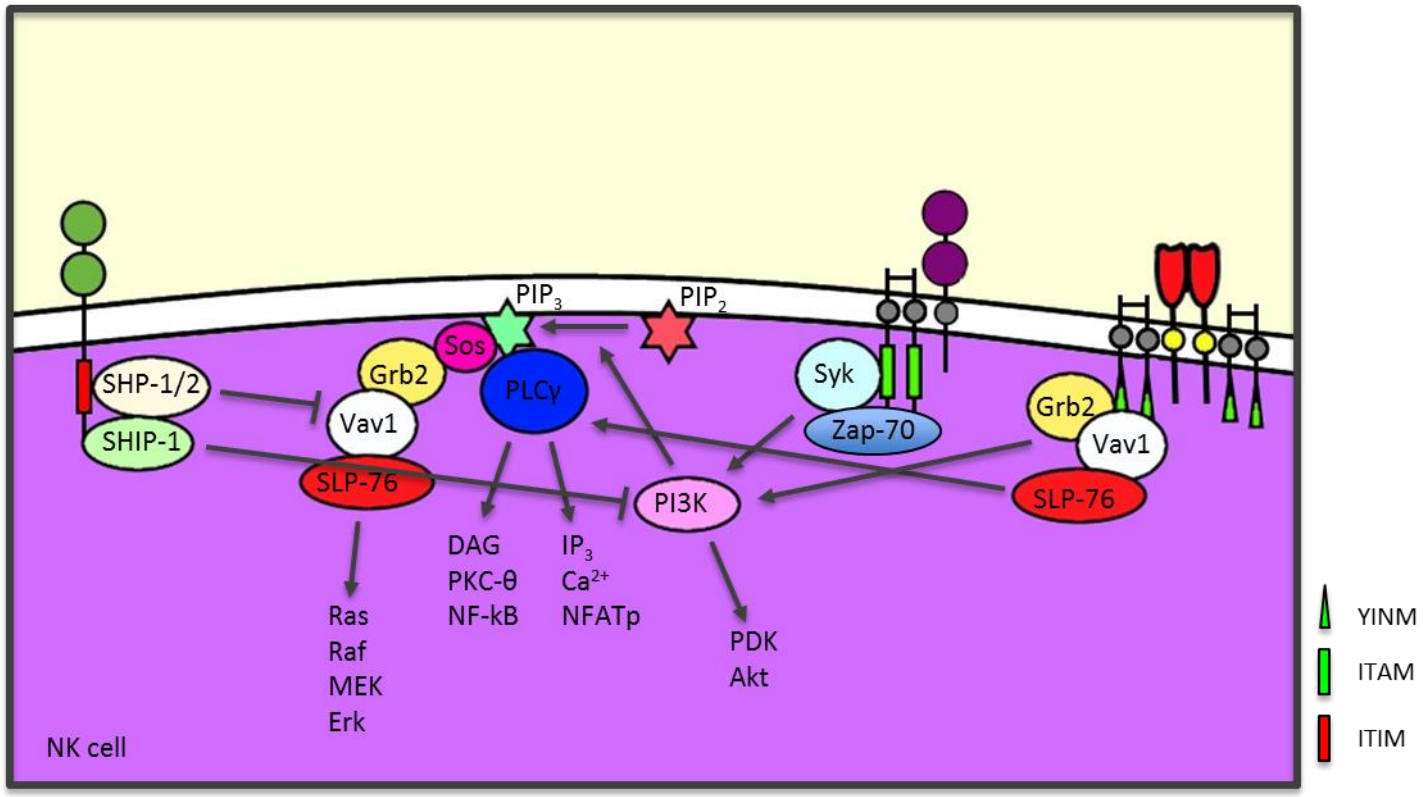

Figure 1.8. The integration of signalling downstream of activation and inhibitory receptors. Inhibitory receptors have ITIMs within the cytoplasmic part of the protein. When the receptor is bound by its ligand, the tyrosine residue within the ITIM becomes phosphorylated which leads to the recruitment of phosphatases such as SHIP-1, SHP-1 or SHP-2 that lead to the dephosphorylation of PIP_3 and Vav1 respectively. This opposes the downstream signalling of activation receptors that are coupled to proteins containing activation motifs such as DAP12 and DAP10 that harbour an ITAM and YINM respectively. Binding of the activation receptors leads to the activation of signalling cascades including PI3K, PLCγ and Ras/Raf/MEK pathways. Based on information in (Lanier 2008; Kruse et al. 2014; Long et al. 2013).

1.3.4 Detection within brain tumours

When reviewing the literature of brain infiltrating NK cells it is important to consider how the NK cells were defined and the method used to detect them. In 1988, a study of immune cell infiltrates was performed on both primary and secondary brain tumours which included grade IV gliomas (Stevens et al. 1988). Immunohistochemistry was utilised and NK cells were identified as Leu7 (CD57) positive cells. No NK cells were detected within grade I and II gliomas and low levels of NK cells were detected within grade IV gliomas and those that were present were within perivascular cuffs. The study presents two issues; firstly, if the cells only constitute a small proportion of the total number there is a distinct possibility that they will not be detected and secondly, not only is CD57 only expressed on a subset of NK cells, it is also present on a large proportion of T cells (Lopez-Vergès et al. 2010). Other markers used are not without their problems either; Leu11b (CD16) was used to study NK cell infiltration within oligodendrogliomas (Rossi et al. 1991) but it is not expressed on all NK cells. Although each study comes with its own restrictions, these consistently find that NK cells make up only a very small proportion of infiltrating cells if they are detected at all (Kmiecik et al. 2014).

1.4 Rationale for using cell based immunotherapies

The current standard treatment for GBM involves surgical resection, radiotherapy and the administration of the chemotherapeutic drug temozolomide (Stupp et al. 2005). However, the prognosis of GBM patients remains poor. Although surgical resection removes the visible tumour mass, it does not eliminate the diffuse, migratory cells that are characteristic of GBM and inevitably the tumour recurs. Temozolomide is an alklyating agent that adds methyl groups to the oxygen at position 6 of guanine. This causes DNA fragmentation that prevents DNA replication, leading to tumour suppression and apoptotic cell death (Zhang et al. 2012). Treatment with temozolomide eventually yields populations that have acquired resistance by upregulating the DNA repair enzyme O^6-methylguanine-DNA methyltransferase (MGMT) (Bandres et al. 2005). Alongside acquired resistance, the use of chemotherapies can also be restricted by the BBB as it disrupts the efficient delivery of systemically administered drugs (Doolittle et al. 2005). These challenges reiterate the need for novel strategies to improve the outcome of patients with GBM. Cell based immunotherapies are an exciting prospect as immune cells identify cancer cells based on molecular surface properties so could potentially identify cells that have spread from the tumour bulk. Importantly, activated immune cells can cross the BBB (Sehgal & Berger 2000).

NK cells are of particular interest when considering immunotherapies because they can kill transformed cells without prior sensitisation (Herberman et al. 1975), help prime the adaptive immune response by the release of regulatory cytokines such as GM-CSF and IFNγ (O'Connor et al. 2006) and are important responders in cancer antibody therapies (Caligiuri 2008). However, in order for this to be achieved for patients with GBM, the NK cells must be capable of homing to the tumour and, once there, they must have functional cytotoxic activities.

1.5 Glucocorticoids

When considering the use of cell based immunotherapies for the treatment of GBM, and indeed other cancers, it is important to consider the effects of other clinical treatments on immune cells. GBM patients often experience cerebral oedema that is treated with synthetic glucocorticoids (GCs), such as dexamethasone (Kostaras et al. 2014).

Naturally occurring GCs are steroidal hormones that are synthesised in the adrenal cortex. The name glucocorticoid (glucose + cortex + steroid) reflects their role in regulation of glucose metabolism, site of synthesis and steroidal structure (De Bosscher 2010). GCs are also potent anti-inflammatory molecules. In fact, it was this property that led to the initial identification of adrenal cortex hormones by Edward Kendall, Philip Hench and Tadeus Reichstein for which they were awarded the Nobel Prize for Physiology and Medicine in 1950 (Hench 1950). The initial success observed with the administration of cortisone for the treatment of rheumatoid arthritis (Hench & Kendall 1949) lead to the development of related synthetic compounds such as dexamethasone and methylprednisolone that retained the anti-inflammatory properties, but reduced the associated side effects (Herzog et al. 1955; Bunim et al. 1958). GCs are still widely used in current clinical practice to treat an array of inflammatory, immune and allergic disorders (such as arthritis and asthma), blood cancers, and are administered following transplant surgery to prevent rejection (Sundahl et al. 2015). The clinical use of GCs predates knowledge of the mechanism of action. For example, it was not until 1985 that the glucocorticoid receptor (GR) was shown to bind DNA and regulate transcription initiation (Yamamoto 1985). There is now evidence that GCs exert their effects in different ways, examples of which are discussed below.

It is generally accepted that GCs are fat soluble and diffuse across the cell membrane to the cytosol where they are able to bind the GR (De Bosscher et al. 2003). GRs are made up of different functional domains including an N-terminal transactivation domain (NTD), a conserved DNA-binding domain (DBD) and a C-terminal ligand-binding domain (LBD) (Ratman et al. 2013). In the absence of ligand, the GR resides in the cytoplasm within a complex of chaperone proteins containing heat shock proteins

(HSP) and immunophilins (Echeverria & Picard 2010). The interaction of the GR with HSP70/HSP90 is important to ensure the steroid-binding cleft is available to ligands (Pratt et al. 2004). Once the ligand is bound, the activated receptor is able to translocate to the nucleus where it can bind to both positive and negative GR response elements (GREs) (Franchimont 2004). Positive GREs are palindromic sequences within the promoter regions of genes that are bound by a homodimeric activated GR to promote gene expression (De Bosscher et al. 2008). Transcription can also be negatively regulated, a process known as transrepression, and this can involve DNA binding of the GC receptor/ligand complex or by blocking the binding of other transcription factors by direct protein-protein interaction, a process referred to as squelching (Ratman et al. 2013). Originally it was believed that the anti-inflammatory actions of GCs were due to transrepression of key transcriptional regulators of pro-inflammatory genes such as NF-κB and AP-1 but it is now known that some anti-inflammatory effects also occur through transcriptional activation (Clark 2007). These include the transcription of the NF-κB inhibitor (IκBα), IL-10, IL-4, TGF-β and mitogen-activated protein kinase (MAPK) phosphatase 1 (De Bosscher et al. 2003; Auphan et al. 1995; Scheinman et al. 1995; Abraham et al. 2006).

More recently it has been discovered that GCs also exhibit non-genomic effects. Although the rapid action of GCs, within minutes, indicates that there are non-genomic effects, the research is very much in its infancy compared to the genomic actions. For example, a study using two commonly administered GCs, beclomethasone dipropionate (BDP) and prednisolone acetate (PDNA), showed that GCs increased the maximum isometric force produced by mouse slow-twitch muscle fibre bundles (Pérez et al. 2013). Experiments using an inhibitor of the GR or an antibody that binds to the GR prevented the observed increase in force. From this, the authors concluded that the GR is located within the membrane and somehow leads to the activation of focal adhesion kinase (FAK), Grb2 and ERK. However, it could be the case that the antibody also binds GCs which would result in a reduced concentration, mimicking the effect of blocking the interaction. More research is required to confirm the membrane bound protein.

Non-genomic actions have also been reported in T cell signalling. When the T-cell receptor (TCR) is activated, Src kinases such as Lck and Fyn are activated and play a

critical role in TCR-mediated signal transduction (Zamoyska et al. 2003). Dexamethasone has been shown to prevent early events in T cell activation such as the formation of the T-cell-receptor-associated protein complex that contains Lck and Fyn (Löwenberg et al. 2006), preventing phosphorylation of Lck and Fyn targets (Löwenberg et al. 2005), thus inhibiting signalling through the TCR.

These examples further highlight the complexity of the behaviour of GCs, in that they have tissue specific actions. Although the GR is expressed in most tissues (Ballard et al. 1974), regulation is dependent on other factors such as the bioavailability of GCs, the topology of the DNA and tissue specific expression of certain histone modifying proteins that mediate access to the receptor/ligand complex (De Bosscher et al. 2003).

Most commonly used for its anti-inflammatory properties, dexamethasone is likely to reduce the effectiveness of immunotherapies for patients with GBM. Indeed, dexamethasone was shown to inhibit the immune-stimulatory activities of lenalidomide on NK and T cells against multiple myeloma (MM) (Gandhi et al. 2010). However, when used in a mouse model of melanoma, dexamethasone was found to cause lymphopenia but did not inhibit the anti-tumour activity of activated CD8+ T cells (Hinrichs et al. 2005).

More research into the actions of GCs on NK cells will help to integrate immunotherapies with the current use of glucocorticoids that are essential for treating brain tumour induced cerebral oedema.

1.6 Aims

The prognosis for patients with glioblastoma multiforme remains poor and alternative therapies are clearly required. Cell based immunotherapy could prove an exciting avenue for new treatment options. The properties of NK cells, eliminating transformed cells without prior sensitisation, make them ideal candidates for therapeutic manipulation. However, the existence of GBM as a clinical entity indicates that they have already undergone the immunoediting process and are resistant to NK cell lysis. A limited number of studies exist that assess the amount of NK cell infiltration into human GBM tumours and no studies exist that extensively characterise the infiltrating NK cells.

The aim of this study was to analyse the NK cells located within human GBM tumours and to establish their phenotype. Defining the phenotype is crucial to help elucidate mechanisms deployed by the tumour to inhibit NK cell function, which could be targeted for treatment. Glucocorticoids are frequently administered to GBM patients to reduce brain oedema; a second aim of this work was to investigate the effects that glucocorticoids have on NK cell function. This will help predict the impact that glucocorticoids have on any future NK cell based immunotherapies.

Chapter 2 Materials and Methods

2.1 Cell culture

2.1.1 Adherent cells

GBM1, GBM4, GBM11, GBM13 and GBM20 are tumour stem-like cells derived from patients with GBM. The primary lines, GBM1 and GBM4, were generated at the Scripps Institute by Dr Heiko Wurdak in the laboratory of Professor Peter G. Schultz (Wurdak et al. 2010). GBM11, GBM13 and GBM20 were derived by Dr Anjana Patel and Dr Heiko Wurdak at the University of Leeds using the same method. The cells were a kind gift from Dr Anjana Patel and Dr Heiko Wurdak. Cells were grown on laminin (Sigma-Aldrich, UK)-coated flasks (Corning, MA USA) in Neurobasal Medium (Gibco, Invitrogen, UK) supplemented with 0.5 % B27 Serum-Free Supplement (Gibco), 0.5 % N2 Supplement (Gibco), 40 ng/mL recombinant human EGF (R&D Systems), 40 ng/mL recombinant human bFGF (PeproTech, New Jersey, USA). Cells were incubated at 37°C in a humidified atmosphere containing 5% CO_2. No antibiotics were used.

The neural progenitor cells (NP1) were isolated by the Wurdak group from a patient who had a section of brain removed to treat epilepsy. Cells were grown on laminin-coated surfaces in Dulbecco's Modified Eagle Medium: Nutrient Mixture F-12 (DMEM-F12) (Gibco) supplemented with 0.5 % B27 Serum-Free Supplement, 0.5 % N2 Supplement, 20 ng/mL recombinant human EGF, 20 ng/mL recombinant human bFGF, 1 % glutamine (Gibco) and 5% foetal bovine serum (FBS) (Gibco). Cells were incubated at 37°C in a humidified atmosphere containing 5% CO_2. No antibiotics were used.

Adherent cells were harvested using 0.25% trypsin (Sigma-Aldrich)/EDTA (Sigma-Aldrich) (0.25 % w/v trypsin and 0.2 % w/v ethylenediaminetetraacetic acid (EDTA) in PBS (Sigma-Aldrich)). Culture medium was discarded, cells were washed with PBS (phosphate buffered saline; 137 mM NaCl, 2.7 mM KCl, 1.8 mM KH_2PO_4, 10 mM Na_2HPO_4 pH 7.4), and incubated with 1 mL of trypsin/EDTA solution at 37°C until they detached. Growth medium was added to dilute the trypsin and the cells were pelleted by centrifugation at 350 g for 5 minutes at room temperature (RT).

2.1.2 Suspension cells

K562 is a well-known tumour target cell used to examine NK cell effector function. It originates from a 53-year-old female chronic myeloid leukaemia (CML) patient in blast crisis. Cells were cultured in RPMI (Sigma-Aldrich, UK) supplemented with 10% FBS. Cells were maintained at approximately 1 x 10^6 cells/mL and incubated at 37°C in a humidified atmosphere containing 5% CO_2. No antibiotics were used.

2.2 Primary NK cells

2.2.1 Peripheral blood mononuclear cell isolation

Peripheral blood mononuclear cells (PBMCs) were either obtained from an apheresis cone or from the blood of a healthy donor. Blood from the apheresis cone was diluted four-fold with PBS, whereas blood from a donor was diluted two-fold. Approximately 30 mL of diluted blood was carefully layered onto 15 mL Ficoll (Axis-Shield PoC, Oslo, Norway) in a 50 mL falcon tube (Corning). PBMCs were separated by density gradient separation at 800 g for 20 minutes and disabling the brake function. The PBMC fraction lies at the interface between the Ficoll and plasma layers (Figure 2.1). The PBMCs were removed using a Pasteur pipette (Thermo Fisher Scientific, USA), washed in a five-fold volume of PBS and collected by centrifugation at 220 g for 15 minutes. PBMCs were resuspended in cold MACS buffer (0.5% w/v bovine serum albumin (BSA) and 2mM sodium EDTA in PBS) and counted using a haemocytometer.

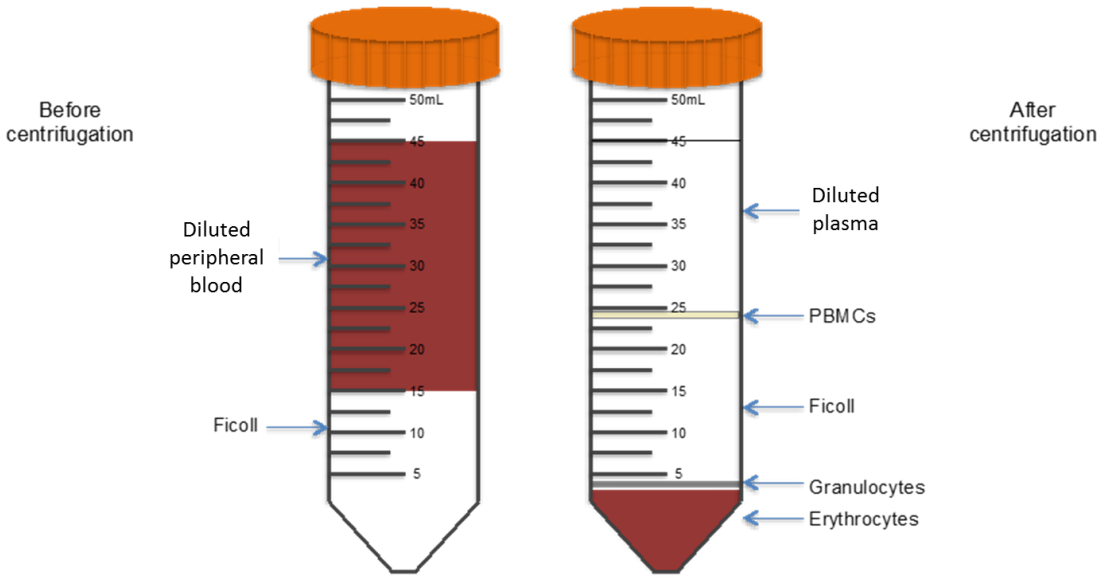

Figure 2.1. Peripheral blood mononuclear cell isolation by density gradient centrifugation. Diluted peripheral blood was layered onto Ficoll and centrifuged at 800 g for 20 minutes without the brake. The PBMC layer can be seen post centrifugation between the Ficoll and plasma layers.

2.2.2 NK cell isolation

Untouched NK cells were isolated from PBMCs using an NK cell isolation kit (Miltenyi Biotec, Bergisch Gladbach, Germany) in line with the manufacturer's protocol. A cocktail of biotin-conjugated monoclonal antibodies against non-NK cell antigens is used to negatively select the NK cell population. Magnetically labelled anti-biotin antibodies were added. The cells were passed through a MACS cell separation column within a magnetic field and the non-NK cells were retained on the column. The eluted NK cell fraction was washed with PBS and pelleted at 300 g for 10 minutes. NK cells were cultured in DMEM supplemented with 10% FBS and 10% heat inactivated human AB serum at approximately 1 x 10^6 cells/mL.

2.2.3 NK cell cytokine and drug treatments

Freshly isolated NK cells were activated with 100 $IUmL^{-1}$ of IL-15 (Miltenyi Biotec).

NK cells were seeded at approximately 1 x 10^6 cells/mL in a 24-well plate. Drug concentrations of 2 x 10^{-7} M dexamethasone (Sigma-Aldrich), 2 x 10^{-6} M methylprednisolone (Sigma-Aldrich), 1 x 10^{-4} M c-Myc inhibitor 10074-G5 (Sigma-Aldrich) or 5 ng/mL TGF-β (Miltenyi Biotec) were added to the cells and mixed

thoroughly. For dual treatments, the glucocorticoids, TGF-β or c-Myc inhibitor was added immediately before the IL-15.

2.3 Matched GBM tumour and blood sample

2.3.1 Ethical approval

Ethical approval to collect blood and tumour samples after informed consent was obtained from the ethics committee at the Leeds Teaching Hospitals NHS Trust (REC number 10-H1306-7).

2.3.2 Tumour Processing

After ethical approval and patient consent had been given, the tumour samples were taken from astrocytoma patients as part of resection surgery. Samples either arrived as a solid lump of tissue (varied in size but were approximately 2 cm^3) in a specimen tube containing PBS or within the sterile suction trap of a cavitron ultrasonic surgical aspirator (CUSA). A study assessing the use of CUSA trap samples as a source of material for histopathological study and tissue culture concluded that the CUSA trap provides viable cells that are a representative sample of tumour histology, as well as an adequate and sterile biosource of material for tissue culture studies (Schroeteler et al. 2014). Upon arrival, the solid sample was placed in a petri dish and washed in PBS. The sample was pushed through a 40 µm cell sieve (Thermo Fisher Scientific) using the plunger part of a 10 mL syringe and collected in a 50 mL falcon tube (Figure 2.2). The filter was washed using PBS until a final volume of 50 mL had been collected. The cells were collected by centrifugation at 400 g for 5 minutes. The supernatant was removed and the remaining pellet was washed twice by resuspending in 50 mL of PBS. After the second wash, the cell pellet was resuspended in fluorescence-activated cell sorting (FACS) buffer (PBS with 0.5% BSA (Sigma-Aldrich) and 0.05% sodium azide (Sigma-Aldrich) and stained with appropriate antibodies (see antibody staining section). Approximately 1 x 10^7 cells/tube were stained. Data was acquired using the BD LSRII machine fitted with 4 lasers. Approximately 2 x 10^6 events were collected.

2.3.3 Blood Processing

Between 4 and 12mL of blood sample were collected from the same patient. The blood sample was diluted with PBS to a final volume of 35 mL. PBMCs were extracted

using Ficoll as detailed above. As with the cells from the tumour sample, PBMCs were resuspended in FACS buffer, stained with antibodies (section 2.4) and analysed on the BD LSRII machine. Approximately 3 x 10^4 events were collected.

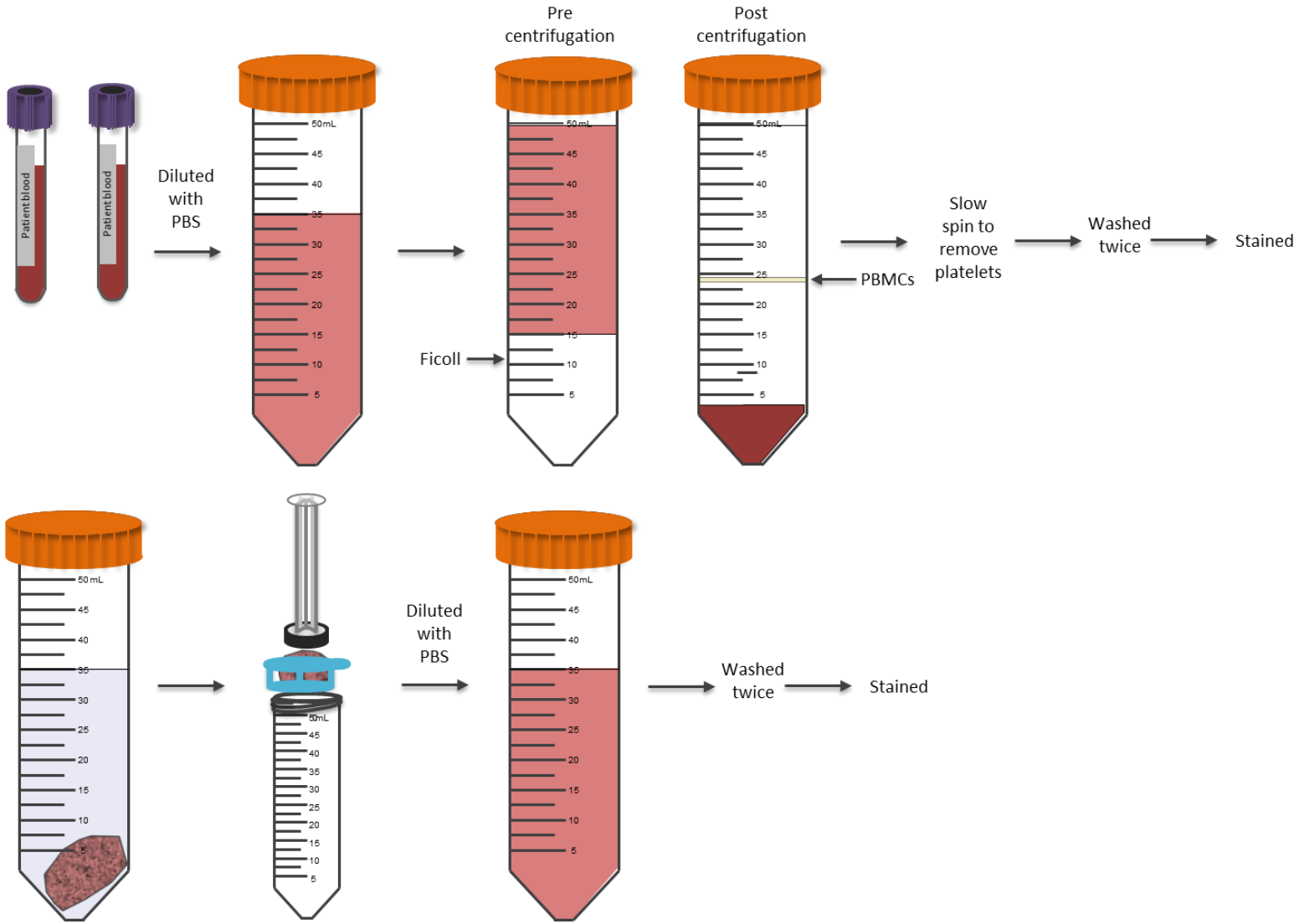

Figure 2.2. Flow diagram of sample processing. (Top) The patient blood sample was diluted with PBS to a final volume of 35 mL. PBMCs were isolated on a ficoll gradient, washed and stained. (Bottom) The tumour sample was pushed through a 40 µm filter, washed and stained.

2.4 Antibody staining

Cells were washed with PBS and resuspended in ice-cold FACS buffer with a maximum density of 1 x 10^7 cells/mL. An optimised concentration of antibody was added (Table 2.1) and incubated in the dark, on ice for 20-30 minutes. Isotype control antibodies were used to exclude unspecific antibody binding. When assessing the percentage of cells positive for a particular antigen an isotype binding of 2% was used as a baseline. Subsequently cells were washed with PBS, pelleted by centrifugation at 350 g, 4 °C for 5 minutes and stained with a dead cell discriminator, Zombie NIR: PBS 1:200 PBS for 15 minutes in the dark. Cells were washed with FACS buffer before being analysed using a LSRII flow cytometer. Details of the antibodies are listed in Table 2.1.

Table 2.1. Details of antibodies used for flow cytometry.

CD number or specificity	Conjugate	Clone	Manufacturer, product number	Host	Target	Class	Optimised concentration (Volume(µL) per 100 µL or 1 x 10^6 cells)
CD2	PE	RPA-2.10	BD Biosciences, 555327	Mouse	Human	IgG1k	5
CD3	PerCP	BW264/56	Miltenyi Biotec, 130-094-965	Mouse	Human	IgG2a	8
CD9	PE	M-L13	BD Biosciences, 555372	Mouse	Human	IgG1	5
CD24	PE	32D12	Miltenyi Biotec, 130-095-953	Mouse	Human	IgG1	10
CD45	FITC	HI30	BD Biosciences, 555482	Mouse	Human	IgG1k	5
CD48	FITC	BJ40	BioLegend, 336707	Mouse	Human	IgG1k	5
CD69	BV421	FN50	BioLegend, 310929	Mouse	Human	IgG1k	3
CD69	FITC	FN50	BioLegend, 310904	Mouse	Human	IgG1k	3
CD90	VioBlue	DG3	Miltenyi Biotec, 130-099-271	Mouse	Human	IgG1	5
CD107a	PE	H4A3	BD Biosciences, 555801	Mouse	Human	IgG1k	5
CD112 (Nectin-2)	PE	R2.525	BD Biosciences, 551057	Mouse	Human	IgG1k	10
CD132 (IL-2 Rγ)	PE	AG184	BD Biosciences, 555900	Mouse	Human	IgG1k	3
CD152 (CTLA-4)	PE	BNI3	Miltenyi Biotec, 130-097-684	Mouse	Human	IgG2a	10
CD184	PEVio770	12G5	Miltenyi Biotec, 130-103-798	Mouse	Human	IgG2a	10
CD223 (LAG-3)	PE	REA351	Miltenyi Biotec, 130-105-452	Mouse	Human		10
CD226 (DNAM-1)	PE	DX11	Miltenyi Biotec, 130-092-476	Mouse	Human	IgG1	5
CD244 (2B4)	PE	REA112	Miltenyi Biotec, 130-099-051	Mouse	Human		10
CD273 (PD-L2)	PE	MIH18	BD Biosciences, 558066	Mouse	Human	IgG1k	5
CD274 (PD-L1)	PE	MIH1	BD Biosciences, 557924	Mouse	Human	IgG1k	5
CD279 (PD-1)	PE	PD1.3.1.3	Miltenyi Biotec, 130-096-164	Mouse	Human	IgG2b	5
CD314 (NKG2D)	PE	1D11	BD Biosciences, 557940	Mouse	Human	IgG1k	5
CD317 (Tetherin)	PE	REA202	Miltenyi Biotec, 130-101-707	Mouse	Human		5

CD335 (NKp46)	APC	9E2/NKp46	BD Biosciences, 558051	Mouse	Human	IgG1k	5
CD336 (NKp44)	PE	2.29	Miltenyi Biotec, 130-092-480	Mouse	Human	IgG1	10
CD337 (NKp30)	PE	P30-15	BD Biosciences, 558407	Mouse	Human	IgG1k	5
B7H6	APC	875001	R&D Systems, FAB 7144	Mouse	Human	IgG1	5
HLA-A,B,C	APC	W6/32	BioLegend, 311410	Mouse	Human	IgG2a	5
MIC A/B	PE	6D4	BD Biosciences, 558352	Mouse	Human	IgG2ak	10
ULBP1	PE	170818	R&D Systems, FAB 1380P	Mouse	Human	IgG2a	10
mTOR (pS2448)	PE	O21-404	BD Biosciences, 563489	Mouse	Human	IgG1k	5
SMAD2 (pS465/pS467)/ SMAD3 (pS423/pS425)	PE	O72-670	BD Biosciences, 562586	Mouse	Human	IgG1k	5
STAT5 (pY694)	PerCP Cy5.5	47/Stat5(pY694)	BD Biosciences, 560118	Mouse	Human	IgG1k	20
S6 (pS235/pS236)	PE	N7-548	BD Biosciences, 560433	Mouse	Human	IgG1k	20
Isotype	APC	MOPC-21	BD Biosciences, 555751	Mouse		IgG1k	
Isotype	BV421	MOPC-21	BioLegend, 400157	Mouse		IgG1k	
Isotype	FITC	MOPC-21	BD Biosciences, 555748	Mouse		IgG1k	
Isotype	PE	MOPC-21	BD Biosciences, 559320	Mouse		IgG1k	
Isotype	PE	G155-178	BD Biosciences, 555574	Mouse		IgG2ak	
Isotype	PerCP Cy5.5	MOPC-21	BD Biosciences, 552834	Mouse		IgG1k	
Isotype	PEVio770	S43.10	Miltenyi Biotec, 130-096-638	Mouse		IgG2a	
Isotype	APC	IS5-21F5	Miltenyi Biotec, 130-092-214	Mouse		IgG1k	
Isotype	VioBlue	IS5-21F5	Miltenyi Biotec, 130-094-670	Mouse		IgG1	

2.5 NK cell functional assays

2.5.1 Cytotoxicity assay

The target cells were harvested using 0.25% trypsin/EDTA and resuspended in media containing a cell tracker dye (see multiplex screen section, 2.6) at a concentration of 1 x 10^6 cells/mL. The cells were incubated in the staining solutions for 1 hour at 37°C and 5% CO_2. Once stained, the cells were washed with PBS and resuspended in media. NK cells (the effectors) were pelleted by centrifugation at 300 g for 5 minutes and co-cultured with a total of 2 x 10^5 cells per well in a 100 μl reaction volume with the stained targets in a U-bottomed 96-well plate for five hours at 37°C and 5% CO_2. Different concentrations of effector to target ratios were used ranging from 1:1 to 5:1. A zero hour control was set up alongside each reaction that included the same number of effector and target cells and was mixed immediately before staining with the dead cell discriminator. This allowed the background level of death to be established. After five hours the cells were pelleted and the supernatant was removed. The cells were resuspended in ice-cold Zombie near infrared (NIR) (Biolegend, UK) dead cell discriminator in PBS (1:200 v/v) and incubated on ice, in the dark for 10 minutes. Zombie NIR reacts with the primary amine group on proteins. Although Zombie NIR has access to the proteins on the surface of the cell, when the cell is dead the membrane becomes compromised and the dye can additionally bind to cytoplasmic proteins. Therefore, the dead cells stain more brightly. After a 10 minute incubation with the dead cell discriminator, the cells were washed with ice-cold FACS buffer, resuspended in FACS buffer and analysed using a LSRII Flow cytometer (BD Bioscience). Approximately 5 x 10^4 events were collected.

2.5.2 Cytotoxicity assay with two targets

The target cells were harvested separately using 0.25% trypsin/EDTA and resuspended in media containing either cell tracker violet or cell tracker green (see multiplex screen section) at a concentration of 1 x 10^6 cells/mL. The cells were incubated in the staining solutions for 1 hour at 37°C and 5% CO_2. Once stained, the cells were washed with PBS and resuspended in media. The cells were mixed in a 1:1 ratio and collectively used as the targets. The assay was then carried out as described in method 2.5.1.

2.5.3 Degranulation assay

Prior to the assay NK cells were stained with 0.4 µM cell tracker green-CMFDA (Invitrogen) for 1 hour at 37°C and then washed with PBS. NK cells were co-cultured with K562 target cells at an E:T ratio of 1:1 for 5 hours. After an hour of incubation GolgiStop (BD Biosciences) was added at 1:1000 to prevent the internalisation of CD107a after degranulation. At the end of the 5 hour incubation, the cells were pelleted, resuspended in ice-cold FACS buffer and stained with anti-CD107a-PE, anti-CD56-APC or the correct isotype control (Table 2.1) for 20 minutes on ice. Cells were then washed with ice-cold PBS and resuspended in ice-cold Zombie NIR :PBS 1:200 and incubated on ice, in the dark for 10 minutes. Cells were washed with ice-cold FACS buffer, resuspended in FACS buffer and analysed using a LSRII Flow cytometer (BD Bioscience). Approximately 5 x 10^4 events were collected.

2.6 Multiplex screen

The antibody panel used was the 'Human Cell Surface Marker Screening Panel' from BD Bioscience. The panel is supplied as three ninety-six well plates with lyophilised rat or a mouse primary antibodies against two hundred and forty two human cell surface antigens and a panel of appropriate isotype controls. The lyophilised antibodies were reconstituted in 100 µL of PBS. The multiplex surface antigen screen allowed four cell lines to be analysed at a time. The screen was repeated to gather data on 5 GBM stem cell lines (GBM1, GBM4, GBM11, GBM13 and GBM20). Cells were harvested using 0.25% trypsin/EDTA, washed with PBS and counted using a haemocytometer. The cells were stained by resuspending in media containing the appropriate dye; GBM1 with 5 µM calcein blue-AM (Invitrogen), GBM4 with 2µM cell tracker violet-BMQC (Invitrogen), GBM11 with 2 µM cell tracker orange-CMRA (Invitrogen), GBM13 with 5 µM calcein blue-AM (Invitrogen) and GBM20 with 0.4 µM cell tracker green-CMFDA (Invitrogen). Cells were incubated in the staining solutions for 1 hour at 37°C and 5% CO_2. Once stained, the cells were washed with PBS, resuspended in FACS buffer, pooled together and aliquoted at 100 µl/well into 4 U-bottomed 96-well plates. 20 µL of unlabelled primary antibody was added to the appropriate well and incubated on ice in the dark for 30 minutes. The cells were washed with FACS buffer, resuspended in the appropriate AlexaFluor 647 conjugated goat anti-mouse or goat anti-rat secondary

antibody and incubated on ice for 20 minutes in the dark. The cells were subsequently washed with PBS and resuspended in 100 µL of 1:100 Zombie NIR:PBS to stain the dead cells. A final wash step was completed before collecting the data using a LSRII (BD) Flow cytometer (4 laser) with a 96 well plate reader. Analysis and compensation was done using FACS Diva (BD) and Kaluza (Beckman Coulter, High Wycombe UK) software. The fluorophores used in the screen were selected based on their excitation and emission values and could be compensated to give a clear signal for the individual fluorophores.

2.7 Cell cycle analysis

NK cells were isolated and treated (see methods 2.2.2-2.2.3) for 24-72 hours. A minimum of 1.5 x 10^6 cells/treatment was used. BrdU (Sigma-Aldrich) was added to a final concentration of 50 µM. The experiment was performed in two different ways; BrdU was either added immediately after treatment or 1 hour before collection. After incubation, cells were washed with ice-cold PBS and collected by centrifugation at 450 g for 10 minutes at 4°C. The pellet was resuspended in 2 mL of ice-cold PBS and fixed by adding 8 mL 100% EtOH in a dropwise fashion, whilst vortexing. Fixed cells were stored at -20°C at least overnight before staining. Cells were centrifuged for 10 minutes at 600 g at 4°C and the supernatant was discarded. The pellet was resuspended in 1.5 mL of pepsin solution (0.5 mg/mL pepsin (Fisher Scientific, UK), 30 mM HCl). Cells were incubated in a water bath at 37°C for 20 minutes and vortexed every 5 minutes. Cells were centrifuged for 10 minutes at 600 g. The supernatant was carefully removed using a needle and syringe. The cells were resuspended in 1 mL of 2 M HCl and incubated at RT for 20 minutes. Cells were diluted with 0.5 mL of PBS and centrifuged for 10 minutes at 600 g. The supernatant was removed and the cells were washed with 1.5 mL PBS. Cells were resuspended in 100 µL of anti-BrdU (BD Biosciences) antibody solution; 1:4 anti-BrdU: Bu buffer (0.5 % FCS, 0.5 % Tween 20, 20 mM Hepes in PBS). Cells were stained for 1 hour at RT, then diluted with 1.5 mL PBS and stored at 4°C overnight. Cells were centrifuged for 10 minutes at 600 g and resuspended in 100 µL of the first secondary antibody; 1:49 rabbit anti-mouse AF594 (Invitrogen): Bu buffer. After a 1-hour incubation at RT the cells were diluted with 1.5 mL PBS and stored at 4°C overnight. Cells were centrifuged for 10 minutes at 600 g and

resuspended in 100 µL of the second secondary antibody; 1:49 donkey anti-rabbit AF594 (Invitrogen): Bu buffer. Cells were incubated at RT for 1 hour and washed with PBS. Cells were resuspended in 300 µL Hoechst solution; 2.5 µM Hoechst 33342 (Biotium, California, USA) in PBS, 0.05% Tween. Data was collected using a LSRII flow cytometer.

2.8 Preparation of NK cell lysates

NK cells were diluted five-fold with ice-cold PBS and centrifuged at 450 g for 5 minutes at 4°C. The supernatant was discarded and the cells were resuspended in 50 µL RIPA buffer (10 mM Tris-HCl pH 8, 1 mM EDTA, 0.5 mM EGTA, 140 mM NaCl, 1 % Triton X-100, 0.1 % sodium deoxycholate, 0.1 % v/v SDS, dH_20) supplemented with protease inhibitor (Roche, Basel, Switerland) and phosphatase inhibitor (Roche) according to the manufacturer's guidelines. Cells were incubated on ice for 10 minutes and either used immediately or frozen at -20°C.

2.9 SDS PAGE

A discontinuous protein gel was made consisting of a 5% stacking gel (5% acrylamide, 0.125 M Tris-HCl pH 6.8, 0.1% SDS, 0.1% APS, 0.001% TEMED) and either a 10% or 15% resolving gel (10% or 15% acrylamide, 0.375 M Tris-HCl pH 8.8, 0.1% SDS, 0.1% APS, 0.001% TEMED). An equal volume of protein sample buffer (100 mM tris-HCl, 4% SDS, 20% glycerol, 0.2% bromophenol blue, 10% β-mercaptoethanol) was added to the samples and boiled for 5 mins at 95 °C to denature and reduce the protein. The lysates were loaded onto the gel along with molecular weight markers. Equal numbers of cells were analysed. Laemmli running buffer (25 mM tris, 192 mM glycine, 0.1% SDS) was used. The gel was run at 120V until the running front reached the bottom of the gel.

2.10 Western blot

Western blot was performed by sandwiching the gel between a sheet of polyvinylidene difluoride (PVDF) and three pieces of Whatman 3 MM Chr paper that had been pre-soaked in transfer buffer (25 mM tris, 192 mM glycine, 20 % MeOH). The proteins were transferred at 15 V for 1 hour using a semi-dry transfer apparatus (Bio-Rad, UK).

2.11 Probing

Following the transfer, membranes were blocked for 1 hour at RT with blocking buffer; TBST (25 mM Tris base, 134 mM sodium chloride, pH 7.5, 0.1 % v/v Tween-20) containing 5 % w/v BSA. The blots were probed with a primary antibody (Table 2.2) diluted 1:1000 in blocking buffer for 2 hours at RT or overnight at 4°C on a shaker. The membrane was washed three times for 5 minutes with TBST, with continuous rocking. A secondary HRP-conjugated antibody was added diluted in blocking buffer and incubated at RT for 1 hour or at 4°C overnight, with continuous rocking. The membrane was washed again three times with TBST and protein was detected using a chemiluminescence reagent (GE Healthcare, UK), a light proof cassette, CL-XPosure film (Thermo-Fisher Scientific) and a Konica SRX-101A Tabletop X-ray Film Processor (Konica, UK). The expression of β-actin was used to assess the equal loading of protein samples.

Table 2.2. Details of antibodies used for Western blots.

Specificity	Conjugate	Manufacturer, product number	Blocking buffer	Host	Size (KDa)	% gel
c-Myc	Purified	Cell Signaling Technology, 9402	TBST 5%BSA	Rabbit	57-70	10
Total S6	Purified	Cell Signaling Technology, 2217	TBST 5%BSA	Rabbit	32	15
pS6 235/236	Purified	Cell Signaling Technology, 4858	TBST 5%BSA	Rabbit	32	15
pS6 240/244	Purified	Cell Signaling Technology, 5364	TBST 5%BSA	Rabbit	32	15
phospho p70S6K 389	Purified	Cell Signaling Technology, 9234	TBST 5%BSA	Rabbit	70,85	10
4EBP1	Purified	Cell Signaling Technology, 9644	TBST 5%BSA	Rabbit	15-20	15
p4EBP1 T37/40	Purified	Cell Signaling Technology, 2855	TBST 5%BSA	Rabbit	15-20	15
non phospho 4EBP1 T46	Purified	Cell Signaling Technology, 4923	TBST 5%BSA	Rabbit	15-20	15
Granzyme B	Purified	BD Biosciences, 550558	TBST 5%BSA	Mouse	32	10
Rabbit	Peroxidase	Cell Signaling Technology, 7074	TBST 5%BSA	Goat		
Mouse	Peroxidase	Sigma-Aldrich, a4416	TBST 5%BSA	Goat		

2.12 Microarray

NK cells from healthy donors were isolated (method 2.2.2) and treated under six different conditions (method 2.2.3-2.2.3) for 48 hours; untreated (resting) or addition of dexamethasone, TGF-β, IL-15, IL-15+dexamethasone and IL-15+TGF-β. A minimum of 5 x 10^6 cells were treated for each condition. Both the morphology of the cells and the cell surface expression of CD69 and NKp30 were used to assess the donor response (described in Chapter 5). Cells were diluted in a five-fold volume of PBS and centrifuged at 450 g, 5 minutes. The supernatant was discarded and the cell pellet was resuspended in 300 µL RNAprotect cell reagent (Qiagen, Hilden, Germany) and vortexed. The samples were transferred to barcode (provided by the company) labelled Eppendorf tubes and stored at -20°C. The samples from all donors were collectively sent to an external service provider (Hologic, Manchester, UK) who processed the samples and performed the microarray. Standard techniques were used to isolate mRNA, synthesize complementary DNA (cDNA), fluorescently label the cDNA, hybridise it to the array (GeneChip® Human Transcriptome Array 2.0, Affymetrix, California, USA) and acquire the data. The raw intensity files were received and analysed using the Affymetrix expression and transcript analysis consoles. Dr Alastair Droop facilitated the initial stages of the analysis using the computer programming language R.

2.13 Statistics

T tests were performed using GraphPad Prism (GraphPad).

Chapter 3 Lymphocyte infiltration of human GBM tumours

3.1 Introduction

The successful implementation of NK cell based immunotherapy of GBM requires the NK cells to enter the tumour. Previous studies have shown that NK cells account for a very small proportion of infiltrating cells within high grade gliomas (Kmiecik et al. 2014). However, in some cases these analyses were not restricted to GBM (and included other types of brain tumours) and the markers used to identify NK cells were restricted to certain subsets of NK cells or not unique to NK cells. During one study that focused on T cell characterisation, it was noted that NK cells account for less than 3% of infiltrating lymphocytes in GBM (Kmiecik et al. 2013). The lack of detailed characterisation of NK cell infiltration into GBM prompted a more in depth analysis.

NK cell infiltration alone is insufficient for anti-tumour activity as the NK cell must be activated to exert its effector functions. For example, activation receptors must be displayed on the NK cell surface where they can engage and respond to tumour expressed ligands. Immunosuppressive mechanisms operating in other tumour microenvironments have been reported to reduce expression of activation receptors such as NKp30, NKG2D, DNAM-1 (Mamessier et al. 2011; Rocca et al. 2013) and tilt the balance in favour of NK cell inhibition.

To date, there are no reports detailing the phenotype of NK cells within human GBM tumours. Therefore, not only was it necessary to assess the extent of NK cell infiltration into human GBM tumours, it was as essential to characterise their cell surface phenotype. An understanding of how GBM tumours are able to evade the cytotoxic effects of NK cells (be it by preventing recruitment or activation) will enable the development of immunotherapies that target the appropriate evasion strategy.

3.2 NK cells are present within the tumour

Patients undergoing tumour resection surgery gave their consent for the extracted tissue and a peripheral blood sample to be used for research. A tumour dissociation method and a staining panel to phenotype NK cells using flow cytometry was

optimised (data not shown). The samples were processed and data collected on the same day as the surgery. Briefly, the tumour sample was reduced to a single cell suspension and the PBMCs were isolated from the blood sample using a density gradient. The samples were subsequently stained with fluorescently labelled antibodies and a dead cell discriminator, and analysed by flow cytometry. The lymphocyte population was identified within the blood sample according to its size and granularity (FSC and SSC respectively, Figure 3.1). Within this population the live, CD45+ cells (pan-leukocyte marker) were selected. NK cells were then defined as CD3negNKp46+ and T cells as CD3+NKp46neg. The same gating strategy was applied to evaluate both blood and tumour samples. Note that studies of human NK cells frequently define NK cells as CD56+CD3neg cells. However, CD56 (also known as Neural Cell Adhesion Molecule 1) is highly expressed by cells in the brain and cannot be used to identify NK cells.

Tumour and blood samples from 11 patients were analysed for the presence of NK and T cells, both subsets were found within the tumour. NK cells and T cells accounted for 3.6±3.1% and 37.8±24.4% of CD45+ cells within the tumour respectively, compared to 12.3±12.5% and 64.9±13.3% within the blood (Table 3.1). However, the CD45+ populations in healthy blood and brain have quite different compositions (for example, the brain contains large numbers of CD45+ microglia). Therefore, the ratio of NK cells to T cells in blood and brain was used to assess the selective infiltration of these two subsets.

There was no significant difference in the NK:T cell ratio between the patient blood and tumour samples, nor compared to healthy blood donor samples (Figure 3.2). This suggests that both NK cells and T cells are recruited into the tumour and that infiltration of neither NK cells nor T cells is favoured.

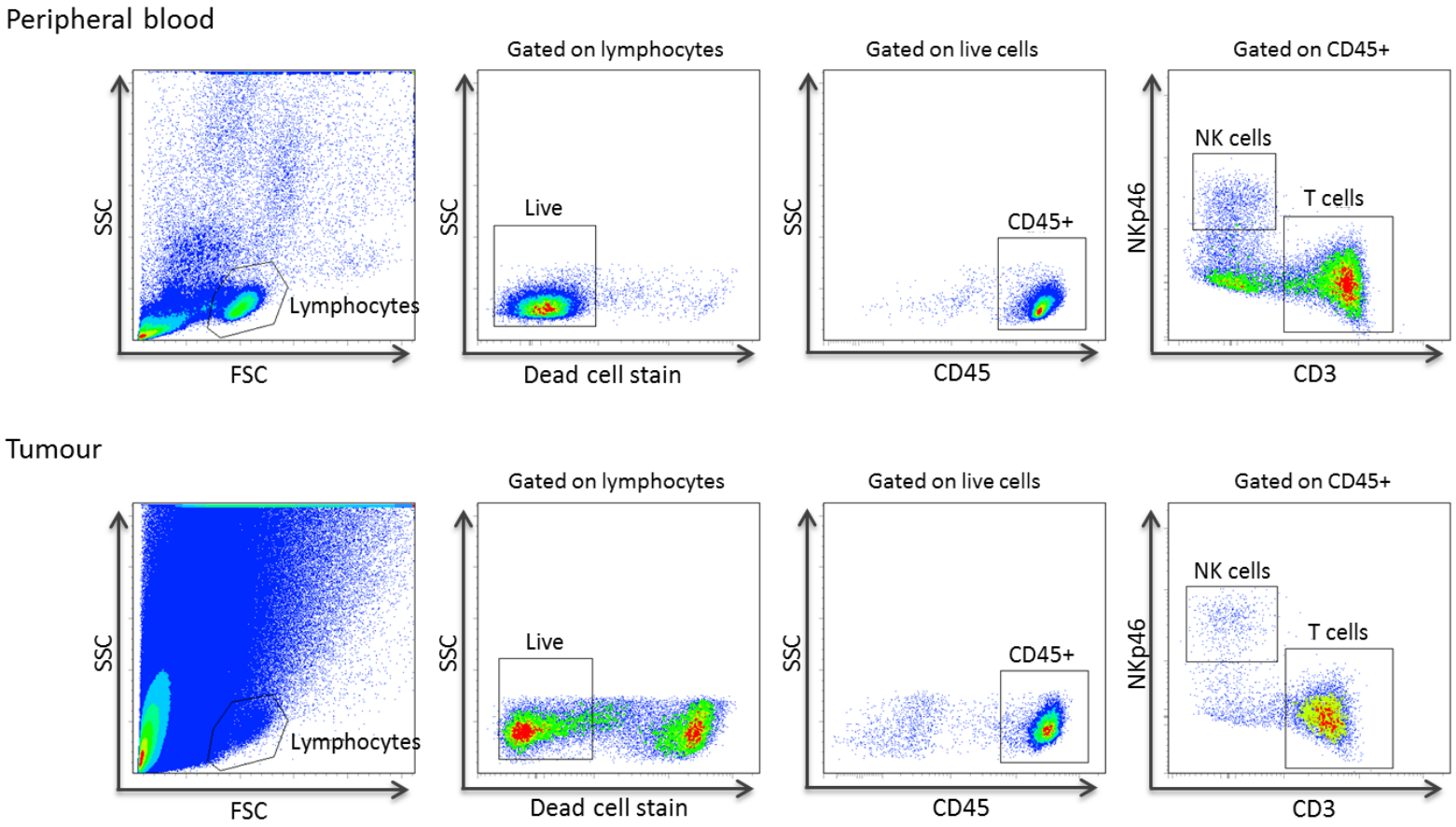

Figure 3.1. The gating strategy used to identify NK and T cells. Samples were processed and analysed by flow cytometry. The same gating strategy was applied to both the peripheral blood (top panel) and tumour sample (bottom panel). The lymphocytes were identified by their forward scatter (FSC) and side scatter (SSC). These are measures of size and granularity respectively. Within this gate the live cells were defined as negatively stained with the dead cell discriminator. The CD45 positive cells were selected. NK cells and T cells were identified as CD3negNKp46+ and CD3+NKp46neg respectively.

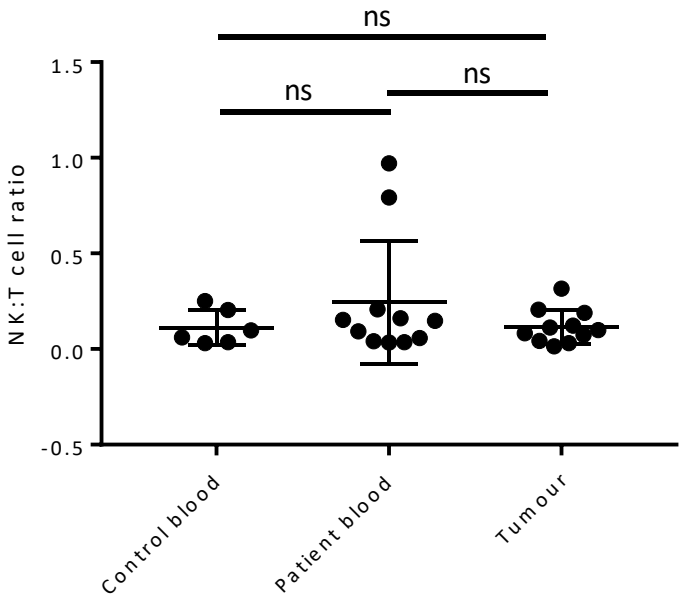

Figure 3.2. NK cell infiltration. PMBCs isolated from blood samples and a single cell suspension of tumour cells were stained and analysed by flow cytometry. Within the CD45+, live, lymphocyte gates NK cells and T cells were identified as CD3negNKp46+ and CD3+NKp46neg respectively. A ratio of the number of NK cells to T cells was calculated for each sample within each group (left-right); control blood, patient blood and tumour. Each dot represents a single sample (n=6 control blood, n=11 patient samples); the bar indicates the mean± s.d. Statistical analysis was performed by ratio t-tests (paired or unpaired where appropriate). ns: not significant.

3.3 Peripheral blood and tumour lymphocytes are phenotypically distinct

Brain tumours are highly vascularised and it was possible that the NK:T cell ratios in the peripheral blood and tumour samples were the same because I simply sampled blood-resident lymphocytes within the tumour vasculature. However, analysis of the cell surface phenotype revealed significant differences between the blood and tumour-resident lymphocytes.

The lymphocyte activation marker CD69 (Ziegler et al. 1993) was expressed on a significantly higher proportion of both NK and T cells within the tumour compared to those in the peripheral blood of the same patient (Figure 3.3 and figure 3.4); the average percentage of NK cells expressing CD69 in the patients' peripheral blood samples was 13.1% compared to 49.3% in the tumours ($p< 0.001$). A similar pattern is seen on T cells where 9.1% express CD69 in the blood compared to 74.6% in the tumour ($p< 0.0001$).

This result indicated that the sampling method was effective and could be used to study the phenotype of tumour infiltrating lymphocytes in more detail.

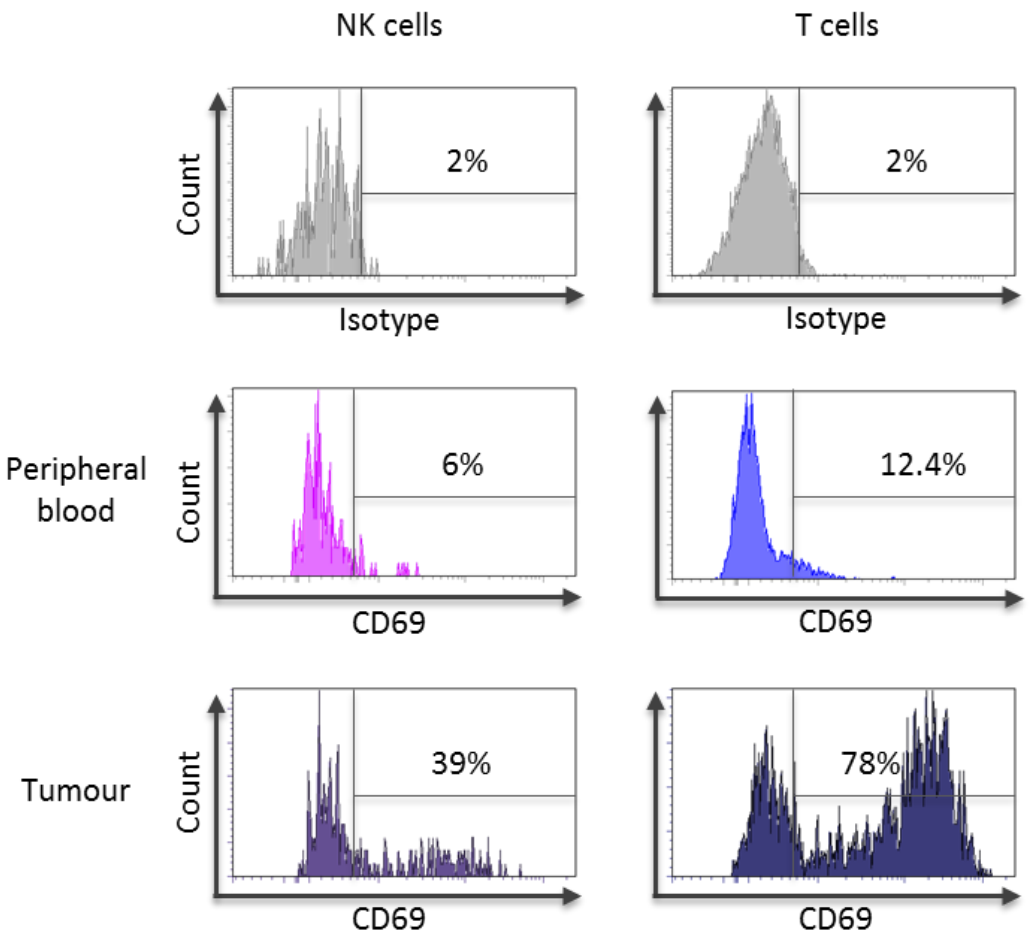

Figure 3.3. CD69 expression on NK and T cells within the blood and tumour. Flow cytometry was used to evaluate the expression of activation marker CD69 on NK cells (left) and T cells (right) within the patient's peripheral blood (middle row) and tumour (bottom row). Data is representative of 8 samples. An isotype control antibody (top row) was used to exclude non-specific binding.

3.4 NK cell activation receptors are down regulated on GBM infiltrating NK cells

A panel of surface proteins was chosen to compare the phenotype of the lymphocytes within the blood and tumour samples (Figure 3.4). These included the prototypic activation marker CD69, activation (or coactivation) receptors such as NKp30, NKG2D, DNAM-1, CD2, and 2B4 and the checkpoint inhibitors PD-1, CTLA-4 and LAG-3. Expression of tetherin was also analysed as it is induced by type I interferons and IL-15 so is a marker of activation (Neil et al. 2008; Homann et al. 2011; El-Sherbiny et al. 2015). In contrast, CD9 is upregulated by TGF-β (Keskin et al. 2007) and might indicate the presence of this immunosuppressive cytokine within the tumour microenvironment. The expression of CD69 on the tumour infiltrating NK cells suggests that a proportion of NK cells are activated when they enter the tumour microenvironment.

In contrast, the activation receptors NKp30, NKG2D and DNAM-1 were down regulated on NK cells located within the tumour compared to the peripheral blood (Figure 3.4 and table 3.2). Approximately 10% fewer tumour infiltrating NK cells expressed these activation receptors (Table 3.2). This suggests that tumour-resident NK cells are less likely to respond to ligands expressed by the tumour. The cell surface molecule CD2 is essential for the development of NK cytotoxicity and cytokine secretion (Kim et al. 2010) and also showed the same pattern of down regulation as the activation receptors (Figure 3.4 and table 3.2). This supports the hypothesis that tumour resident NK cells have a reduced capacity for anti-tumour activity due to the reduced expression of these key activation receptors.

The upregulation of CD9 on tumour infiltrating NK cells suggests that TGF-β is present within the tumour microenvironment. TGF-β suppresses NK cell activity (Rook et al. 1986) and this might be one mechanism by which the tumour evades immune destruction. Tetherin is constitutively expressed by NK cells and further upregulated by type I interferons and activating cytokines such as IL-15 (El-Sherbiny et al. 2015). However, tetherin expression was significantly downregulated on the tumour infiltrating NK cells compared to NK cells in the blood. This suggests that NK cells are

inhibited within the tumour microenvironment, demonstrated by the down-regulation of multiple activatory receptors.

Previous reports have demonstrated NK cell expression of checkpoint inhibitors such as PD-1 (Norris et al. 2012) and CTLA-4 (Stojanovic et al. 2014). However, I found no evidence of their expression in any of the groups (control blood, patient blood nor the tumour infiltrating NK cells).

Though there were statistically significant differences in expression of activation receptors between matched NK cells within the patients' blood and tumour, I found no evidence for significant differences between the blood of patients and those of healthy controls (Figure 3.4). This indicates that it is the tumour microenvironment that specifically causes the immunosuppressed NK cell phenotype.

A similar study investigating NKG2D expression on NK and T cells in patients with gliomas found NKG2D was downregulated on peripheral NK cells from GBM patients compared with those isolated from patients with meningioma or other benign tumors (Crane et al. 2010). The group showed that the reduced expression of NKG2D in the peripheral blood of GBM patients correlated with serum TGF-β levels. The expression of NKG2D on peripheral NK cells was reassessed post resection surgery and was found to be increased to around 70%, still much less than the 90% observed within my patient blood cohort. A key difference is that their study was based on recurrent GBM patients. Presumably, the patients analysed in their study had a higher tumour burden than those analysed here hence the main effects observed in my study were restricted to the tumour microenvironment.

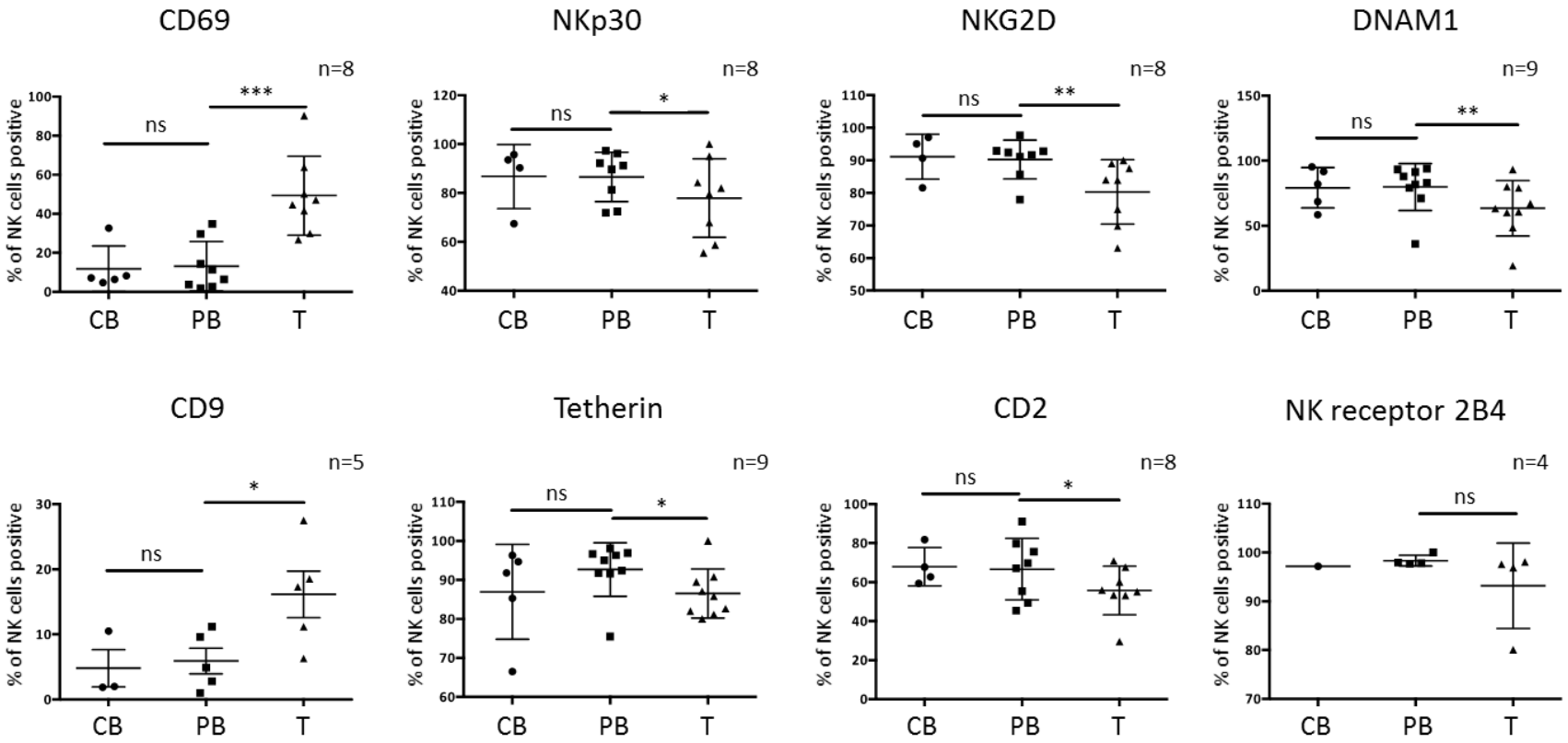

Figure 3.4. NK cell phenotype within the patient peripheral blood and tumour. NK cells (CD45+CD3negNKp46+) from control blood (CB), patient's peripheral blood (PB) or tumour (T) were analysed by flow cytometry for the expression of the surface proteins listed. The gates were set at 2% of the isotype control stain. The number of patient samples analysed is adjacent to each graph. Each dot represents a single sample and the bar indicates the mean± s.d. Statistical analysis was performed using t-tests (paired or unpaired where appropriate). *P<0.05, **P<0.01; ***P<0.001; n.s: not significant.

3.5 T cell inhibitory receptors are upregulated on GBM infiltrating T cells

The use of anti-CD3 antibody (to identify NKp46+CD3neg NK cells) also allowed the phenotype of T cells (CD3+) to be examined (Figure 3.5). Limitations due to the sample size prevented the incorporation of additional markers, such as CD4 and CD8, into the panel so information about specific subsets of T cells could not be ascertained. However, phenotyping the bulk population of tumour resident T cells provided additional insight into the immune status within the tumour.

As witnessed in the NK cell analysis, DNAM-1, tetherin and CD2 were all downregulated on T cells within the tumour compared to those in the peripheral blood (Figure 3.5 and table 3.3). Furthermore, similar to the data with NK cells, CD69 was upregulated in the tumour infiltrating T cells compared to the matched blood (Figure 3.5 and table 3.3). Hence, the tumour microenvironment influences the phenotype of T cells and NK cells in a similar manner.

One of the major differences observed between NK cells and T cells is the upregulation of checkpoint inhibitors on T cells within the tumour. Both PD-1 and LAG-3 are significantly upregulated on tumour T cells compared to the peripheral blood T cells and a similar trend is seen for CTLA-4. These checkpoint inhibitors are not expressed by NK cells. It appears that T cell suppression within the tumour microenvironment is twofold; activation receptors (e.g DNAM-1 and CD2) are down regulated and checkpoint inhibitors (PD-1 and LAG-3) are upregulated.

As with NK cells, the phenotype of the T cells is not significantly different between the blood of a healthy controls and the patients.

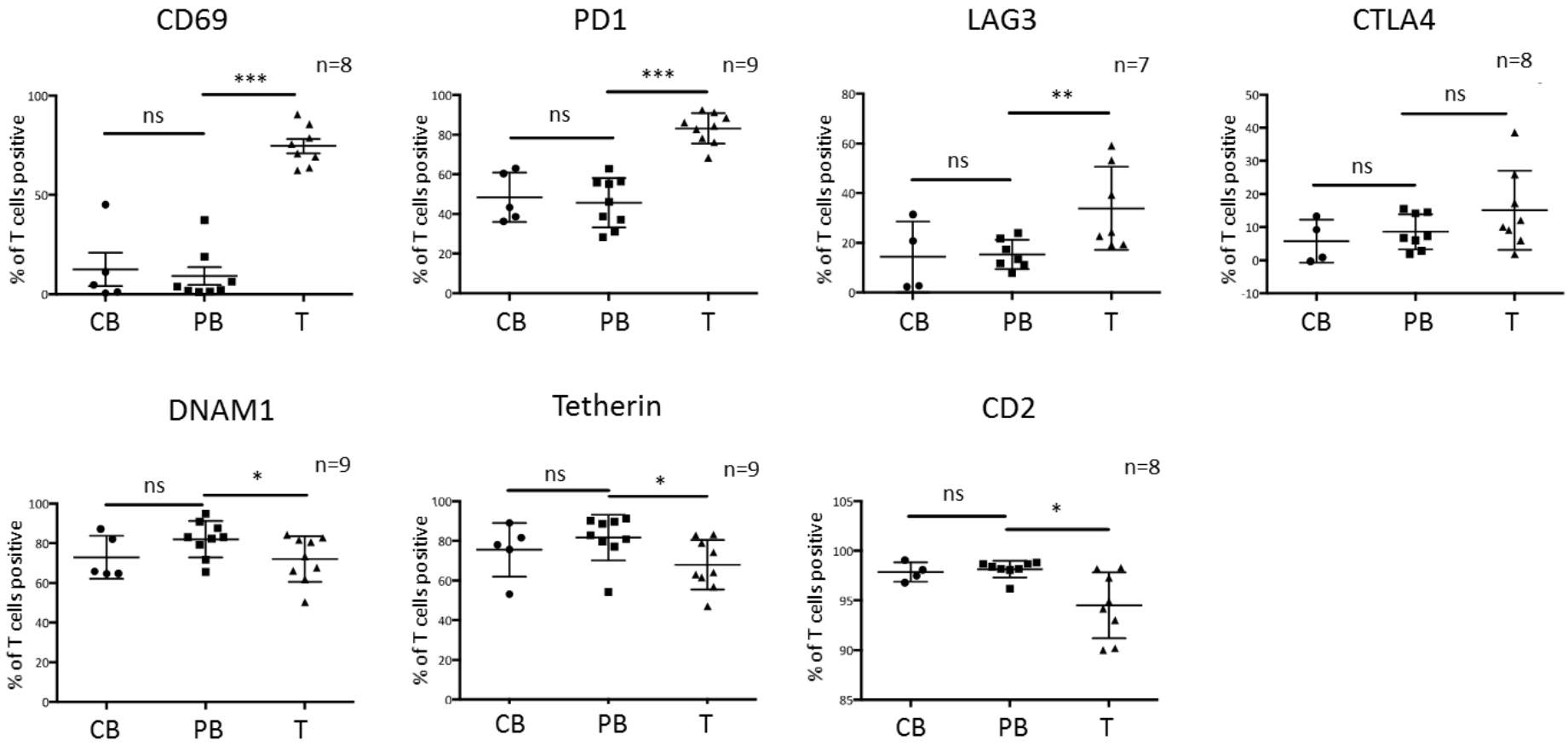

Figure 3.5. T cell phenotype within the patient peripheral blood and tumour. T cells (CD45+CD3+NKp46neg) from the control blood (CB), patient's peripheral blood (PB) or tumour (T) were analysed by flow cytometry for the expression of the surface proteins listed. The gates were set at 2% of the isotype control stain. The number of patient samples analysed is adjacent to each graph. Each dot represents a single sample and the bar

indicates the mean± s.d. Statistical analysis was performed using t-tests (paired or unpaired where appropriate). *P<0.05, **P<0.01; ***P<0.001; n.s: not significant.

	Peripheral blood	Tumour
NK cells	12.3 ± 12.5%	3.6 ± 3.1%
T cells	64.9 ± 13.3%	37.8 ± 24.4%

Table 3.1 Proportion of NK and T cells out of CD45+. NK (CD45+CD3negNKp46+) and T cells (CD45+CD3+NKp46neg) were identified within the peripheral blood and tumour using flow cytometry. The proportion of NK and T cells out of CD45+ cells was calculated. n=11. Numbers represent mean± s.d.

	Control blood	Peripheral blood of patient	Tumour
CD69	11.8 ± 11.7%	13.1 ± 12.7%	49.3 ± 20.2%
NKp30	86.8 ± 13.1%	86.5 ± 10.1%	77.9 ± 16.1%
NKG2D	91.1 ± 6.9%	90.3 ± 6.0%	80.3 ± 9.9%
DNAM-1	79.2 ± 15.6%	79.8 ± 18.0%	63.5 ± 21.3%
CD9	4.8 ± 4.9%	5.9 ± 4.4%	16.2 ± 8.0%
Tetherin	86.9 ± 12.2%	92.7 ± 6.9%	86.6 ± 6.3%
CD2	67.9 ± 9.8%	66.7 ± 15.7%	55.7 ± 12.5%

Table 3.2 Proportion of NK cells expressing surface protein. Flow cytometry was used to analyse the proportion of NK cells (CD45+CD3negNKp46+) that were stained with antibodies for the particular antigens. The gates were set at 2% of the isotype control antibody stain. Numbers represent mean± s.d, number of patient samples analysed is given in figure 3.4.

	Control blood	Peripheral blood of patient	Tumour
CD69	12.5 ± 18.7%	9.1 ± 12.9%	74.6 ± 10.0%
PD-1	48.4 ± 12.5%	45.7 ± 12.5%	83.2 ± 7.8%
LAG-3	14.3 ± 14.3%	15.3 ± 5.9%	33.9 ± 16.8%
CTLA-4	5.8 ± 6.6%	8.6 ± 5.4%	15.1 ± 12.0%
DNAM-1	72.9 ± 10.9%	82.0 ± 9.1%	72.0 ± 11.5%
Tetherin	75.5 ± 13.5%	81.7 ± 11.5%	68.0 ± 12.5%
CD2	97.9 ± 1.0%	98.2 ± 0.8%	94.5 ± 3.3%

Table 3.3 Proportion of T cells expressing surface protein. Flow cytometry was used to analyse the proportion of T cells (CD45+CD3+NKp46neg) that were stained with antibodies for the particular antigens. The gates were set at 2% of the isotype control antibody stain. Numbers represent mean± s.d, number of patient samples analysed is given in figure 3.5.

3.6 Discussion and conclusion

NK cells, defined as CD3negNKp46+, were identified within human GBM tumours, accounting for 3.6±3.1% of CD45+ cells. This agrees with a previous study that reported NK cells (defined as CD3−CD14−CD56+) accounted for 2.11% ±0.54 of CD45+ cells (Kmiecik et al. 2013). To assess whether T cells or NK cells selectively infiltrated the tumour, I compared the proportion of NK cells in both the blood and tumour sample. As previously mentioned, the presence of CD45+ microglia in the tumour sample means that the comparison cannot be made using the proportion of CD45+ cells. The ratio of NK to T cells was used and no infiltration preference was observed between these two cell types. It is important to realise that no information about the infiltration of specific T cell subsets can be obtained using this ratio; knowledge of CD4 and CD8 T cell infiltrates will likely be more relevant to patient prognosis. For example, conflicting historical reports exist that correlate gross lymphocyte infiltration and prognosis (Safdari et al. 1985; Brooks et al. 1978; Böker et al. 1984). However, the use of subset markers has linked the levels of CD3+ and CD8+ cells with prolonged survival in GBM patients (Kmiecik et al. 2013) and Treg accumulation (scored using the FOXP3 molecule as a marker) increases with tumour grade (El Andaloussi & Lesniak 2006).

For several other cancers the number of NK cells present in the tumour positively correlates with patient survival. For example, in squamous cell lung carcinoma patients with low levels of tumour infiltrating NK cells had a 2.5 fold increase in the risk of death (Villegas et al. 2002). However, these studies were performed using 50 patients and a much larger GBM cohort would be required to carry out similar studies.

Tumour infiltrating immune cells often show an altered phenotype which is associated with a loss of an antitumor activity and, in some cases, pro-tumour activities (de Visser et al. 2006). This process is known as tumour-induced polarisation and has been well documented for macrophages (Mantovani & Sica 2010), dendritic cells, mast cells, B cells and T cells (Coffelt et al. 2010; DeNardo et al. 2010). It has also been proposed for NK cells (Noonan et al. 2008) as the $CD56^{bright}$CD16neg subset, that are known to produce angiogenic factors such as VEGF, PIGF and IL-8, are predominant in human non-small cell lung cancer (NSCLC) (Carrega et al. 2008). Having established that NK cells were able to gain entry into the GBM tumour, it was important to analyse their

cell surface phenotype to assess any tumour-induced polarisation and evidence of immunosuppression.

The upregulation of CD69 on tumour infiltrating NK and T cells suggests that the cells are or have been active. When considering the development of immunotherapies for these patients, the upregulation of CD69 is promising because it suggests that the immune cells are capable of recognising and responding to the tumour cells. However, when NK cells are treated with the activating cytokine IL-15 a far greater proportion of cells (typically 60-70%; see chapter 5), express CD69. In contrast, the bimodal CD69 histogram (Figure 3.3) shows that a minority of the tumour infiltrating NK cells are activated and the majority of NK cells within the tumour are CD69 negative. This suggests that, whilst NK cell activation can occur in the tumour microenvironment, the majority of NK cells are not activated and are unlikely to be contributing to an anti-tumour response. The ability to therapeutically activate these CD69neg NK cells has the potential to enhance the anti-tumour activity, for example using a TGF-β blocking antibody could prevent the down regulation of activation receptors (see below).

A down regulation of activation and coactivation receptors NKp30, NKG2D, DNAM-1 and CD2 was observed on NK cells located within the tumour compared to the peripheral blood (Figure 3.4). This has been reported for NKp30, NKG2D, DNAM-1 in other tumours such as breast (Mamessier et al. 2011) and colon cancer (Rocca et al. 2013). In both cases these NK cells had an impaired cytotoxicity. This is not surprising as reducing the amount of receptor available at the surface means that activation signals cannot be relayed. In fact, a direct association has been made between the surface density of NCRs such as NKp30 and NK cell cytotoxic activity (Sivori et al. 1999). Although the cytotoxic ability of the GBM infiltrating NK cells identified in this study was not tested (as the numbers present in the samples preclude such an analysis), I would predict that it is reduced.

Similarly, evidence of immunosuppression is seen when examining the GBM infiltrating T cell population; inhibitory receptors PD-1 and LAG-3 were significantly upregulated and the same trend is shown for CTLA-4 (Figure 3.5). A study analysing malignant brain tumours found a 3.3 fold increase of CTLA-4 on T regs (defined as CD4+FoxP3+CD25^{high}CD127^{low}) infiltrating brain metastases compared to those within the blood (Jacobs et al. 2009). Although the figures given reflect an increase in the amount of CTLA-4 rather than the proportion of cells that display the antigen, the

same trend is observed in my data that shows approximately 2 fold more cells expressing CTLA-4 within the tumour compared to the patients' blood. The same study also reported that PD-1 was expressed on CD4+ cells present in 26% of tumours but no indication was given as to the of proportion of T cells expressing PD-1. My research concludes that the average proportion of T cells within the tumour expressing PD-1 was 83.2 ± 7.8%, comparatively much higher. However, this could be due to differences in the types of tumour analysed as the study mentioned included different types of brain tumours. Although the expression of LAG-3 has not been analysed previously on GBM infiltrating lymphocytes, its expression is enriched on CD8+ epithelial ovarian cancer (EOC) infiltrating T cells compared to those in the peripheral blood (Matsuzaki et al. 2010).Overexpression of inhibitory receptors is a feature of exhausted T cells which have reduced effector functions (Jiang et al. 2015). Exhausted T cells are no longer able to produce granzyme B that is a key component of lytic granules found in cytotoxic T cells (Wherry et al. 2003). A reduced cytokine and cytotoxic response by T cells leads to the failure of cancer elimination (Jiang et al. 2015). Restoring this function using immunotherapies has shown real clinical promise. A recent clinical trial targeting CTLA-4 and PD-1 in GBM patients showed tumour regression (Nduom et al. 2016). Antibodies are being used in trials in GBM, combining that with second generation checkpoint inhibitors (e.g. LAG-3) and other e.g. anti-TGF-β strategies might prove successful.

CD9 is known to be induced by TGF-β (Keskin et al. 2007) and was significantly upregulated on NK cells within the tumour compared to those in the peripheral blood (Figure 3.4). Interestingly, not only is TGF-β known to reduce the expression of activation receptors NKp30 and NKG2D (Castriconi et al. 2003), it is also a crucial factor during T cell exhaustion (Massagué 2008). TGF-β is expressed by GBM cells, astrocytes and microglia (Constam et al. 1992). Whilst CD9 might be induced by many factors, the presence of CD9 on tumour infiltrating NK cells is consistent with the presence of TGF-β in the tumour microenvironment. In addition to tumour-induced polarisation, TGF-β acts directly on the tumour cells themselves and has been implicated in tumour progression and metastasis (Ikushima & Miyazono 2010).

CD9 is a characteristic marker of decidual NK cells (dNKs). These are specialised NK cells in the gravid uterus that play a role in preventing rejection of the foetal hemi-allograft and placental angiogenesis (Sharma 2014). Within the decidua, NK cells are

the most abundant lymphocyte and they have a different phenotype and function to peripheral blood NK cells. The dNKs are CD56^{superbright}CD16negCD9+, poorly cytotoxic, and associated with induction of CD4+ Tregs and produce IL-10 that potentially contributes to the immunosuppressive nature of the placenta. Indeed, low levels of dNKs are linked to miscarriage (Santoni et al. 2007). The origin of dNKs is controversial but it has been proposed that peripheral NK cells are converted when they enter the decidua and decidual stromal cells are known to produce high levels of TGF-β (Bruno et al. 2014). Perhaps TGF-β within the tumour microenvironment induced a proangiogenic NK cell phenotype that is characteristic of dNKs. Supporting this theory is the finding that dNKs introduced to tumour cell xenografts enhanced tumour growth (Hanna et al. 2006) and that TGF-β contributes to the proangiogenic polarisation of NK cells in NSCLC (Bruno et al. 2013).

Tetherin was also down regulated on the tumour infiltrating NK cells compared to those in the peripheral blood. Tetherin is upregulated in response to type I interferons and is important in controlling viral infections (Jiang et al. 2010; Brass et al. 2009). Down regulation could signify a global suppression of NK cell function. However, little is known of the mechanisms that regulate tetherin beyond IFN and the significance of tetherin downregulation is currently unclear. As well as its role in tethering budding virus particles to the cell membrane, tetherin has a pro-inflammatory signalling role; DCs from virus infected tetherin knock out mice had a significantly reduced expression of MHC class II and co-stimulatory molecule CD80 than wild type mice (Li et al. 2016). Reduced tetherin expression in the tumour may thus have consequences for NK cell effector function.

Flow cytometry proved to be an incredibly powerful method for identifying and phenotyping rare populations of cells. However, it is also important to realise its limitations. One of the main drawback of this technique is that spatial information is lost. It would be interesting to see if NK cells could penetrate the tumour, or if they are paralysed upon entry. Immunofluorescence microscopy using tumour sections would help to provide answers. Nonetheless, it could prove difficult given the low proportion of NK cell infiltration.

Results show that NK and T cells are present in the tumour, albeit at low numbers. There is evidence of immunosuppression of tumour infiltrating cells but not on peripheral lymphocytes, suggesting that the blood resident cells are ‘normal’ until they

encounter the tumour microenvironment. Not only does this suggest that this is part of the tumour's evasion strategy, it also suggests that restoring the immune function within the tumour using immunotherapies could prove an effective treatment for these patients.

In order for NK cell based therapies to be effective, the NK cells must be capable of responding to transformed cells. The results demonstrating CD69 expression on some tumour resident NK cells suggests that some NK cells are activated by a stimulus present in the tumour microenvironment. However, it is unclear whether the NK cells are responding directly to the tumour. Experiments described in the next chapter are aimed at investigating the outcome of NK cell-GBM interactions *in vitro*, outside of the immunosuppressive environment of the tumour.

Chapter 4 NK and target cell interactions

4.1 Introduction

Tumours progress partly because they are not eliminated by the immune system. In the previous chapter I showed that the GBM tumour microenvironment alters the cell surface phenotype of NK cells and T cells, with expression of NK cell activation receptors reduced and T cell inhibitory receptors increased. This is consistent with the hypothesis that NK cell and T cell activity is inhibited in the tumour and that this evasion activity has contributed to tumour progression, a hallmark of cancer (Hanahan & Weinberg 2011). With their ability to recognise and eliminate tumour cells, NK cells have great potential as key effector cells of immunotherapies. However, translating this to the clinic requires that NK cells have the ability to kill GBM cells when they are not subject to the immunosuppressive cues within the tumour microenvironment. Work reported in this chapter aims to address this by analysing GBM cell susceptibility to NK cell mediated death *in vitro*.

Glioma stem cells (GSCs) are resistant to radio- and chemotherapies (Bao et al. 2006; Liu et al. 2006) and repopulate the tumour after treatment, leading to the formation of a recurrent tumour. Therefore, it is critical that we assess how well NK cells target GSCs if they are to be used as an immunotherapy. Patient derived brain tumour-initiating cells (BTICs, also known as cancer stem cells) were used for the *in vitro* assays carried out in this chapter. Four of the primary cell lines were derived from GBM patients undergoing initial resection surgery (GBM1, GBM4, GBM11 and GBM13) whilst GBM20 is from a recurrent GBM tumour. The BTICs, which I will refer to as GBM stem cells, were characterised by Dr Heiko Wurdak (Wurdak et al. 2010) and members of his group, Dr Euan Polson and Dr Anjana Patel. They exhibit an undifferentiated phenotype and are characterised by expression of neural markers such as Nestin and Sox2, the proliferation marker Ki67 and low levels of the astroglial marker GFAP and the neuronal marker TuJ1 (which are characteristic of differentiated cells). They are also able to recapitulate high-grade gliomas *in vivo* using a mouse model, including high cellularity, tumour heterogeneity, proliferation, and massive infiltration into areas adjacent to the implantation site and even into relatively distant brain areas.

I therefore assessed the ability of the GBM cells to alter the surface phenotype of activated NK cells, the ability of NK cells to recognise and kill GBM stem cell tumour targets and characterised the surface landscape of these cells to understand how the targets might influence the immune response.

4.2 GBM stem cells instigate an immunosuppressed NK cell phenotype

GBM infiltrating NK cells analysed in chapter 3 exhibited reduced cell surface expression of NKG2D, NKp30 and DNAM-1. To assess the ability of GBM stem cells to downregulate the expression of NK cell activation receptors, co-culture experiments were carried out.

This type of experiment has previously been used to analyse the interaction between ovarian cancer and NK cells and colorectal cancer and NK cells (Wilson et al. 2011); co-culture using an excess of tumour cells causes TGF-β-dependent changes in the NK cell phenotype, including the downregulation of NKp30, NKG2D and DNAM-1, similar to that observed on the GBM infiltrating NK cells (chapter 3).

I hypothesised that the changes observed in vivo might also be due to GBM expressed TGF-β. To test this, NK cells were isolated from healthy donors and activated for 24 hours with IL-15. They were then washed and co-cultured with 80% confluent GBM stem cells (GBM4, GBM11 and GBM20) for between 24 and 72 hours (specifically, donor 1 24 hours; donor 2, 72 hours; donor 3, 48 hours). Activated NK cells incubated in GBM media were included as a control to account for changes in phenotype attributable to the different media used for culturing NK cells and GBM. The effect of co-culture on the expression of the activation marker CD69 and the activation receptors NKp30, NKG2D, DNAM-1 and NKp44 was analysed using flow cytometry (Figure 4.1). The results indicate that CD69 is expressed at high levels on IL-15 treated NK cells and that this expression was largely unaffected by co-culture with GBM (a slight downregulation of CD69 is seen for donor 2 and 3 when the NK cells are cultured with GBM4 and GBM20, Figure 4.1 top row).

However, more marked changes in expression of activation receptors was observed following co-culture; NK cells from all three donors showed downregulation of activation receptors to varying degrees when co-cultured with the GBM stem cells. The

most pronounced effect is seen in donor 1 whereby co-culture with all GBM cells leads to the decreased expression of NKp30, NKG2D and DNAM-1 (Figure 4.1 left column). This mimics the effects of the tumour microenvironment on NK cells observed in the patient samples (Figure 3.4).

Interestingly, not only do the donor NK cells show different levels of downregulation of activation receptors in response to the GBM cells, but they are also influenced in distinct ways by the individual GBM cells. For example, NK cells from donor 2 showed a down regulation of NKG2D, DNAM-1 and NKp44 when co-cultured with GBM11 cells but there was no expression change in NKp30 when compared to the IL-15 treated cells. In contrast, NK cells from the same donor co-cultured with GBM20 resulted in downregulation of NKp30, but the downregulation of NKG2D and DNAM-1 was not to the same extent as that seen with GBM11 co-cultured NK cells (Figure 4.1 middle column). Incubation of NK cells from donor 3 with any of the GBM cells caused a downregulation of NKG2D.

These experiment show that GBM stem cells are capable of modifying the NK cell surface phenotype *ex vivo*, and that the resultant phenotype broadly resembles that observed for GBM infiltrating NK cells (chapter 3).

However, inclusion of anti-TGF-β antibody or the TGF-β signalling inhibitor (SB431542) in similar co-cultures with the GBM cell line U87 (data not shown) failed to demonstrate a role for TGF-β in these effects and, coupled with the donor variation, the mechanistic basis for this modulation was not pursued further. However, this type of co-culture experiment has the future potential to uncover the mechanism by which GBM cells influence the NK cell phenotype.

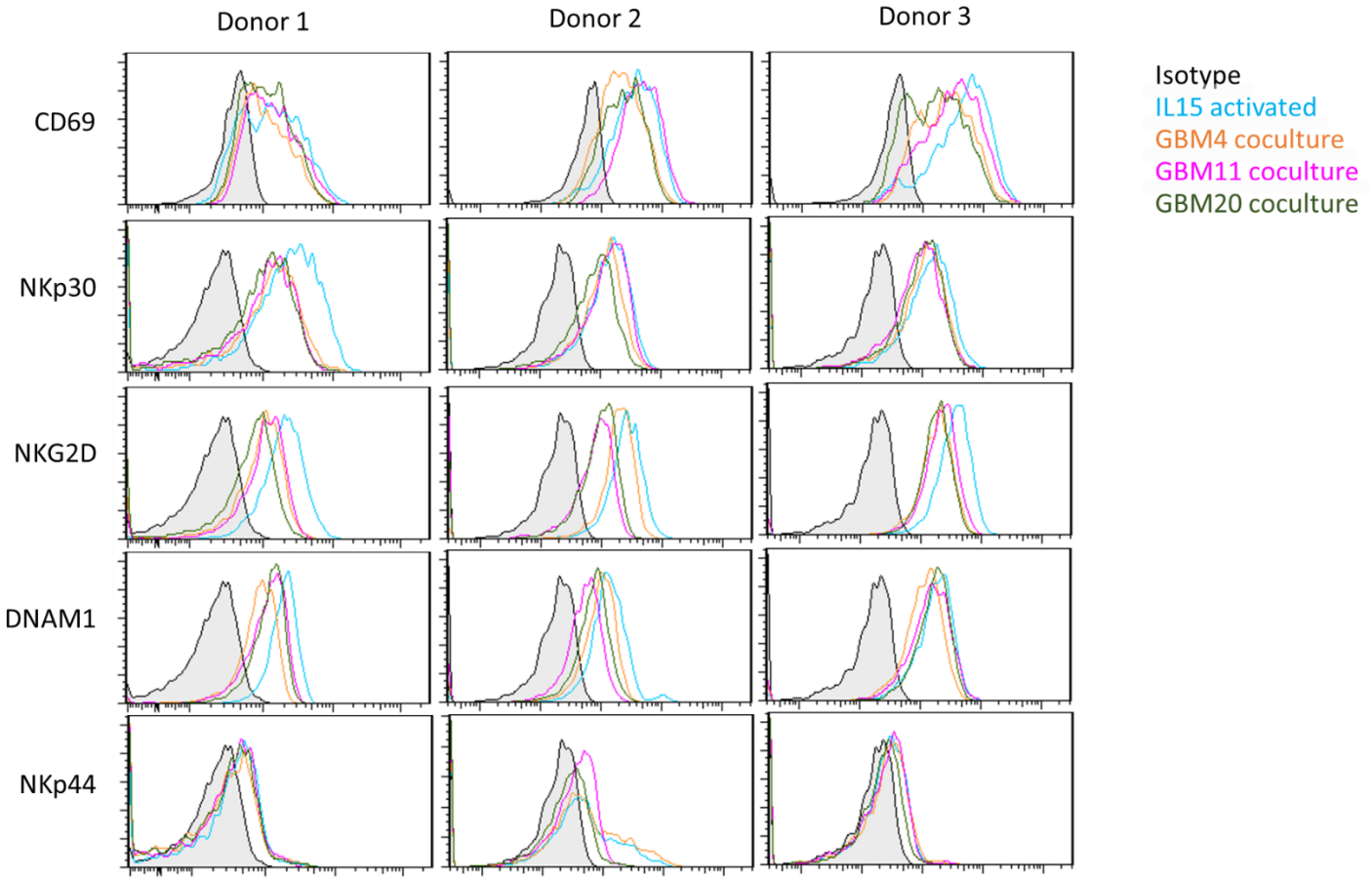

Figure 4.1. Phenotype of NK cells co-cultured with GBM stem cells. NK cells were activated with IL-15 and incubated with GBM stem cells for between 24 and 72 hours. NK cells were analysed using flow cytometry for the expression of the activation receptors shown. Isotype staining (shaded) shows nonspecific binding. Expression of each receptor is shown for cells treated with IL-15 alone (blue) or subsequently co-cultured with GBM4 (orange), GBM11 (pink) or GBM20 (green). Data from 3 experiments using 3 individual donors is presented.

4.3 Patient derived GBM stem cells are susceptible to activated NK cell killing

Having established that the GBM stem cells were capable of modulating the phenotype of activated NK cells, it was important to establish if their cytolytic function was also impaired. Three patient-derived GBM stem cell lines (GBM1, GBM4 and GBM20) were used as targets in cytotoxicity assays to assess the ability of NK cells to recognise and kill GBM cells in the absence of the immunosuppressive microenvironment. NK cell activation is dependent on the integration of both activating and inhibitory signals. To shift this balance to favour NK cell activation, freshly isolated NK cells from healthy donors were cultured with IL-15 prior to the assay. This treatment induces the cell surface expression of activation receptors NKp30, NKG2D and DNAM-1 (See chapter 5); receptors that were shown to be downregulated on the tumour infiltrating NK cells in the GBM resection samples (chapter 3).

Target cells were stained with a cell tracker dye and incubated with different ratios of activated NK cells (effectors). After 5 hours, the level of target cell death was assessed using a dead cell marker and flow cytometry (Figure 4.2a). A zero-hour time point was used as a control to account for non-NK mediated cell death. The experiment was repeated 3 times using NK cells derived from 3 individual donors. All primary GBM stem cells tested (GBM1, GBM4 and GBM20) were susceptible to NK mediated cell death (Figure 4.2b). A higher effector to target ratio correlated with an increase in target cell death. The results also exhibit different donor responses. For example, one donor (red dots on graphs in figure 4.2b) was able to kill a higher proportion of GBM1 and GBM4 cells compared to GBM20 cells and also compared to the other two donors. This variation in donor response can be explained by the fact that NK cells from different individuals can display different inhibitory KIRs (Valiante et al. 1997; Uhrberg et al. 2002).

These experiments demonstrate that activated NK cells are capable of killing primary GBM stem cells and suggests that immunotherapies that enhance NK cell activity might be beneficial for GBM patients.

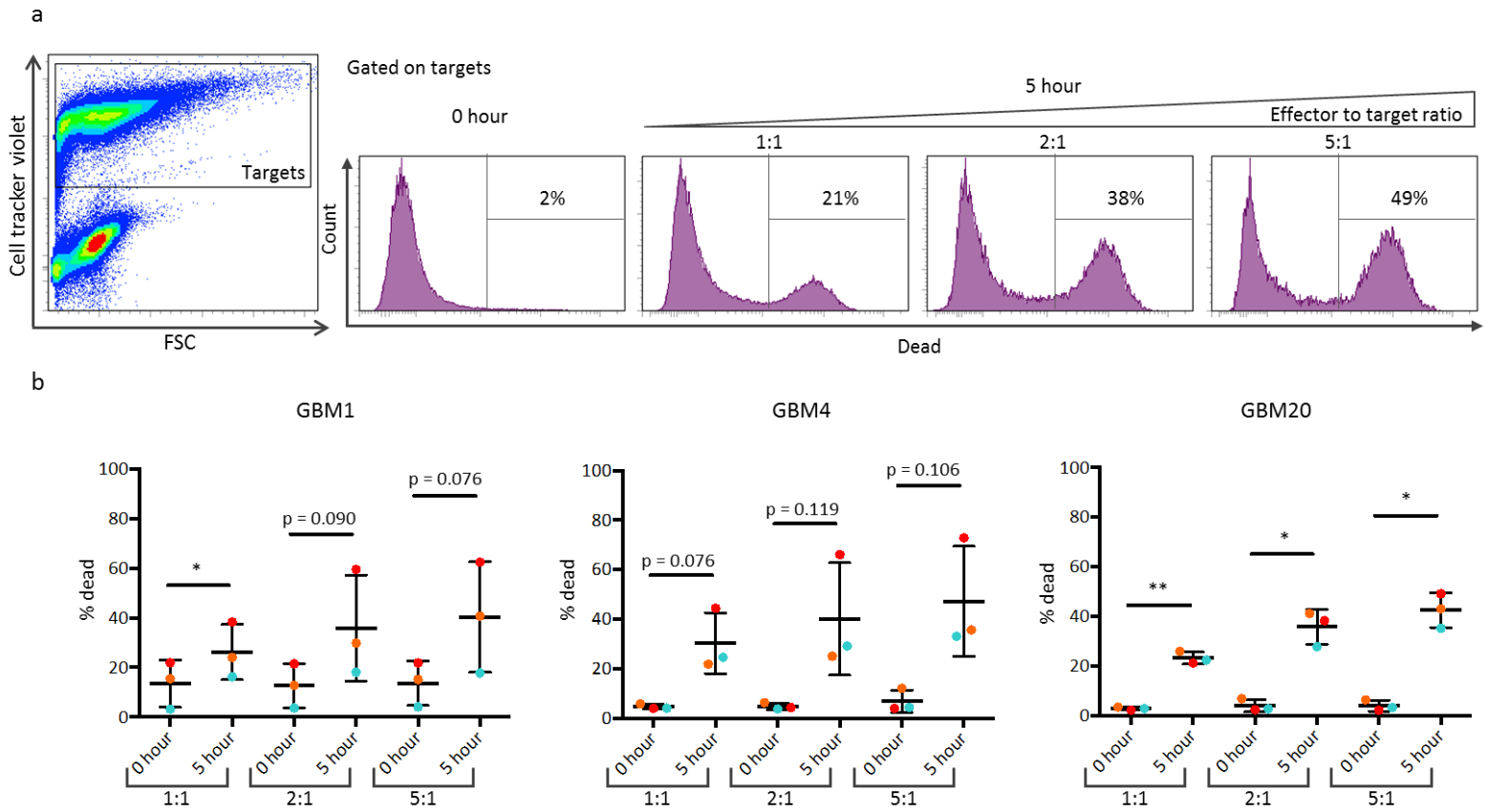

Figure 4.2. Cytotoxic assays. Effectors (activated primary NK cells) were incubated with stained targets (patient derived GBM stem cells) for 5 hours. After the 5 hour incubation period the cells were stained with a dead cell discriminator and assessed by flow cytometry. a) Cell tracker positive targets were identified (left) and cell death was analysed. The histograms show (from left to right) the 0 hour (control) and 5 hour time points with the increasing effector to target ratios; dose dependent killing was observed. b) GBM stem cells (GBM1, GBM4 and GBM20) were assessed for NK cell mediated cytotoxicity. The experiment was repeated with NK cells from 3 individual donors. Dots of the same colour (red, orange and blue) represent data for each donor. The bar indicates the mean± s.d. Statistical analysis was performed using paired t-tests. *P<0.05, **P<0.01.

4.4 GBM stem cell surface antigen screen

The results in figure 4.2 indicate that NK cells can detect (and kill) GBM cells. This implies that GBM cells express ligands for NK cell receptors and presumably ligands of other immune cell types. Furthermore, knowledge of cell surface phenotype of GBM cells could greatly improve our understanding of potential immune evasion strategies employed by the tumour that could underpin development of immunotherapies.

To analyse the GBM cell surface phenotype in detail, I performed a multiplex cell surface antigen screen using five patient-derived glioma stem cell lines (GBM1, GBM4, GBM11, GBM13 and GBM20). The multiplex screen utilises cell tracker dyes to label different cell types in a mixed population (Figure 4.3a). In this way, four cell types could be distinguished (Figure 4.3b) and simultaneously stained for 242 different surface antigens (Figure 4.3c). The screen was performed twice to allow five lines to be analysed. Cell lines screened on both occasions showed that the assay was reproducible (data not shown). Prior to the screen, optimisation was carried out to find the best combination of cell tracker dyes, antibody staining protocol and flow cytometer settings (data not shown). Data was acquired using an LSRII flow cytometer and analysed using BD FACSDiva and Beckman Kaluza software.

Antigens expressed on 20% or more of the cells were taken forward for further analysis. Figure 4.4 summarises the antigens expressed on the five glioma stem cell lines. The percentage expression for each antigen on the five cell lines is listed in Appendix 1. All five lines expressed 44 antigens in common including HLA molecules and CD56 (neural cell adhesion molecule, NCAM), which is a neural marker (Sundberg et al. 2009) as well as being expressed by NK cells.

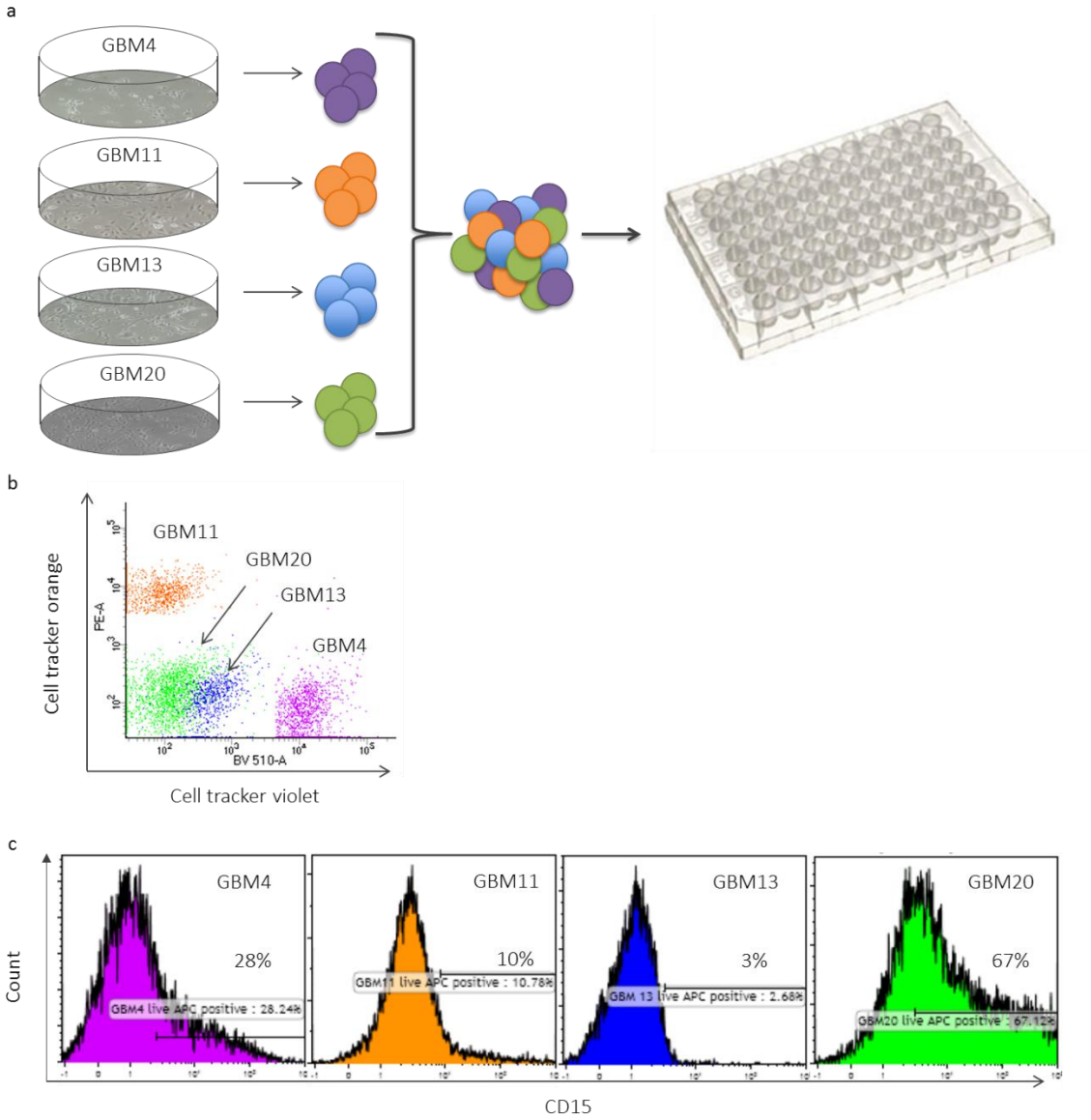

Figure 4.3. Multiplex surface screen. a) Cells were stained with different cell tracker dyes, mixed and aliquoted into 96-well plates. Each plate was subsequently stained for a panel of 242 different surface antigens (one antigen/well). b) Cells were analysed by flow cytometry. Live cells were identified by their morphology (FSC/SSC) and using a fluorescent dead cell discriminator. The cell tracker dyes enabled resolution of the different populations. The dot plot of the violet and orange channels shows separation of GBM11 (orange) and GBM4 (purple) cells. c) Viable cells were assessed for the presence of antigen. An Alexa Fluor 647 conjugated secondary antibody was used to detect the primary antibody bound to the surface protein and the signal acquired in the APC channel (640-680 nm). The histograms show an example of staining (CD15) for each of the four GBM lines used in the second screen.

a

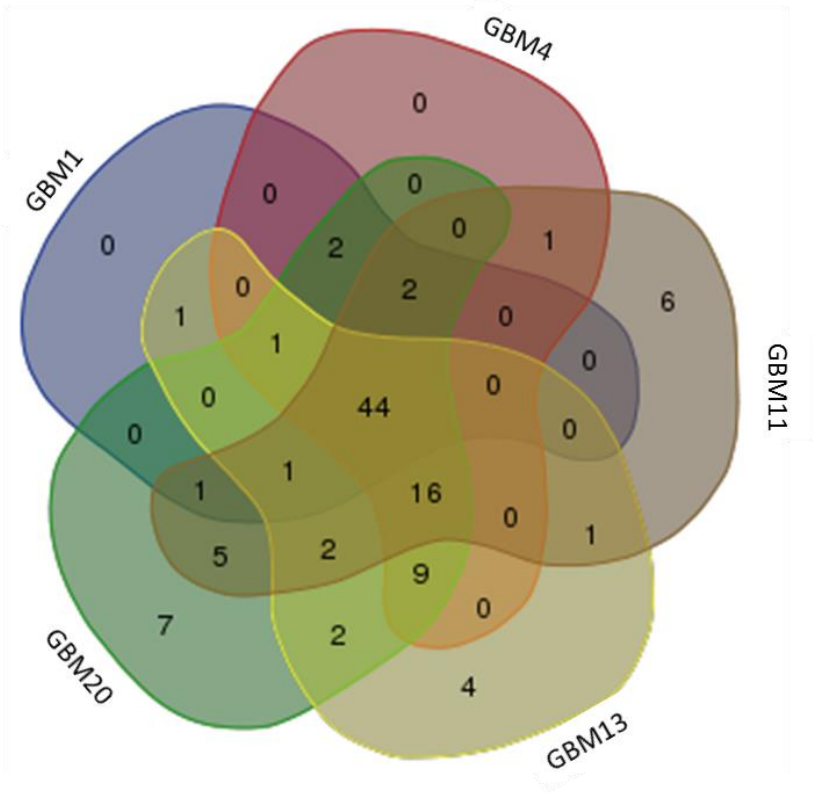

b

GBM stem cells	Total	Antigens (CD no. if applicable)
GBM1 GBM11 GBM13 GBM20 GBM4	44	9 26 29 34 44 46 47 49b 49c 49d 49e 49f 54 56 57 59 63 71 73 81 90 91 94 95 97 98 99 99R 107A 119 142 146 147 151 164 165 166 227 271 340 b2m GD2 HLA ABC HLA DQ
GBM1 GBM11 GBM20 GBM4	2	58 140A
GBM1 GBM13 GBM20 GBM4	1	200
GBM1 GBM11 GBM13 GBM20	1	321
GBM11 GBM13 GBM20 GBM4	16	49f 55 51/61 61 105 107B 112 120A 130 141 172B 184 221 268 274 338
GBM1 GBM20 GBM4	2	15 SSEA1
GBM1 GBM11 GBM20	1	106
GBM13 GBM20 GBM4	9	24 118 140B 152 209 220 egfr HLAA2 MICA/B
GBM11 GBM13 GBM20	2	77 80
GBM1 GBM13	1	49a
GBM11 GBM4	1	109
GBM11 GBM13	1	104
GBM11 GBM20	5	74 205 273 HLA DR HLA DRPQ
GBM13 GBM20	2	50 108
GBM11	6	10 38 40 62P 121B 201
GBM13	4	144 326 329 SSEA4
GBM20	7	75 88 120B 138 171 231

Figure 4.4. Multiplex surface screen. A large scale surface screen was performed using five GBM stem cell lines (GBM1, GBM4, GBM11, GBM13 and GBM20). a) The Venn diagram (generated with http://bioinformatics.psb.ugent.be/webtools/Venn/) details the number of antigens expressed on at least 20% of the cells. b) The table lists the antigens present within each section of the Venn diagram.

4.4.1 Bimodal populations

Flow cytometry allows the expression of antigens to be analysed across a population of cells. This allows heterogeneity of the cell population to be analysed and the expression of antigens within subpopulations to be determined. Bimodal peaks are indicative of two separate populations of cells in relation to a particular antigen. The multiplex screen revealed bimodal peaks as well as single peaks with a smaller shoulder population. For example, expression of human embryonic stem cell marker CD24 (Assou et al. 2007), the neural stem cell markers CD90 and CD184 (Sundberg et al. 2009) and other antigens such as CD15, CD138 and CD172b showed evidence of distinct populations of cells (Figure 4.5). The expression of the stem cell markers on GBM stem cells is not surprising, but their bimodal distribution suggests that the isolated cells exist as heterogeneous populations containing subsets of cells that are enriched with stem cell characteristics.

Interestingly, gene expression data for some of the antigens, including a few of those with a bimodal expression pattern, are associated with differential prognosis. The Repository of Molecular Brain Neoplasia Data (REMBRANDT) database (now housed in Georgetown University's G-DOC System) was used to produce Kaplan-Meier survival curves that assess the association between the mRNA expression level for each antigen and patient survival (Figure 4.6). In the REMBRANDT study, RNA was extracted from whole tumour tissue and information about which cells express the particular mRNA cannot be determined.

The results show that patients with down regulation of signal-regulatory protein beta-1 (SIRPβ1, CD172b) have a poorer survival outcome than patients with an intermediate or high level of expression of this molecule. Signal-regulatory proteins are immunoglobulin-like transmembrane glycoproteins involved in the regulation of leukocyte function (van Beek et al. 2005). SIRPβ1 generates a positive signal via the ITAM of DAP12 (Takizawa & Manz 2007). It is possible that the poor prognosis seen with a lower amount of SIRPβ1 is indicative of inactive immune cells. However, the screen showed expression of SIRPβ1/CD172b on the GBM stem cells themselves so maybe positive regulation of tyrosine signalling promotes cancer cell activities. Likewise, patients with low expression of CD80 had a worse prognosis; CD80 is involved in co-stimulation of T cells (Harris & Ronchese 1999) and a lack of CD80 in the

tumour microenvironment might prevent the activation of T cells, thereby enabling the tumour cells to evade T cell lysis. Although three of the cell lines, GBM4, GBM13 and GBM20, were positive for CD80, only 28%, 25% and 50% of the cells respectively were positive for the antigen. Cells expressing higher levels of CD80 (or other co-stimulatory molecules) are predicted to act as better stimulators of T cell responses, for example triggering CD8 cytotoxic cells. Thus, patients with tumours expressing lower levels of CD80 mRNA might exhibit poorer survival due to weaker T cell responses.

For both lymphocyte antigen 75 (Ly75, CD205) and intracellular adhesion molecule 3 (ICAM3, CD50), high expression within the tumour correlates with a worse prognosis. Ly75 is found on dendritic cells that are able to present antigens on both class I and II MHCs (Palucka & Banchereau 2012), enabling stimulation of other immune cells. Therefore, one might expect a high expression level to reflect more dendritic cells within the tumour that can process antigen, prime T cell responses in the lymph node and generate an anti tumour immune response, in turn improving prognosis. However, high expression of Ly75 has also been found in epithelial ovarian cancer and promotes a metastatic phenotype (Faddaoui et al. 2016). CD50 has been shown to be important for the recruitment of phagocytes to apoptotic lymphocytes and their subsequent clearance (Torr et al. 2012). Perhaps expression of CD50 could lead to recruitment of phagocytes to the tumour and lead to the elimination of anti tumour immune cells. Another pro-tumour role has also been proposed for CD50. An *in vitro* study using a NSCLC cell line overexpressing CD50 suggest it stimulates cancer cell migration and invasion pathways (Park et al. 2010). Clearly, the actual role of any of these molecules requires further study and elucidation of their function in regulating survival requires linking of survival data to expression of mRNA or protein in particular tumour or stromal cell types.

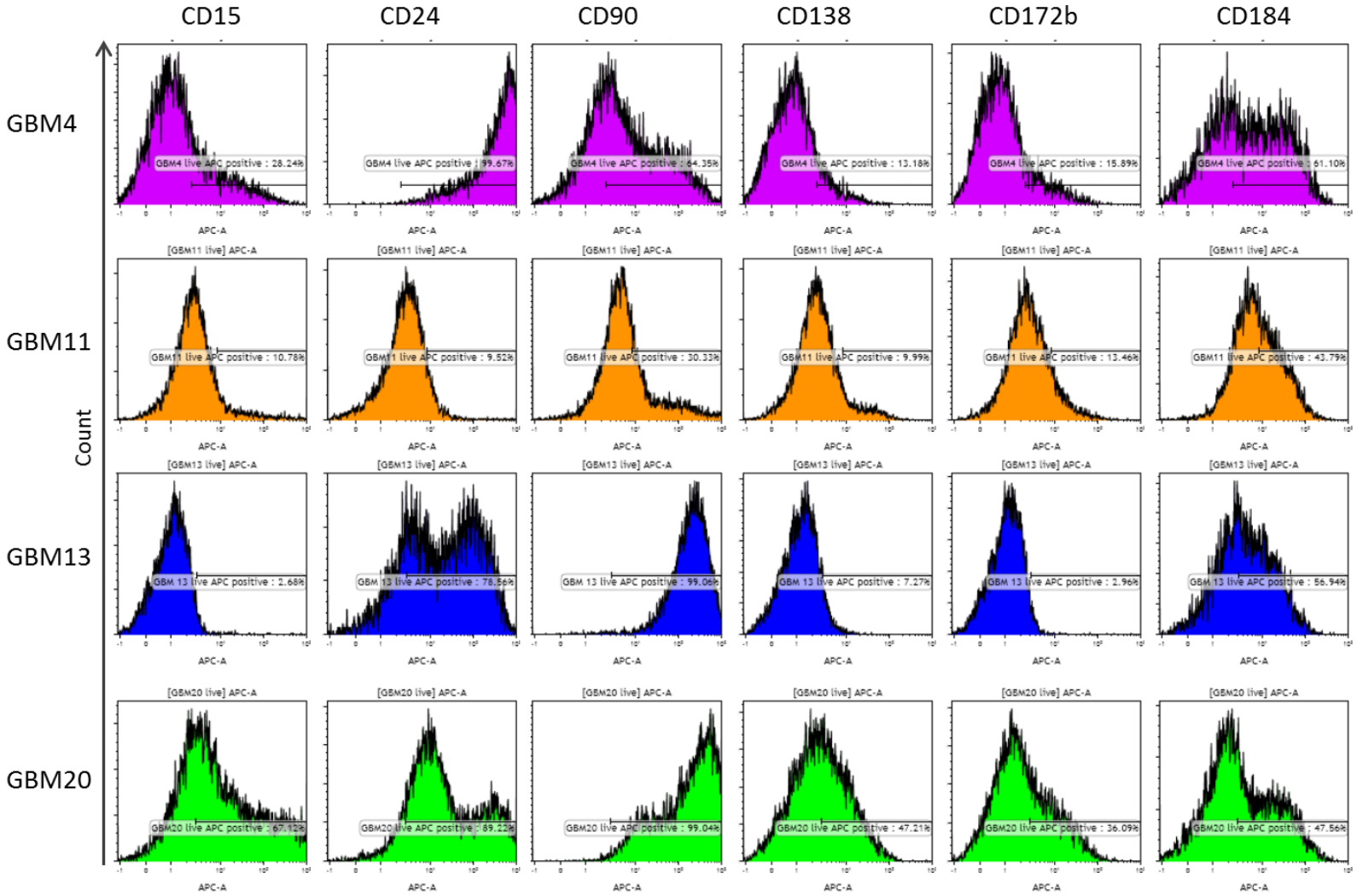

Figure 4.5. Bimodal populations. Histograms for the four GBM lines analysed simultaneously showing the expression of markers that exhibit bimodal or shoulder populations. These include stem cell markers CD15, CD24, CD90 and CD184 and other markers such as CD172b and CD138.

SIRPβ1 gene (CD172B)

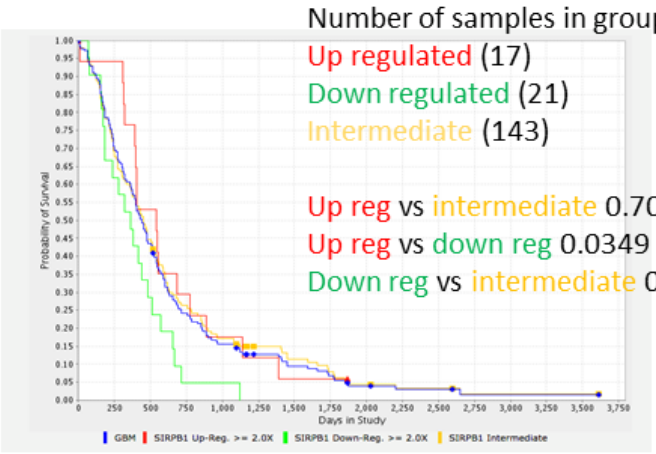

CD80 gene (CD80)

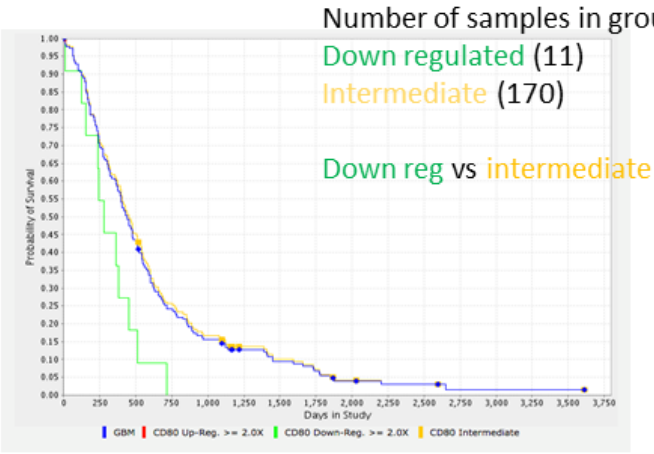

LY75 gene (CD205)

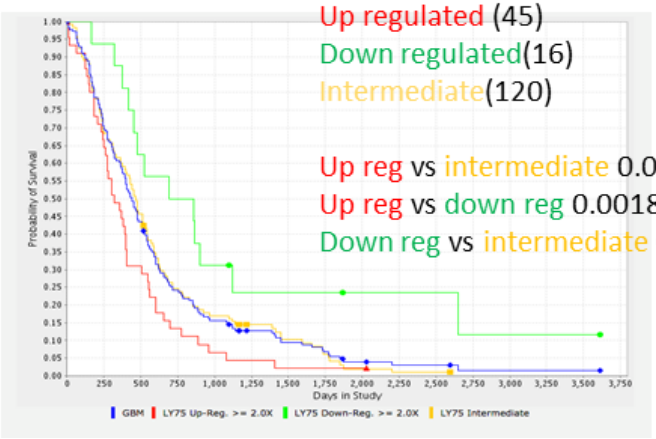

ICAM3 gene (CD50)

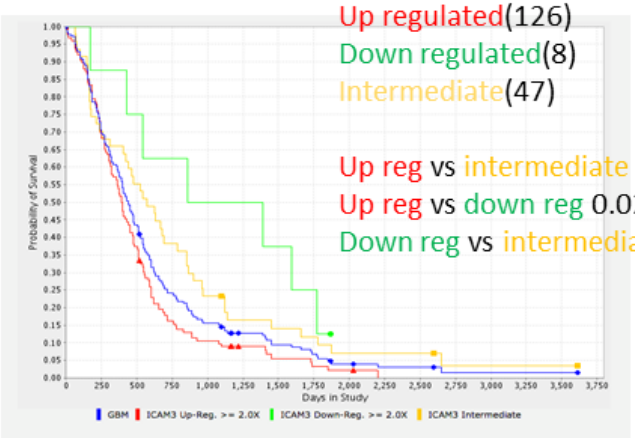

Figure 4.6. Kaplan-Meier survival plots for samples with differential mRNA expression for the genes (and antigens) listed. The REMBRANDT database was used to generate Kaplan-Meier plots that test for association of expression level (up regulated red, intermediate yellow, down regulated green) of each gene based on levels of mRNA extracted from tumour tissue and patient survival. Survival data for GBM patients is shown in blue. The number of samples analysed in each group is listed. The log-rank p-value (for significance of difference of survival between group of samples) is also listed (Institute National Cancer 2005).

4.4.2 Antigens of interest

Many of the antigens detected in the multiplex surface screen were of particular interest because they have previously been implicated in either immune regulation or immune evasion. These are summarised in figure 4.7 and include molecules such as MIC-A and Nectin-2 (CD112) which are ligands for the NK cell activation receptors NKG2D and DNAM-1 respectively. Supporting the detection of GBM and activation of NK cells via these receptor-ligand interactions are *in vitro* cytotoxic assays that use blocking antibodies to prevent receptor-ligand interaction and disrupt killing (Codo et al. 2014).

Antigens of interest for their immune evasion properties include CD73, programmed cell death ligands PD-L1 and PD-L2 and CD200. CD73 (an ectonucleotidase) is found on the membranes of anti-inflammatory immune cells (such as Tregs) and helps to limit the immune response by dephosphorylating AMP to generate adenosine (Antonioli et al. 2013). Adenosine mediates immune-suppressive and anti-inflammatory activities of Tregs by engaging with A_{2A} receptors on T cells (Deaglio et al. 2007), causing inhibition of effector functions of activated cells (Huang et al. 1997). Increased CD73 mRNA has previously been reported in glioma cells compared to normal astrocytes (Wink et al. 2003). However, analysis of the REMBRANDT database reveals that CD73 mRNA levels are not associated with survival (data not shown).

Another protein that keeps the immune response in check and is exploited by cancer cells to avoid immune destruction is PD-1/CD279 (Jadus et al. 2012; Zou & Chen 2008). This molecule is expressed on B cells, NK cells, dendritic cells, monocytes and T cells (Keir et al. 2008). Its ligands, which include PD-L1/CD274 and PD-L2/CD273, were detected on the tumour cells in the screen (Figure 4.4 and appendix 1); these ligands suppress TCR activation and reduce T cell survival, cytokine production and proliferation (Rozali et al. 2012). The use of antibodies targeting the receptor for PD-L1 (PD-1) have shown promising results in clinical trials to treat metastatic melanoma (NCT01927419) and similar trials are underway for patients with GBM (NCT02617589, NCT02017717, NCT02529072). Importantly, results in chapter 3 demonstrated that GBM infiltrating T cells expressed high levels of PD-1 compared to their counterparts in patient blood (Figure 3.5). Detection of the PD-1 ligands, PD-L1 and PD-L2 on the GBM cells themselves indicates that tumour infiltrating T cells will likely be inhibited via the

PD-1:PD-L1/PD-L2 interactions. Indeed, patients expressing high levels of PD-L1 have a worse prognosis (Nduom et al. 2016). This provides a rationale for the use of anti-PD-1 antibodies (e.g. Nivolumab and Pembrolizumab) in this disease. Optimal T cell activation requires engagement via the TCR and via co-stimulatory molecules. Whilst GBM cells express high levels of MHC class I (for antigen presentation to the TCR; Figure 4.4 and appendix 1), I did not detect expression of CD86 and four out of the five lines tested had low or no expression of CD80 (Figure 4.4). Both proteins are known ligands for the costimulatory T cell antigen CD28. This surface antigen screen suggests that GBM cells have a cell surface phenotype that is consistent with inhibiting T cell activity rather than stimulating anti-tumour immunity.

CD200 is a membrane glycoprotein that plays an important role in immunosuppression and regulation of anti-tumor activity (Kretz-Rommel et al. 2007). Overexpression of CD200 correlates with poor prognosis in many human blood cancers (McWhirter et al. 2006; Moreaux et al. 2006; Tonks et al. 2007) and has been directly linked with the suppression of NK cells (Coles et al. 2011). CD200 was expressed on GBM1, GBM4, GBM13 and GBM20 and possibly contributes to NK cell evasion.

Some of the antigens detected in the screen are the targets of current antibody therapies, or receptors for oncolytic viruses (Figure 4.7). For example, CD340/HER2 is targeted with Trastuzumab (best known for its role in the treatment of breast cancer; (Romond et al. 2005; Piccart-Gebhart et al. 2005). The CD33 antigen is targeted by the antibody Gemtuzumab and an antibody-drug conjugate known as Gemtuzumab ozogamicin (Mylotarg) has been used to treat acute myelogenous leukaemia (Cohen et al. 2002). EGFR is targeted by Cetuximab as part of existing therapies for several tumours, including colorectal cancer (Scott et al. 2012). Although EGFR was expressed on GBM4, GBM13 and GBM20, it was not detected in the screen for GBM1 and GBM11. However, EGFR is frequently mutated in human gliomas, and 20-25% of GBM express the EGFRvIII variant (Kogiku et al. 2008; Saikali et al. 2007; Xu et al. 2009). This is a glioma stem cell associated antigen and is being developed as an antigen for use in dendritic cell based immunotherapy for GBM treatment (Sampson et al. 2009). The antibody used in the screen does not detect the mutated variant. The expression of therapeutic antibody targets on the GBM cells may be of relevance to future therapeutic strategies. However, whilst immune cells can cross the blood brain barrier

via the dynamic process of transendothelial migration, molecules greater than 500 Daltons in size (equivalent to a four or five amino acid peptide) are prevented from entering the brain under normal conditions (an IgG antibody has a molecular weight of approximately 150 kDa). However, the blood brain barrier is much less selective in the presence of GBM, evidenced by a higher accumulation of temozolomide (Rosso et al. 2009) and contrasting agents (Zhou & Lu 2013) in glioma tissue compared to normal brain. In addition, strategies are being developed to enhance the permeability of the blood brain barrier for therapeutic delivery (e.g. the localised delivery of TNF to enhance endothelial permeability; (Connell et al. 2013) and focused ultrasound (Rodriguez et al. 2015). The use of bevacizumab (anti-VEGF) in patients changed the vessel morphology within the tumour (Lampson 2011), suggesting that antibodies are able to gain access to the tumour.

The reovirus receptor, CD321 (also known as JAM-A, JAM1 and F11R) was expressed on GBM1 (22%), GBM11 (20%), GBM13 (84%) and GBM20 (42%) but was not detected for GBM4. The presence of the receptor indicates the possibility that reovirus could be used in the treatment of GBM as in many other cancer types where it has reached stage III clinical trials (Adair et al. 2012). Importantly, reovirus (and other oncolytic viruses) exert anti-tumour activity via (at least) two distinct mechanisms; direct killing of the tumour cell upon infection and replication and the promotion of anti-tumour immunity (Turnbull et al. 2015). Reovirus stimulates human NK cell activation *in vivo* (El-Sherbiny et al. 2015) and Reovirus reaches GBM tumours after intravenous delivery (Alan Melcher, personal communication). This suggests that Reovirus might prove a useful therapeutic agent to treat GBM. High expression (above 89%) of CD46 was observed on all of the GBM cell lines screened. The CD46 molecule is a receptor for group B adenoviruses (Gaggar et al. 2003) which are being developed as vectors for cancer gene therapy (Wold & Toth 2013). This too might lend itself for the development of new GBM therapies.

Cancer stem cell markers for solid tumours were observed in the screen. These included those identified in glioma, such as CD98 and CD90, and those that are presented by other tumours; CD44 (breast, colon, liver, ovarian, pancreatic and prostate), CD26 (colon) and CD24 (breast, colon, liver, ovarian and pancreatic) (Medema 2013). Expression of CD98 predicts poor prognosis in many cancers as it

promotes survival, growth and metastasis (Cantor & Ginsberg 2012). Interestingly, ovarian cancer cells bearing CD24 were found to be resistant to chemotherapy yet preferentially lysed by NK cells (Koh et al. 2012). If the same is true of GBM, then assessing CD24 expression at the time of resection might predict the response to subsequent chemo- or immunotherapies.

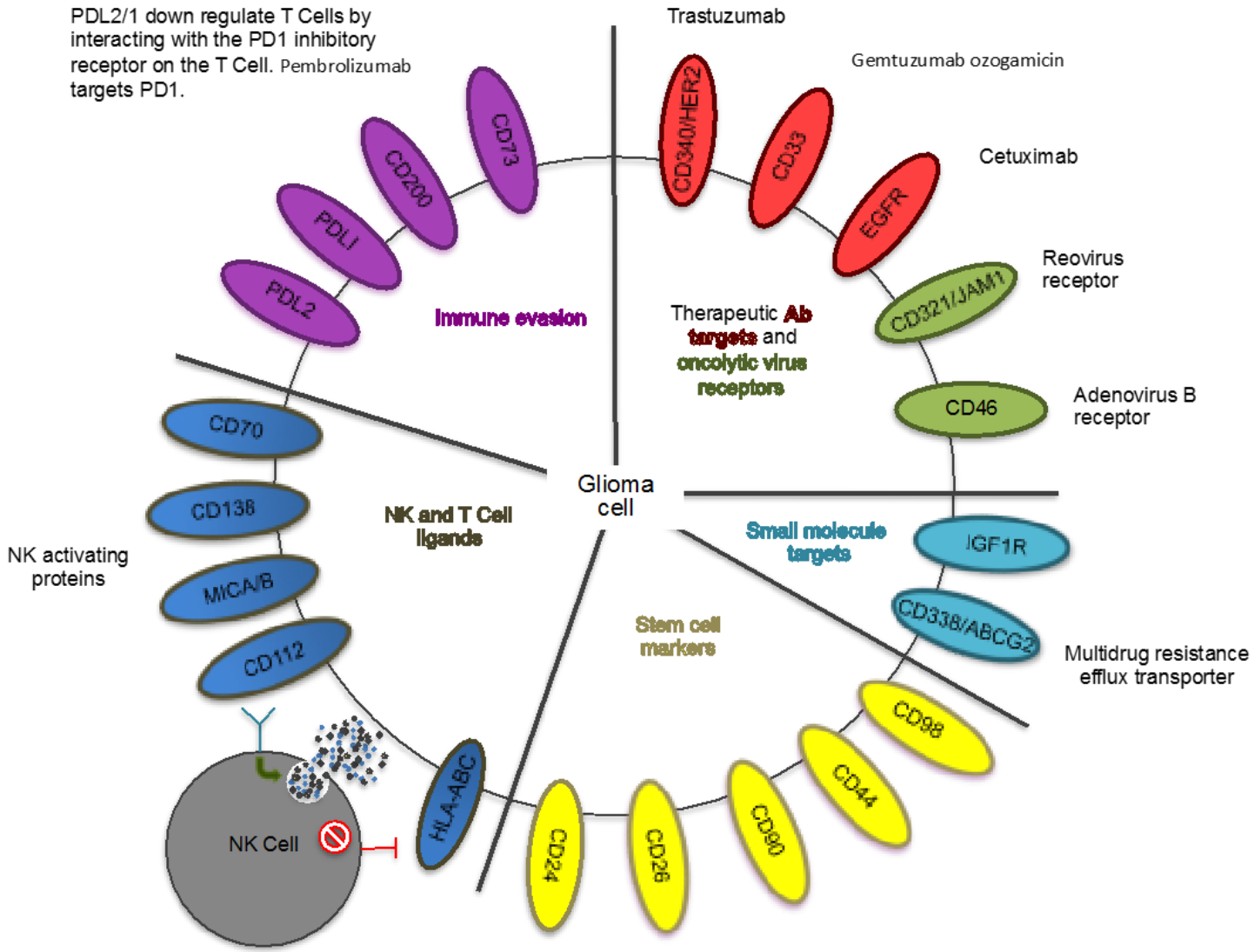

Figure 4.7. Antigen expression on GBM stem cells grouped into functional categories. A selection of screen hits classified into functional categories; immune evasion, T cell and NK cell ligands, stem cell markers, small molecule targets, antibody targets (antibodies are listed) and oncolytic virus receptors.

4.5 Characterising neural progenitor cells

Successful cancer therapies must target the tumour cells, but spare non-transformed healthy cells. This is especially important in the brain where damage to healthy cells could result in severe morbidity. Highly sophisticated mechanisms employed by the immune system ensure that responses are specific to infected or malignant cells. Hence, exploitation of the immune system is of great interest for the development of cancer therapies. However, the immune system is not fool proof, and it can damage healthy tissues, as shown by the prevalence and severity of autoimmune and autoinflammatory diseases, including those occurring in the brain, such as multiple sclerosis (Goldenberg 2012). The immune response to cancer cells is, by definition, an autoimmune reaction (or at least, a response to altered self) and effective tumour elimination with minimal collateral damage is a challenge.

To address the specificity of NK cells towards tumour cells compared to healthy brain tissue, I made use of non-malignant, neural progenitor cells. Characterising non-malignant, neural progenitor cells was undertaken to identify potential immune cell interactions that help protect these stem cells from an immune response. The cells studied (NP1) were derived from an epilepsy patient (without cancer). The NP1 cells were established by the Wurdak group using the same method to isolate the GBM stem cells. The GBM cell lines express the stem cell markers CD24 (GBM4 99%, GBM13 78% and GBM20 89%), CD90 (GBM1 81%, GBM4 64%, GBM11 30%, GBM13 99%, GBM20 99%) and CD184 (GBM4 61%, GBM11 44%, GBM13 57% and GBM20 48%) (Figure 4.5 and appendix 1) and flow cytometry showed that these molecules were also expressed to a similar level by the NP1 cells (CD24 72%, CD90 99% and CD184 44%) (Figure 4.8), indicating a degree of similarity between the malignant GBM cells and the normal NP1 cells.

The expression of ligands for the NK cell activation receptors DNAM-1, NKG2D and NKp30 was also assessed. Surprisingly, NP1 cells expressed high levels of Nectin-2 (CD112) and ULBP1 (Figure 4.8), which are ligands for DNAM-1 and NKG2D respectively. Lower levels of a second NKG2D ligand, MIC-A/B (Figure 4.8), and the NKp30 ligand, B7H6 were also detected. The expression of these molecules suggests that the NP1 cells would be susceptible to NK cell cytotoxicity. However, the NP1 cells also express high levels of HLA class I proteins; these interact with KIRs and other

inhibitory receptors to downregulate NK cell activity. Interestingly, the PD-1 ligands, CD274 (PD-L1) and CD273 (PD-L2) were also expressed by the NP1 cells (99% and 58% respectively) (Figure 4.8); this suggests that NP1 cells might inhibit the activity of T cells.

Having established that NP1 cells display ligands for both activating and inhibitory NK cell receptors, functional assays were performed to assess if these non-malignant neural progenitor cells were susceptible to NK cell cytotoxicity.

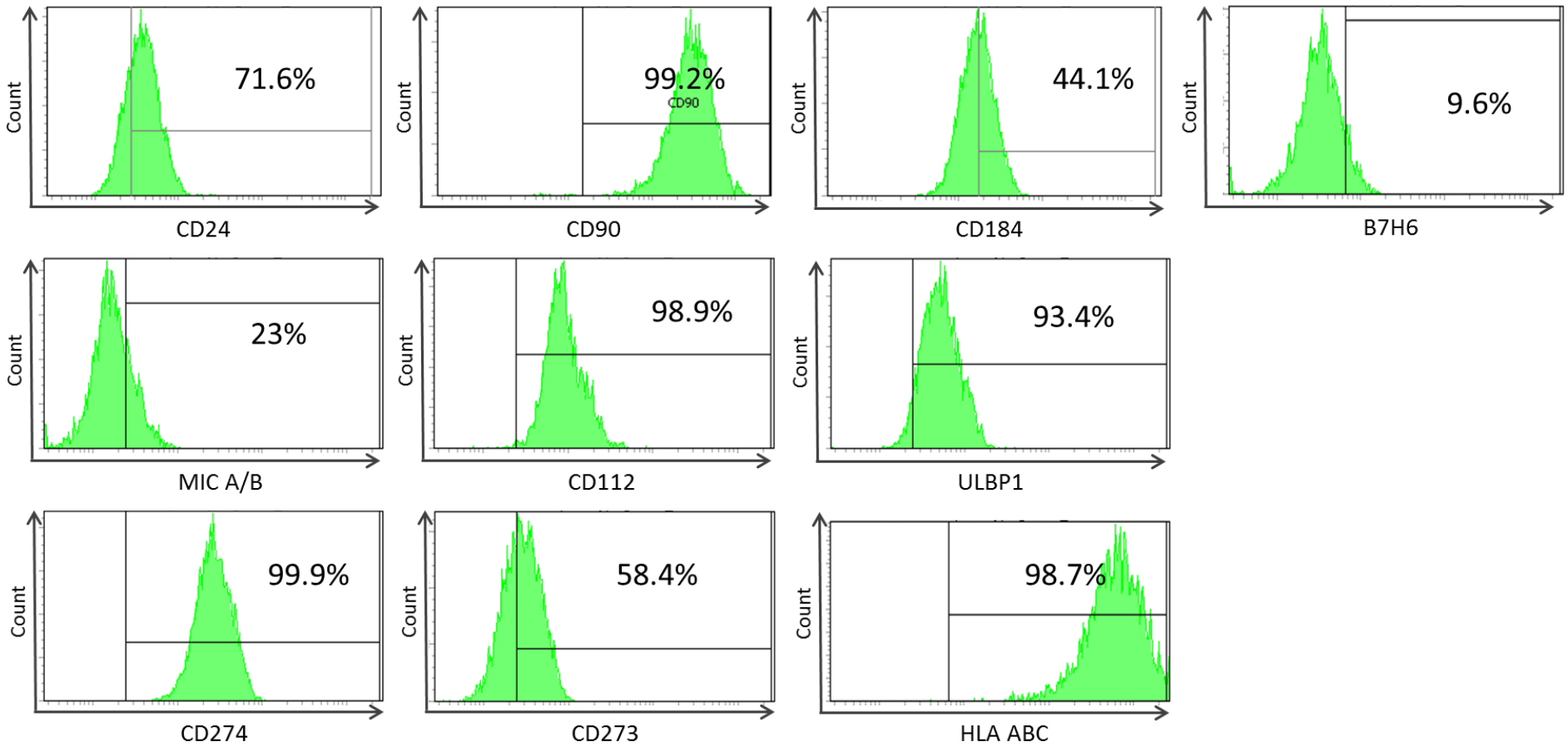

Figure 4.8. Neural progenitor (NP1) phenotype. NP1 cells were tested for stem cell markers and NK and T cell ligands using flow cytometry. The gates were set at 2% of the isotype control stain. Data is representative of three separate analyses.

4.6 Selective killing of GBM stem cells

In section 4.2 above, I demonstrated that activated NK cells can kill GBM stem cells *ex vivo* (Figure 4.2), supporting the hypothesis that immunotherapies which restore NK cell function might benefit GBM patients. However, the expression of NK cell activation ligands by NP1 neural progenitor cells (Section 4.5; Figure 4.8) suggests that non-malignant cells in the brain might also be susceptible to NK cell mediated death. This could cause severe side effects during immunotherapy. It was therefore paramount to compare the capacity of NK cells to selectively target the GBM stem cells.

To directly compare the susceptibility of the GBM and NP1 cells in a mixed population (as would be found in a brain tumour), I modified the standard cytotoxicity assay. GBM stem cells (GBM) and neural progenitors (NP) were stained with different cell tracker dyes and then mixed in a 1:1 ratio to provide the target cells (denoted GBM+NP1). Green and violet cell tracker dyes were used to identify the GBM+NP1 targets. These dyes did not affect cell death; neither directly, nor by making them more susceptible to NK cell mediated cytotoxicity (data not shown). Donor derived NK cells (effectors) were activated with IL-15 and incubated with the GBM+NP1 targets for 5 hours at an E:T ratio of 5:1. After the 5 hour incubation period, the cells were stained with a dead cell discriminator and assessed by flow cytometry. Death of the GBM and NP cells due to NK cell activity was calculated as the difference between the 5 hour and 0 hour samples.

Competitive assays were performed with three GBM stem cell lines (GBM1, GBM4 and GBM20) paired with the neural progenitor cells (NP1). The experiments were repeated using NK cells from a minimum of three donors. The same trends are observed for all pairings (Figure 4.9); at the zero-hour time point a similar, minimal cell death is recorded for both cell types (Figure 4.9a left). However, after 5 hours the proportion of GBM cells that have been killed is far greater than the proportion of NP1 cells. This difference was statistically significant for GBM4+NP1 cells, but the pattern is also evident (but not statistically significant) for the GBM1+NP1 and GBM20+NP1 pairs (Figure 4.9b). These results show that, despite expressing ligands for NK cell activation receptors, the non-malignant neural progenitors are more resistant to NK mediated cytotoxicity than the GBM stem cells. This indicates that NK cell based

immunotherapies might be effective at targeting the GBM stem cells but sparing others.

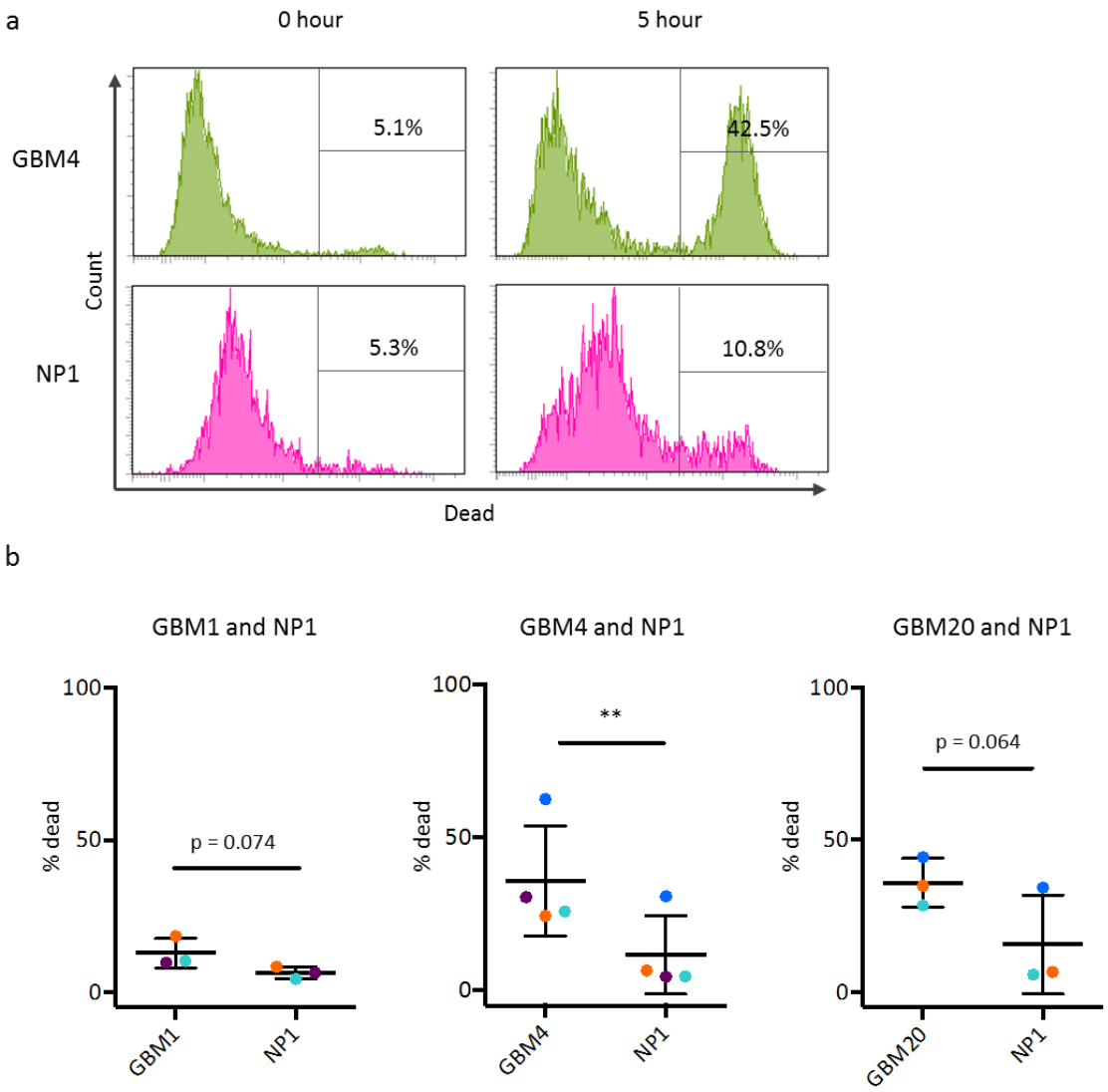

Figure 4.9. Competitive cytotoxicity. GBM stem cells (GBM) and neural progenitors (NP) were stained with different cell tracker dyes and mixed in a 1:1 ratio to collectively be the target cells. Effectors (activated primary NK cells) were incubated with the targets for 5 hours at an E:T ratio of 5:1. After the 5 hour incubation period the cells were stained with a dead cell discriminator and assessed by flow cytometry. a) Cell tracker positive targets were identified and the NK cell mediated death was calculated by subtracting the 0 hour time point from the 5 hour time point. b) A comparison of NK cell mediated cytotoxicity was made between GBM stem cells and neural progenitors. The experiment was repeated with NK cells from at least 3 individual donors. Dots of the same colour represent data for each donor. The bar indicates the mean± s.d. Statistical analysis was performed using paired t-tests. *P<0.05, **P<0.01.

4.7 Discussion and conclusion

In chapter 3, I showed that the cell surface phenotype of NK cells infiltrating GBM tumours was altered compared to NK cells from the patients' blood. A similar phenotype was observed when IL-15 treated cells were co-cultured with GBM cells *in vitro*. The downregulation of NK cell activation receptors observed in the tumour microenvironment suggests that NK cells in the tumour are less responsive or inhibited. This suggests that therapies that prevent NK cell inhibition in the tumour microenvironment might enhance the anti-tumour response for patients with GBM. However, for the NK centred immunotherapies to be effective, the NK cells must be capable of killing the tumour cells once the immunosuppressive brakes of the tumour microenvironment are lifted and show specificity for the tumour.

In vitro cytotoxic assays using IL-15 activated NK cells from healthy donors revealed that NK cells successfully kill primary GBM stem cells (Figure 4.2). This finding supports an existing publication that used both IL-2 and IL-15 activated NK cells to target glioma stem cells (Castriconi et al. 2009). Without the use of activating cytokines, patient-derived GBM cells are largely resistant to NK cell lysis (Friese et al. 2003; Wischhusen et al. 2005). In these published studies, NK cell cytotoxicity was enhanced by the plasmid-mediated or adenovirus-mediated overexpression of the NKG2D ligand, MIC-A, on the target cell (Friese et al. 2003) or by downregulating HLA-E, which interacts with the inhibitory NKG2A/CD94 heterodimer (Wischhusen et al. 2005). Although previous studies have shown that GBM cells are susceptible to NK cell mediated killing, to the best of my knowledge there are no published studies comparing the ability of NK cells to recognise and respond to GBM stem cells in comparison to their non-malignant counterparts. This is very important because immunotherapies must be able to specifically target the cancer cells to minimise collateral damage to healthy brain cells.

To assess the specificity of activated NK cell cytotoxicity towards transformed cells, competitive killing assays were carried out. A non-malignant neural stem cell line (NP1) was used in conjunction with three different primary GBM stem cell lines. In all cases selective killing of the GBM stem cells over the non-malignant cells was seen (Figure 4.9). Even when artificially skewed to an activated status (with IL-15), NK cells still kill

target cells in a very specific manner. Interestingly, a recent report using a multiple sclerosis mouse model showed that neural stem cells produce IL-15 and can sustain functionally competent NK cells (Liu et al. 2016). The NK cells used in the cytotoxic assays described here had already been activated with IL-15, but it would be interesting to see if co-culture with NP1 cells could enhance GBM cell lysis via endogenous IL-15 production.

Previous studies that have investigated the susceptibility of neural stem cells to NK cell lysis, with a view to develop neural stem cell therapy for untreatable neurological or psychiatric diseases, have shown conflicting results. One study concluded that neural stem cells do not express MHC antigens and are susceptible to NK cell lysis by recognition of lack of self MHC and also expression of NKG2D ligands, Rae-1, H60 and MULT-1 (Phillips et al. 2013). In contrast, a second study found that despite marginal expression of MHC class I and II on neural stem cells they are not susceptible to NK cell lysis, even when activated with IL-2 (Mammolenti et al. 2004). The agreement between these studies is that neural stem cells lack MHC antigens. This contradicts my results; whereby high levels of HLA class I were observed on the NP1 cells (Figure 4.8). However, these previous studies were both performed in mice and a recent study using human neural stem cells showed similar expression of HLA class I that I report (Schmitt et al. 2015). This study also concluded that HLA-G expression was important for inferring NK cell resistance.

Further characterisation of the NP1 cells revealed high expression of Nectin-2 (CD112) and ULBP-1 which are ligands for NK cell activation receptors DNAM-1 and NKG2D respectively (Figure 4.8). An antibody that detects both MIC-A and MIC-B also showed moderate staining (23%) on NP1 cells. Despite the high expression of these activating ligands, NP1 cells were largely resistant to NK cell lysis. NK cell activation occurs when signals from activating receptors outweighs those from inhibitory ones. The high expression of MHC class I molecules by NP1 is predicted to block the activation signals delivered by DNAM-1 and NKG2D ligands. However, all GBM stem cells also express high levels of MHC class I and the difference in the susceptibility of GBM cells and NP1 cells to NK cells presumably lies with differences in the expression of ligands that activate NK cells. The expression of NKG2D ligands is coupled to the malignant phenotype; DNA damage induces ATM/ATR dependent expression of NKG2D ligands (Gasser et al. 2005), allowing NK cells to detect damaged cells. However, NKG2D

ligands are also upregulated during the cell cycle via E2F (Jung et al. 2012). Hence, any cells maintained in culture are likely to induce expression of NKG2D ligands and this mechanism might be responsible for the expression of ULBP1 and MIC-A/B on the NP1 cells.

The cytotoxicity data demonstrate that GBM cells are selectively targeted in preference to normal neural progenitor cells. A limitation of these experiments is that the NK cells, NP1 cells and GBM cells used in the assays are all derived from different donors. The polymorphism of MHC class I molecules and KIRs means that it is theoretically possible that MHC class I molecules from one donor do not inhibit NK cells from a different donor. Hence, it is possible that the resistance of the NP1 cells results from the expression of MHC class I molecules that inhibit all three donors, whereas the GBM cells express MHC class I molecules that do not inhibit the donor NK cells. In reality, such a scenario is highly unlikely as most donors possess between 6 and 16 different KIRs with several KIRs common to many donors (Uhrberg et al. 2002).

To investigate other potential immune modulating proteins and to better characterise the GBM stem cells a large scale surface screen was carried out. Five patient derived GBM stem cell lines established by the Wurdak group were analysed. The expression of CD112 and MICA/B (ligands of DNAM-1 and NKG2D respectively) was initially detected during the GBM surface antigen screen on most of the GBM stem cells (CD112 on GBM4/11/13/20, MICA/B on GBM4/13/20) (Figure 4.4). This antigen screening assay highlighted the expression on GBM cells of several proteins with the potential to modulate anti-tumour immunity or act as therapeutic targets (summarised in Figure 4.7).

The very existence of GBM tumours shows that they are able to evade the immune system. The previous chapter presented evidence of immunosuppressed GBM infiltrating NK cells and thus supports the rationale for developing NK cell based immunotherapies. Data presented in this section shows that NK cells skewed to an activated status are not only capable of killing GBM stem cells, but that they preferentially kill GBM cells over non-malignant neural stem cells. The surface screen helped characterise the GBM stem cells and revealed proteins that could influence cell fate *in vivo* or that are interesting for other immune based therapies.

In the next chapter, I examine the effects that glucocorticoids, which are currently used to treat the cerebral oedema experienced by many brain tumour patients, have on the phenotype and function of NK cells.

Chapter 5 Steroid mediated NK cell immunosuppression

5.1 Introduction

The data presented in chapters 3 and 4 supports the rationale for developing NK based immunotherapies for the treatment of GBM. However, GBM patients often experience complications such as cerebral oedema, which if left untreated, can be fatal. Cerebral oedema is treated with corticosteroids such as dexamethasone, which are well known for their powerful anti-inflammatory properties; using corticosteroids is likely to render immunotherapy ineffective (Zitvogel et al. 2008). It is remarkable that, despite the fact that corticosteroids have been used in clinic to treat cerebral oedema since the early 1950s (Ingraham et al. 1952), their exact mechanism of action remains unclear. An understanding of how glucocorticoids affect NK cells is required in order to design immunotherapies that are effective in the presence of concomitant lifesaving steroids.

Chapter 3 demonstrated that the phenotype of GBM infiltrating NK cells mirrored that of NK cells that had been treated with TGF-β (Wilson et al. 2011). In this chapter I compare the action of TGF-β, which is detected within GBM tumours (Joseph et al. 2013), with that of dexamethasone, the predominant corticosteroid used to alleviate cerebral oedema in to brain tumours and methylprednisolone, which is used in the treatment of other cancers.

5.2 TGF-β, dexamethasone and methylprednisolone prevent the IL-15 induced activated phenotype

To assess potential immune regulatory effects of corticosteroids on NK cells, freshly isolated NK cells from healthy donors were treated with dexamethasone or methylprednisolone, either alone or in conjunction with IL-15. TGF-β prevents the IL-15 induced upregulation of activation receptors such as NKp30, NKG2D and DNAM-1 and was used as a positive control for NK cell inhibition. The NK cells were treated for 48 hours and assessed for the expression of 7 activation receptors using flow cytometry (Figure 5.1). An isotype control antibody was used to assess non-specific antibody binding. Unstimulated NK cells (resting) were included as a control to measure the basal level of antigen expression. A physiological concentration of TGF-β

(5 ng/mL) was used (Porreca et al. 2002; Fogel-Petrovic et al. 2007) and dexamethasone (2 x 10^{-7} M) and methylprednisolone (2 x 10^{-6} M) were used at a concentration achievable in patients receiving these agents (Kostaras et al. 2014; Baylis et al. 1982). Within the reported range, the minimum concentration that could effectively prevent IL-15 induced CD69 upregulation was used. A time course experiment was also carried out; this revealed that the greatest change in receptor expression occurred at 48 hours. The experiment was repeated with a minimum of NK cells from 3 donors. Results are summarised in figure 5.2.

One of the most striking differences between IL-15 treated cells and those dual treated with IL-15 and dexamethasone or TGF-β, is the change in morphology assessed by flow cytometry (Figure 5.3). When NK cells are treated with IL-15 their size and granularity increase (Figure 5.3). This is known to correlate with an increase in their metabolic activity (Marçais et al. 2014). Both TGF-β and dexamethasone curtail the IL-15 induced morphological changes, suggesting that they prevent the IL-15 mediated increases in metabolic activity.

Figure 5.2 shows that TGF-β, dexamethasone and methylprednisolone all prevent the upregulation of CD69 that is seen with IL-15 treatment. CD69 is one of the first surface expressed proteins displayed subsequent to activation (Ziegler et al. 1993); this result suggested that TGF-β, dexamethasone and methylprednisolone all inhibit NK cell activation.

In addition to inhibiting CD69, steroids and TGF-β also inhibited the IL-15 mediated induction of NKp30 and NKG2D. The same pattern was observed for DNAM-1, NKp46 and CD132 (IL-2 receptor subunit gamma), even though the levels of IL-15 induction were much lower (Figure 5.2). These results demonstrate that TGF-β and the glucocorticoids dexamethasone and methylprednisolone were able to inhibit the IL-15 mediated NK cell activation phenotype to a similar extent.

Interestingly, both dexamethasone and methylprednisolone inhibited the IL-15 induced upregulation of NKp44. However, the same was not true of TGF-β (Figure 5.1 and 5.2). This suggests that the expression of NKp44 is regulated by different pathways than those that control regulation of other activating receptors and that glucocorticoids are able to inhibit the NKp44 pathway, whereas TGF-β cannot.

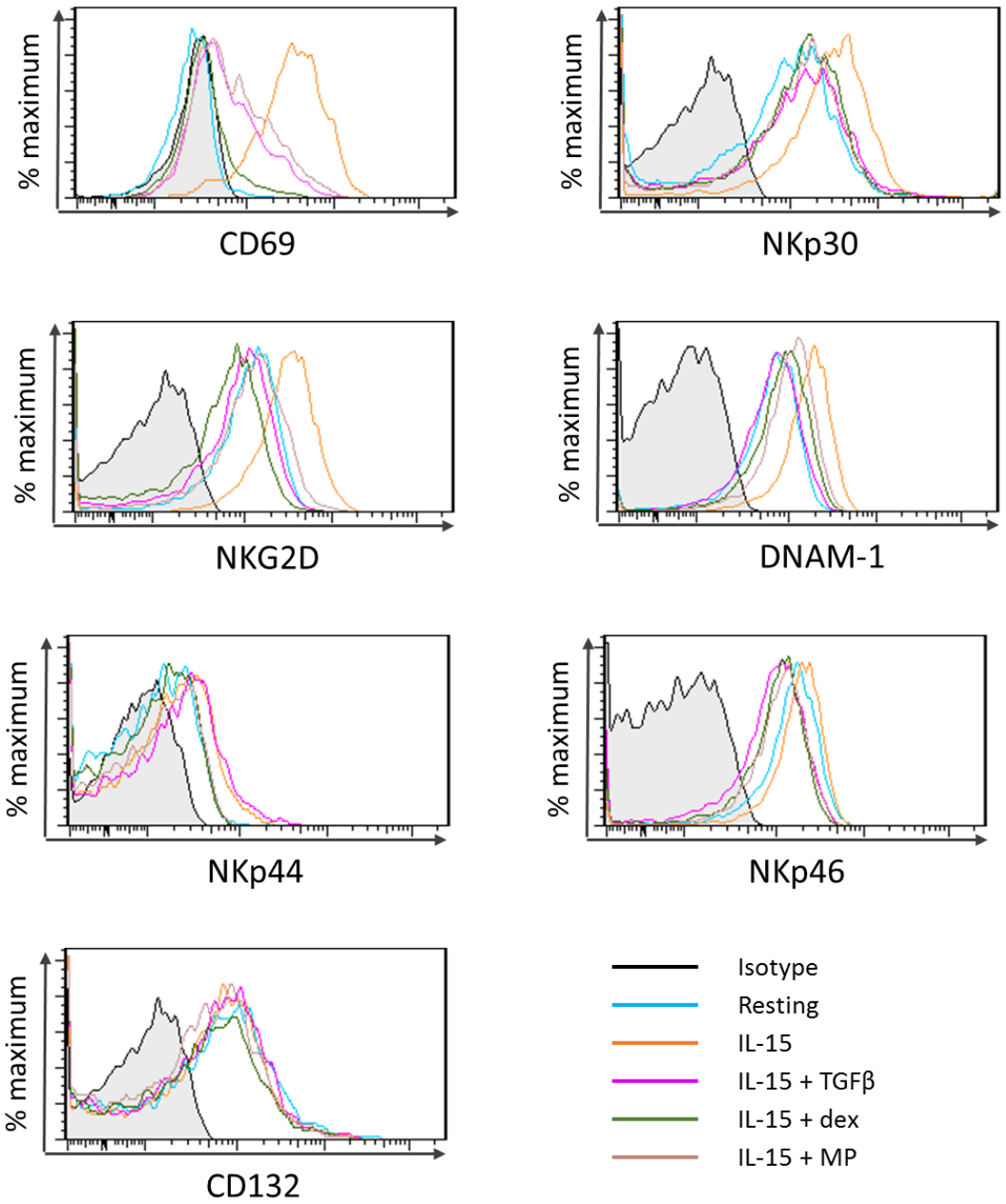

Figure 5.1. Characterisation of NK cells treated with corticosteroids. NK cells isolated from healthy donors were treated at the same time with 100IU/mL IL-15 (orange), IL-15 + 5 ng/mL TGF-β (pink), IL-15 + $2x10^{-7}$ M dexamethasone (green) or IL-15 + methylprednisolone (beige) for 48 hours. An isotype control antibody (black shaded) was used to establish nonspecific binding and untreated cells (blue) were used to establish the resting phenotype. Characterisation was performed using the antibodies listed and flow cytometry. The percentage of NK cells that were positively stained for each antigen was established by analysing the live cells The gates were set at 2% of the isotype control stain. The experiment was repeated 5-7 times. Representative histograms are shown.

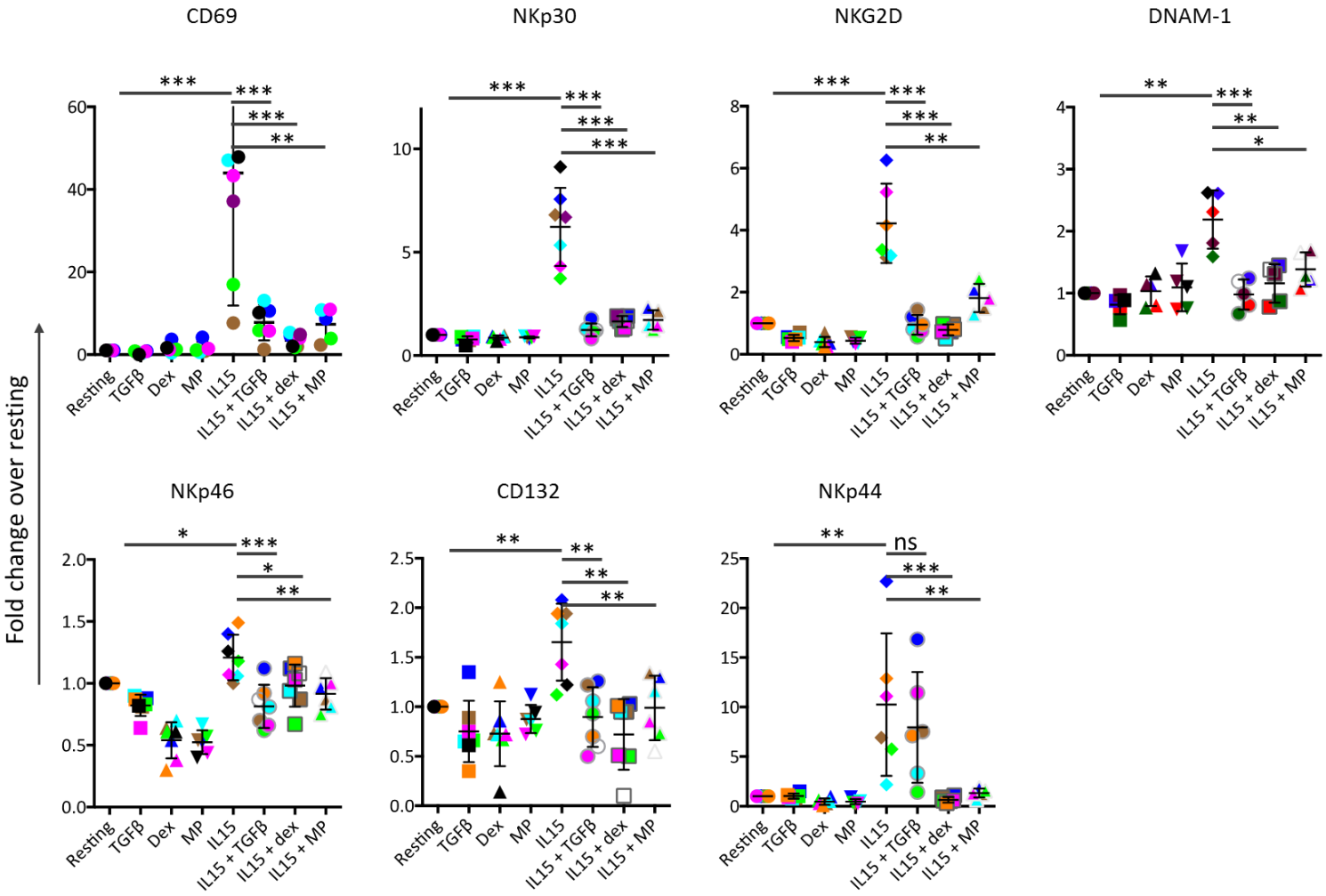

Figure 5.2. Summary of all donors used for the characterisation of corticosteroid treated NK cells. NK cells derived from healthy donors were either left untreated (resting) or treated with 5 ng/mL TGF-β, $2x10^{-7}$ M dexamethasone (dex), $2x10^{-6}$ M methylprednisolone (MP) or a combination of these with 100 IU/mL IL-15. Cells were treated for 48 hours then characterised for the antigens listed using flow cytometry. The median fluorescent intensity was used to calculate the fold change compared to the resting expression level. The experiment was repeated with NK cells from a minimum of 3 individual donors. Dots of the same colour represent data for each donor. The bar indicates the mean± s.d. Statistical analysis was performed using ratio paired t-tests. *P<0.05, **P<0.01, ***P<0.001, ns= not significant.

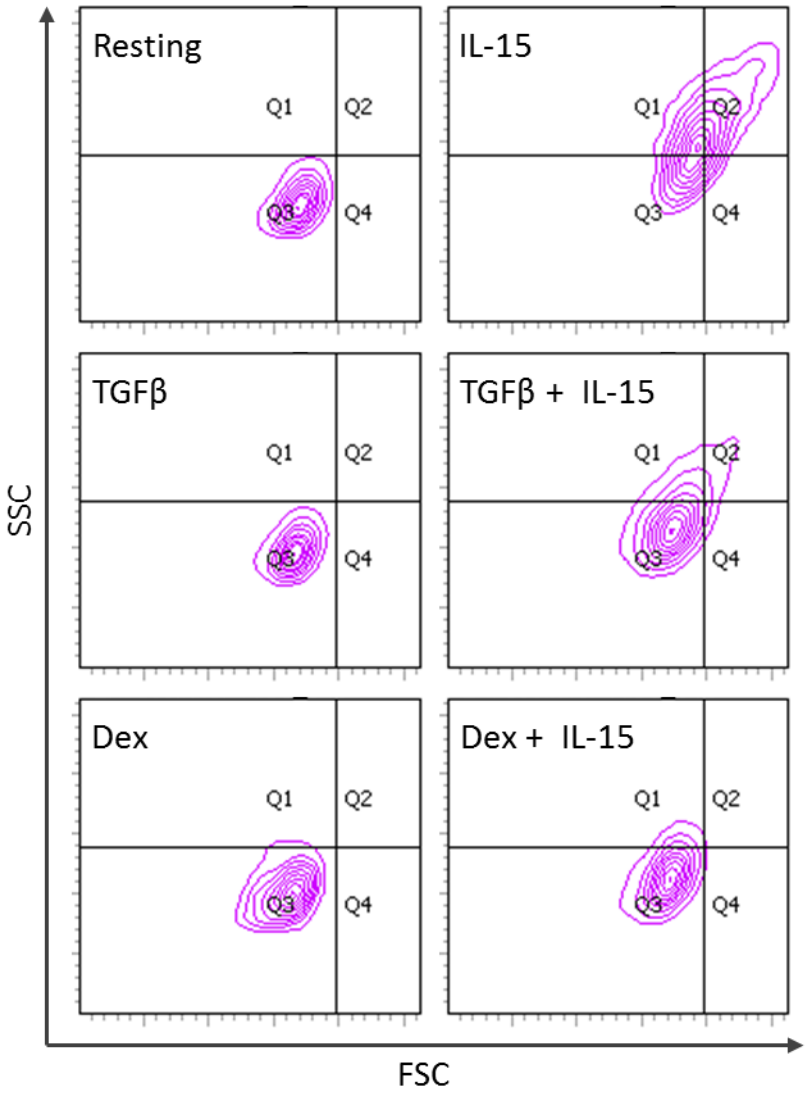

Figure 5.3. Morphological changes observed with TGF-β and dexamethasone treatments. NK cells derived from healthy donors were either left untreated (resting) or treated with 5 ng/mL TGF-β, $2x10^{-7}$ M dexamethasone (dex), or a combination of these with 100 IU/mL IL-15. Cells were treated for 48 hours then characterised using flow cytometry. The forward (FSC) and side (SSC) scatter that are a measure of size and granularity respectively were used to study morphological changes with the different treatments.

5.3 Dexamethasone prevents NK cell degranulation and target cell killing

Finding that dexamethasone inhibits IL-15 induced expression of activation receptors suggested that NK cell effector functions might also be inhibited. Cytotoxicity assays were carried out to assess the ability of dexamethasone treated NK cells to kill the prototypic NK cell target cell line, K562. Prior to the cytotoxic assays, NK cells were treated with either IL-15 or a combination of IL-15 and dexamethasone for 48 hours. Cells were incubated together for 5 hours at different E:T ratios (1:1, 2:1 and 5:1), stained with a dead cell discriminator and assessed by flow cytometry. A zero hour time point was used to establish the background level K562 death. The experiment was repeated 4 times with NK cells from different donors.

The results show that IL-15 treated NK cells are able to kill K562 in a dose dependent manner (Figure 5.4a). However, when NK cells were pre-treated with IL-15 and dexamethasone their ability to kill the target cells was greatly reduced (Figure 5.4a bottom); NK cells from all donors followed this pattern (Figure 5.4b).

The cytotoxic function of NK cells depends on them being able to recognise targets and respond by releasing the contents of their cytotoxic, secretory lysosomes. Therefore, the observed inability of dexamethasone treated NK cells to kill target cells could either be due to an inability to respond appropriately or because the lysosomes do not contain sufficient lytic proteins.

To assess the NK cell response to target cells, degranulation assays were performed. When an NK cell degranulates, the lysosomal membrane fuses with the plasma membrane such that the luminal side of the lysosome is displayed on the cell surface; CD107a, also known as lysosomal-associated membrane protein 1 (LAMP-1), is expressed on the luminal side of the secretory lysosomes, thus it is exposed to the cell surface when the cell degranulates. During degranulation assays (first described using T cells by (Betts et al. 2003)), the surface expression of CD107a is used to quantify the response of NK cells to target cells.

Prior to the degranulation assay, NK cells derived from healthy donors were either treated with IL-15 or IL-15 and dexamethasone for 48 hours. NK and K562 target cells were incubated at a 1:1 ratio for 5 hours. NK cells were identified using a cell tracker

dye and an antibody for the NK cell marker, CD56. The expression of CD107a was established using antibodies and flow cytometry. The surface expression of CD107a was determined both with and without the presence of K562 target cells. The expression of CD107a without the presence of K562 was used to establish the basal level of cell surface expression.

In the absence of target cells, neither treatment caused degranulation (Figure 5.5a). However, in the presence of K562, IL-15 treated NK cells were able to degranulate and this was significantly reduced when NK cells had been pre-treated with a combination of IL-15 and dexamethasone. The experiments were performed using NK cells from 4 donors and the same pattern was observed (Figure 5.5b).

Secretory lysosomes contain perforin and granzyme family members that function to pierce the target cell and initiate the apoptotic cascade. The absence of such proteins greatly decreases the lytic function of NK cells (Trapani & Smyth 2002). For example, absence of active granzymes greatly compromises NK cell activity (Heusel et al. 1994; Simon et al. 1997; Pardo et al. 2002). NK cells derived from healthy donors were treated with either TGF-β, dexamethasone, methylprednisolone, or these agents combined with IL-15, for 48 hours. Cells were lysed and the level of granzyme B was assessed using a Western blot. The results show (Figure 5.5c) that IL-15 induces granzyme B levels and that both steroids and TGF-β prevent IL-15 induced granzyme B accumulation.

These results show that dexamethasone is able to impair the cytotoxic activity of IL-15 activated NK cells. This is achieved by both reducing the ability of the NK cell to respond to its target (via reduced expression of target-sensing activation receptors) and release the contents of its lytic granules and by the reduction in the amount of the key cytotoxic protein, granzyme B.

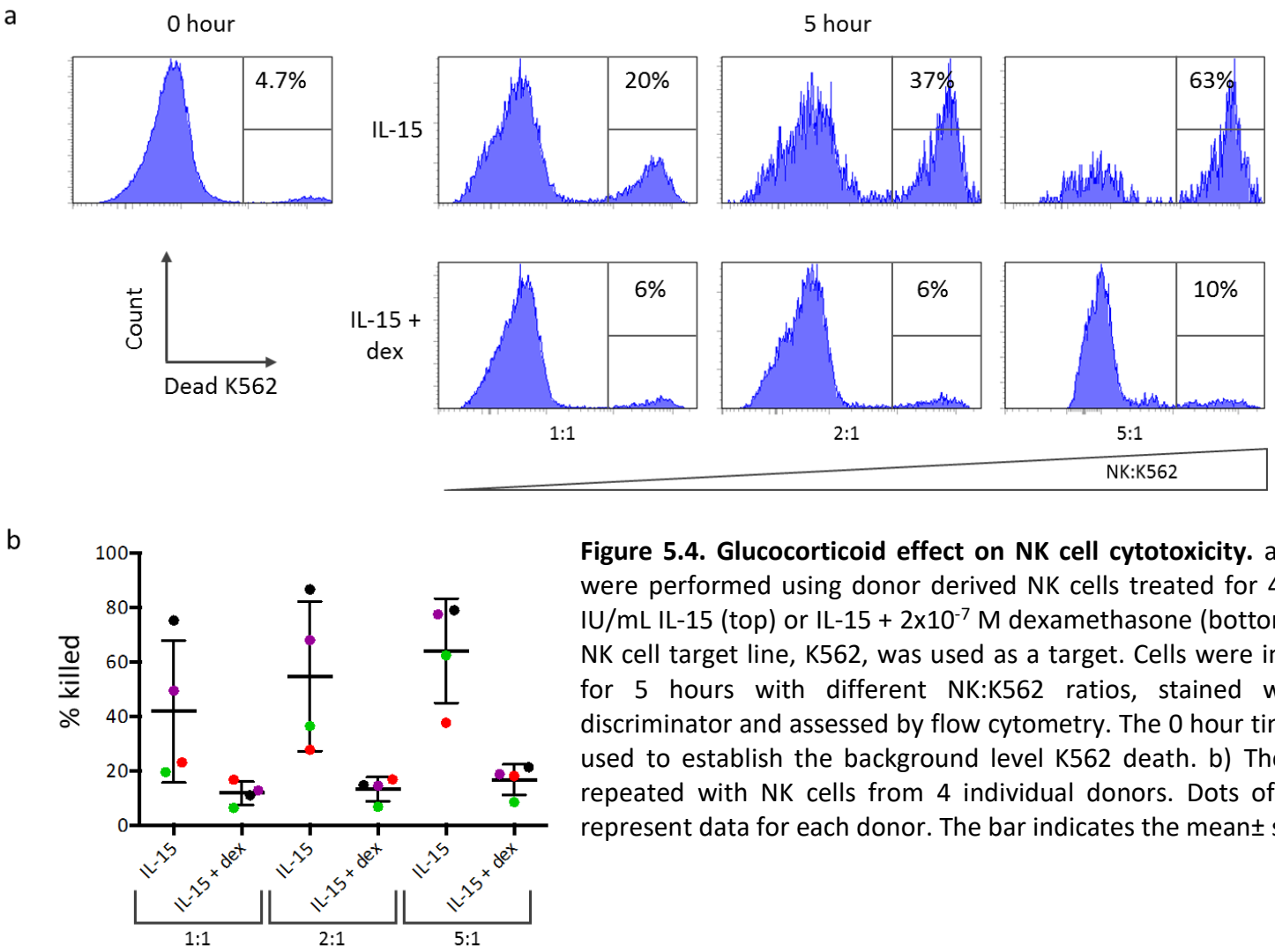

Figure 5.4. Glucocorticoid effect on NK cell cytotoxicity. a) Cytotoxic assays were performed using donor derived NK cells treated for 48 hours with 100 IU/mL IL-15 (top) or IL-15 + $2x10^{-7}$ M dexamethasone (bottom). The prototypic NK cell target line, K562, was used as a target. Cells were incubated together for 5 hours with different NK:K562 ratios, stained with a dead cell discriminator and assessed by flow cytometry. The 0 hour time point (left) was used to establish the background level K562 death. b) The experiment was repeated with NK cells from 4 individual donors. Dots of the same colour represent data for each donor. The bar indicates the mean± s.d.

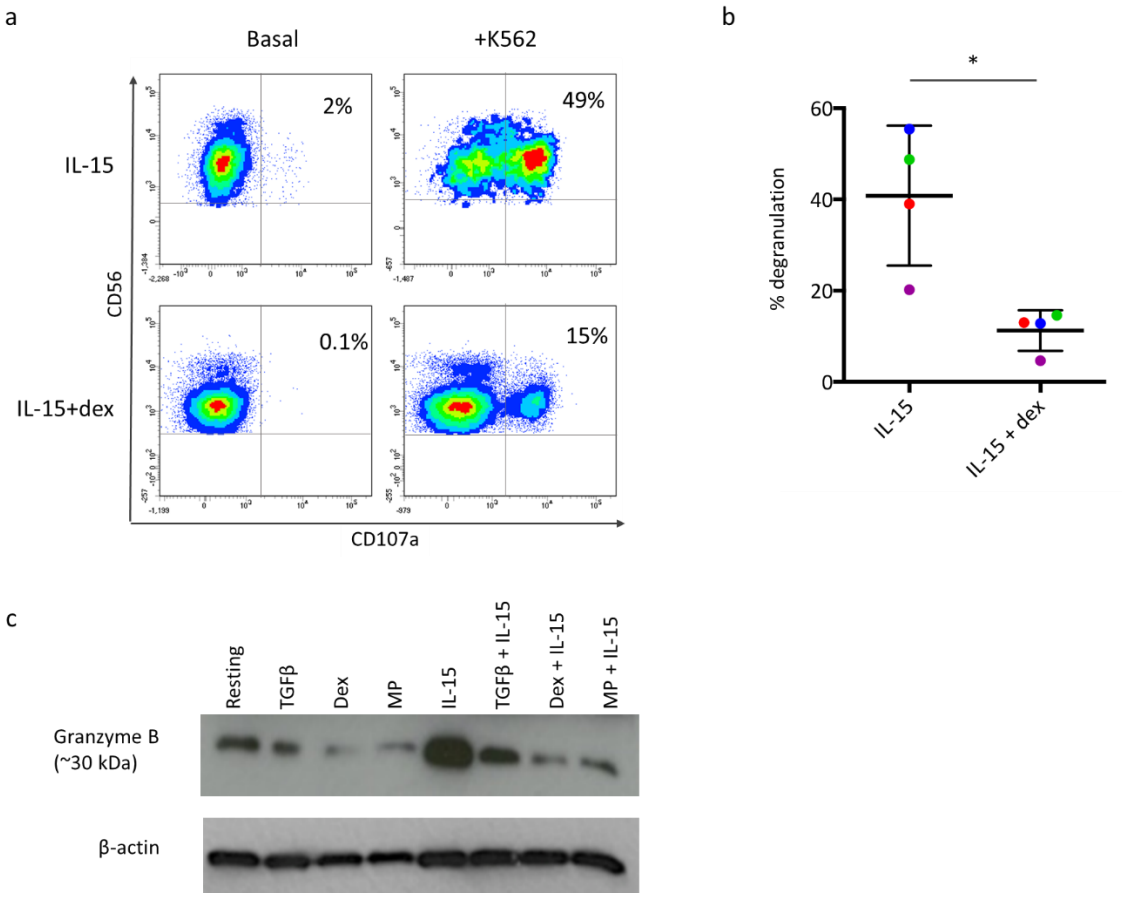

Figure 5.5. Glucocorticoid effect on degranulation and granzyme B. a) Degranulation assays were performed using donor derived NK cells treated for 48 hours with IL-15 (top) or IL-15 + dexamethasone (bottom). The prototypic NK cell target line, K562, was used as a target. Cells were incubated together for 5 hours at a 1:1 ratio of NK to K562 cells. Degranulation was quantified using they luminal lysosomal marker CD107a and flow cytometry. The basal level of expression of CD107a was assessed (left) without the presence of K562. b) The experiment was repeated with NK cells from 4 individual donors. Dots of the same colour represent data for each donor. The bar indicates the mean± s.d. Statistical analysis was performed using paired t-tests. *P<0.05. c) Expression of granzyme B assessed using a Western blot. β actin staining was used as a loading control.

5.4 How do TGF-β and steroids inhibit NK cell activation?

The results presented above indicated that dexamethasone and TGF-β have a similar effect on the NK cells; both acting to prevent IL-15 activation. To investigate the inhibitory mechanisms of dexamethasone and TGF-β on IL-15 activation, gene expression profiling using a microarray was performed. This global view of the effects of these agents on NK cells should reveal whether dexamethasone and TGF-β act in a similar manner to generate the same overall phenotype.

NK cells from healthy donors were isolated and treated under six different conditions for 48 hours; untreated (resting) or addition of dexamethasone, TGF-β, IL-15, IL-15+dexamethasone and IL-15+TGF-β. Both the morphology of the cells and the cell surface expression of CD69 and NKp30 were used to assess the donor response (Figure 5.6). IL-15 activation causes NK cells to clump together and this is prevented by the addition of dexamethasone and TGF-β (Figure 5.6b), consistent with the ability of these agents to block the activation signal. Likewise, IL-15 causes the upregulation of both CD69 and NKp30, but both dexamethasone and TGF-β counteract this response (Figure 5.7). Seven donors were treated in total, with two of the seven showing a weak response. The remaining five donors showed strong induction of the activated phenotype with IL-15 and antagonism of this effect by dexamethasone and TGF-β. Cells from these five donors were used to prepare mRNA for the microarray. The surface phenotype of CD69 and NKp30 for these five donors are presented in figure 5.7.

Following collection, the samples were sent to an external service provider (see materials and methods) who performed the microarray. Standard techniques were used to isolate mRNA, synthesize complementary DNA (cDNA), fluorescently label the cDNA, hybridise it to the array and acquire the data. The raw intensity files were received and analysed using the Affymetrix expression and transcript analysis consoles. A bioinformatician (Dr Alastair Droop) facilitated the initial stages of the analysis using the computer programming language R. In addition to the quality controls incorporated in the Affymetrix expression console, a principal component analysis (PCA) was carried out to assess the similarity of the six treatments for each of the five donors. The microarray provided expression data across over 60,000 probes

(encompassing protein coding and non-coding genes) for the thirty individual samples (five donors and six treatments), generating a total of over 1.5 million data points. Principal component analysis is a mathematical algorithm that allows the simplification of such a large data set while retaining information on the variance. This is achieved by establishing directions in the data (known as the principal components) along which the variation in the data set is at its greatest (Ringnér 2008). For my data set, 39.6% of the variation is described by the first principal component (Figure 5.8).

Importantly, the principal component analysis (Figure 5.8) shows that the same treatments cluster together, confirming that the different donors respond to the treatments in a similar way. Cells left untreated (resting) or treated with dexamethasone or TGF-β cluster together, as do those treated with IL-15+TGF-β or IL-15+dexamethasone. The cluster of IL-15 treated cells is far away from the other samples; this reflects the dramatic change in phenotype observed with IL-15, with dexamethasone and TGF-β blunting these effects and dragging the data closer to the phenotype observed for untreated cells. This is also illustrated by the cell surface phenotype data. For example, for CD69 (Figure 5.7b) whereby expression levels remain low (close to 0% of cells expressing CD69) in the resting, dexamethasone or TGF-β treated cells, but greatly upregulated with IL-15 (approximately 60% of cells express CD69). The combination treatments significantly inhibit the IL-15 induced CD69 expression, with approximately 10-20% of cells expressing the antigen. These samples are phenotypically more similar to the resting, dexamethasone and TGF-β treated samples. The PCA indicated that the global transcription within the cells supports the biological changes observed *in vitro*.

The expression of several genes were analysed further using quantitative RT-PCR. This analysis (performed by Dr Erica Wilson) validated the results observed within the microarray, with the same trends in expression observed for the different treatments.

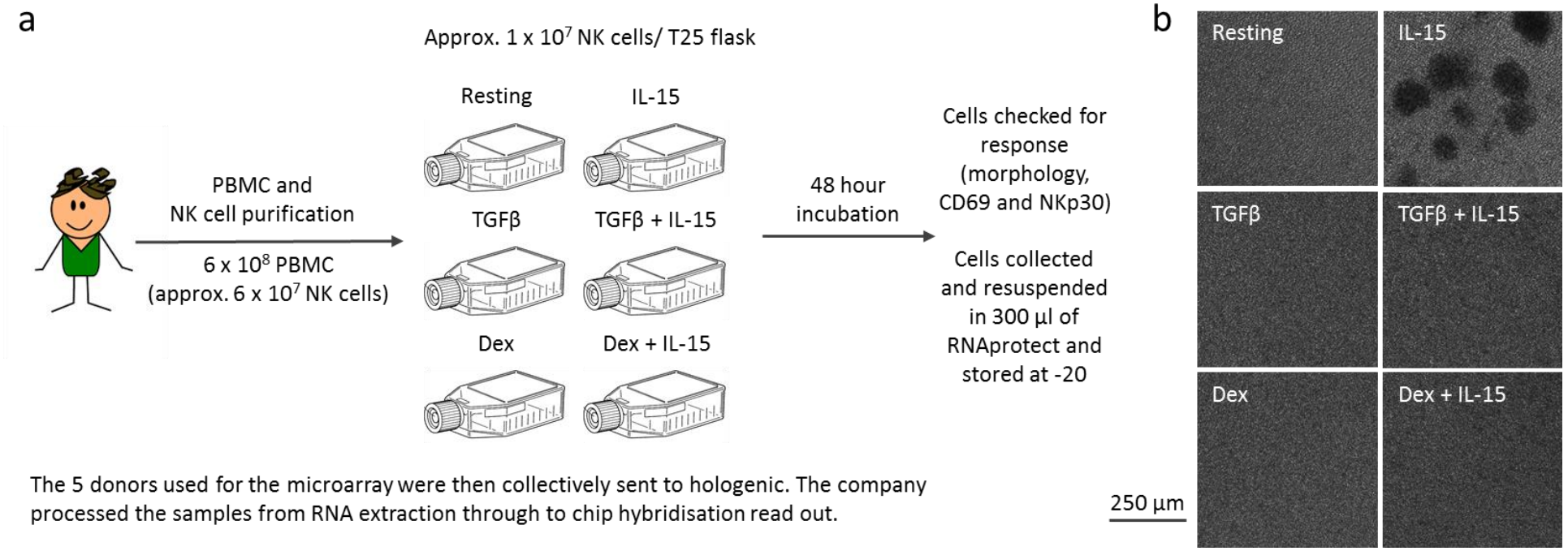

Figure 5.6. Protocol for sample treatment and collection for the microarray. a) Approximately 6 x 10^7 NK cells were isolated (1 x 10^7/ treatment) and either left untreated or treated with 5 ng/Ml TGF-β, 2X10^{-7} M dexamethasone or these in combination with IL-15. Cells were incubated for 48 hours before being harvested by centrifugation and resuspended in RNAprotect. Cells were stored at -20°C until all samples had been obtained. Prior to collection cells were analysed for their response to the treatments both morphologically (b) and by characterisation of NKp30 and CD69 using flow cytometry (figure 5.7).

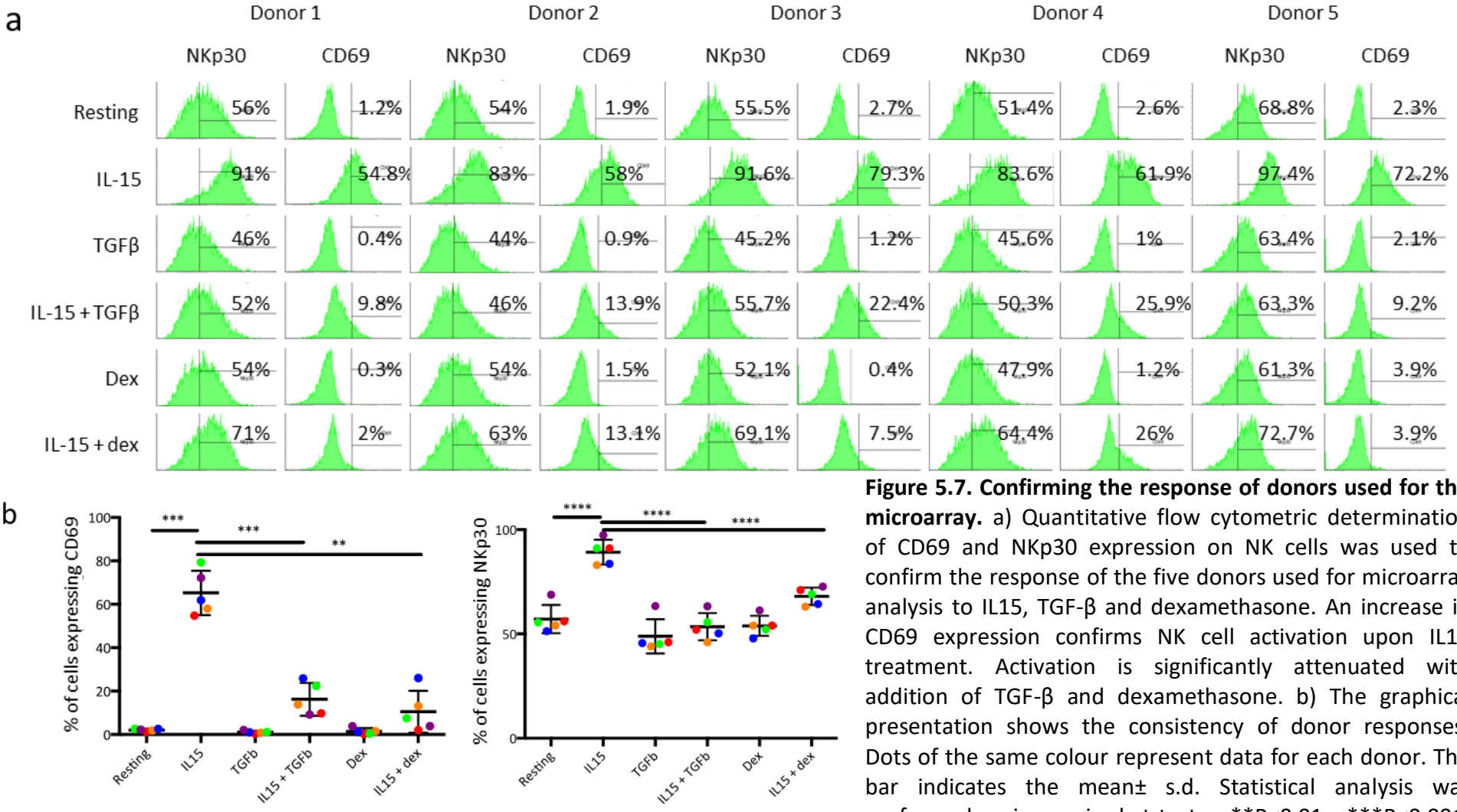

Figure 5.7. Confirming the response of donors used for the microarray. a) Quantitative flow cytometric determination of CD69 and NKp30 expression on NK cells was used to confirm the response of the five donors used for microarray analysis to IL15, TGF-β and dexamethasone. An increase in CD69 expression confirms NK cell activation upon IL15 treatment. Activation is significantly attenuated with addition of TGF-β and dexamethasone. b) The graphical presentation shows the consistency of donor responses. Dots of the same colour represent data for each donor. The bar indicates the mean± s.d. Statistical analysis was performed using paired t-tests. **P<0.01, ***P<0.001,

****P<0.0001.

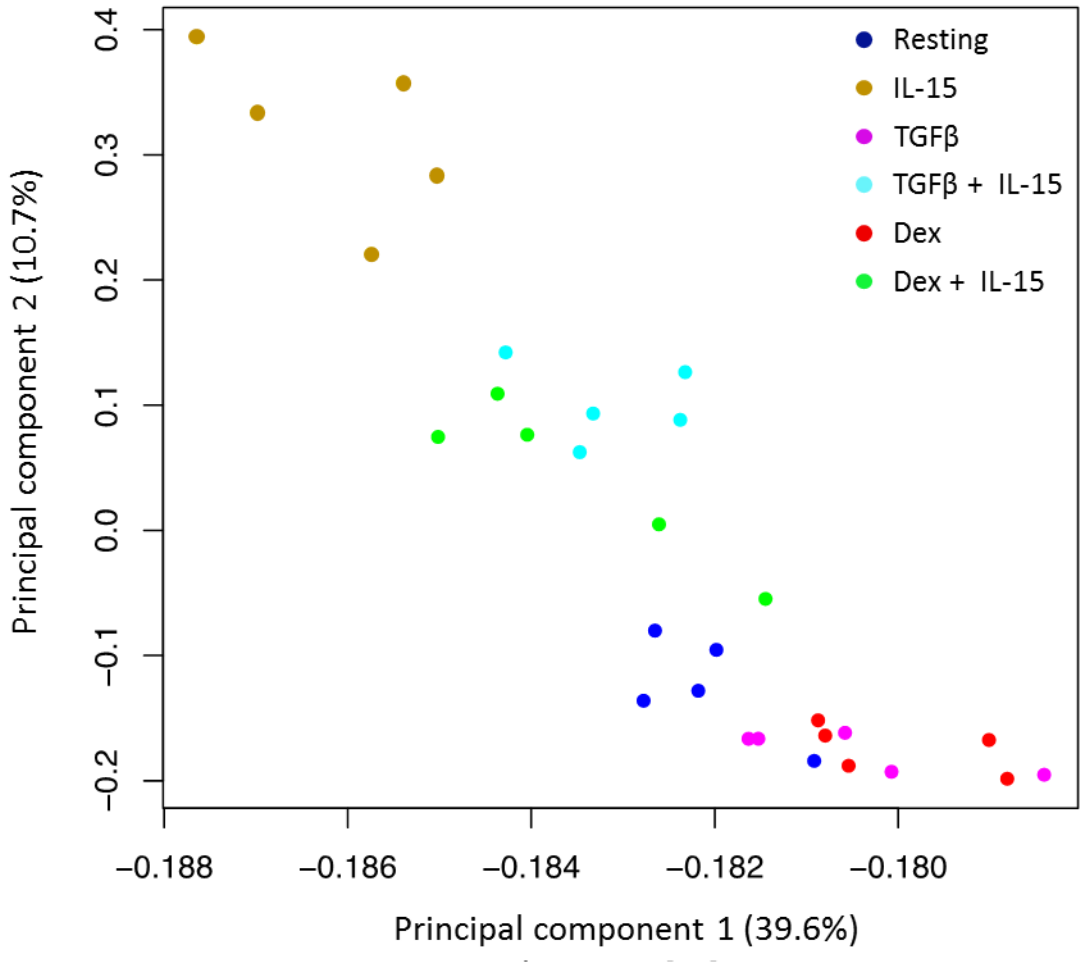

Figure 5.8. Principal component analysis. Principal component analysis (PCA) plot of principal components 1 and 2 for the gene expression profile of NK cells from 5 donors, with 6 treatments. Each sample is represented by one dot. Each colour corresponds to a separate treatment. The graph was generated by Alastair Droop using R.

The Affymetrix transcriptome analysis software enabled the comparison of two treatments for the five donors. A paired analysis was carried out to generate the average fold change for the five donors for each gene between two treatments. An average fold change of 1.5 or more and a p value of 0.05 or less was used as a threshold. To assess the suppressive effects of TGF-β and dexamethasone on IL-15 activation, three paired analyses were carried out; resting vs IL-15, IL-15 vs IL-15 + TGF-β and IL-15 vs IL-15 + dexamethasone. A comparison of the results is summarised in the Venn diagram in figure 5.9. Three regions of the Venn diagram are of particular interest. The central overlap containing 564 genes identifies those that are upregulated by IL-15 and downregulated in the presence of IL-15+TGF-β and IL-15+dexamethasone, i.e inhibition is common to both agents. These genes were further analysed to identify any potential inhibitory mechanisms that are common to both TGF-β or dexamethasone. Two other regions were also analysed in greater detail to identify genes that are unique to suppression either by TGF-β or dexamethasone; Venn diagram overlaps between 'Up in IL-15' and either 'Down in IL-15+TGF-β' (132 genes) or 'Down in IL-15+dex' (409 genes) respectively.

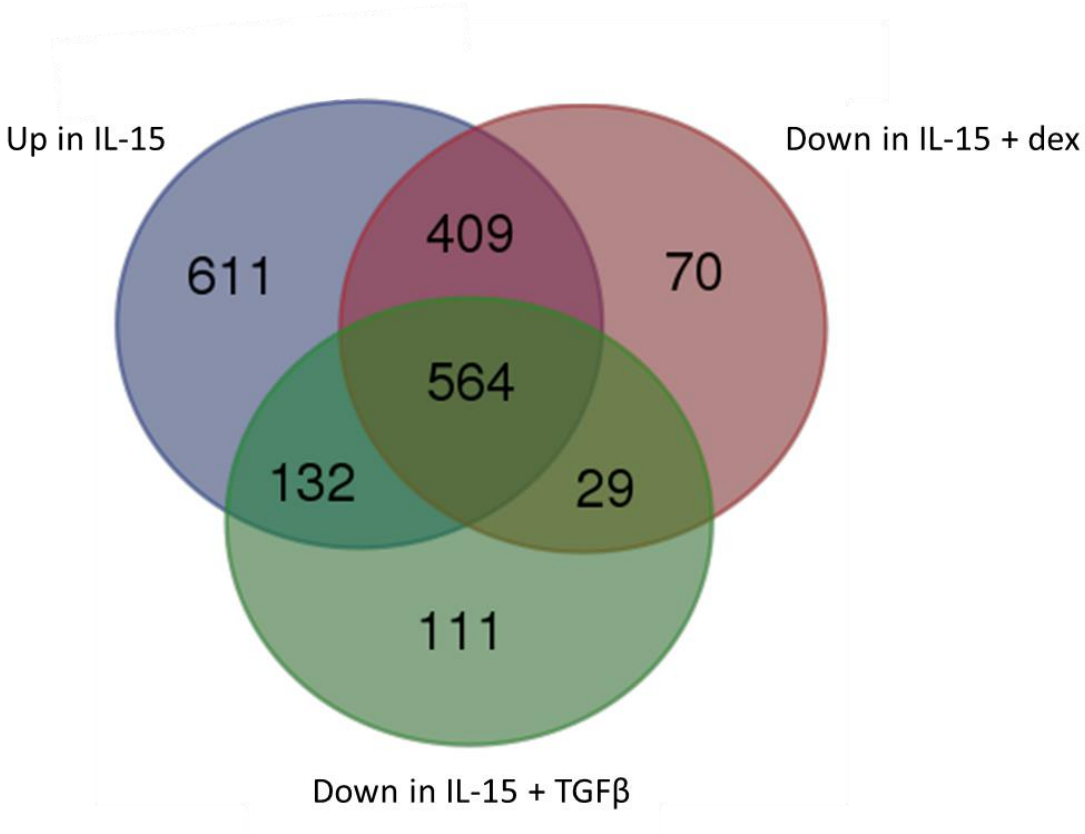

Figure 5.9. Venn diagram to compare the suppressive effects of TGF-β and dexamethasone on IL-15 activated NK cells. Three paired analyses were carried out; resting vs IL-15, IL-15 vs IL-15 + TGF-β and IL-15 vs IL-15 + dexamethasone. A fold change of 1.5 and a p value of 0.05 or less was used as thresholds. To analyse suppression, the genes up regulated in IL-15 treated NK cells vs resting (Up in IL-15) were compared with those down regulated in combination treatments of dexamethasone (Down in IL-15 + dex) or TGF-β vs IL-15 (Down in IL-15 + TGF-β) treated cells.

5.4.1 Strategies to reveal common mechanisms of regulation

The 564 mRNA transcripts within the central overlap of the Venn diagram are those that are upregulated in IL-15 treated cells compared to resting cells and downregulated in the presence of IL-15+dexamethasone or IL-15+TGF-β. Analysing this region will help to elucidate the suppressive mechanisms common to both dexamethasone and TGF-β.

Presented with a list of RNA transcripts, there are a number of ways to approach the analysis (Figure 5.10a). Although each transcript is potentially interesting in its own right, analysing the transcripts as a whole allows the identification of enriched pathways and the potential cellular functions that they regulate (Figure 5.10a right). Once the pathways are established, it is also possible to predict the downstream transcription factors that regulate the expression of effector genes (Figure 5.10a left). Another approach is to ask which transcription factors are known to regulate the expression of the genes for which the transcripts are present (Figure 5.10a bottom). These are the ways in which the data was analysed.

Metacore software was used to analyse the data. Metacore software encompasses an integrated knowledge database. The manually curated software allows the incorporation of established biological functions into the analysis of whole cell transcriptional changes. This enables identification of pathways enriched within different data sets and can suggest key transcription factors and pathways regulated by the treatments in the data set.

The transcription factors that regulate the transcription of the RNA within the central Venn overlap are listed in figure 5.10b. Metacore contains data about established links (published in the literature) between transcription factors and their target genes. The software then searches the dataset for these targets and reports functions controlled by the target proteins (Figure 5.10c).

The results strongly suggested that dexamethasone and TGF-β act to prevent IL-15 induced cell division and that this is potentially mediated by transcription factors such as CREB1, c-MYC, E2F1 and/or any of the other transcription factors listed in figure 5.10b.

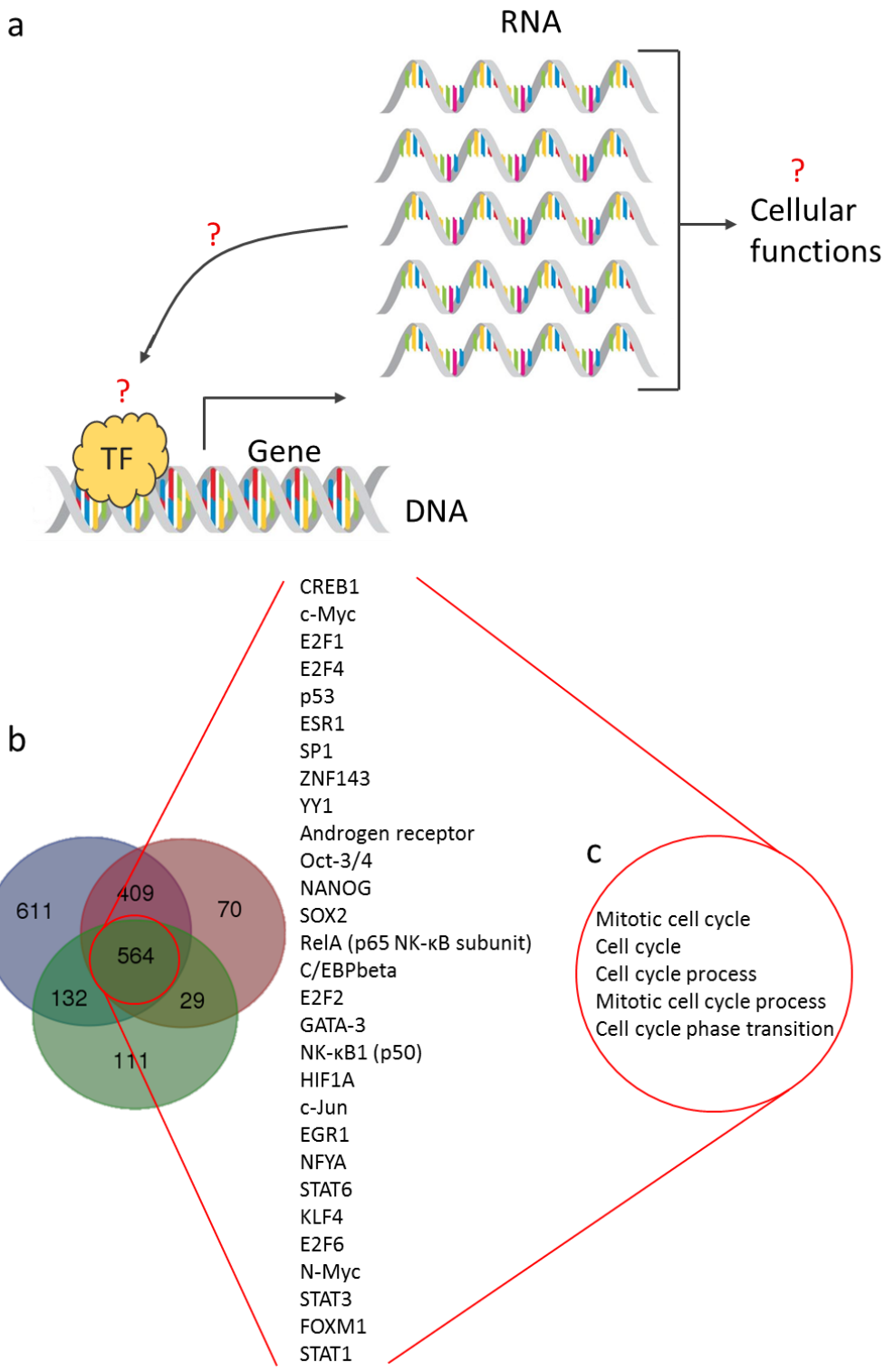

Figure 5.10. Analysis of common gene targets and pathways inhibited by TGF-β and dexamethasone. a) Possible approaches to analyse the RNA transcripts collectively. The cellular functions of the proteins encoded by the RNA can be identified. The presence of multiple RNA transcripts within one pathway indicate pathways activated by the treatment. Downstream transcription factors of these pathways can also be established. A second approach is to consider transcription factors that are known to regulate the expression of RNA within the dataset. b) Transcription factors that regulate the expression of the transcripts within the central region of the Venn diagram were identified. c) The functions regulated by these transcription factors.

Metacore was also instrumental in the second type of analysis performed; identification of pathways enriched within the transcripts listed in the central overlap of the Venn diagram (Figure 5.9). The cellular functions of these pathways are summarised in figure 5.11a. As observed during the transcription factor analysis, functions include cell cycle progression. In addition to cell cycle processes, pathways involved in the innate immune response and metabolism are also upregulated with treatment of IL-15 and inhibited in the presence of dexamethasone and TGF-β. The morphological changes observed with the different treatments (Figures 5.1 and 5.6b) support the finding that metabolic pathways are enriched in the overlap.

The key transcription factors that are predicted to regulate the observed gene expression changes are shown in figure 5.11b. This implicates NF-κB, E2F1/DP1 and c-Myc as important transcription factors regulating IL-15 induced cell cycle, metabolic upregulation and activation of the innate immune response in NK cells.

The identification of genes reciprocally regulated by IL-15 and these agents implicated c-Myc as a key regulator of NK cell activation. This suggests c-Myc is a common point at which TGF-β and dexamethasone block pathways induced by IL-15. This finding led to further investigation of Myc reported in section 5.5 and 5.6.

a

Processes identified within enriched pathways (p value < 10^{-20})

Cell cycle
Cell cycle process
Mitotic cell cycle
Response to stress
Mitotic cell cycle process
Positive regulation of cellular metabolic process
Regulation of innate immune response
Innate immune response-activating signal transduction
Activation of innate immune response

b

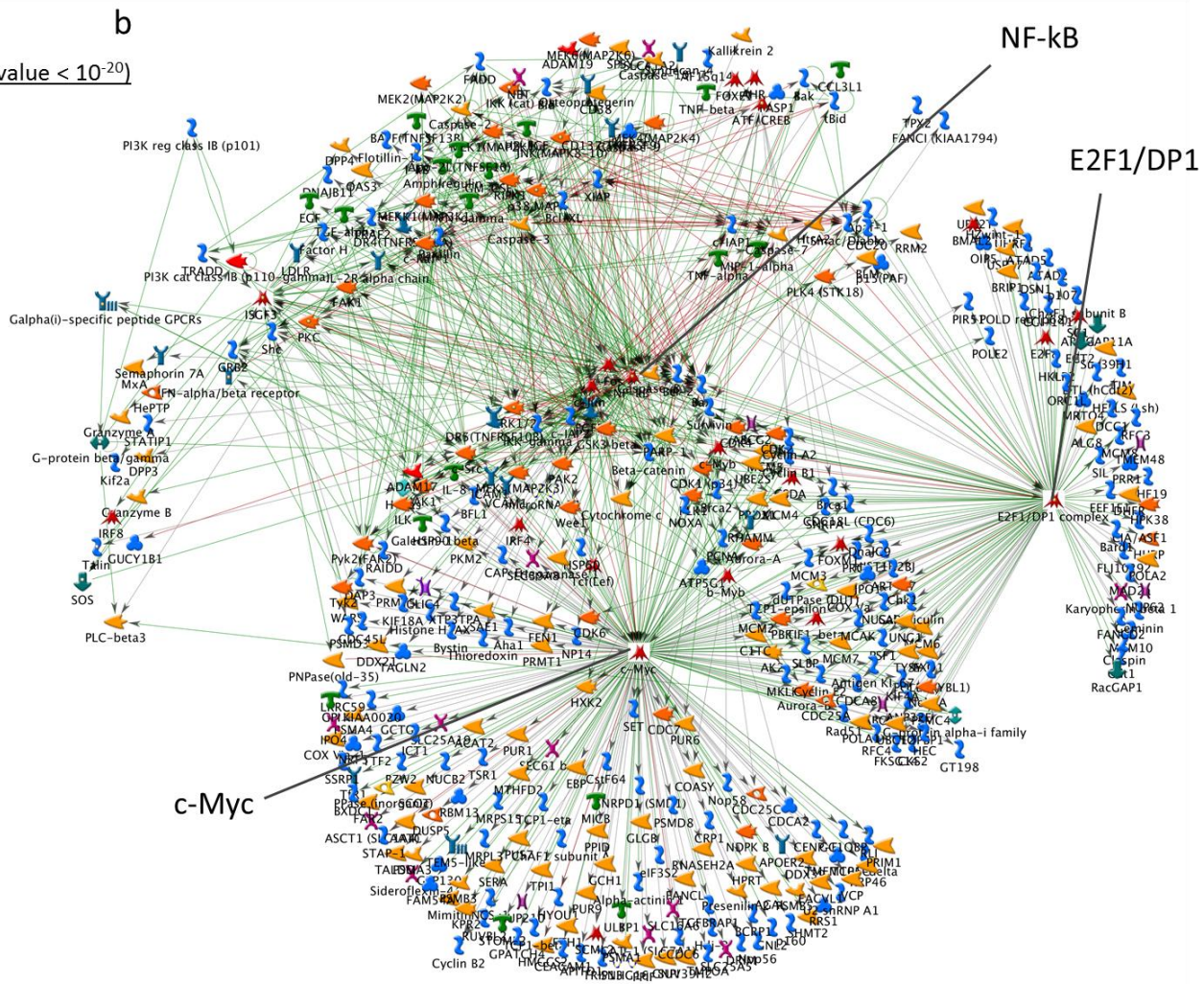

Figure 5.11 Cellular functions and key transcription factors. a) A list of cell cycle processes that are associated with pathways enriched within the central Venn diagram overlap. b) Key transcription factors are identified that are downstream of proteins within enriched pathways (generated using Metacore).

5.4.2 Mechanisms specific to dexamethasone or TGF-β suppression of IL15 induction

Analysis of the transcripts that are differentially expressed between the two treatments (Figure 5.12) indicated several transcription factors are common to both sets of genes, suggesting that these transcription factors are downstream of different signals and regulate multiple pathways independently. The listed functions (Figure 5.12 b and d) indicate that, whilst TGF-β and dexamethasone both exhibit inhibitory functions, TGF-β seems to alter expression of genes that regulate glucose uptake whilst dexamethasone has other inhibitory effects.

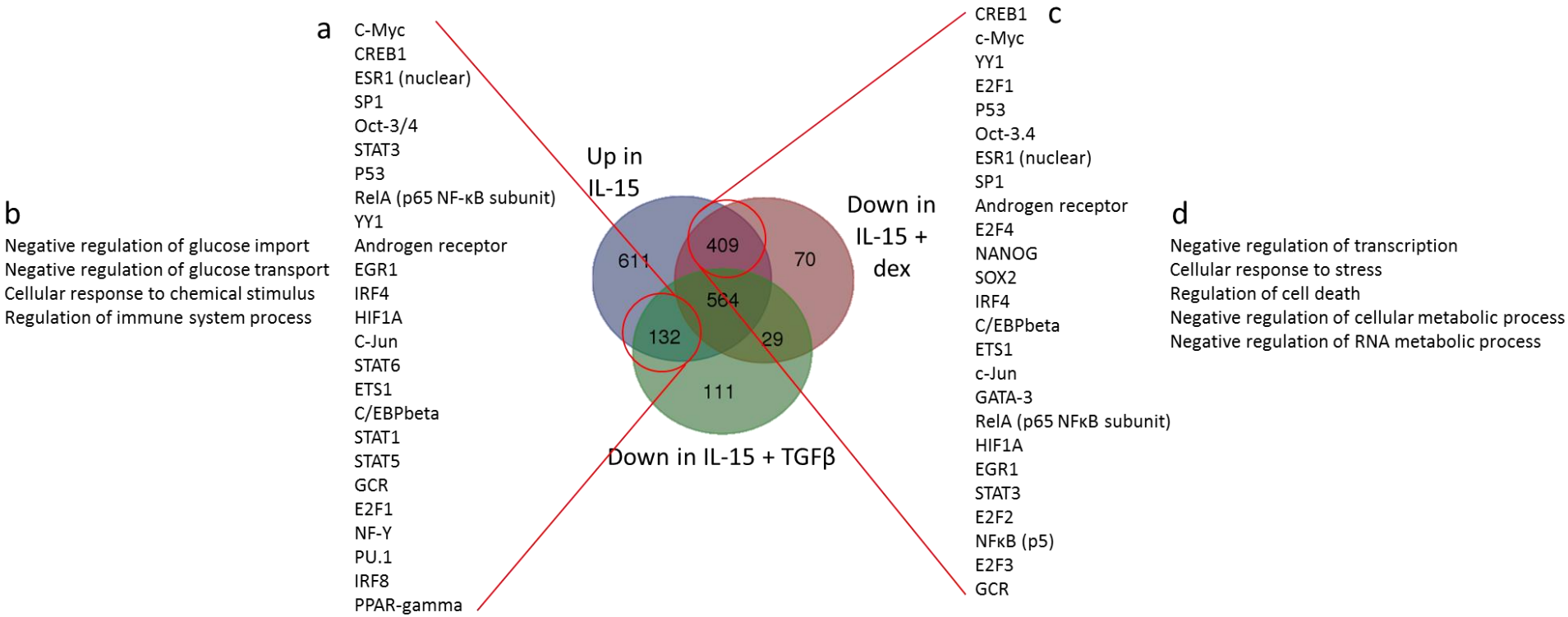

Figure 5.12. Cellular functions and key transcription factors that are upregulated by IL-15 and down regulated by either dexamethasone or TGF-β. Key transcription factors (a and c) and functions (b and d) regulated by the addition of TGF-β or dexamethasone respectively.

5.5 Cell cycle analysis

Changes in gene expression observed using the microarray suggested that IL-15 mediated cell cycle control was disrupted by both dexamethasone and TGF-β. The transcription factor, c-Myc, was also identified in the microarray; first as a hub for regulating the expression of genes that are both upregulated with IL-15 and downregulated with the addition of either dexamethasone or TGF-β and secondly, as a transcription factor that regulates the cell cycle (Figure 5.10b). I therefore analysed the effect of IL-15, TGF-β and dexamethasone on the NK cell cycle. Cell cycle analysis was performed using BrdU, a thymidine analogue, and a DNA stain (Hoechst), to detect newly synthesised DNA and total DNA respectively. Isolated NK cells were either left untreated (resting) or treated with TGF-β, dexamethasone or in combination with IL-15. A c-Myc inhibitor (Zhao et al. 2015) was also used to confirm the role of c-Myc in cell cycle control.

Cells were treated for 24, 48 and 72 hours and the amount of BrdU incorporation into newly synthesised DNA was quantified. The assay was initially performed by incubating the cells with BrdU throughout the experiment, but this method was adapted by adding BrdU one hour prior to collecting the cells to reduce any effects of BrdU associated toxicity. However, the trends observed were the same for both variations on the method (Figure 5.13b). The cells were collected and washed in ice cold PBS then fixed by gradually increasing the concentration of ethanol to 80%. The samples were stored at -20°C until all time points had been collected. Nuclei were prepared by treating the cells with pepsin and hydrochloric acid to break down cellular proteins and expose the DNA including the incorporated BrdU. The BrdU was detected using an antibody and a fluorescent (AF594) conjugated secondary antibody. In addition, the fluorescent DNA stain, Hoechst 33342, allowed the cell cycle to be analysed using flow cytometry. This method was optimised for the analysis of primary NK cells by Dr Laura Wetherill (for use in an unrelated study).

Cell cycle analysis is based on the knowledge that cells in the G_0 or G_1 phase of the cell cycle will have the normal diploid contents of DNA, G_2 cells will have twice that amount and cells in S phase will have an intermediate quantity. It is important that only single nuclei (singlets) are included in the analysis, as two conjoined G_0 nuclei will have the same total amount of DNA as one G_2 nucleus. Singlets were identified based

on the pulse width and area on the channel used to detect total DNA (i.e the Hoechst stain was detected using the pacific blue channel). When a particle passes through the laser beam, a pulse is generated (Figure 5.13a). The width is the time taken for an object to pass through the laser beam and it is proportional to the object size and the duration of signal. The height of the pulse is the intensity of the signal. Both a cell in the G_2 phase of the cell cycle and two G_0 cells stuck together will have the same intensity. However, they can be distinguished based on the width of the pulse; a G_2 nucleus will take less time to pass the laser beam than two nuclei together. Unfortunately, the separation of the pacific blue signal based width was not pronounced (Figure 5.13b(i)) and the cell cycle profile subsequently generated based on the 'singlets' gate (Figure 5.13b(ii)) contained a pattern associated with conjoined nuclei. To overcome this problem, the 'singlets' gate was modified (Figure 5.13b(iii)) to exclude the conjoined nucleus stain pattern (Figure 5.13b(iv)).

The gating strategy identified in figure 5.13b was used to generate cell cycle profile plots for the different treatments (Figure 5.14a). The experiment was carried out using NK cells from 3 donors (only 2 donors with the c-Myc inhibitor). During the initial experiment, the 24-hour time point revealed that less than 5% of cells had entered S phase (data not shown). Therefore, future experiments were set up with just the 48 and 72 hour time points. The amount of cells in S phase and cell death was analysed. Data for all donors is presented in figure 5.14b. The results show that the mitogenic activity of IL-15 on NK cells is antagonised by both TGF-B and dexamethasone, as suggested by the microarray data. By 48 hours, approximately 10% of the IL-15 treated cells have entered S phase, whereas this is inhibited (approximately 2 fold) in the cells treated with IL-15 in combination with dexamethasone or TGF-β. This effect is more pronounced by 72 hours. Importantly, the same trend was also observed with the addition of the c-Myc inhibitor, suggesting that c-Myc regulates the transcription of genes required for cell cycle entry, as indicated by the transcription factor analysis of the microarray data (Figure 5.10b).

Interestingly, when analysing the differences in cell death it became apparent that IL-15 is capable of preventing the cell death that is seen with the treatment of dexamethasone alone. However, this rescue effect of IL-15 is not observed when the cells are treated with IL-15 together with the c-Myc inhibitor. This suggests that c-Myc is required for the pro-survival functions of IL-15.

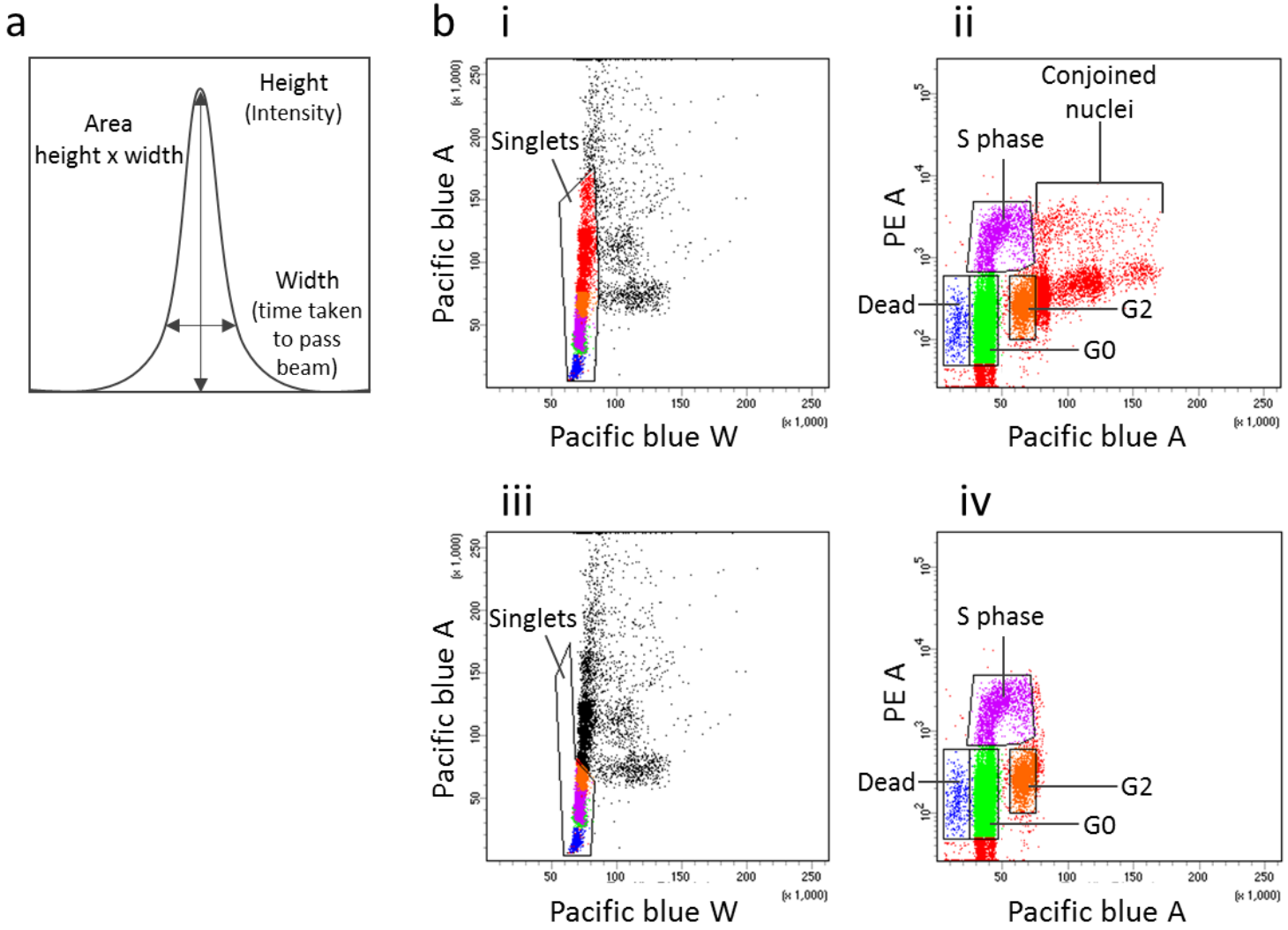

Figure 5.13. Analysis of the cell cycle by flow cytometry. a) The width and height of the pulse generated when a particle passes through the laser beam can be used to infer the amount of taken for the object to pass and the intensity of the signal respectively. The width is therefore proportion to the size of the object. b) The original 'singlets' gate (i) had to be modified (iii) to exclude patterns associated with conjoined nuclei (ii). Subsequent gates were established to identify nuclei of dead cells (blue), G0 (green), S phase (purple) and G2 cells (orange) (iv).

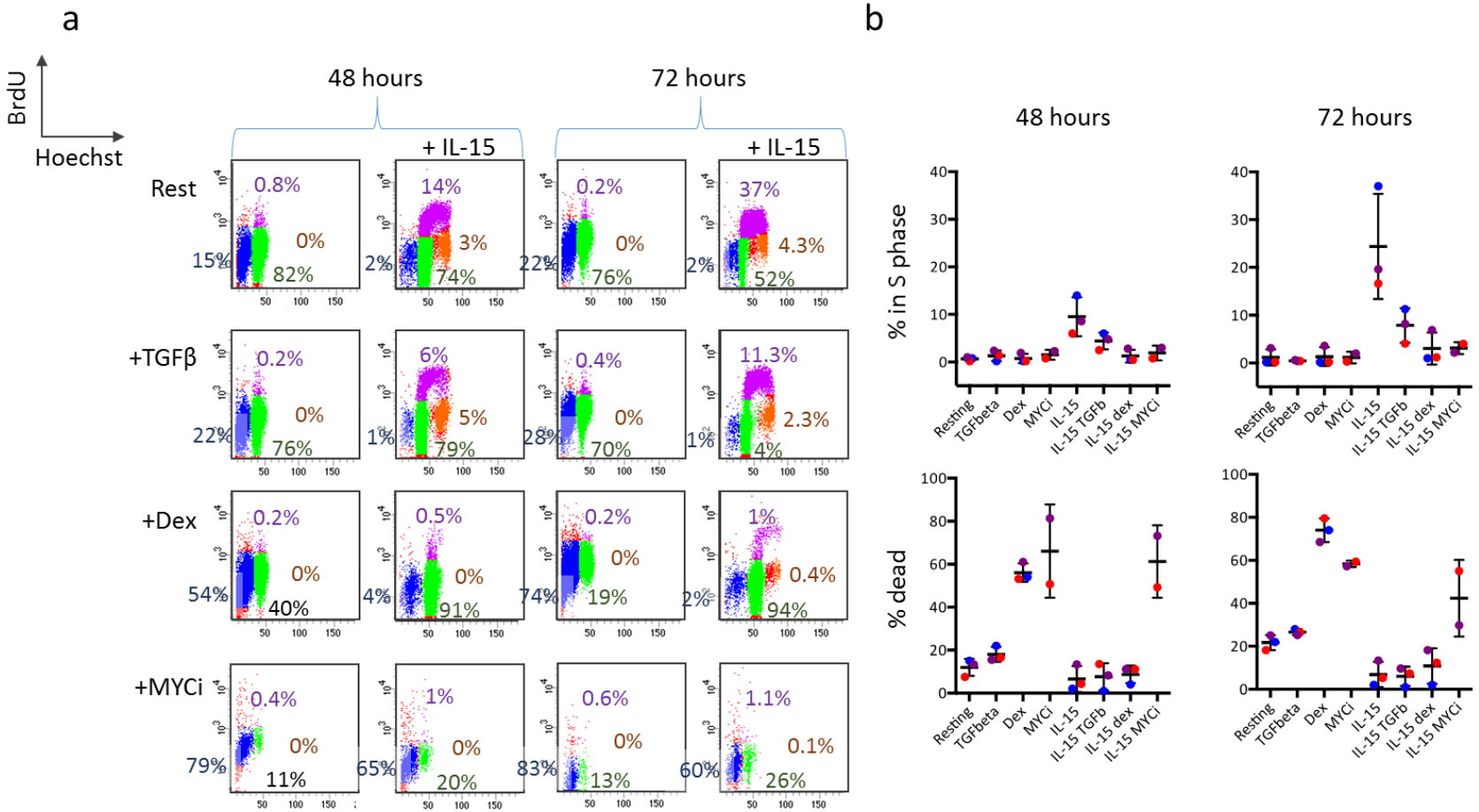

Figure 5.14. Cell cycle analysis. a) Example cell cycle plots are shown for the treatments with 5 ng/Ml TGF-β, $2X10^{-7}$ M dexamethasone (dex) in the presence (right) or absence of 100 IU/mL IL-15 at 48 and 72hours. The colours identify nuclei from dead cells (blue), G0 (green), S phase (purple) and G2 cells (orange), along with the proportion of cells within each phase. b) The experiment was carried out using NK cells from 3 donors (only 2 donors with the c-Myc inhibitor). Dots of the same colour represent data for each donor. The bar indicates the mean± s.d.

5.6 Intracellular signalling

Both the microarray and the c-Myc inhibitor used in the cell cycle assays indicate that c-Myc plays a central role in IL-15 induced NK cell proliferation and survival. Collectively, the data suggests that c-Myc is a regulatory hub for pro- and anti-activation pathways, the latter coordinating the inhibitory functions of TGF-β and the corticosteroids. I therefore analysed the effect of IL-15, TGF-β and dexamethasone on c-Myc protein by Western blotting. The results showed that IL-15 upregulates c-Myc expression compared to resting cells and that this response is suppressed by TGF-β, dexamethasone and methylprednisolone (Figure 5.15). The same effect was observed at both 48 and 72 hours post treatment.

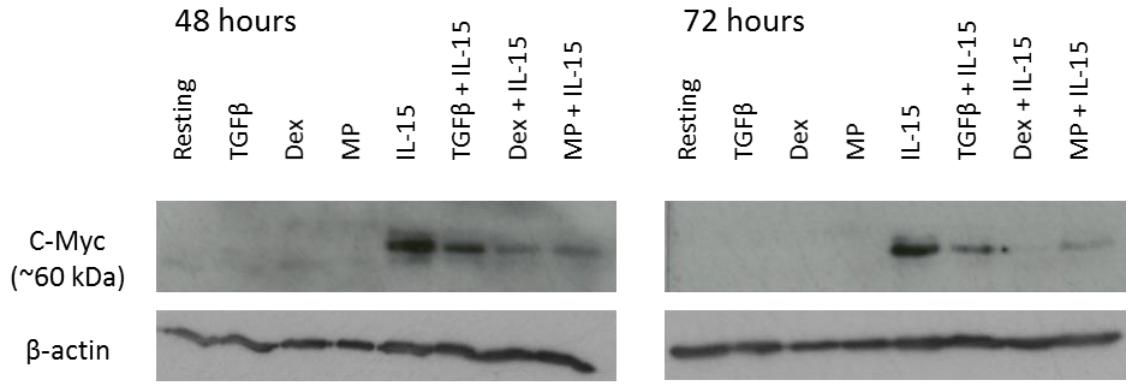

Figure 5.15. Western blot analysis of c-Myc. NK cells derived from a healthy donor were treated with either 5 ng/mLl TGF-β, $2x10^{-7}$ M dexamethasone, $2x10^{-6}$ M methylprednisolone or these treatments in conjunction with 100 IU/mL IL-15. Cells were collected after the specified time, lysed and prepared for analysis by Western blot. An equal number of cells were analysed for each sample. βactin has been used as a loading control.

To investigate potential differences in the suppressive mechanisms of dexamethasone and TGF-β on IL-15 signalling, proteins acting downstream of the IL-15 and TGF-β receptors were investigated.

The IL-15 receptor consists of three subunits; α, β and γ (Ma et al. 2006). When bound by IL-15, Janus kinases 1 and 3 (JAK1 and JAK3) are auto-phosphorylated and initiate at least three signalling cascades; Ras-Raf-MEK, PI3K-AKT-mTOR and signal transduction and activation of transcription (STAT) 5 pathways (Nandagopal et al. 2014). As expected, treatment of NK cells with IL-15 was shown to induce the phosphorylation of STAT5 (Figure 5.16). NK cells treated with both IL-15 and TGF-β did not alter the phosphorylation of STAT5, a result consistent with previous data from our laboratory using human NK cells (Wilson et al. 2011) and a recent publication using mouse NK cells (Viel et al. 2016). Conversely, dexamethasone and methylprednisolone were both able to prevent IL-15 induced STAT5 phosphorylation. This supports the finding that dexamethasone prevents IL-2 induced STAT5 phosphorylation in NK cells (Michelo et al. 2016).

The TGF-β receptor is a tetrameric complex made up of two TGF-βRI chains and two TGF-βRII chains. When bound by TGF-β, the type I chains phosphorylate the type II chains which enables the phosphorylation of transcription factors Smad2 and Smad3 (Smad2/3). The SMAD2/3 complex is then able to translocate to the nucleus where it interacts with Smad4 and other proteins to regulate transcription (Derynck & Zhang 2003). In keeping with this mechanism, TGF-β induced the phosphorylation of Smad2/3 (Figure 5.16). This was not observed for dexamethasone or methylprednisolone treated cells where no difference in SMAD2/3 phosphorylation was observed compared to the IL-15 treated cells. Differential activation of the SMAD and STAT signalling pathways identifies differences between the actions of TGF-β and dexamethasone.

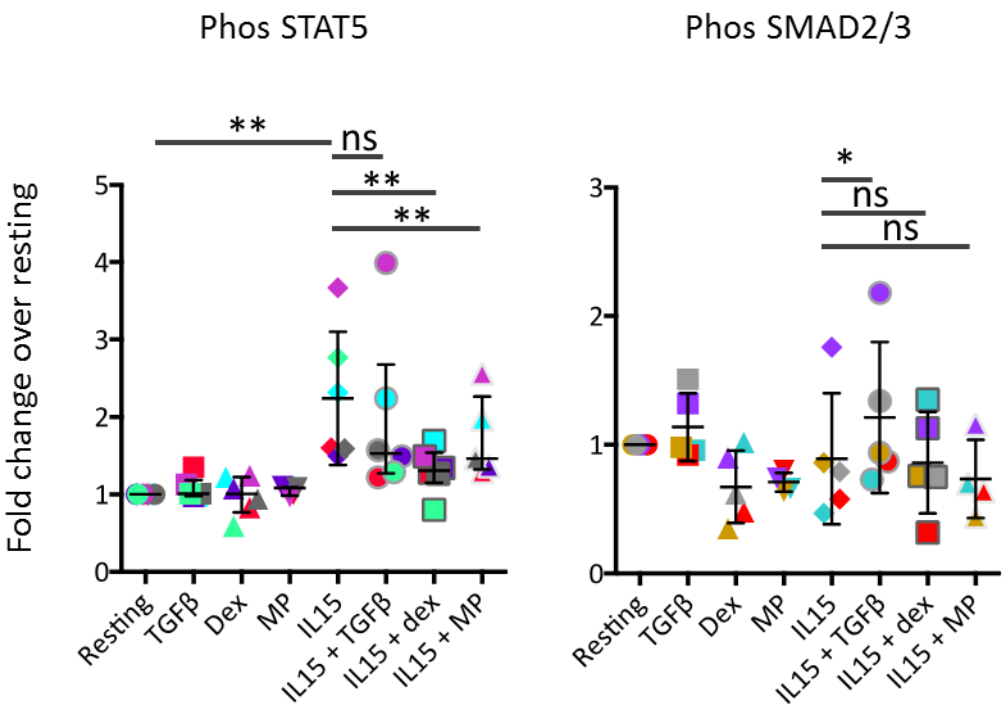

Figure 5.16. Flow cytometry to assess phosphorylated STAT5 and phosphorylated SMAD2/3. NK cells derived from healthy donors were either left untreated (resting) or treated with 5 ng/Ml TGF-β, $2x10^{-7}$ M dexamethasone (dex), $2x10^{-6}$ M methylprednisolone (MP) or a combination of these with 100 IU/mL IL-15. Cells were treated for 48 hours then characterised for phosphorylated STAT5 or phosphorylated SMAD2/3 using flow cytometry. The surface phenotype and cell death were analysed by flow cytometry. Only live cells were included in the analysis. The median fluorescent intensity was used to calculate the fold change compared to the resting expression level. The experiment was repeated with NK cells from a minimum of 4 individual donors. Dots of the same colour represent data for each donor. The bar indicates the mean± s.d. Statistical analysis was performed using ratio paired t-tests. *P<0.05, **P<0.01, ns= not significant.

The treatment of NK cells with IL-15 causes an increase in the size and granularity of cells (Figure 5.1) and initiates the cell cycle (Figure 5.14), with TGF-β and dexamethasone attenuating these responses. The serine/threonine protein kinase mammalian target of rapamycin (mTOR) was discovered due to its role in inhibiting cell proliferation (Thomson et al. 2009) and is now known to be downstream of the IL-15 signalling pathway (Marçais & Walzer 2014). Therefore, I analysed the effect of TGF-β and dexamethasone on the mTOR signalling pathway.

Two of the most well-studied downstream targets of mTOR are the p70 S6 kinase pathway and the 4EBP1/eIF4E pathway (Figure 5.17a) which act in parallel to control translation (Fingar et al. 2004). The eukaryotic translation initiation factor 4E (eIF4E) forms part of a translational complex. When bound by 4E-binding protein 1 (4E-BP1), it is inhibited from forming this complex and translation is reduced. Phosphorylation of 4E-BP1 by mTOR causes the release of eIF4E and the brake on translation is lifted (Fingar et al. 2004). Additionally, mTOR is able to phosphorylate p70 S6 kinase, which in turn phosphorylates the 40S ribosomal S6 protein, which is also thought to increase translation (Fingar et al. 2004).

NK cells treated with TGF-β, dexamethasone, methylprednisolone alone or in combination with IL-15 were incubated for 48 hours and analysed for sustained changes in signalling pathways using flow cytometry or Western blotting. The results show that IL-15 treatment of NK cells causes an increase in the amounts of phosphorylated mTOR (Figure 5.17b), phosphorylated p70 S6 kinase (Figure 17c) and phosphorylated S6 (Figures 5.17b/c). These phosphorylation events were reduced when NK cells were treated with IL-15 in combination with TGF-β, dexamethasone or methylprednisolone (Figure 5.17b and c), identifying similarities in the actions of these immunosuppressive molecules.

Analysis of the 4EBP1/eIF4E pathway reveals that IL-15 treatment induced the overall expression of 4E-BP1 and this is reduced with the addition of methylprednisolone or dexamethasone (Figure 5.17d). However, the same is not true of the IL-15/TGF-β treatment. The blot reveals different isoforms of 4E-BP1, as previously reported (Gingras et al. 1999; Wang et al. 2006; Takabatake et al. n.d.). Results show that TGF-β, dexamethasone and methylprednisolone all induce the α form (compared to resting NK cells). Interestingly, a previous paper investigating the mTOR pathway in an

osteosarcoma cell line showed that inhibition of S6 kinase or treatment with Rapamycin (an inhibitor of mTOR) restricted 4E-BP1expression to just the α form (Fingar et al. 2004). It is possible that the α form has a greater affinity for eIF4E and is preferentially expressed with these treatments. The IL-15 induced phosphorylation of 4E-BP1 at threonine 37/40 is reduced with the addition of the steroid treatments but not with TGF-β. However, it has been suggested that the phosphorylation at Thr37/40 is essential for the phosphorylation of other sites on 4E-BP1 that are in the binding site for eIF4E, but they themselves do not alter the pairing (Gingras et al. 1999). The amount of the non-phosphorylated form of 4E-BP1 is also reduced, but not undetectable, with the addition of IL-15 in all treatments. The antibody used recognises threonine 46 without a phosphate; hypophosphorylated 4E-BP1 interacts strongly with eIF4E (Gingras et al. 1999) and prevents its association with mRNA. The Western blots for the phosphorylated and non-phosphorylated forms of 4E-BP1 are consistent with patterns seen for the surface phenotype, the microarray and cell cycle analysis; dexamethasone and TGF-β dampen the IL-15 response but do not completely inhibit it.

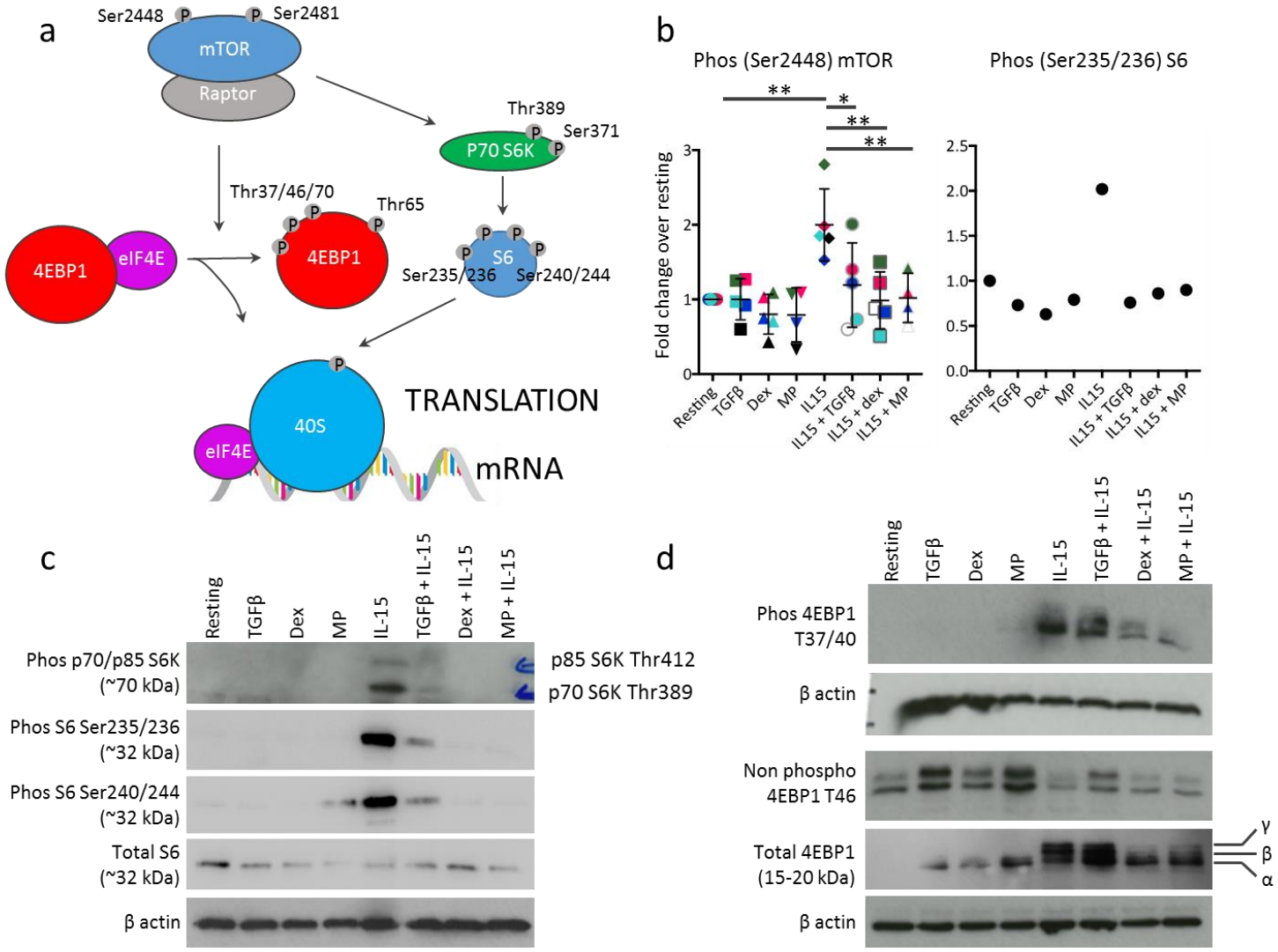

Figure 5.17. mTOR pathway analysis. a) Schematic of the mTOR pathway. The phosphorylation of 4E-BP1by mTOR causes the release of eIF4E that forms part of a translation complex. mTOR also phosphorylates p70 S6 kinase (p70 S6K), that phosphorylates S6, which in turn phosphorylates 40S ribosomal protein which also forms part of the translation complex (Based on information in (Fingar et al. 2004). b) Flow cytometry data for phosphorylated mTOR and S6. A separate colour has been used for each donor. pS6 tested for in one donor. The bar indicates the mean± s.d. Statistical analysis was performed using ratio paired t-tests. *P<0.05, **P<0.01. c) Western blots for phosphorylated p70 S6 kinase, total and phosphorylated S6. d) Western blots for 4E-BP1analysis; total protein as well as phosphorylated and non-phosphorylated protein. β actin was used as a loading

control

5.7 Reactivation of NK cells after glucocorticoid treatment.

These data demonstrate that dexamethasone is able to antagonise the effects of IL-15; downregulating NK cell activation receptor expression, preventing NK cell cytotoxicity, inducing cell death and preventing NK cells from entering the cell cycle *in vitro*. If the same is true *in vivo*, then the administration of dexamethasone to treat tumour induced cerebral oedema is predicted to render NK cell based immunotherapies ineffective. Indeed, evidence suggests that the administration of dexamethasone could negatively impact GBM patient prognosis (Hohwieler Schloss et al. 1989). The lifesaving action of steroids means that avoiding their use is not an option. My results show that future therapies must consider the combination of immunotherapy and steroids such that the steroids do not inhibit the anti-tumour activity of NK cells or other immune cell types.

I attempted to model the effects of steroid treatment on subsequent NK cell activation by IL-15 *in vitro.* Figure 5.18 shows the experimental design. NK cells were isolated from healthy donors, aliquoted into two 24-well plates and treated as follows; resting (R), dexamethasone (D), methylprednisolone (MP) or these treatments in combination with IL-15. One plate was incubated for 24 hours and the other for 48 hours. After initial incubation, cells were characterised by flow cytometry for panel of NK cell activation receptors to establish the surface phenotype (p in figure 5.18) and to quantify cell death. Cells were subsequently washed with PBS and resuspended in media containing IL-15. Cells were characterised again at both 24 and 48 hours after IL-15 treatment. The experiment was carried out using NK cells isolated from 2 individual donors.

The cell death observed during the cell cycle analysis with dexamethasone treatment alone was replicated in this analysis (Figure 5.14 and 5.19). So too was the finding that IL-15 in conjunction with dexamethasone acts to prevent death. Methylprednisolone also follows this pattern. Unsurprisingly, the amount of death increases as the time of dexamethasone or methylprednisolone exposure increases. Interestingly, when NK cells were initially treated with dexamethasone or methylprednisolone, washed and re-cultured in IL-15, the same survival effect as that seen when cells are simultaneously cultured with IL-15 and dexamethasone or methylprednisolone was

not observed. This suggests that a proportion of cells are already committed to cell death before the IL-15 survival signal is presented. The plateau of the death curves may indicate that only cells not already dying respond to the survival cue from IL-15.

When analysing the cell surface expression of CD69, a similarity between the two donors is seen (Figure 5.19). As previously described, NK cells treated with IL-15 upregulate CD69 expression compared to all other conditions including resting, steroid and dual steroid/IL-15 treatments.

The same trend is clearly seen for NKp30 and NKG2D and to a lesser extent NKp46 and DNAM-1. This supports the data presented in section 5.2. Once the cells had been washed and treated with IL-15 the general trend showed an increase in the expression of all antigens studied (CD69, NKp30, NKp46, NKG2D and DNAM-1). For CD69, NKG2D and NKp30 (48 hour treatment) the level of expression had increased by 24 hours and again by 48 hours. However, when NK cells were pre-treated with steroids, the induction of NK cell receptors by IL-15 was blunted. This is most apparent when examining the CD69 data whereby cells initially treated with methylprednisolone, dexamethasone or dexamethasone/IL-15 before IL-15 treatment have a much lower expression than cells initially left resting or treated with IL-15 (Figure 5.19). Specifically, only 42% and 23% of the 48 hour dexamethasone treated cells for donor 1 and 2 respectively expressed CD69 when subsequently activated with IL-15. Furthermore, the longer the initial exposure to dexamethasone, the lower the CD69 expression with subsequent IL-15 treatment.

If this finding mirrors the patient response to treatment with dexamethasone, then a suitable window for immunotherapy would likely be 2-3 days following the withdrawal of dexamethasone. After extended periods exposed to dexamethasone it would be sensible to assess the number of NK cells present within the patient's blood before embarking on NK cell centred immunotherapies.

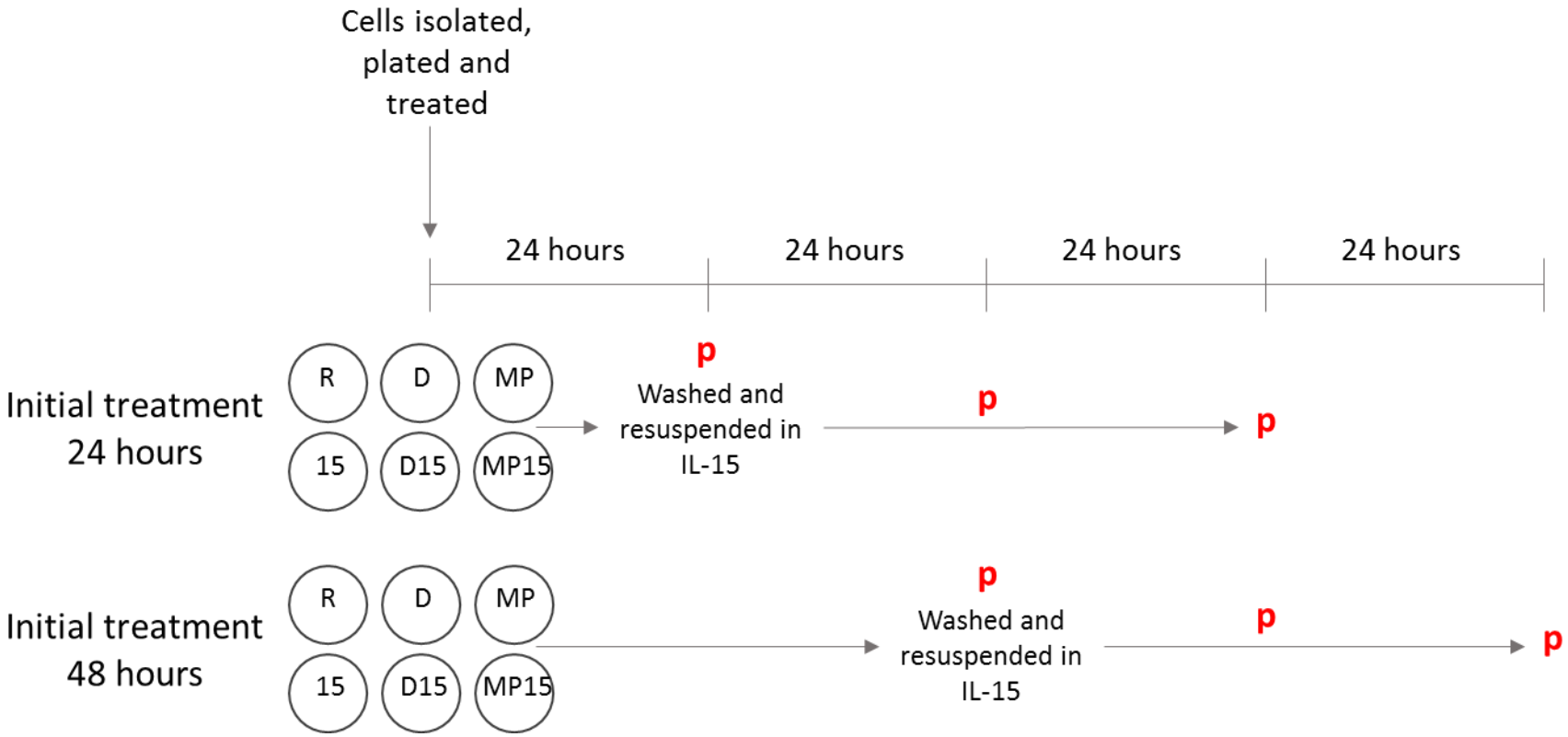

Figure 5.18. Schedule for the characterisation of NK cells reactivated after initial treatment with glucocorticoids. NK cells were isolated, plated into two 24 well plates and either left untreated (R) or treated with $2x10^{-7}$ M dexamethasone (D), $2x10^{-6}$ M methylprednisolone (MP) or these with the addition of 100 IU/mL IL-15 (15). One plate was incubated for 24 hours and the other for 48 hours. The surface phenotype (p) was characterised before the cells were washed with PBS and resuspended in media containing IL-15. The cells were then incubated for a further 24 or 48 hours before being re-characterised.

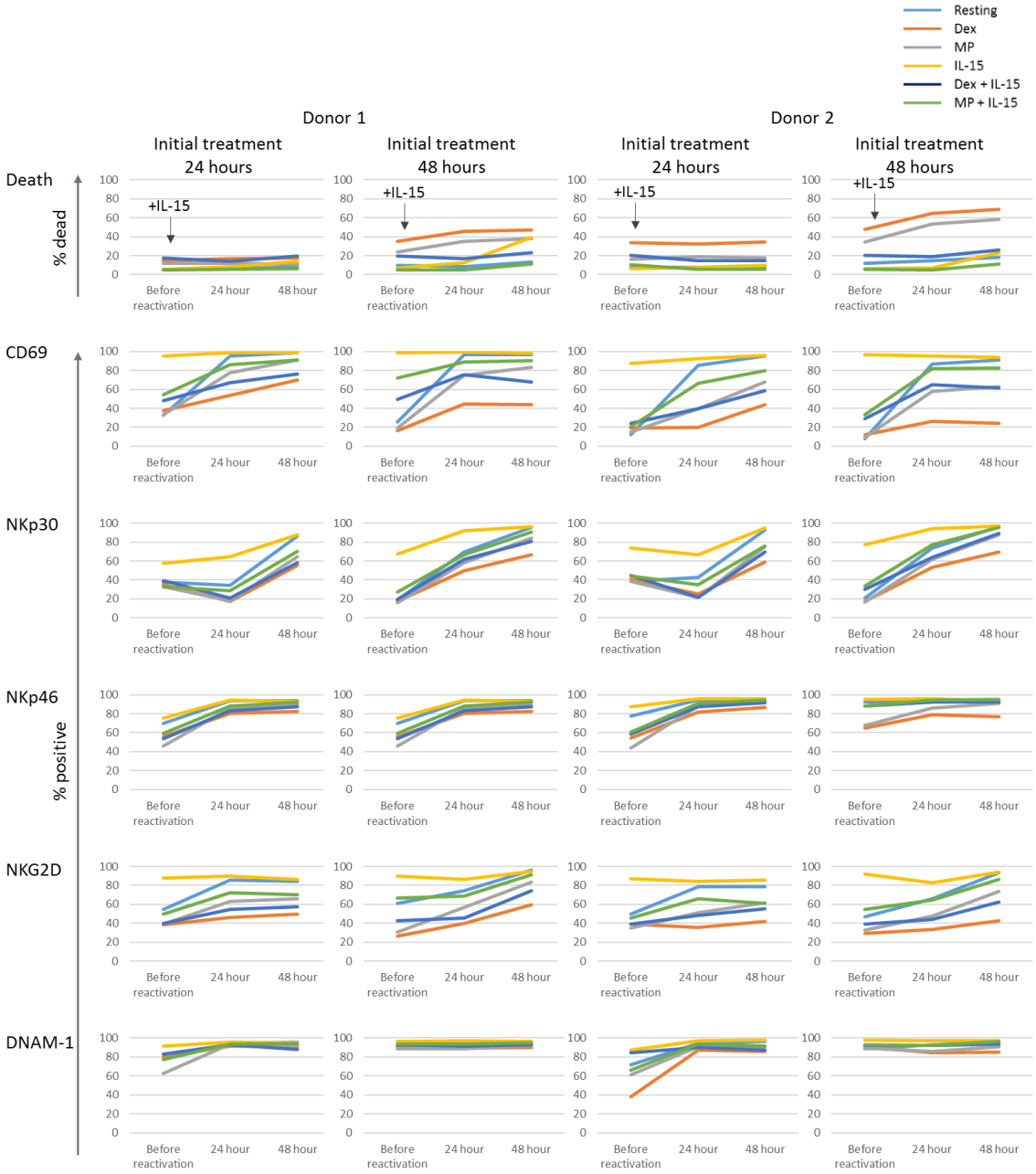

Figure 5.19. Characterisation of NK cells reactivated after initial treatment with glucocorticoids. NK cells were isolated, plated into two 24 well plates and either left untreated (light blue) or treated with $2x10^{-7}$ M dexamethasone (orange), $2X10^{-6}$ M methylprednisolone (grey) or these with the addition of 100 IU/Ml IL-15 (yellow, dark blue and green respectively). One plate was initially incubated for 24 hours (initial treatment 24 hours) and the other for 48 hours (initial treatment 48 hours). The amount of cell death (top) and the surface phenotype (antigens listed) were characterised before the cells were washed with PBS (Before reactivation) and resuspended in media containing IL-15 (+IL-15). The cells were then incubated for a further 24 or 48 hours before being re-characterised. Data is shown for two donors. The surface phenotype and cell death were analysed by flow cytometry. The percentage of NK cells that were positively stained for each antigen was established by analysing the live cells The gates were set at 2% of the isotype control stain.

5.8 Discussion and conclusion

The data presented in this chapter shows that NK cells are suppressed by both TGF-β and the glucocorticoids, dexamethasone and methylprednisolone. All three agents inhibit the IL-15 induced upregulation of activation receptors NKp30, NKG2D, DNAM-1, CD132, with IL-15 induced NKp44 expression blocked by the steroids but not TGF-β. The different patterns of expression observed between IL-15 and IL-15/TGF-β treated blood NK cells (Figure 5.2 and 5.3) mirrored those seen between the patient blood and tumour samples (Figure 3.4). This supports the hypothesis that TGF-β is an important suppressor molecule in GBM patients (Crane et al. 2010; Joseph et al. 2013). My data also supports previous publications that implicate TGF-β in preventing the upregulation of NK cell activating receptors (Wilson et al. 2011; Ikushima & Miyazono 2010; Friese et al. 2004; Lee et al. 2004). Dexamethasone has also previously been shown to prevent both the surface expression of NK cell activation receptors and effector functions. For example, the lenalidomide-induced upregulation of NKG2D and NKp46 was thwarted with the addition of dexamethasone. So too was the NK cell cytotoxic activity towards the K562 target cell line (Hsu et al. 2011). This is in agreement with the functional data presented here, whereby dexamethasone inhibits NK cell cytotoxicity (Figure 5.4), by both decreasing the amount of degranulation against target cells (which might be related to reduced expression of activation receptors) and reducing the amount of the pro-apoptotic serine protease granzyme B (Figure 5.5). Other reports show that methylprednisolone inhibits surface expression of NKp30 and NKp44 (Chiossone et al. 2007).

Gene expression profiling revealed that pathway components regulated by the transcription factor c-Myc were differentially expressed between the IL-15 treated NK cells and those treated with IL-15/TGF-β and IL-15/dexamethasone (Figure 5.10). Western blot analysis supported this hypothesis, as levels of c-Myc were higher in IL-15 treated cells compared to resting cells and cells treated with IL-15/TGF-β and IL-15/dexamethasone (Figure 5.15). The suppression of c-Myc by TGF-β was observed in keratinocytes in the late 1980s and was shown to be due to transcriptional inhibition (Pietenpol et al. 1990). Similarly, dexamethasone has previously been reported to prevent c-Myc transcription in PBMCs that have been treated with the lectin mitogen phytohemagglutinin (PHA) and recombinant IL-2 (Reed et al. 1985). Although it is

known that IL-15 activation of NK cells induces c-Myc, the inhibition of such signals have not previously been reported for dexamethasone or methylprednisolone in NK cells.

The results of the microarray suggested that IL-15 induces NK cell proliferation and that this is inhibited by TGF-β and dexamethasone. Cell cycle analysis confirmed this finding *in vitro* (Figure 5.14), which is supported by a recent publication demonstrating that TGF-β is able to prevent IL-15 induced activation, including proliferation, and that this is achieved by inhibition of the mTOR pathway (Viel et al. 2016). For many cell types it has also been reported that corticosteroids such as dexamethasone and methylprednisolone inhibit proliferation. For example, dexamethasone inhibits the proliferation of smooth muscle cells (SMC) (Reil et al. 1999), basic fibroblast growth factor-(bFGF) stimulated rat gastric epithelial cell proliferation (Luo et al. 2008) and T cells (Gutsol et al. 2013). However, a paper that presents data based on a very similar set of experiments to those described in this chapter, including expression of activation receptors, degranulation assays, and cell cycle analysis using glucocorticoids in conjunction with IL-15 on NK cells, reveals contradictory results. The paper reports that glucocorticoids (hydrocortisone, methylprednisolone and dexamethasone enhance IL-15 mediated NK cell division and that there is no change in NK cell degranulation against K562 target cells (Moustaki et al. 2011). The difference in results cannot be explained by differential amounts of IL-15 or glucocorticoids used, as a similar concentration of IL-15 was used, an identical concentration of methylprednisolone and double the concentration of dexamethasone was used in this report compared to mine. However, a different method was used to analyse cell proliferation; a CFSE assay, at different time points. The authors investigated the effects of the glucocorticoids on NK cells after 6 and 8 days in culture. Interestingly, their results at day 6 show that the IL-15 cells are proliferating more than the cells treated with dexamethasone and most have only gone through one cell division. However, according to the authors, by day 8, 50% or more of the cells have undergone 5 cell divisions or more; this seems very unlikely given that the first division took five days. The authors also state that the analysis was 'gated on live NK cells' but there is no indication of how this was performed. In my study, when optimising the loading of both NK cells and GBM cells with different cell tracker dyes, it became apparent that as cells begin to die they start to leak the dye and this can precede morphological

changes (data not shown). Dead cells incorporated in CFSE analysis would mimic dilution of dye due to cell division. My data shows that by 72 hours (with half the concentration of dexamethasone used in this study) approximately 60-80% of cells are dead, close to the proportion of NK cells reported that have divided in the contrary study.

A separate study investigating the effects of methylprednisolone on IL-2 or IL-15 treated NK cells supports the results within this chapter (Chiossone et al. 2007); methylprednisolone was found to inhibit the upregulation of IL-15 induced NKp30 and NKp44, prevent NK cell cytotoxic activity and reduce granule exocytosis. The paper also reports that IL-15 prevented glucocorticoid induced apoptosis, validating the IL-15 rescue effect that is evident in the cell cycle assay (Figure 5.14). IL-15 signalling has been implicated in the maintenance of anti-apoptotic factor Bcl-2 (Ranson et al. 2003; Huntington et al. 2007) which could counteract glucocorticoid induced apoptosis. In one study (Chiossone et al. 2007) the down regulation of IL-15 induced phosphorylated STAT5 by methylprednisolone shows the agent is able to inhibit the JAK/STAT pathway. This result was mirrored in my results for both methylprednisolone and dexamethasone, but was not seen with TGF-β (Figure 5.16). The finding that STAT5 phosphorylation was unchanged by IL-15/TGF-β also supports published findings (Viel et al. 2016).

The inhibitory effects of TGF-β, dexamethasone and methylprednisolone on IL-15 activated NK cells seems to be mediated by the mTOR pathway, with c-Myc implicated as an important transcriptional regulator. When considering NK cell based immunotherapies for patients with GBM, it is worrying that the clinically administered glucocorticoid dexamethasone employs the same immunosuppressive pathways as TGF-β. If the use of dexamethasone is unavoidable, then a suitable time to issue immunotherapy needs to be established. Experiments that aimed to investigate if NK cells could be activated after treatment with dexamethasone or methylprednisolone revealed that it was possible to increase the concentration of activation receptors but that extended treatments with the steroids without a survival signal caused large amounts of cell death (Figure 5.19). Dexamethasone is also known to cause lymphopenia (Anderson et al. 1999) *in vivo*. The phenotypic data in figure 5.19 suggests that NK cells can be activated after the withdrawal of glucocorticoids

dexamethasone and methylprednisolone. Assessing their cytotoxic activity after withdrawal of dexamethasone and activation with IL-15 would confirm this prediction.

Summary and discussion

In this work I have analysed the immune response to human glioblastoma multiforme, focussing on the interactions between NK cells and the cancer cells. The impetus for this work is the clear need to develop new therapies against this disease. Current treatments of surgery combined with chemotherapy (using temozolomide) extend a patient's life by just 9 months (Perry et al. 2016); immunotherapy holds the potential to improve this. This is best demonstrated by recent success in melanoma, where use of checkpoint inhibitors has extended survival times (Callahan et al. 2014) and trials are now underway to test these antibody therapies for use in GBM.

Natural killer (NK) cells have potent anti-tumour function and hold great potential for immunotherapy (Vivier et al. 2011; Pahl & Cerwenka 2015). Indeed, NK cells are already harnessed in standard therapies. For example, the efficacy of both rituximab (anti-CD20, for haematological malignancies) and Herceptin (trastuzumab, anti-HER2, for breast cancer) is, at least in part, due to the ability of NK cells to kill antibody coated target cells via ADCC (Dall'Ozzo et al. 2004; Roda et al. 2007; Carson et al. 2001). Furthermore, NK cell activity is harnessed in graft versus leukemia responses (Ruggeri et al. 2002). NK cells are also being exploited in several trial therapies. For example, antibodies that block KIR-MHC class I interactions are in clinical trials (Romagné et al. 2009). These antibodies inhibit NK cell inactivation by MHC class I+ tumour cells and their action is akin to releasing an NK cell checkpoint. Oncolytic viruses also exert some of their action via NK cells; the anti-viral activity of NK cells allows the oncolytic virus to activate NK cells (via type I interferon responses) and this heightened NK cell activation allows greater anti-tumour activity (El-Sherbiny et al. 2015). These existing and emerging NK cell based therapies suggest that NK cells do indeed offer great potential for NK cell based therapies in the future. However, there is a lack of information on the interaction between NK cells and GBM. Indeed, the difficulty in accessing brain tumour samples and analysing immune infiltration and immune responses has greatly limited the study of the immune response to GBM. My study aimed to address this.

Principal findings

1. NK cells and T cells infiltrate human GBM tumours but have an altered cell surface phenotype compared to their counterparts in patients' blood and healthy donor blood (chapter 3). Importantly, NK cells in the tumour microenvironment exhibited reduced cell surface expression of key tumour-cell detecting activation receptors such as NKp30, NKG2D and DNAM-1. Analysis of bulk tumour infiltrating T cells demonstrated the increased expression of key inhibitory checkpoint molecules on the T cells, namely PD-1, LAG-3 and CTLA-4. This is the first study to report such phenotypic changes on GBM infiltrating NK cells and T cells.
2. GBM stem cells are more susceptible to NK cell lysis *in vitro* compared to a non-cancerous neural progenitor cell line and GBM cells express numerous ligands that regulate NK cell activity and other components of the immune system (Chapter 4).
3. A multiplex cell surface antigen screen analysing expression of 242 cell surface antigens identified 44 antigens in common between the five GBM cancer stem cell-like cell lines. The GBM cells expressed multiple ligands known to activate NK cells (including MIC-A/B and Nectin-2) as well as a number of other cell surface molecules known to modulate T cell activity and other immune cell types, in addition to a number of molecules under investigation in other systems as therapeutic targets.
4. Analysis of the effect of corticosteroids on NK cell activation revealed them to have a potent inhibitory effect, consistent with the use of these molecules as anti-inflammatory agents (e.g in the treatment of inflammatory and autoimmune disease). In brain cancer, corticosteroids are administered to prevent oedema. My results show that steroid use is likely to severely limit any NK cell-based immunotherapy and these results have implications for the timing of immunotherapy relative to steroid treatment.
5. Gene expression profiling identified c-MYC as a key regulatory hub in NK cell activation. Biochemical studies showed that IL-15 potently induces c-MYC and this induction is inhibited in the presence of dexamethasone and the immunosuppressive cytokine TGF-β. Both steroids and TGF-β inhibit IL-15

mediated mTOR signalling. The fact that NK cells utilise mTOR and c-Myc is also highly relevant to designing new therapeutic strategies as both molecules are identified as important targets for inhibition in cancer cells themselves (Pópulo et al. 2012; Huang et al. 2014). Clearly, immunotherapy requiring mTOR activation and c-Myc dependent pathways is unlikely to be optimal in patients receiving mTOR inhibitors (e.g. rapamycin and derivative rapalogues, such as tacrolimus) or c-MYC inhibitors.

Discussion

Studies in other cancers have revealed that T lymphocyte infiltration of tumours is generally a good prognostic marker. For example, in melanoma, T cell infiltration is correlated with improved survival (reviewed in (Lee et al. 2016)). Recent studies have used transcriptome data from the bulk tumour to look for evidence of infiltration of particular lymphocytes. For example, in colorectal cancer (Bindea et al. 2013) T cell infiltrates reduce as the tumours progress. The interpretation of T cell data is difficult because of the existence of multiple subsets with different roles. For example, whereas CD8+ cytotoxic T cells might provide an anti-tumour activity, FOXP3+ Treg are associated with a poorer prognosis as they inhibit anti-tumour immunity (Curiel et al. 2004; Wolf et al. 2005; Deng et al. 2010). However, the role of Tregs is complex as they have also been reported to prevent tumour progression by limiting inflammatory activity that promotes tumour development (Whiteside 2015). For GBM patients, Tregs seem to have a detrimental role as infiltration of Tregs correlates with grade (El Andaloussi & Lesniak 2006). In my work, only bulk T cells were analysed as the samples were too small to perform the necessary phenotyping. However, my results show that whatever T cells are present, they express high levels of checkpoint molecules (especially PD-1) which are indicative of an inhibited T cell response (unlike the blood). This indicates that patients could benefit from antibody therapy targeting checkpoints and these are being trialled (despite limitations of the BBB and Ab penetration).

NK cell infiltration is also prognostic in several cancers (Coca et al. 1997; Takanami et al. 2001; Ishigami et al. 2000; Villegas et al. 2002). However, NK cells in the tumour microenvironment have an altered phenotype. For example, reduced expression of activation receptors ((Wilson et al. 2011; Carlsten et al. 2009; Carlsten et al. 2007) or

even a pro-angiogenic phenotype (Bruno et al. 2014). In GBM I found reduced expression of NKp30, DNAM-1 and NKG2D, suggestive of an impaired ability to respond to the tumour cells, although numbers of cells present prevented me from testing effector functions. In the ovarian cancer study (Wilson et al. 2011) TGF-β, an immunosuppressive cytokine known to be important in tumour progression and the immune response (Flavell et al. 2010) mimics the effects of the tumour microenvironment and inhibition of TGF-β activity restores the NK cell phenotype and anti-tumour function in vitro (Wilson et al. 2011). The phenotype of GBM resident NK cells (chapter 3) resembles that of TGF-β exposed NK cells. TGF-β is elevated in the serum of GBM patients with a large tumour burden and alters the phenotype of blood NK cells (Crane et al. 2010). Although GBM cells are known to make TGF-β (Constam et al. 1992), I could not find a role for TGF-β in the in the downregulation of NK cell activation receptors in the NK-GBM *in vitro* co-cultures.

An important result of the study is that NK cells and T cells are able to traffic to the tumour, either through the BBB, or maybe the BBB is impaired in GBM. NK cells are present in low numbers, though the ratio to bulk T cells is similar. This demonstrates that NK cells can traffic to the tumour and hence the design of therapies that enhance activity in the tumour microenvironment are likely to offer some benefit (as opposed to a situation where NK cell infiltration is absent). Whether TGF-β inhibitors or anti-KIR antibodies might help to restore NK cell function in the tumour microenvironment is unclear and it is premature to make predictions as there are many ways that tumors can evade NK cells as well as other immune cell types (Pahl & Cerwenka 2015; Vitale et al. 2014; Drake et al. 2006).

Results from chapter 4 showed that, when activated optimally (with IL-15), NK cells were able to recognize and kill GBM. Furthermore, GBM cells were preferentially killed over NP1 cells. Whilst this seems like an obvious result, most studies of NK cell-tumour cell interactions ignore the specificity of NK cells for the tumour cell compared to healthy normal tissue. This is particularly important in the brain where healthy tissue damaged by immune response is less likely to be repaired/regenerate compared to other tissues and is also likely to have severe morbidity. The mechanism behind the recognition and killing of GBM by NK cells was not explored in detail. My cell surface

antigen screen (chapter 4) identified expression of several well charactersied NK cell receptor ligands (e.g. ligands of NKG2D and DNAM-1) but these were expressed alongside high levels of MHC class I. Other studies have used blocking Ab to determine the roles of particular receptor-ligand interactions in anti-tumour activity (e.g. results from this lab; (Holmes et al. 2011; El-Sherbiny et al. 2007), in Ewings sarcoma and myeloma respectively). However, I did not perform these studies in GBM. It is noteworthy that the NK cells infiltrating the tumour exhibited a reduced surface expression of NKG2D, DNAM and NKp30 and the assumption is made that this will affect GBM recognition and killing. However, formally I haven't shown that these receptors are important in GBM recognition. Future experiments could use NK cell receptor blocking antibodies and RNA interference methods to investigate these interactions.

In addition to NK cell receptor ligands, the surface antigen screen identified several proteins of interest. PDL-1 was expressed on four of the five GBM cell lines tested, providing a plausible mechanism by which GBM evades T cell activity as my results from chapter 3 clearly demonstrate expression of PD-1 on the infiltrating T cells. In addition, several other proteins were identified that are targets of clinically approved antibody therapies. However, efficacy of these treatments might be restricted as the BBB could prevent the penetration of antibodies into the brain and research is underway to optimise BBB permeability for treatment delivery (Connell et al. 2013). Interestingly, in this study, TNF enhanced the uptake of trastuzumab targeting Her-2; my surface antigen screen revealed the expression of Her2 on all of the GBM cell lines analysed. Other targets identified, include proteins contributed to chemotherapy resistance such as type I insulin-like growth factor receptor (IGFR1) and ABCG transporter (CD338) (Chen & Sharon 2013; Leonard et al. 2003). GBM patients that acquire resistance to chemotherapy might benefit from treatments targeting these receptors.

TGF-β is recognised as playing a major role in tumour immune evasion (Flavell et al. 2010). TGF-β works by antagonising the activation of NK cells by IL-15 (Wilson et al. 2011; Viel et al. 2016). Interestingly, steroids also inhibit the cytokine activation of NK cells (Chiossone et al. 2007) and the resultant cell surface phenotype resembles that induced by TGF-β, i.e. reduced activation and induced expression of NKG2D, DNAM

and NKp30. Use of steroids in brain cancer is unavoidable, but I hypothesized that steroid treatment mimics the effects of TGF-β and is therefore is likely to limit the efficacy of immunotherapy when combined. In chapter 5, I analysed the effects of steroids on IL-15 induced NK cell activation in more detail. I used gene expression profiling in an attempt to identify common pathways of inhibition by steroids and TGF-β. This approach identified 564 genes that were reciprocally regulated by IL-15 and by IL-15+ TGF-β and IL-15+dex. Importantly, this list of genes included proteins crucial for NK cell effector functions, such as granzymes and IFN, as well as key receptors (e.g DNAM-1), highlighting the inhibitory effect of these agents in NK cell function. Bioinformatics analysis implicated the transcription c-Myc as a key molecule in the regulation of these 564 genes. Further biochemical studies in chapter showed that IL-15 induces c-Myc protein and that this induction is blocked by both TGF-β and steroids. In T cells, it is established that SMAD2/3 repress the expression of MYC in a Foxp1 dependent manner (Stephen et al. 2014). Furthermore, c-Myc orchestrates several T cell activation functions, not least the induction of the metabolic pathways that provide energy and the building blocks for biosynthesis required for cellular activation and proliferation (Buck et al. 2015). My results show that TGF-β and steroids inhibit IL-15 induced Myc protein production in NK cells and further experiments from my colleagues show that this occurs at the level of c-Myc transcription. It seems likely that TGF-β exerts these effects in a similar manner to that described in T cells. However, the mechanism by which steroids might regulate Myc is currently unclear. The importance of Myc as a regulator of NK cell activation is perhaps not surprising given that it is regulates many thousands of genes in many different cell types (Nie et al. 2012; Littlewood et al. 2012; Sabò et al. 2014). In one model, Myc acts as an amplifier of ongoing gene expression (Nie et al. 2012; Littlewood et al. 2012) and the ability of TGF-β to counteract the effects of IL-15 are consistent with this role, whereby blocking MYC induction would prevent the amplification of this expression. Furthermore, such a model is consistent with the fact that TGF-β does not completely block expression of many genes, but abrogates the IL-15 mediated increases in gene expression (Wilson et al. 2011). Whatever the mechanism, my results indicate that Myc is important to NK cell activation and this is blocked by steroids and by TGF-β. The most accepted mechanism of steroid activity is that they bind a cytosolic GR, which translocates to the nucleus and regulates gene expression. Steroids have been shown

to interfere with the NF-κB pathway and to block Myc induction in many cell types (Chang et al. 1997; Crinelli et al. 2000; Aghai et al. 2006). Clearly, further studies are required to elucidate the mechanisms by which steroids and TGF- β block Myc induction in NK cells. Furthermore, my data with Myc inhibitors are somewhat limited because they are toxic to NK cells (Chapter 5). This is probably related to the fact that preventing Myc activity blocks the IL-15 induced survival functions of NK cells. The induction of mTOR activity and Myc is important in T cell activation. However, it is not clear how mTOR and Myc are linked; studies in this lab have shown that Myc induction is unaffected by rapamycin (Erica Wilson, personal communication) and there is not a simple linear pathway between IL-15, mTOR and Myc. However, the observation that NK cells require mTOR and Myc for efficient activation has important consequences for future cancer therapy. mTOR inhibitors are in trials for several cancers as a means to block the high metabolic activity of tumour cells, reviewed in (Zaytseva et al. 2012). However, mTOR inhibitors will block T cell and NK cell activation and hence they will be incompatible with immunotherapy (Chaoul et al. 2015). Similarly, c-Myc inhibitors would not be compatible with immunotherapy. Together with my results showing that steroids block immune activation, it is clear that the effective exploitation of immunotherapy will require detailed studies of the best way to apply these different drugs, such that the anti-tumour activities of these agents do not prevent immune activation. Whilst this appears to be highly complex, it could be resolved by the appropriate sequencing and timing of different agents, as my experiments with steroid pretreatment in chapter 5 illustrate.

In summary, NK cells are capable of reaching the tumour site and recognizing and killing GBM cells. However, the optimisation of NK cells and indeed other immunotherapy approaches will clearly require a more complete understanding of the mechanisms used by immune cells to recognize and be activated by GBM cells and how different therapies might interact, either positively or negatively.

References

Abraham, S.M. et al., 2006. Antiinflammatory effects of dexamethasone are partly dependent on induction of dual specificity phosphatase 1. *The Journal of experimental medicine*, 203(8), pp.1883–9.

Adair, R.A. et al., 2012. Cell carriage, delivery, and selective replication of an oncolytic virus in tumor in patients. *Science translational medicine*, 4(138), p.138ra77.

Aghai, Z.H. et al., 2006. Dexamethasone suppresses expression of Nuclear Factor-kappaB in the cells of tracheobronchial lavage fluid in premature neonates with respiratory distress. *Pediatric research*, 59(6), pp.811–5.

Ahmad, A.S., Ormiston-Smith, N. & Sasieni, P.D., 2015. Trends in the lifetime risk of developing cancer in Great Britain: comparison of risk for those born from 1930 to 1960. *British journal of cancer*, 112(5), pp.943–7.

Ahmed, R. et al., 2014. Malignant gliomas: current perspectives in diagnosis, treatment, and early response assessment using advanced quantitative imaging methods. *Cancer management and research*, 6, pp.149–70.

Alcami, A. & Koszinowski, U.H., 2000. Viral mechanisms of immune evasion. *Immunology today*, 21(9), pp.447–55.

Algarra, I. et al., 2004. The selection of tumor variants with altered expression of classical and nonclassical MHC class I molecules: implications for tumor immune escape. *Cancer immunology, immunotherapy : CII*, 53(10), pp.904–10.

Alvarez-Breckenridge, C.A. et al., 2012. NK cells impede glioblastoma virotherapy through NKp30 and NKp46 natural cytotoxicity receptors. *Nature medicine*, 18(12), pp.1827–34.

El Andaloussi, A. & Lesniak, M.S., 2006. An increase in CD4+CD25+FOXP3+ regulatory T cells in tumor-infiltrating lymphocytes of human glioblastoma multiforme. *Neuro-oncology*, 8(3), pp.234–43.

Anderson, B.H., Watson, D.L. & Colditz, I.G., 1999. The effect of dexamethasone on some immunological parameters in cattle. *Veterinary research communications*, 23(7), pp.399–413.

Antonioli, L. et al., 2013. CD39 and CD73 in immunity and inflammation. *Trends in molecular medicine*, 19(6), pp.355–67.

Assou, S. et al., 2007. A meta-analysis of human embryonic stem cells transcriptome integrated into a web-based expression atlas. *Stem cells (Dayton, Ohio)*, 25(4), pp.961–73.

Auphan, N. et al., 1995. Immunosuppression by glucocorticoids: inhibition of NF-kappa B activity through induction of I kappa B synthesis. *Science (New York, N.Y.)*, 270(5234), pp.286–90.

Bailey, P. & Cushing, H., 1926. Bailey P, Cushing H: A Classification of the Tumors of the Glioma Group on a Histogenetic Basis With a Correlated Study of Prognosis. Philadelphia: Lippincott, 1926. *British Journal of Surgery*, 14(55), pp.554–555.

Ballabh, P., Braun, A. & Nedergaard, M., 2004. The blood-brain barrier: an overview: structure, regulation, and clinical implications. *Neurobiology of disease*, 16(1), pp.1–13.

Ballard, P.L. et al., 1974. General presence of glucocorticoid receptors in mammalian tissues. *Endocrinology*, 94(4), pp.998–1002.

Bandres, E. et al., 2005. Gene expression profile induced by BCNU in human glioma cell lines with differential MGMT expression. *Journal of neuro-oncology*, 73(3),

pp.189–98.
Bao, S. et al., 2006. Glioma stem cells promote radioresistance by preferential activation of the DNA damage response. *Nature*, 444(7120), pp.756–60.
Barrow, A.D. & Trowsdale, J., 2008. The extended human leukocyte receptor complex: diverse ways of modulating immune responses. *Immunological reviews*, 224, pp.98–123.
Baylis, E.M. et al., 1982. High dose intravenous methylprednisolone "pulse" therapy in patients with rheumatoid disease. Plasma methylprednisolone levels and adrenal function. *European journal of clinical pharmacology*, 21(5), pp.385–8.
van Beek, E.M. et al., 2005. Signal regulatory proteins in the immune system. *Journal of immunology (Baltimore, Md. : 1950)*, 175(12), pp.7781–7.
Betts, M.R. et al., 2003. Sensitive and viable identification of antigen-specific CD8+ T cells by a flow cytometric assay for degranulation. *Journal of immunological methods*, 281(1–2), pp.65–78.
Bielamowicz, K., Khawja, S. & Ahmed, N., 2013. Adoptive cell therapies for glioblastoma. *Frontiers in oncology*, 3, p.275.
Bindea, G. et al., 2013. Spatiotemporal dynamics of intratumoral immune cells reveal the immune landscape in human cancer. *Immunity*, 39(4), pp.782–95.
Böker, D.K. et al., 1984. Mononuclear infiltrates in human intracranial tumors as a prognostic factor. Influence of preoperative steroid treatment. I. Glioblastoma. *Clinical neuropathology*, 3(4), pp.143–7.
De Bosscher, K., 2010. Selective Glucocorticoid Receptor modulators. *The Journal of steroid biochemistry and molecular biology*, 120(2–3), pp.96–104.
De Bosscher, K. et al., 2008. Selective transrepression versus transactivation mechanisms by glucocorticoid receptor modulators in stress and immune systems. *European journal of pharmacology*, 583(2–3), pp.290–302.
De Bosscher, K., Vanden Berghe, W. & Haegeman, G., 2003. The interplay between the glucocorticoid receptor and nuclear factor-kappaB or activator protein-1: molecular mechanisms for gene repression. *Endocrine reviews*, 24(4), pp.488–522.
Bottino, C. et al., 2003. Identification of PVR (CD155) and Nectin-2 (CD112) as cell surface ligands for the human DNAM-1 (CD226) activating molecule. *The Journal of experimental medicine*, 198(4), pp.557–67.
Brandt, C.S. et al., 2009. The B7 family member B7-H6 is a tumor cell ligand for the activating natural killer cell receptor NKp30 in humans. *The Journal of experimental medicine*, 206(7), pp.1495–503.
Brass, A.L. et al., 2009. The IFITM proteins mediate cellular resistance to influenza A H1N1 virus, West Nile virus, and dengue virus. *Cell*, 139(7), pp.1243–54.
Brodbelt, A. & Stoodley, M., 2007. CSF pathways: a review. *British journal of neurosurgery*, 21(5), pp.510–20.
Brooks, W.H. et al., 1978. Relationship of lymphocyte invasion and survival of brain tumor patients. *Annals of neurology*, 4(3), pp.219–24.
Bruno, A. et al., 2014. A think tank of TINK/TANKs: tumor-infiltrating/tumor-associated natural killer cells in tumor progression and angiogenesis. *Journal of the National Cancer Institute*, 106(8), p.dju200.
Bruno, A. et al., 2013. The proangiogenic phenotype of natural killer cells in patients with non-small cell lung cancer. *Neoplasia (New York, N.Y.)*, 15(2), pp.133–42.
Buck, M.D., O'Sullivan, D. & Pearce, E.L., 2015. T cell metabolism drives immunity. *The*

Journal of experimental medicine, 212(9), pp.1345–60.
Bunim, J.J. et al., 1958. Studies on dexamethasone, a new synthetic steroid, in rheurheumatoid arthritis: a preliminary report; adrenal cortical, metabolic and early clinical effects. *Arthritis and rheumatism*, 1(4), pp.313–31.
Burnet, F.M., 1970. The concept of immunological surveillance. *Progress in experimental tumor research*, 13, pp.1–27.
Caligiuri, M.A., 2008a. Human natural killer cells. *Blood*, 112(3), pp.461–9.
Caligiuri, M.A., 2008b. Human natural killer cells. *Blood*, 112(3), pp.461–9.
Callahan, M.K., Postow, M.A. & Wolchok, J.D., 2014. CTLA-4 and PD-1 Pathway Blockade: Combinations in the Clinic. *Frontiers in oncology*, 4, p.385.
Cancer Genome Atlas Research Network, 2008. Comprehensive genomic characterization defines human glioblastoma genes and core pathways. *Nature*, 455(7216), pp.1061–8.
Cancer Research UK, 2016a. Cancer mortality statistics. Available at: http://www.cancerresearchuk.org/health-professional/cancer-mortality-statistics accessed [Accessed June 7, 2016].
Cancer Research UK, 2016b. Survival statistics for brain tumours. Available at: http://www.cancerresearchuk.org/about-cancer/type/brain-tumour/treatment/statistics-and-outlook-for-brain-tumours#glioma [Accessed June 14, 2016].
Cantor, J.M. & Ginsberg, M.H., 2012. CD98 at the crossroads of adaptive immunity and cancer. *Journal of cell science*, 125(Pt 6), pp.1373–82.
Carlsten, M. et al., 2007. DNAX accessory molecule-1 mediated recognition of freshly isolated ovarian carcinoma by resting natural killer cells. *Cancer research*, 67(3), pp.1317–25.
Carlsten, M. et al., 2009. Primary human tumor cells expressing CD155 impair tumor targeting by down-regulating DNAM-1 on NK cells. *Journal of immunology (Baltimore, Md. : 1950)*, 183(8), pp.4921–30.
Carrega, P. et al., 2008. Natural killer cells infiltrating human nonsmall-cell lung cancer are enriched in CD56 bright CD16(-) cells and display an impaired capability to kill tumor cells. *Cancer*, 112(4), pp.863–75.
Carson, W.E. et al., 2001. Interleukin-2 enhances the natural killer cell response to Herceptin-coated Her2/neu-positive breast cancer cells. *European journal of immunology*, 31(10), pp.3016–25.
Castriconi, R. et al., 2009. NK cells recognize and kill human glioblastoma cells with stem cell-like properties. *Journal of immunology (Baltimore, Md. : 1950)*, 182(6), pp.3530–9.
Castriconi, R. et al., 2003. Transforming growth factor beta 1 inhibits expression of NKp30 and NKG2D receptors: consequences for the NK-mediated killing of dendritic cells. *Proceedings of the National Academy of Sciences of the United States of America*, 100(7), pp.4120–5.
Catalfamo, M. & Henkart, P.A., 2003. Perforin and the granule exocytosis cytotoxicity pathway. *Current opinion in immunology*, 15(5), pp.522–7.
Chan, J.K., Ng, C.S. & Hui, P.K., 1988. A simple guide to the terminology and application of leucocyte monoclonal antibodies. *Histopathology*, 12(5), pp.461–80.
Chang, C.K., Llanes, S. & Schumer, W., 1997. Effect of dexamethasone on NF-kB activation, tumor necrosis factor formation, and glucose dyshomeostasis in septic rats. *The Journal of surgical research*, 72(2), pp.141–5.
Chaoul, N. et al., 2015. Rapamycin Impairs Antitumor CD8+ T-cell Responses and

Vaccine-Induced Tumor Eradication. *Cancer research*, 75(16), pp.3279–91.
Chen, H.X. & Sharon, E., 2013. IGF-1R as an anti-cancer target--trials and tribulations. *Chinese journal of cancer*, 32(5), pp.242–52.
Chiossone, L. et al., 2007. Molecular analysis of the methylprednisolone-mediated inhibition of NK-cell function: evidence for different susceptibility of IL-2- versus IL-15-activated NK cells. *Blood*, 109(9), pp.3767–75.
Clark, A.R., 2007. Anti-inflammatory functions of glucocorticoid-induced genes. *Molecular and cellular endocrinology*, 275(1–2), pp.79–97.
Coca, S. et al., 1997. The prognostic significance of intratumoral natural killer cells in patients with colorectal carcinoma. *Cancer*, 79(12), pp.2320–8.
Codo, P. et al., 2014. MicroRNA-mediated down-regulation of NKG2D ligands contributes to glioma immune escape. *Oncotarget*, 5(17), pp.7651–62.
Coffelt, S.B. et al., 2010. Elusive identities and overlapping phenotypes of proangiogenic myeloid cells in tumors. *The American journal of pathology*, 176(4), pp.1564–76.
Cohen, A.D. et al., 2002. Gemtuzumab ozogamicin (Mylotarg) monotherapy for relapsed AML after hematopoietic stem cell transplant: efficacy and incidence of hepatic veno-occlusive disease. *Bone marrow transplantation*, 30(1), pp.23–8.
Coles, S.J. et al., 2011. CD200 expression suppresses natural killer cell function and directly inhibits patient anti-tumor response in acute myeloid leukemia. *Leukemia*, 25(5), pp.792–9.
Connell, J.J. et al., 2013. Selective permeabilization of the blood-brain barrier at sites of metastasis. *Journal of the National Cancer Institute*, 105(21), pp.1634–43.
Constam, D.B. et al., 1992. Differential expression of transforming growth factor-beta 1, -beta 2, and -beta 3 by glioblastoma cells, astrocytes, and microglia. *Journal of immunology (Baltimore, Md. : 1950)*, 148(5), pp.1404–10.
Cooper, M.A. et al., 2001. Human natural killer cells: a unique innate immunoregulatory role for the CD56bright subset. *Blood*, 97(10).
Crane, C.A. et al., 2010. TGF-beta downregulates the activating receptor NKG2D on NK cells and CD8+ T cells in glioma patients. *Neuro-oncology*, 12(1), pp.7–13.
Crinelli, R. et al., 2000. Selective inhibition of NF-kB activation and TNF-alpha production in macrophages by red blood cell-mediated delivery of dexamethasone. *Blood cells, molecules & diseases*, 26(3), pp.211–22.
Curiel, T.J. et al., 2004. Specific recruitment of regulatory T cells in ovarian carcinoma fosters immune privilege and predicts reduced survival. *Nature medicine*, 10(9), pp.942–9.
Daga, A. et al., 2011. New perspectives in glioma immunotherapy. *Current pharmaceutical design*, 17(23), pp.2439–67.
Dall'Ozzo, S. et al., 2004. Rituximab-dependent cytotoxicity by natural killer cells: influence of FCGR3A polymorphism on the concentration-effect relationship. *Cancer research*, 64(13), pp.4664–9.
Deaglio, S. et al., 2007. Adenosine generation catalyzed by CD39 and CD73 expressed on regulatory T cells mediates immune suppression. *The Journal of experimental medicine*, 204(6), pp.1257–65.
DeNardo, D.G., Andreu, P. & Coussens, L.M., 2010. Interactions between lymphocytes and myeloid cells regulate pro- versus anti-tumor immunity. *Cancer metastasis reviews*, 29(2), pp.309–16.
Deng, L. et al., 2010. Accumulation of foxp3+ T regulatory cells in draining lymph nodes correlates with disease progression and immune suppression in colorectal cancer

patients. *Clinical cancer research : an official journal of the American Association for Cancer Research*, 16(16), pp.4105–12.
Denysenko, T. et al., 2010. Glioblastoma cancer stem cells: heterogeneity, microenvironment and related therapeutic strategies. *Cell biochemistry and function*, 28(5), pp.343–51.
Derynck, R. & Zhang, Y.E., 2003. Smad-dependent and Smad-independent pathways in TGF-beta family signalling. *Nature*, 425(6958), pp.577–84.
Desjardins, A. et al., 2016. Patient survival on the dose escalation phase of the Oncolytic Polio/Rhinovirus Recombinant (PVSRIPO) against WHO grade IV malignant glioma (MG) clinical trial compared to historical controls. | 2016 ASCO Annual Meeting | Abstracts | Meeting Library.
Dighe, A.S. et al., 1994. Enhanced in vivo growth and resistance to rejection of tumor cells expressing dominant negative IFN gamma receptors. *Immunity*, 1(6), pp.447–56.
Dillman, R.O. et al., 1997. Intralesional lymphokine-activated killer cells as adjuvant therapy for primary glioblastoma. *Journal of immunotherapy (Hagerstown, Md. : 1997)*, 32(9), pp.914–9.
Ding, P. et al., 2014. Expression of tumor-associated macrophage in progression of human glioma. *Cell biochemistry and biophysics*, 70(3), pp.1625–31.
Dong, Z. et al., 2009. Essential function for SAP family adaptors in the surveillance of hematopoietic cells by natural killer cells. *Nature immunology*, 10(9), pp.973–80.
Doolittle, N.D. et al., 2005. New frontiers in translational research in neuro-oncology and the blood-brain barrier: report of the tenth annual Blood-Brain Barrier Disruption Consortium Meeting. *Clinical cancer research : an official journal of the American Association for Cancer Research*, 11(2 Pt 1), pp.421–8.
Drake, C.G., Jaffee, E. & Pardoll, D.M., 2006. Mechanisms of immune evasion by tumors. *Advances in immunology*, 90, pp.51–81.
Dunn, G.P. et al., 2002. Cancer immunoediting: from immunosurveillance to tumor escape. *Nature immunology*, 3(11), pp.991–8.
Dunn, G.P., Dunn, I.F. & Curry, W.T., 2007. Focus on TILs: Prognostic significance of tumor infiltrating lymphocytes in human glioma. *Cancer immunity*, 7, p.12.
Echeverria, P.C. & Picard, D., 2010. Molecular chaperones, essential partners of steroid hormone receptors for activity and mobility. *Biochimica et biophysica acta*, 1803(6), pp.641–9.
El-Sherbiny, Y.M. et al., 2015. Controlled infection with a therapeutic virus defines the activation kinetics of human natural killer cells in vivo. *Clinical and experimental immunology*, 180(1), pp.98–107.
El-Sherbiny, Y.M. et al., 2007. The requirement for DNAM-1, NKG2D, and NKp46 in the natural killer cell-mediated killing of myeloma cells. *Cancer research*, 67(18), pp.8444–9.
Faddaoui, A. et al., 2016. The mannose receptor LY75 (DEC205/CD205) modulates cellular phenotype and metastatic potential of ovarian cancer cells. *Oncotarget*, 7(12), pp.14125–42.
Fellner, C., 2012. Ipilimumab (yervoy) prolongs survival in advanced melanoma: serious side effects and a hefty price tag may limit its use. *P & T : a peer-reviewed journal for formulary management*, 37(9), pp.503–30.
Filipe-Santos, O. et al., 2006. Inborn errors of IL-12/23- and IFN-gamma-mediated immunity: molecular, cellular, and clinical features. *Seminars in immunology*, 18(6), pp.347–61.

Fingar, D.C. et al., 2004. mTOR controls cell cycle progression through its cell growth effectors S6K1 and 4E-BP1/eukaryotic translation initiation factor 4E. *Molecular and cellular biology*, 24(1), pp.200–16.

Flavell, R.A. et al., 2010. The polarization of immune cells in the tumour environment by TGFbeta. *Nature reviews. Immunology*, 10(8), pp.554–67.

Fogel-Petrovic, M. et al., 2007. Physiological concentrations of transforming growth factor beta1 selectively inhibit human dendritic cell function. *International immunopharmacology*, 7(14), pp.1924–33.

Ford, A.L. et al., 1996. Microglia induce CD4 T lymphocyte final effector function and death. *The Journal of experimental medicine*, 184(5), pp.1737–45.

Franchimont, D., 2004. Overview of the actions of glucocorticoids on the immune response: a good model to characterize new pathways of immunosuppression for new treatment strategies. *Annals of the New York Academy of Sciences*, 1024, pp.124–37.

Freud, A.G. & Caligiuri, M.A., 2006. Human natural killer cell development. *Immunological reviews*, 214, pp.56–72.

Friese, M.A. et al., 2003. MICA/NKG2D-mediated immunogene therapy of experimental gliomas. *Cancer research*, 63(24), pp.8996–9006.

Friese, M.A. et al., 2004. RNA interference targeting transforming growth factor-beta enhances NKG2D-mediated antiglioma immune response, inhibits glioma cell migration and invasiveness, and abrogates tumorigenicity in vivo. *Cancer research*, 64(20), pp.7596–603.

Gaggar, A., Shayakhmetov, D.M. & Lieber, A., 2003. CD46 is a cellular receptor for group B adenoviruses. *Nature medicine*, 9(11), pp.1408–12.

Galea, I., Bechmann, I. & Perry, V.H., 2007. What is immune privilege (not)? *Trends in immunology*, 28(1), pp.12–8.

Gandhi, A.K. et al., 2010. Dexamethasone synergizes with lenalidomide to inhibit multiple myeloma tumor growth, but reduces lenalidomide-induced immunomodulation of T and NK cell function. *Current cancer drug targets*, 10(2), pp.155–67.

Garni-Wagner, B.A. et al., 1993. A novel function-associated molecule related to non-MHC-restricted cytotoxicity mediated by activated natural killer cells and T cells. *Journal of immunology (Baltimore, Md. : 1950)*, 151(1), pp.60–70.

Gasser, S. et al., 2005. The DNA damage pathway regulates innate immune system ligands of the NKG2D receptor. *Nature*, 436(7054), pp.1186–90.

Gilbert, M.R. et al., 2014. A randomized trial of bevacizumab for newly diagnosed glioblastoma. *The New England journal of medicine*, 370(8), pp.699–708.

Gingras, A.C. et al., 1999. Regulation of 4E-BP1 phosphorylation: a novel two-step mechanism. *Genes & development*, 13(11), pp.1422–37.

Goldenberg, M.M., 2012. Multiple sclerosis review. *P & T : a peer-reviewed journal for formulary management*, 37(3), pp.175–84.

Goldmann, J. et al., 2006. T cells traffic from brain to cervical lymph nodes via the cribroid plate and the nasal mucosa. *Journal of leukocyte biology*, 80(4), pp.797–801.

Grauer, O.M. et al., 2007. CD4+FoxP3+ regulatory T cells gradually accumulate in gliomas during tumor growth and efficiently suppress antiglioma immune responses in vivo. *International journal of cancer*, 121(1), pp.95–105.

Grégoire, C. et al., 2007. The trafficking of natural killer cells. *Immunological reviews*, 220, pp.169–82.

Gutsol, A.A. et al., 2013. Dexamethasone effects on activation and proliferation of immune memory T cells. *Bulletin of experimental biology and medicine*, 155(4), pp.474–6.
Hadjipanayis, C.G. & Van Meir, E.G., 2009. Tumor initiating cells in malignant gliomas: biology and implications for therapy. *Journal of molecular medicine (Berlin, Germany)*, 87(4), pp.363–74.
Hall, A., 2006. *Textbook of Medical Physiology* 11th ed., Philadelphia: Elsevier Saunders.
Han, J. et al., 2015. TGFβ Treatment Enhances Glioblastoma Virotherapy by Inhibiting the Innate Immune Response. *Cancer research*, 75(24), pp.5273–82.
Hanahan, D. & Weinberg, R.A., 2011. Hallmarks of cancer: the next generation. *Cell*, 144(5), pp.646–74.
Hanahan, D. & Weinberg, R.A., 2000. The hallmarks of cancer. *Cell*, 100(1), pp.57–70.
Hanna, J. et al., 2006. Decidual NK cells regulate key developmental processes at the human fetal-maternal interface. *Nature medicine*, 12(9), pp.1065–74.
Harris, N.L. & Ronchese, F., 1999. The role of B7 costimulation in T-cell immunity. *Immunology and cell biology*, 77(4), pp.304–11.
He, Y. et al., 2016. Lymphocyte-activation gene-3, an important immune checkpoint in cancer. *Cancer Sci*, 107, pp.1193–1197.
Heimberger, A.B. et al., 2005. Prognostic effect of epidermal growth factor receptor and EGFRvIII in glioblastoma multiforme patients. *Clinical cancer research : an official journal of the American Association for Cancer Research*, 11(4), pp.1462–6.
Hench, P., 1950. The reversibility of certain rheumatic and non-rheumatic conditions by the use of cortisone or of the pituitary adrenocorticotropic hormone. In *Nobel Lecture*.
Hench, P. & Kendall, E.C., 1949. The effect of a hormone of the adrenal cortex (17-hydroxy-11-dehydrocorticosterone; compound E) and of pituitary adrenocorticotropic hormone on rheumatoid arthritis. *Proceedings of the staff meetings. Mayo Clinic*, 24(8), pp.181–97.
Herberman, R.B. et al., 1975. Natural cytotoxic reactivity of mouse lymphoid cells against syngeneic and allogeneic tumors. II. Characterization of effector cells. *International journal of cancer*, 16(2), pp.230–9.
Herberman, R.B. & Holden, H.T., 1978. Natural cell-mediated immunity. *Advances in cancer research*, 27, pp.305–77.
Herzog, H.L. et al., 1955. New antiarthritic steroids. *Science (New York, N.Y.)*, 121(3136), p.176.
Heusel, J.W. et al., 1994. Cytotoxic lymphocytes require granzyme B for the rapid induction of DNA fragmentation and apoptosis in allogeneic target cells. *Cell*, 76(6), pp.977–87.
Hinrichs, C.S. et al., 2005. Glucocorticoids do not inhibit antitumor activity of activated CD8+ T cells. *Journal of immunotherapy (Hagerstown, Md. : 1997)*, 28(6), pp.517–24.
Hishii, M. et al., 1995. Human glioma-derived interleukin-10 inhibits antitumor immune responses in vitro. *Neurosurgery*, 37(6), pp.1160-6-7.
Hohwieler Schloss, M. et al., 1989. Glucocorticoid dependency as a prognostic factor in radiotherapy for cerebral gliomas. *Acta oncologica (Stockholm, Sweden)*, 28(1), pp.51–5.
Holmes, T.D. et al., 2011. A human NK cell activation/inhibition threshold allows small changes in the target cell surface phenotype to dramatically alter susceptibility to

NK cells. *Journal of immunology (Baltimore, Md. : 1950)*, 186(3), pp.1538–45.
Homann, S. et al., 2011. Upregulation of BST-2/Tetherin by HIV infection in vivo. *Journal of virology*, 85(20), pp.10659–68.
Hsu, A.K. et al., 2011. The immunostimulatory effect of lenalidomide on NK-cell function is profoundly inhibited by concurrent dexamethasone therapy. *Blood*, 117(5), pp.1605–13.
Huang, H. et al., 2014. Attacking c-Myc: targeted and combined therapies for cancer. *Current pharmaceutical design*, 20(42), pp.6543–54.
Huang, S. et al., 1997. Role of A2a extracellular adenosine receptor-mediated signaling in adenosine-mediated inhibition of T-cell activation and expansion. *Blood*, 90(4), pp.1600–10.
Huntington, N.D. et al., 2007. Interleukin 15-mediated survival of natural killer cells is determined by interactions among Bim, Noxa and Mcl-1. *Nature immunology*, 8(8), pp.856–63.
Hussain, S.F. et al., 2006. The role of human glioma-infiltrating microglia/macrophages in mediating antitumor immune responses. *Neuro-oncology*, 8(3), pp.261–79.
Ichim, C. V, 2005. Revisiting immunosurveillance and immunostimulation: Implications for cancer immunotherapy. *Journal of translational medicine*, 3(1), p.8.
Ikushima, H. & Miyazono, K., 2010. TGFbeta signalling: a complex web in cancer progression. *Nature reviews. Cancer*, 10(6), pp.415–24.
Ingraham, F.D., Matson, D.D. & McLaurin, R.L., 1952. Cortisone and ACTH as an adjunct to the surgery of craniopharyngiomas. *The New England journal of medicine*, 246(15), pp.568–71.
Institute National Cancer, 2005. The Repository of Molecular Brain Neoplasia Data (REMBRANDT). Available at: http://rembrandt.nci.nih.gov [Accessed February 25, 2015].
Ishigami, S. et al., 2000. Prognostic value of intratumoral natural killer cells in gastric carcinoma. *Cancer*, 88(3), pp.577–83.
Jacobs, J.F.M. et al., 2009. Regulatory T cells and the PD-L1/PD-1 pathway mediate immune suppression in malignant human brain tumors. *Neuro-oncology*, 11(4), pp.394–402.
Jadus, M.R. et al., 2012. Lung cancer: a classic example of tumor escape and progression while providing opportunities for immunological intervention. *Clinical & developmental immunology*, 2012, p.160724.
Jain, R.K. et al., 2007. Angiogenesis in brain tumours. *Nature reviews. Neuroscience*, 8(8), pp.610–22.
Jiang, D. et al., 2010. Identification of five interferon-induced cellular proteins that inhibit west nile virus and dengue virus infections. *Journal of virology*, 84(16), pp.8332–41.
Jiang, Y., Li, Y. & Zhu, B., 2015. T-cell exhaustion in the tumor microenvironment. *Cell death & disease*, 6, p.e1792.
Johnston, J.A. et al., 1995. Tyrosine phosphorylation and activation of STAT5, STAT3, and Janus kinases by interleukins 2 and 15. *Proceedings of the National Academy of Sciences of the United States of America*, 92(19), pp.8705–9.
Joseph, J. V et al., 2013. TGF-β as a therapeutic target in high grade gliomas - promises and challenges. *Biochemical pharmacology*, 85(4), pp.478–85.
Jovčevska, I., Kočevar, N. & Komel, R., 2013. Glioma and glioblastoma - how much do we (not) know? *Molecular and clinical oncology*, 1(6), pp.935–941.
Joyce, M.G. & Sun, P.D., 2011. The structural basis of ligand recognition by natural

killer cell receptors. *Journal of biomedicine & biotechnology*, 2011, p.203628.
Jung, H. et al., 2012. RAE-1 ligands for the NKG2D receptor are regulated by E2F transcription factors, which control cell cycle entry. *The Journal of experimental medicine*, 209(13), pp.2409–22.
Kärre, K., 2002. NK cells, MHC class I molecules and the missing self. *Scandinavian journal of immunology*, 55(3), pp.221–8.
Keir, M.E. et al., 2008. PD-1 and its ligands in tolerance and immunity. *Annual review of immunology*, 26, pp.677–704.
Kelly, E. & Russell, S.J., 2007. History of oncolytic viruses: genesis to genetic engineering. *Molecular therapy : the journal of the American Society of Gene Therapy*, 15(4), pp.651–9.
Keskin, D.B. et al., 2007. TGFbeta promotes conversion of CD16+ peripheral blood NK cells into CD16- NK cells with similarities to decidual NK cells. *Proceedings of the National Academy of Sciences of the United States of America*, 104(9), pp.3378–83.
Kiessling, R., Klein, E. & Wigzell, H., 1975. Natural'' killer cells in the mouse. I. Cytotoxic cells with specificity for mouse Moloney leukemia cells. Specificity and distribution according to genotype. *European journal of immunology*, 5(2), pp.112–7.
Kim, E.-O. et al., 2010. Homotypic cell to cell cross-talk among human natural killer cells reveals differential and overlapping roles of 2B4 and CD2. *The Journal of biological chemistry*, 285(53), pp.41755–64.
Kim, R., Emi, M. & Tanabe, K., 2007. Cancer immunoediting from immune surveillance to immune escape. *Immunology*, 121(1), pp.1–14.
Kivisäkk, P. et al., 2003. Human cerebrospinal fluid central memory CD4+ T cells: evidence for trafficking through choroid plexus and meninges via P-selectin. *Proceedings of the National Academy of Sciences of the United States of America*, 100(14), pp.8389–94.
Kmiecik, J. et al., 2013. Elevated CD3+ and CD8+ tumor-infiltrating immune cells correlate with prolonged survival in glioblastoma patients despite integrated immunosuppressive mechanisms in the tumor microenvironment and at the systemic level. *Journal of neuroimmunology*, 264(1–2), pp.71–83.
Kmiecik, J., Zimmer, J. & Chekenya, M., 2014. Natural killer cells in intracranial neoplasms: presence and therapeutic efficacy against brain tumours. *Journal of neuro-oncology*, 116(1), pp.1–9.
Kogiku, M. et al., 2008. Prognosis of glioma patients by combined immunostaining for survivin, Ki-67 and epidermal growth factor receptor. *Journal of clinical neuroscience : official journal of the Neurosurgical Society of Australasia*, 15(11), pp.1198–203.
Koh, J. et al., 2012. Susceptibility of CD24(+) ovarian cancer cells to anti-cancer drugs and natural killer cells. *Biochemical and biophysical research communications*, 427(2), pp.373–8.
Koh, L., Zakharov, A. & Johnston, M., 2005. Integration of the subarachnoid space and lymphatics: is it time to embrace a new concept of cerebrospinal fluid absorption? *Cerebrospinal fluid research*, 2, p.6.
Koks, C.A.E. et al., 2015. Immune Suppression during Oncolytic Virotherapy for High-Grade Glioma; Yes or No? *Journal of Cancer*, 6(3), pp.203–17.
Kostaras, X. et al., 2014. Use of dexamethasone in patients with high-grade glioma: a clinical practice guideline. *Current oncology (Toronto, Ont.)*, 21(3), pp.e493-503.

Kretz-Rommel, A. et al., 2007. CD200 expression on tumor cells suppresses antitumor immunity: new approaches to cancer immunotherapy. *Journal of immunology (Baltimore, Md. : 1950)*, 178(9), pp.5595–605.
Kruse, P.H. et al., 2014. Natural cytotoxicity receptors and their ligands. *Immunology and cell biology*, 92(3), pp.221–9.
Krzewski, K. & Coligan, J.E., 2012. Human NK cell lytic granules and regulation of their exocytosis. *Frontiers in immunology*, 3, p.335.
Krzewski, K. & Strominger, J.L., 2008. The killer's kiss: the many functions of NK cell immunological synapses. *Current opinion in cell biology*, 20(5), pp.597–605.
Lampson, L.A., 2011. Monoclonal antibodies in neuro-oncology: Getting past the blood-brain barrier. *mAbs*, 3(2), pp.153–60.
Lanier, L.L., 2008. Up on the tightrope: natural killer cell activation and inhibition. *Nature immunology*, 9(5), pp.495–502.
Laouar, Y. et al., 2005. Transforming growth factor-beta controls T helper type 1 cell development through regulation of natural killer cell interferon-gamma. *Nature immunology*, 6(6), pp.600–7.
Lee, J.-C. et al., 2004. Elevated TGF-beta1 secretion and down-modulation of NKG2D underlies impaired NK cytotoxicity in cancer patients. *Journal of immunology (Baltimore, Md. : 1950)*, 172(12), pp.7335–40.
Lee, N. et al., 2016. Tumour-infiltrating lymphocytes in melanoma prognosis and cancer immunotherapy. *Pathology*, 48(2), pp.177–87.
Leonard, G.D., Fojo, T. & Bates, S.E., 2003. The role of ABC transporters in clinical practice. *The oncologist*, 8(5), pp.411–24.
Li, S.X. et al., 2016. Tetherin/BST-2 promotes dendritic cell activation and function during acute retrovirus infection. *Scientific reports*, 6, p.20425.
Lin, J.X. et al., 1995. The role of shared receptor motifs and common Stat proteins in the generation of cytokine pleiotropy and redundancy by IL-2, IL-4, IL-7, IL-13, and IL-15. *Immunity*, 2(4), pp.331–9.
Littlewood, T.D., Kreuzaler, P. & Evan, G.I., 2012. All things to all people. *Cell*, 151(1), pp.11–3.
Liu, G. et al., 2006. Analysis of gene expression and chemoresistance of CD133+ cancer stem cells in glioblastoma. *Molecular cancer*, 5, p.67.
Liu, Q. et al., 2016. Neural stem cells sustain natural killer cells that dictate recovery from brain inflammation. *Nature neuroscience*, 19(2), pp.243–52.
Long, E.O. et al., 2013. Controlling natural killer cell responses: integration of signals for activation and inhibition. *Annual review of immunology*, 31, pp.227–58.
Lopez-Vergès, S. et al., 2010. CD57 defines a functionally distinct population of mature NK cells in the human CD56dimCD16+ NK-cell subset. *Blood*, 116(19), pp.3865–74.
Louis, D.N. et al., 2007. The 2007 WHO classification of tumours of the central nervous system. *Acta neuropathologica*, 114(2), pp.97–109.
Louis, D.N. et al., 2016. The 2016 World Health Organization Classification of Tumors of the Central Nervous System: a summary. *Acta neuropathologica*, 131(6), pp.803–20.
Louis, D.N., Holland, E.C. & Cairncross, J.G., 2001. Glioma classification: a molecular reappraisal. *The American journal of pathology*, 159(3), pp.779–86.
Louveau, A. et al., 2015. Structural and functional features of central nervous system lymphatic vessels. *Nature*, 523(7560), pp.337–41.
Löwenberg, M. et al., 2006. Glucocorticoids cause rapid dissociation of a T-cell-receptor-associated protein complex containing LCK and FYN. *EMBO reports*,

7(10), pp.1023–9.
Löwenberg, M. et al., 2005. Rapid immunosuppressive effects of glucocorticoids mediated through Lck and Fyn. *Blood*, 106(5), pp.1703–10.
Lun, M.P., Monuki, E.S. & Lehtinen, M.K., 2015. Development and functions of the choroid plexus-cerebrospinal fluid system. *Nature reviews. Neuroscience*, 16(8), pp.445–57.
Luo, J.-C. et al., 2008. Dexamethasone inhibits basic fibroblast growth factor-stimulated gastric epithelial cell proliferation. *Biochemical pharmacology*, 76(7), pp.841–9.
Ma, A., Koka, R. & Burkett, P., 2006. Diverse functions of IL-2, IL-15, and IL-7 in lymphoid homeostasis. *Annual review of immunology*, 24, pp.657–79.
Maher, S.G. et al., 2007. Interferon: cellular executioner or white knight? *Current medicinal chemistry*, 14(12), pp.1279–89.
Mamessier, E. et al., 2011. Human breast cancer cells enhance self tolerance by promoting evasion from NK cell antitumor immunity. *The Journal of clinical investigation*, 121(9), pp.3609–22.
Mammolenti, M. et al., 2004. Absence of major histocompatibility complex class I on neural stem cells does not permit natural killer cell killing and prevents recognition by alloreactive cytotoxic T lymphocytes in vitro. *Stem cells (Dayton, Ohio)*, 22(6), pp.1101–10.
Mandelboim, O. et al., 1999. Human CD16 as a lysis receptor mediating direct natural killer cell cytotoxicity. *Proceedings of the National Academy of Sciences of the United States of America*, 96(10), pp.5640–4.
Mantovani, A. & Sica, A., 2010. Macrophages, innate immunity and cancer: balance, tolerance, and diversity. *Current opinion in immunology*, 22(2), pp.231–7.
Marçais, A. et al., 2014. The metabolic checkpoint kinase mTOR is essential for IL-15 signaling during the development and activation of NK cells. *Nature immunology*, 15(8), pp.749–57.
Marçais, A. & Walzer, T., 2014. mTOR: a gate to NK cell maturation and activation. *Cell cycle (Georgetown, Tex.)*, 13(21), pp.3315–6.
Massagué, J., 2008. TGFbeta in Cancer. *Cell*, 134(2), pp.215–30.
Matsuzaki, J. et al., 2010. Tumor-infiltrating NY-ESO-1-specific CD8+ T cells are negatively regulated by LAG-3 and PD-1 in human ovarian cancer. *Proceedings of the National Academy of Sciences of the United States of America*, 107(17), pp.7875–80.
McCoy, K.D. & Le Gros, G., 1999. The role of CTLA-4 in the regulation of T cell immune responses. *Immunology and cell biology*, 77(1), pp.1–10.
McDermott, D.F. & Atkins, M.B., 2013. PD-1 as a potential target in cancer therapy. *Cancer medicine*, 2(5), pp.662–73.
McWhirter, J.R. et al., 2006. Antibodies selected from combinatorial libraries block a tumor antigen that plays a key role in immunomodulation. *Proceedings of the National Academy of Sciences of the United States of America*, 103(4), pp.1041–6.
Medema, J.P., 2013. Cancer stem cells: the challenges ahead. *Nature cell biology*, 15(4), pp.338–44.
Van Meir, E.G. et al., 2010. Exciting new advances in neuro-oncology: the avenue to a cure for malignant glioma. *CA: a cancer journal for clinicians*, 60(3), pp.166–93.
Melcher, A. et al., 2011. Thunder and lightning: immunotherapy and oncolytic viruses collide. *Molecular therapy : the journal of the American Society of Gene Therapy*, 19(6), pp.1008–16.

Michelo, C.M. et al., 2016. Added effects of dexamethasone and mesenchymal stem cells on early Natural Killer cell activation. *Transplant immunology*, 37, pp.1–9.
Mishra, A., Sullivan, L. & Caligiuri, M.A., 2014. Molecular pathways: interleukin-15 signaling in health and in cancer. *Clinical cancer research : an official journal of the American Association for Cancer Research*, 20(8), pp.2044–50.
Miyazaki, T. et al., 1994. Functional activation of Jak1 and Jak3 by selective association with IL-2 receptor subunits. *Science (New York, N.Y.)*, 266(5187), pp.1045–7.
Morantz, R.A. et al., 1979. Macrophages in experimental and human brain tumors. Part 2: studies of the macrophage content of human brain tumors. *Journal of neurosurgery*, 50(3), pp.305–11.
Moreaux, J. et al., 2006. CD200 is a new prognostic factor in multiple myeloma. *Blood*, 108(13), pp.4194–7.
Morvan, M.G. & Lanier, L.L., 2016. NK cells and cancer: you can teach innate cells new tricks. *Nature reviews. Cancer*, 16(1), pp.7–19.
Moustaki, A. et al., 2011. Effect of the simultaneous administration of glucocorticoids and IL-15 on human NK cell phenotype, proliferation and function. *Cancer immunology, immunotherapy : CII*, 60(12), pp.1683–95.
Murdoch, C. et al., 2008. The role of myeloid cells in the promotion of tumour angiogenesis. *Nature reviews. Cancer*, 8(8), pp.618–31.
Nagaraj, S. & Gabrilovich, D.I., 2007. Myeloid-derived suppressor cells. *Advances in experimental medicine and biology*, 601, pp.213–23.
Nandagopal, N. et al., 2014. The Critical Role of IL-15-PI3K-mTOR Pathway in Natural Killer Cell Effector Functions. *Frontiers in immunology*, 5, p.187.
Nduom, E.K. et al., 2016. PD-L1 expression and prognostic impact in glioblastoma. *Neuro-oncology*, 18(2), pp.195–205.
Neil, S.J.D., Zang, T. & Bieniasz, P.D., 2008. Tetherin inhibits retrovirus release and is antagonized by HIV-1 Vpu. *Nature*, 451(7177), pp.425–30.
Nguyen, L.T. & Ohashi, P.S., 2015. Clinical blockade of PD1 and LAG3--potential mechanisms of action. *Nature reviews. Immunology*, 15(1), pp.45–56.
Nie, Z. et al., 2012. c-Myc is a universal amplifier of expressed genes in lymphocytes and embryonic stem cells. *Cell*, 151(1), pp.68–79.
Noonan, D.M. et al., 2008. Inflammation, inflammatory cells and angiogenesis: decisions and indecisions. *Cancer metastasis reviews*, 27(1), pp.31–40.
Norris, S. et al., 2012. PD-1 expression on natural killer cells and CD8(+) T cells during chronic HIV-1 infection. *Viral immunology*, 25(4), pp.329–32.
O'Connor, G.M., Hart, O.M. & Gardiner, C.M., 2006. Putting the natural killer cell in its place. *Immunology*, 117(1), pp.1–10.
Orange, J.S., 2013. Natural killer cell deficiency. *The Journal of allergy and clinical immunology*, 132(3), p.515–25; quiz 526.
Ostrand-Rosenberg, S., 2010. Myeloid-derived suppressor cells: more mechanisms for inhibiting antitumor immunity. *Cancer immunology, immunotherapy : CII*, 59(10), pp.1593–600.
Pàez-Ribes, M. et al., 2009. Antiangiogenic therapy elicits malignant progression of tumors to increased local invasion and distant metastasis. *Cancer cell*, 15(3), pp.220–31.
Pahl, J. & Cerwenka, A., 2015. Tricking the balance: NK cells in anti-cancer immunity. *Immunobiology*.
Palucka, K. & Banchereau, J., 2012. Cancer immunotherapy via dendritic cells. *Nature reviews. Cancer*, 12(4), pp.265–77.

Pardo, J. et al., 2002. The differential contribution of granzyme A and granzyme B in cytotoxic T lymphocyte-mediated apoptosis is determined by the quality of target cells. *European journal of immunology*, 32(7), pp.1980–5.

Park, J.K. et al., 2010. ICAM-3 enhances the migratory and invasive potential of human non-small cell lung cancer cells by inducing MMP-2 and MMP-9 via Akt and CREB. *International journal of oncology*, 36(1), pp.181–92.

Pérez, M.H.-A. et al., 2013. A membrane glucocorticoid receptor mediates the rapid/non-genomic actions of glucocorticoids in mammalian skeletal muscle fibres. *The Journal of physiology*, 591(20), pp.5171–85.

Perry, J., Laperriere, N. & O'Callaghan, C., 2016. A phase III randomized controlled trial of short-course radiotherapy with or without concomitant and adjuvant temozolomide in elderly patients with glioblastoma (CCTG CE.6, EORTC 26062-22061, TROG 08.02, NCT00482677).tle. In *2016 ASCO Annual Meeting*.

Perry, V.H. & Teeling, J., 2013. Microglia and macrophages of the central nervous system: the contribution of microglia priming and systemic inflammation to chronic neurodegeneration. *Seminars in immunopathology*, 35(5), pp.601–12.

Phillips, L.K. et al., 2013. Natural killer cell-activating receptor NKG2D mediates innate immune targeting of allogeneic neural progenitor cell grafts. *Stem cells (Dayton, Ohio)*, 31(9), pp.1829–39.

Piccart-Gebhart, M.J. et al., 2005. Trastuzumab after adjuvant chemotherapy in HER2-positive breast cancer. *The New England journal of medicine*, 353(16), pp.1659–72.

Pietenpol, J.A. et al., 1990. TGF-beta 1 inhibition of c-myc transcription and growth in keratinocytes is abrogated by viral transforming proteins with pRB binding domains. *Cell*, 61(5), pp.777–85.

Pointer, K.B. et al., 2014. Glioblastoma cancer stem cells: Biomarker and therapeutic advances. *Neurochemistry international*, 71, pp.1–7.

Pópulo, H., Lopes, J.M. & Soares, P., 2012. The mTOR signalling pathway in human cancer. *International journal of molecular sciences*, 13(2), pp.1886–918.

Porreca, E. et al., 2002. Increased transforming growth factor-beta(1) circulating levels and production in human monocytes after 3-hydroxy-3-methyl-glutaryl-coenzyme a reductase inhibition with pravastatin. *Journal of the American College of Cardiology*, 39(11), pp.1752–7.

Pratt, W.B. et al., 2004. Role of molecular chaperones in steroid receptor action. *Essays in biochemistry*, 40, pp.41–58.

Prigent, S.A. et al., 1996. Enhanced tumorigenic behavior of glioblastoma cells expressing a truncated epidermal growth factor receptor is mediated through the Ras-Shc-Grb2 pathway. *The Journal of biological chemistry*, 271(41), pp.25639–45.

Qian, B.-Z. & Pollard, J.W., 2010. Macrophage diversity enhances tumor progression and metastasis. *Cell*, 141(1), pp.39–51.

Quaresma, M., Coleman, M.P. & Rachet, B., 2015. 40-year trends in an index of survival for all cancers combined and survival adjusted for age and sex for each cancer in England and Wales, 1971-2011: a population-based study. *Lancet (London, England)*, 385(9974), pp.1206–18.

Rajagopalan, S. & Long, E.O., 2005. Understanding how combinations of HLA and KIR genes influence disease. *The Journal of experimental medicine*, 201(7), pp.1025–9.

Ransohoff, R.M. & Engelhardt, B., 2012. The anatomical and cellular basis of immune surveillance in the central nervous system. *Nature reviews. Immunology*, 12(9), pp.623–35.

Ransohoff, R.M., Kivisäkk, P. & Kidd, G., 2003. Three or more routes for leukocyte migration into the central nervous system. *Nature reviews. Immunology*, 3(7), pp.569–81.

Ranson, T. et al., 2003. IL-15 is an essential mediator of peripheral NK-cell homeostasis. *Blood*, 101(12), pp.4887–93.

Ratman, D. et al., 2013. How glucocorticoid receptors modulate the activity of other transcription factors: a scope beyond tethering. *Mol Cell Endocrinol*, 5(380(1-2)), pp.41–54.

Raulet, D.H., 2003. Roles of the NKG2D immunoreceptor and its ligands. *Nature reviews. Immunology*, 3(10), pp.781–90.

Reed, J.C., Nowell, P.C. & Hoover, R.G., 1985. Regulation of c-myc mRNA levels in normal human lymphocytes by modulators of cell proliferation. *Proceedings of the National Academy of Sciences of the United States of America*, 82(12), pp.4221–4.

Reil, T.D. et al., 1999. Dexamethasone suppresses vascular smooth muscle cell proliferation. *The Journal of surgical research*, 85(1), pp.109–14.

Ringnér, M., 2008. What is principal component analysis? *Nature biotechnology*, 26(3), pp.303–4.

Rocca, Y.S. et al., 2013. Altered phenotype in peripheral blood and tumor-associated NK cells from colorectal cancer patients. *Innate immunity*, 19(1), pp.76–85.

Roda, J.M. et al., 2007. The activation of natural killer cell effector functions by cetuximab-coated, epidermal growth factor receptor positive tumor cells is enhanced by cytokines. *Clinical cancer research : an official journal of the American Association for Cancer Research*, 13(21), pp.6419–28.

Rodriguez, A., Tatter, S.B. & Debinski, W., 2015. Neurosurgical Techniques for Disruption of the Blood-Brain Barrier for Glioblastoma Treatment. *Pharmaceutics*, 7(3), pp.175–87.

Rodríguez, P.C. & Ochoa, A.C., 2008. Arginine regulation by myeloid derived suppressor cells and tolerance in cancer: mechanisms and therapeutic perspectives. *Immunological reviews*, 222, pp.180–91.

Romagné, F. et al., 2009. Preclinical characterization of 1-7F9, a novel human anti-KIR receptor therapeutic antibody that augments natural killer-mediated killing of tumor cells. *Blood*, 114(13), pp.2667–77.

Romond, E.H. et al., 2005. Trastuzumab plus adjuvant chemotherapy for operable HER2-positive breast cancer. *The New England journal of medicine*, 353(16), pp.1673–84.

Rook, A.H. et al., 1986. Effects of transforming growth factor beta on the functions of natural killer cells: depressed cytolytic activity and blunting of interferon responsiveness. *Journal of immunology (Baltimore, Md. : 1950)*, 136(10), pp.3916–20.

Rossi, M.L. et al., 1991. Characterization of the mononuclear cell infiltrate and HLA-Dr expression in 19 oligodendrogliomas. *Surgical neurology*, 36(2), pp.119–25.

Rosso, L. et al., 2009. A new model for prediction of drug distribution in tumor and normal tissues: pharmacokinetics of temozolomide in glioma patients. *Cancer research*, 69(1), pp.120–7.

Rozali, E.N. et al., 2012. Programmed Death Ligand 2 in Cancer-Induced Immune Suppression. *Clinical and Developmental Immunology*, 2012, pp.1–8.

Ruggeri, L. et al., 2002. Effectiveness of donor natural killer cell alloreactivity in mismatched hematopoietic transplants. *Science (New York, N.Y.)*, 295(5562),

pp.2097–100.
Russell, J.H. & Ley, T.J., 2002. Lymphocyte-mediated cytotoxicity. *Annual review of immunology*, 20, pp.323–70.
Saas, P. et al., 1997. Fas ligand expression by astrocytoma in vivo: maintaining immune privilege in the brain? *The Journal of clinical investigation*, 99(6), pp.1173–8.
Sabò, A. et al., 2014. Selective transcriptional regulation by Myc in cellular growth control and lymphomagenesis. *Nature*, 511(7510), pp.488–92.
Safdari, H., Hochberg, F.H. & Richardson, E.P., 1985. Prognostic value of round cell (lymphocyte) infiltration in malignant gliomas. *Surgical neurology*, 23(3), pp.221–6.
Saikali, S. et al., 2007. Expression of nine tumour antigens in a series of human glioblastoma multiforme: interest of EGFRvIII, IL-13Ralpha2, gp100 and TRP-2 for immunotherapy. *Journal of neuro-oncology*, 81(2), pp.139–48.
Sampson, J.H. et al., 2009. An epidermal growth factor receptor variant III-targeted vaccine is safe and immunogenic in patients with glioblastoma multiforme. *Molecular cancer therapeutics*, 8(10), pp.2773–9.
Sampson, J.H. et al., 2008. Tumor-specific immunotherapy targeting the EGFRvIII mutation in patients with malignant glioma. *Seminars in immunology*, 20(5), pp.267–75.
Santoni, A. et al., 2007. Natural killer (NK) cells from killers to regulators: distinct features between peripheral blood and decidual NK cells. *American journal of reproductive immunology (New York, N.Y. : 1989)*, 58(3), pp.280–8.
Schatzle, J.D. et al., 1999. Characterization of inhibitory and stimulatory forms of the murine natural killer cell receptor 2B4. *Proceedings of the National Academy of Sciences of the United States of America*, 96(7), pp.3870–5.
Scheinman, R.I. et al., 1995. Role of transcriptional activation of I kappa B alpha in mediation of immunosuppression by glucocorticoids. *Science (New York, N.Y.)*, 270(5234), pp.283–6.
Schmitt, J. et al., 2015. Human Parthenogenetic Embryonic Stem Cell-Derived Neural Stem Cells Express HLA-G and Show Unique Resistance to NK Cell-Mediated Killing. *Molecular medicine (Cambridge, Mass.)*, 21, pp.185–96.
Schroeteler, J. et al., 2014. Glioma tissue obtained by modern ultrasonic aspiration with a simple sterile suction trap for primary cell culture and pathological evaluation. *European surgical research. Europäische chirurgische Forschung. Recherches chirurgicales européennes*, 53(1–4), pp.37–42.
Schwartz, R.H., 2003. T cell anergy. *Annual review of immunology*, 21, pp.305–34.
Scott, A.M., Wolchok, J.D. & Old, L.J., 2012. Antibody therapy of cancer. *Nature reviews. Cancer*, 12(4), pp.278–87.
Sehgal, A. & Berger, M.S., 2000. Basic concepts of immunology and neuroimmunology. *Neurosurgical focus*, 9(6), p.e1.
Seidel, U.J.E., Schlegel, P. & Lang, P., 2013. Natural killer cell mediated antibody-dependent cellular cytotoxicity in tumor immunotherapy with therapeutic antibodies. *Frontiers in immunology*, 4, p.76.
Seo, D.R., Kim, K.Y. & Lee, Y.B., 2004. Interleukin-10 expression in lipopolysaccharide-activated microglia is mediated by extracellular ATP in an autocrine fashion. *Neuroreport*, 15(7), pp.1157–61.
Shaked, I. et al., 2005. Protective autoimmunity: interferon-gamma enables microglia to remove glutamate without evoking inflammatory mediators. *Journal of neurochemistry*, 92(5), pp.997–1009.

Sharma, S., 2014. Natural killer cells and regulatory T cells in early pregnancy loss. *The International journal of developmental biology*, 58(2–4), pp.219–29.
Shibuya, A. et al., 1996. DNAM-1, a novel adhesion molecule involved in the cytolytic function of T lymphocytes. *Immunity*, 4(6), pp.573–81.
Shibuya, A., Lanier, L.L. & Phillips, J.H., 1998. Protein kinase C is involved in the regulation of both signaling and adhesion mediated by DNAX accessory molecule-1 receptor. *Journal of immunology (Baltimore, Md. : 1950)*, 161(4), pp.1671–6.
Shibuya, K. et al., 1999. Physical and functional association of LFA-1 with DNAM-1 adhesion molecule. *Immunity*, 11(5), pp.615–23.
Simon, M.M. et al., 1997. In vitro- and ex vivo-derived cytolytic leukocytes from granzyme A x B double knockout mice are defective in granule-mediated apoptosis but not lysis of target cells. *The Journal of experimental medicine*, 186(10), pp.1781–6.
Singh, S.K. et al., 2003. Identification of a cancer stem cell in human brain tumors. *Cancer research*, 63(18), pp.5821–8.
Singh, S.K. et al., 2004. Identification of human brain tumour initiating cells. *Nature*, 432(7015), pp.396–401.
Sivori, S. et al., 1999. NKp46 is the major triggering receptor involved in the natural cytotoxicity of fresh or cultured human NK cells. Correlation between surface density of NKp46 and natural cytotoxicity against autologous, allogeneic or xenogeneic target cells. *European journal of immunology*, 29(5), pp.1656–66.
Sivori, S. et al., 1997. p46, a novel natural killer cell-specific surface molecule that mediates cell activation. *The Journal of experimental medicine*, 186(7), pp.1129–36.
Spits, H. et al., 2013. Innate lymphoid cells--a proposal for uniform nomenclature. *Nature reviews. Immunology*, 13(2), pp.145–9.
Stephen, T.L. et al., 2014. Transforming growth factor β-mediated suppression of antitumor T cells requires FoxP1 transcription factor expression. *Immunity*, 41(3), pp.427–39.
Stern, P. et al., 1980. Natural killer cells mediate lysis of embryonal carcinoma cells lacking MHC. *Nature*, 285(5763), pp.341–2.
Stevens, A., Klöter, I. & Roggendorf, W., 1988. Inflammatory infiltrates and natural killer cell presence in human brain tumors. *Cancer*, 61(4), pp.738–43.
Stojanovic, A. et al., 2014. CTLA-4 is expressed by activated mouse NK cells and inhibits NK Cell IFN-γ production in response to mature dendritic cells. *Journal of immunology (Baltimore, Md. : 1950)*, 192(9), pp.4184–91.
Stonier, S.W. & Schluns, K.S., 2010. Trans-presentation: a novel mechanism regulating IL-15 delivery and responses. *Immunology letters*, 127(2), pp.85–92.
Stupp, R. et al., 2005. Radiotherapy plus concomitant and adjuvant temozolomide for glioblastoma. *The New England journal of medicine*, 352(10), pp.987–96.
Sundahl, N. et al., 2015. Selective glucocorticoid receptor modulation: New directions with non-steroidal scaffolds. *Pharmacology & therapeutics*, 152, pp.28–41.
Sundberg, M. et al., 2009. CD marker expression profiles of human embryonic stem cells and their neural derivatives, determined using flow-cytometric analysis, reveal a novel CD marker for exclusion of pluripotent stem cells. *Stem cell research*, 2(2), pp.113–24.
Takabatake, M. et al., Aberrant expression and phosphorylation of 4E-BP1, a main target of mTOR signaling, in rat mammary carcinomas: an association with etiology. *In vivo (Athens, Greece)*, 25(6), pp.853–60.

Takanami, I., Takeuchi, K. & Giga, M., 2001. The prognostic value of natural killer cell infiltration in resected pulmonary adenocarcinoma. *The Journal of thoracic and cardiovascular surgery*, 121(6), pp.1058–63.

Takizawa, H. & Manz, M.G., 2007. Macrophage tolerance: CD47-SIRP-alpha-mediated signals matter. *Nature immunology*, 8(12), pp.1287–9.

Teng, M.W.L. et al., 2008. Immune-mediated dormancy: an equilibrium with cancer. *Journal of leukocyte biology*, 84(4), pp.988–93.

Teo, E.C., Chew, Y. & Phipps, C., 2016. A review of monoclonal antibody therapies in lymphoma. *Critical reviews in oncology/hematology*, 97, pp.72–84.

Thomson, A.W., Turnquist, H.R. & Raimondi, G., 2009. Immunoregulatory functions of mTOR inhibition. *Nature reviews. Immunology*, 9(5), pp.324–37.

Tonks, A. et al., 2007. CD200 as a prognostic factor in acute myeloid leukaemia. *Leukemia*, 21(3), pp.566–8.

Torr, E.E. et al., 2012. Apoptotic cell-derived ICAM-3 promotes both macrophage chemoattraction to and tethering of apoptotic cells. *Cell death and differentiation*, 19(4), pp.671–9.

Trapani, J.A. & Smyth, M.J., 2002. Functional significance of the perforin/granzyme cell death pathway. *Nature reviews. Immunology*, 2(10), pp.735–47.

Tremblay, M.-È., Lowery, R.L. & Majewska, A.K., 2010. Microglial interactions with synapses are modulated by visual experience. *PLoS biology*, 8(11), p.e1000527.

Trinchieri, G., 1989. Biology of natural killer cells. *Advances in immunology*, 47, pp.187–376.

Trinchieri, G. & Santoli, D., 1978. Anti-viral activity induced by culturing lymphocytes with tumor-derived or virus-transformed cells. Enhancement of human natural killer cell activity by interferon and antagonistic inhibition of susceptibility of target cells to lysis. *The Journal of experimental medicine*, 147(5), pp.1314–33.

Tuettenberg, J. et al., 2009. Recurrence pattern in glioblastoma multiforme patients treated with anti-angiogenic chemotherapy. *Journal of cancer research and clinical oncology*, 135(9), pp.1239–44.

Turnbull, S. et al., 2015. Evidence for Oncolytic Virotherapy: Where Have We Got to and Where Are We Going? *Viruses*, 7(12), pp.6291–312.

Uhrberg, M., Parham, P. & Wernet, P., 2002. Definition of gene content for nine common group B haplotypes of the Caucasoid population: KIR haplotypes contain between seven and eleven KIR genes. *Immunogenetics*, 54(4), pp.221–9.

Vajdic, C.M. & van Leeuwen, M.T., 2009. Cancer incidence and risk factors after solid organ transplantation. *International journal of cancer*, 125(8), pp.1747–54.

Valiante, N.M. et al., 1997. Functionally and structurally distinct NK cell receptor repertoires in the peripheral blood of two human donors. *Immunity*, 7(6), pp.739–51.

Veillette, A., 2010. SLAM-family receptors: immune regulators with or without SAP-family adaptors. *Cold Spring Harbor perspectives in biology*, 2(3), p.a002469.

Veillette, A., Dong, Z. & Latour, S., 2007. Consequence of the SLAM-SAP signaling pathway in innate-like and conventional lymphocytes. *Immunity*, 27(5), pp.698–710.

Verhaak, R.G.W. et al., 2010. Integrated genomic analysis identifies clinically relevant subtypes of glioblastoma characterized by abnormalities in PDGFRA, IDH1, EGFR, and NF1. *Cancer cell*, 17(1), pp.98–110.

Viel, S. et al., 2016. TGF-β inhibits the activation and functions of NK cells by repressing the mTOR pathway. *Science signaling*, 9(415), p.ra19.

Villegas, F.R. et al., 2002. Prognostic significance of tumor infiltrating natural killer cells subset CD57 in patients with squamous cell lung cancer. *Lung cancer (Amsterdam, Netherlands)*, 35(1), pp.23–8.
de Visser, K.E., Eichten, A. & Coussens, L.M., 2006. Paradoxical roles of the immune system during cancer development. *Nature reviews. Cancer*, 6(1), pp.24–37.
Vitale, M. et al., 2014. Effect of tumor cells and tumor microenvironment on NK-cell function. *European journal of immunology*, 44(6), pp.1582–92.
Vivier, E. et al., 2008. Functions of natural killer cells. *Nature immunology*, 9(5), pp.503–10.
Vivier, E. et al., 2011. Innate or adaptive immunity? The example of natural killer cells. *Science (New York, N.Y.)*, 331(6013), pp.44–9.
Waldmann, T.A., 2006. The biology of interleukin-2 and interleukin-15: implications for cancer therapy and vaccine design. *Nature reviews. Immunology*, 6(8), pp.595–601.
Walker, P.R., Calzascia, T. & Dietrich, P.-Y., 2002. All in the head: obstacles for immune rejection of brain tumours. *Immunology*, 107(1), pp.28–38.
Wallach, D., Fellous, M. & Revel, M., 1982. Preferential effect of gamma interferon on the synthesis of HLA antigens and their mRNAs in human cells. *Nature*, 299(5886), pp.833–6.
Walzer, T. et al., 2005. Natural-killer cells and dendritic cells: "l'union fait la force". *Blood*, 106(7), pp.2252–8.
Walzer, T. et al., 2007. Natural killer cells: from CD3(-)NKp46(+) to post-genomics meta-analyses. *Current opinion in immunology*, 19(3), pp.365–72.
Wang, H. et al., 2006. Dexamethasone represses signaling through the mammalian target of rapamycin in muscle cells by enhancing expression of REDD1. *The Journal of biological chemistry*, 281(51), pp.39128–34.
Warren, H.S. & Smyth, M.J., 1999. NK cells and apoptosis. *Immunology and Cell Biology*, 77(1), pp.64–75.
Watters, J.J., Schartner, J.M. & Badie, B., 2005. Microglia function in brain tumors. *Journal of neuroscience research*, 81(3), pp.447–55.
Wherry, E.J. et al., 2003. Viral persistence alters CD8 T-cell immunodominance and tissue distribution and results in distinct stages of functional impairment. *Journal of virology*, 77(8), pp.4911–27.
Whiteside, T.L., 2015. The role of regulatory T cells in cancer immunology. *ImmunoTargets and therapy*, 4, pp.159–71.
Wilson, E.B. et al., 2011. Human tumour immune evasion via TGF-β blocks NK cell activation but not survival allowing therapeutic restoration of anti-tumour activity. *PloS one*, 6(9), p.e22842.
Wink, M.R. et al., 2003. Thyroid hormone upregulates ecto-5'-nucleotidase/CD73 in C6 rat glioma cells. *Molecular and cellular endocrinology*, 205(1–2), pp.107–14.
Wintterle, S. et al., 2003. Expression of the B7-related molecule B7-H1 by glioma cells: a potential mechanism of immune paralysis. *Cancer research*, 63(21), pp.7462–7.
Wischhusen, J. et al., 2005. HLA-E protects glioma cells from NKG2D-mediated immune responses in vitro: implications for immune escape in vivo. *Journal of neuropathology and experimental neurology*, 64(6), pp.523–8.
Wold, W.S.M. & Toth, K., 2013. Adenovirus vectors for gene therapy, vaccination and cancer gene therapy. *Current gene therapy*, 13(6), pp.421–33.
Wolf, D. et al., 2005. The expression of the regulatory T cell-specific forkhead box transcription factor FoxP3 is associated with poor prognosis in ovarian cancer.

Clinical cancer research : an official journal of the American Association for Cancer Research, 11(23), pp.8326–31.

Wurdak, H. et al., 2010. An RNAi screen identifies TRRAP as a regulator of brain tumor-initiating cell differentiation. *Cell stem cell*, 6(1), pp.37–47.

Xu, L.W. et al., 2014. Current vaccine trials in glioblastoma: a review. *Journal of immunology research*, 2014, p.796856.

Xu, Q. et al., 2009. Antigen-specific T-cell response from dendritic cell vaccination using cancer stem-like cell-associated antigens. *Stem cells (Dayton, Ohio)*, 27(8), pp.1734–40.

Yamamoto, K.R., 1985. Steroid Receptor Regulated Transcription of Specific Genes and Gene Networks. *Annual Review of Genetics*, 19(1), pp.209–252.

Zamoyska, R. et al., 2003. The influence of the src-family kinases, Lck and Fyn, on T cell differentiation, survival and activation. *Immunological reviews*, 191, pp.107–18.

Zaytseva, Y.Y. et al., 2012. mTOR inhibitors in cancer therapy. *Cancer letters*, 319(1), pp.1–7.

Zhang, J., Stevens, M.F.G. & Bradshaw, T.D., 2012. Temozolomide: mechanisms of action, repair and resistance. *Current molecular pharmacology*, 5(1), pp.102–14.

Zhao, Q. et al., 2015. Inhibition of c-MYC with involvement of ERK/JNK/MAPK and AKT pathways as a novel mechanism for shikonin and its derivatives in killing leukemia cells. *Oncotarget*, 6(36), pp.38934–51.

Zhou, Z. & Lu, Z.-R., 2013. Gadolinium-based contrast agents for magnetic resonance cancer imaging. *Wiley interdisciplinary reviews. Nanomedicine and nanobiotechnology*, 5(1), pp.1–18.

Ziegler, S.F. et al., 1993. Molecular characterization of the early activation antigen CD69: a type II membrane glycoprotein related to a family of natural killer cell activation antigens. *European journal of immunology*, 23(7), pp.1643–8.

Zitvogel, L. et al., 2008. Immunological aspects of cancer chemotherapy. *Nature reviews. Immunology*, 8(1), pp.59–73.

Zou, W. & Chen, L., 2008. Inhibitory B7-family molecules in the tumour microenvironment. *Nature reviews. Immunology*, 8(6), pp.467–77.

Zussman, B.M. & Engh, J.A., 2015. Outcomes of the ACT III Study: Rindopepimut (CDX-110) Therapy for Glioblastoma. *Neurosurgery*, 76(6), p.N17.

Appendix

Appendix 1.

The percentage expression for each antigen on the five cell lines.

CD number	Gene name	% expression on GBM1 cells
47	CD47	91.6
147	BSG	90.9
HLA ABC		90.8
81	CD81	89.8
46	CD46	89.3
49b	ITGA2	89.1
151	151	89
165	X	87.8
166	ALCAM	87.3
99	CD99	87.2
71	TFRC	87.1
97	CD97	86
b2m	B2M	83.8
146	MCAM	83.3
63	CD63	83.2
56	NCAM1	82.7
142	F3	82.6
90	THY1	81.3
59	CD59	80.9
58	CD58	77.2
164	CD164	76.7
98	SLC3A2	75.6
119	IFNGR	75.1
95	FAS	73.8
44	CD44	71.6
57	B3GAT1	71.3
200	CD200	70.6
94	KLRD1	70.5
49e	ITGA5	68.6
49f	ITGA5	63.8
29	ITGB1	62
SSEA1		58.9
91	LRP1	57.7
GD2		53.8
271	NGFR	53.4
227	MUC1	50.5
107A	LAMP1	41.4
HLA DQ		40.3
73	NT5E	37.9
15	FUT4	36.8

99R		36.7
49a	ITGA1	34.9
34	CD34	33.8
26	DPP4	32
49d	ITGA4	31
49c	ITGA3	29.2
140A	THBD	28.2
340	Her2	26.8
9	CD9	26.7
106	VCAM1	25.6
54	ICAM1	23.6
321	F11R	21.5

CD number	**Gene name**	**% expression on GBM4 cells**
47	CD47	100
98	SLC3A2	100
147	BSG	100
49b	ITGA2	99.99
97	CD97	99.99
99	CD99	99.99
46	CD46	99.98
59	CD59	99.98
HLA ABC		99.97
9	CD9	99.96
63	CD63	99.92
165	X	99.92
151	151	99.86
b2m	B2M	99.81
81	CD81	99.8
71	TFRC	99.75
24	CD24	99.67
57	B3GAT1	98.98
119	IFNGR	98.89
164	CD164	98.76
49f	ITGA5	98.52
105	ENG	98.24
166	ALCAM	98.03
95	FAS	97.53
44	CD44	97.35
HLAA2		97.18
200	CD200	95.55
340	Her2	94.98
29	ITGB1	94.81
146	MCAM	94.54
271	NGFR	93.53

HLA DQ		93.52
94	KLRD1	92.85
99R		92.65
GD2		92.33
142	F3	92
130	IL6ST	91.14
91	LRP1	90.62
221	IGF1R	88.91
49e	ITGA5	88.34
141	PDGFRB	86
49c	ITGA3	83.81
CD49f		83.26
112	PVRL2	79.71
172B	SIRPB1	75.75
107A	LAMP1	73.59
55	CD55	73.42
54	ICAM1	73.14
56	NCAM1	69.62
90	THY1	64.35
184	CXCR4	61.1
73	NT5E	60.17
140B	PDGFRA	55.76
51/61	ITGAV	55.64
227	MUC1	55.26
34	CD34	54.75
49d	ITGA4	51.39
140A	THBD	50.48
220	INSR	50.1
120A	TNFRSF1A	47.52
268	TNFRSF13C	46.26
26	DPP4	45.72
MICA/B	MICA	40.37
107B	LAMP2	38.39
118	LIFR	36.06
61	ITGB3	31.87
SSEA1		31.86
egfr	EGFR	31.04
15	FUT4	28.24
152	CTLA-4	27.17
209	CD209	26.39
338	ABCG2	21.76
109	CD109	20.36
274	CD274	20.2

CD number	Gene name	% expression on GBM11 cells
9	CD9	100
44	CD44	100
46	CD46	100
49c	ITGA3	100
49e	ITGA5	100
59	CD59	100
98	SLC3A2	100
47	CD47	99.99
71	TFRC	99.99
147	BSG	99.99
73	NT5E	99.98
97	CD97	99.98
164	CD164	99.98
HLA DR		99.98
49b	ITGA2	99.97
HLA ABC		99.97
63	CD63	99.96
b2m	B2M	99.96
HLA DRPQ		99.95
GD2		99.94
99	CD99	99.86
81	CD81	99.84
56	NCAM1	99.75
166	ALCAM	99.68
165	X	99.67
49f	ITGA5	99.67
205	LY75	99.62
HLA DQ		99.46
54	ICAM1	99.41
107A	LAMP1	99.4
91	LRP1	99.32
34	CD34	99.26
119	IFNGR	99.06
104	ITGB4	98.99
55	CD55	98.61
106	VCAM1	98.22
107B	LAMP2	98.22
271	NGFR	98.13
95	FAS	98.11
274	CD274	97.28
51/61	ITGAV	96.93
49d	ITGA4	96.86
146	MCAM	96.73

CD49f		95.89
227	MUC1	95.48
74	CD74	95.29
120A	TNFRSF1A	93.31
61	ITGB3	91.58
57	B3GAT1	88.91
99R		88.77
151	151	88.73
340	Her2	86.48
77	A4GALT	85.22
273	PDCD1LG2	81.29
142	F3	78.23
94	KLRD1	75.71
26	DPP4	70.04
141	PDGFRB	61.41
130	IL6ST	56.11
10	MME	48.99
105	ENG	48.77
184	CXCR4	43.79
268	TNFRSF13C	41.13
201	PROCR	40.7
29	ITGB1	39.52
338	ABCG2	38.87
221	IGF1R	37.27
38	CD38	36.44
40	CD40	34.05
172B	SIRPB1	34.05
112	PVRL2	32.23
90	THY1	30.33
109	CD109	29.73
80	CD80	28.97
140A	THBD	23.9
121B	IL1R2	23.32
62P	SELP	20.62
321	F11R	20.37

CD number	**Gene name**	**% expression on GBM13 cells**
9	CD9	100
44	CD44	100
46	CD46	100
49c	ITGA3	100
55	CD55	100
97	CD97	100
98	SLC3A2	100

99	CD99	99.99
147	BSG	99.99
HLA ABC		99.99
47	CD47	99.98
49b	ITGA2	99.98
165	X	99.98
73	NT5E	99.97
GD2		99.96
59	CD59	99.95
b2m	B2M	99.94
49e	ITGA5	99.93
63	CD63	99.92
151	151	99.89
271	NGFR	99.87
81	CD81	99.83
49f	ITGA5	99.77
95	FAS	99.76
HLA DQ		99.72
56	NCAM1	99.56
71	TFRC	99.55
166	ALCAM	99.47
99R		99.45
91	LRP1	99.25
HLAA2		99.22
142	F3	99.19
90	THY1	99.06
141	PDGFRB	98.98
119	IFNGR	98.85
146	MCAM	98.83
200	CD200	98.67
CD49f		98.28
94	KLRD1	97.98
340	Her2	97.36
57	B3GAT1	96.16
164	CD164	96.08
54	ICAM1	94.73
130	IL6ST	93.38
51/61	ITGAV	93.03
29	ITGB1	91.72
172B	SIRPB1	89.85
105	ENG	88.5
107A	LAMP1	88.26
61	ITGB3	84.77
321	F11R	84.49

220	INSR	81.34
221	IGF1R	78.72
24	CD24	78.56
274	CD274	75.63
120A	TNFRSF1A	71.32
112	PVRL2	71.2
104	ITGB4	70.65
26	DPP4	70.49
108	SEMA7A	65.92
77	A4GALT	64.76
CD326		63.61
227	MUC1	62.9
209	CD209	61.79
184	CXCR4	56.94
34	CD34	55.04
107B	LAMP2	54.28
egfr	EGFR	53.2
268	TNFRSF13C	50.41
118	LIFR	44.6
MICA/B	MICA	43.86
144	CDH5	41.24
338	ABCG2	38.32
152	CTLA-4	37.74
140B	PDGFRA	37.51
49a	ITGA1	35.63
329	SIGLEC8	34.7
SSEA4		32.18
80	CD80	25.44
49d	ITGA4	23.75
50	ICAM3	21.35

CD number	**Gene name**	**% expression on GBM20 cells**
47	CD47	100
81	CD81	100
98	SLC3A2	100
147	BSG	100
b2m	B2M	100
99	CD99	99.99
46	CD46	99.98
151	151	99.98
9	CD9	99.97
97	CD97	99.97
165	X	99.97
49c	ITGA3	99.96

63	CD63	99.95
HLA ABC		99.95
HLAA2		99.94
59	CD59	99.92
73	NT5E	99.87
44	CD44	99.84
49e	ITGA5	99.83
GD2		99.82
56	NCAM1	99.75
57	B3GAT1	99.75
71	TFRC	99.64
49b	ITGA2	99.33
90	THY1	99.04
200	CD200	98.92
271	NGFR	98.5
HLA DQ		98.28
119	IFNGR	98.14
130	IL6ST	98.03
99R		97.86
142	F3	97.51
164	CD164	97.38
146	MCAM	96.92
95	FAS	96.69
HLA DR		96.45
HLA DRPQ		95.51
141	PDGFRB	94.31
51/61	ITGAV	94.17
166	ALCAM	94.15
91	LRP1	94.09
49f	ITGA5	93.66
227	MUC1	91.57
338	ABCG2	90.98
94	KLRD1	89.63
24	CD24	89.22
61	ITGB3	88.07
49d	ITGA4	82.31
220	INSR	81.45
340	Her2	79.74
107A	LAMP1	78.66
MICA/B	MICA	77.53
152	CTLA-4	75.76
108	SEMA7A	75.15
105	ENG	74.88
268	TNFRSF13C	73.6

274	CD274	72.22
107B	LAMP2	71.14
172B	SIRPB1	70.02
120A	TNFRSF1A	69.01
egfr	EGFR	68.68
15	FUT4	67.12
140B	PDGFRA	66.96
SSEA1		66.06
77	A4GALT	65.45
29	ITGB1	65.05
CD49f		61.16
221	IGF1R	58
80	CD80	57.11
34	CD34	56.14
112	PVRL2	55.1
26	DPP4	55.02
184	CXCR4	47.56
209	CD209	47.54
88	C5AR1	47.35
138	SDC1	47.21
106	VCAM1	45.03
321	F11R	42.19
120B	TNFRSF1B	41.99
54	ICAM1	38.51
74	CD74	37.5
171	L1CAM	36.09
273	PDCD1LG2	34.4
55	CD55	34.17
50	ICAM3	31.08
140A	THBD	26.31
75	ST6GAL1	22.84
231	TSPAN7	21.87
205	LY75	20.88
118	LIFR	20.41